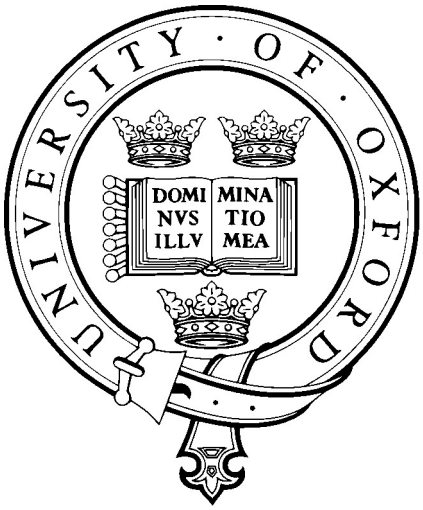
EFFECT OF PHOTOACCLIMATION ON BIO-OPTICAL PROPERTIES OF MARINE PHYTOPLANKTON

by

Sornsiri Phongphattarawat
St Cross College

A thesis submitted to the University of Oxford for the degree of Doctor of Philosophy in Earth Sciences



Supervised by
Dr Heather A. Bouman & Dr Qiong Zhang

Department of Earth Sciences
University of Oxford

Trinity Term 2020

To my parents,
who instilled in me the virtues of
perseverance and commitment.

And to Dr Ajcharaporn Piumsomboon and Dr Heather A. Bouman,
who introduced me to biological oceanography,
and taught me *everything* I know about marine plankton!

Declaration

This thesis is the result of my own work. Any assistance and collaboration with others has been acknowledged. It does not exceed the page limit set out by the degrees committee and is not substantially the same as any work that has been, or is being submitted to any other university for any degree, diploma or other qualifications.

Sornsiri Phongphattarawat

Abstract

Photoacclimation in marine phytoplankton is manifested through changes in pigment composition and has a significant impact on *in vivo* light absorption. Results obtained from this thesis work clearly show that the variability in the chlorophyll *a* (Chl-*a*)-specific absorption coefficient of phytoplankton at 440 nm ($a^*_{ph}(440)$) observed over a broad latitudinal gradient of the Atlantic Basin was influenced significantly by changes in the concentration of non-photosynthetic pigments (NPPs) relative to total pigments (the NPP index), whereas pigment indices of cell size showed a weaker correlation with $a^*_{ph}(440)$. Spatial and seasonal changes in the NPP index were the combined result of photoacclimation and the photoadaptive variation in pigment composition of dominant prokaryotic and eukaryotic groups. Variability in the spectral shape (indexed by the spectral slope) of phytoplankton absorption could be largely explained by NPPs, particularly zeaxanthin (a marker for marine picocyanobacteria) which was highly abundant in the (sub)tropical oligotrophic gyres due to the predominance of the marine picocyanobacterium *Prochlorococcus*. In *Prochlorococcus*-dominated waters, depth-dependent variation in the NPP index was driven primarily by variation in the intracellular concentration of photosynthetic pigments (PSPs), rather than NPPs, which was the result of both photoacclimation and a shift in dominant ecotypes. Photoacclimation of this globally-significant genus was also clearly reflected in the strong vertical change in the intracellular concentration of the dominant light harvesting pigment, divinyl Chl-*a* (DVChl-*a*). The flexibility in the DVChl-*a* cell^{-1} in *Prochlorococcus* leads to a more highly variable carbon-to-DVChl-*a* ratio (θ_{Pro}) observed in this genus than in other phytoplankton groups. θ_{Pro} was shown to be highly correlated with both the NPP index and the spectral slope between 443 and 550 nm, which suggests that both of these indices may serve as useful predictors of θ_{Pro}. In strongly-stratified, oligotrophic waters where the NPP index may be considered a proxy of ambient light levels, the NPP index could account for a significant fraction of the variability in the parameters describing the photosynthesis-irradiance (*PE*) response curve. Using estimates of θ_{Pro} derived from its relationship with the NPP index, the maximum growth rates for surface *Prochlorococcus* populations ($\mu_{m, Pro}$) were calculated from maximum Chl-*a*-specific photosynthetic rates measured at the *Prochlorococcus*-dominated stations, yielding an average $\mu_{m, Pro}$ value of 0.22 d^{-1}, which is consistent with field and culture studies. Thus, the NPP index can be considered a useful proxy of both the photoacclimatory status and photophysiological characteristics of phytoplankton in subtropical marine ecosystems.

Extended Abstract

Marine phytoplankton possess a variety of pigments enabling them to absorb light energy across the visible spectrum. The light harvested by the ocean's microflora provides almost all of the energy for the entire marine trophic system and is responsible for half of the photosynthesis on our planet. Amongst the environmental factors known to affect phytoplankton photosynthesis, light shows the most extreme variation within the aquatic medium. Phytoplankton respond to fluctuating growth irradiances (i.e. photoacclimation) by adjusting the total amount of pigment per cell or the ratio of different pigments, or both.

Using a large *in situ* dataset that covers a wide range of oceanographic domains in the Atlantic Ocean (from the poles to the tropics), the first part of this thesis examines how changes in pigment composition are related to the basin-scale variation in *in vivo* light absorption spectra of phytoplankton ($a_{ph}(\lambda)$) in the surface ocean and the relative importance that shifts in gross community structure and photoacclimatory status play in shaping these patterns. The results clearly show that changes in the relative concentration of non-photosynthetic pigments (NPPs) to total pigments (NPP index) accounted for a significant fraction of the large-scale variability in the chlorophyll *a* (Chl-*a*)-specific absorption coefficient of phytoplankton at 440 nm (a^*_{ph}(440)), whereas there was only a weak correlation between $a^*_{ph}(440)$ and pigment indices of phytoplankton size, although there was an overall tendency for pigment markers associated with larger cells to coincide with lower $a^*_{ph}(440)$ values. The observed relationships between pigment-based indices of phytoplankton biomass (total Chl-*a* concentration, TChl-*a*), photoacclimatory status (NPP index), and size structure are proposed to be largely dictated by the contrasting photophysiological strategies of dominant prokaryotic and eukaryotic primary producers. The relative contribution of NPPs (particularly zeaxanthin) to the total pigment concentration significantly altered the shape of $a_{ph}(\lambda)$, especially in the blue-green part of the spectrum, and there was a strong correlation between the NPP index and the spectral slope of $a_{ph}(\lambda)$. These results highlight the impact of NPPs on phytoplankton light absorption and that the photoacclimatory response of phytoplankton should be considered when using the absorptive characteristics of phytoplankton to derive information on their size and taxonomic composition.

A seasonal component to the variability in the NPP index is clearly demonstrated in the second part of the thesis with a general increase in surface values of the NPP index from the winter-spring phytoplankton communities dominated by low light-acclimated eukaryotic microalgae to the summer and early autumn communities dominated by high light-acclimated picocyanobacteria. Further, given that picocyanobacteria-dominated systems have been found to exhibit strong changes in pigment composition, the photoacclimatory characteristics at the cellular

level of this group of phytoplankton, particularly the genus *Prochlorococcus*, are also examined. *Prochlorococcus* is the most abundant photosynthetic organism on Earth that is distributed throughout the euphotic zone of the vast (sub)tropical ocean. It is the only phytoplankter known to contain divinyl Chl-*a* (DVChl-*a*) as a major photosynthetic pigment (PSP). Through the use of flow cytometry, *Prochlorococcus* can be identified and counted *in situ* and the wild populations can be distinguished from the rest of picophytoplankton community. These unique characteristics allowed examination of changes in the concentrations of PSPs and NPPs in individual *Prochlorococcus* cells. It is clear from these results that the intracellular concentration of DVChl-*a* varied markedly in response to variation in the relative availability of light with depth, whilst the intracellular concentration of the NPP zeaxanthin was relatively uniform with depth. The depth-dependent increase in the cellular content of DVChl-*a* was shown to correspond to the cellular photoacclimation of each ecotype to low light and a shift from high light-adapted to low light-adapted ecotypes that inherently display higher DVChl-*a* cell^{-1}. The ability of *Prochlorococcus* to significantly adjust the DVChl-*a* cell^{-1} over vertical gradients of available light was reflected by the observed wide range of estimates of the carbon-to-DVChl-*a* ratio (θ_{Pro}) computed from flow cytometry counts, pigment data, and published conversion factors. Understanding these fundamental sources of variability in pigmentation of picocyanobacteria is critical if their pigment concentrations and optical properties are to be used in studies on their abundance, distribution, and diversity, both *in situ* and by remote sensing. The unique ability to examine how *Prochlorococcus* adjusts its pigment content allows assessment of the physiological plasticity of this globally-significant group of phytoplankton and will aid us in understanding how the long-term effect of global warming and its anticipated impact on upper ocean stratification may affect this picocyanobacterium that dominates a large fraction of the global ocean.

From a photophysiological point of view, variability in the NPP index indicates a variable proportion of light energy absorbed by PSPs that is directly used for photochemistry compared to that which is lost through thermal dissipation by NPPs. Therefore, photoacclimation by means of changes in the NPP index is likely to affect the photosynthetic properties of marine phytoplankton and the depth distribution of solar heating. Using a global dataset of the photosynthesis-irradiance (*PE*) parameters, the third section of this thesis examines vertical variations in the photosynthetic parameters measured across different trophic domains of the open-ocean environments and the extent to which they could be explained by changes in the NPP index. The *PE* parameters show strong depth-dependence for the oligotrophic domain (i.e. surface TChl-*a* < 0.2 mg Chl-*a* m^{-3}): the maximum Chl-*a*-normalised photosynthetic rate or the assimilation number (P_m^B) and the photoadaptation parameter (E_k) decreased with depth, while the

Chl-*a*-normalised initial slope of the *PE* curve (α^B) and the maximum quantum yield of photosynthesis (ϕ_m) increased. In contrast, there were no discernible vertical patterns of the *PE* parameters at eutrophic stations (> 2 mg Chl-*a* m^{-3}). The depth-dependent variation in the photosynthetic properties was weak for the mesotrophic domain (0.2-2 mg Chl-*a* m^{-3}), although it was significant at mesotrophic stations in the high nutrient-low chlorophyll (HNLC) region of the South Pacific. In the oligotrophic domain, P_m^B and E_k exhibited a strong positive relationship with the NPP index, while α^B and ϕ_m were inversely correlated with the NPP index. Both the NPP index and the spectral slope between 443 and 550 nm were shown to be robust predictors of θ_{Pro} in the oligotrophic region of the (sub)tropical ocean. θ_{Pro} estimated from the observed NPP-θ_{Pro} relationship was used alongside information on P_m^B for *Prochlorococcus*-dominated communities identified using diagnostic pigment criteria to calculate the maximum growth rates for surface *Prochlorococcus* populations ($\mu_{m,\,Pro}$). Estimates of $\mu_{m,\,Pro}$ varied between *ca* 0.1 and 0.8 d^{-1} with a mean value of 0.22 d^{-1}. Developing new strategies of examining the natural variability in *Prochlorococcus* growth rates is fundamental for understanding its contribution to the ocean carbon cycle as well as evaluating mechanisms conferring ecological success to this globally-significant cyanobacterial genus.

Acknowledgement

Finishing a DPhil has been challenging for me, intellectually and mentally, and I cannot imagine how I would have possibly done it without the tremendous help from my supervisor, Dr Heather Bouman. Heather has been supportive, encouraging, and extremely patient throughout my thesis work, especially during the writing stage. She was there during my most trying moments to which I am eternally grateful. I thank Dr Qiong (Joan) Zhang, my thesis co-supervisor, for regular discussions on the results of my data analysis and for comments on my progress report for Confirmation of Status. Also, I would like to extend my sincere appreciation and thanks to my thesis examiners, Dr Stuart Robinson and Dr Bob Brewin for participating in my *viva voce*, especially during this unprecedented time of global public health crises.

I also had the privilege of working with various oceanographic datasets generously provided by Bedford Institute of Oceanography, the British Oceanographic Data Centre, the French Research Institute for Exploitation of the Sea, the Japan Agency for Marine-Earth Science and Technology, the NASA Ocean Biology Processing Group, and the Scottish Association for Marine Science. The International Ocean-Colour Coordinating Group (IOCCG) and the Natural Environment Research Council (NERC) are acknowledged for awarding me travel funds to attend their training courses at the Laboratoire d'Océanographie de Villefranche (2018) and Plymouth Marine Laboratory (2017), respectively. I would also like to thank the Burdetts-Coutts Fund and St Cross College for the financial support for my participation in the Ocean Sciences Meeting 2020 in San Diego, USA to present my thesis work. Thanks also to the Department of Earth Sciences and my College for ideal learning environment and the facilities they have provided.

I would particularly like to take this opportunity to thank the following people whose meaningful conversations and emotional support throughout these challenging years in Oxford rebuilt my lost confidence when I had almost given up: Paramin Sangwongngam and his fiancée, Jane; Atcharawan (Nok) Kotsarn; Montita (Nina) Wijitgoon; and Priscilla Lange. Also heartfelt thanks to my dear friends at Bangkok House for their unwavering support.

I thank my parents and my brother for their unconditional love and support in all the good and bad times. They mean the world to me, and they are truly the reason behind my successes and the inspiration behind my endeavours.

My studentship (since undergraduate level) has been fully funded by the Ministry of Education, Royal Thai Government through the Development and Promotion of Science and Technology Talents (DPST) Project. Thank you for appreciating my research and for believing in the value of the science of oceanography and its potential contribution to the development of our country.

Table of Contents

Declaration …… 2
Abstract …… 3
Extended Abstract …… 4
Acknowledgement …… 7
Table of Contents …….. 9
List of Figures ……... 12
List of Tables …… 15
List of Abbreviations …… 16

Chapter 1 : General Introduction ……..... 19

1.1 Marine Phytoplankton …… 19
1.1.1 Microphytoplankton …….. 20
1.1.2 Nanophytoplankton ……... 21
1.1.3 Picophytoplankton ……. 22
(a) Picocyanobacteria …….. 22
(b) Photosynthetic picoeukaryotes …….. 29

1.2 Methods Used to Identify of Phytoplankton Taxa and Size Classes …... 30
1.2.1 Pigment biomarkers ……... 31
1.2.2 Flow cytometry ……..... 33

1.3 Phytoplankton Optical Properties …… 37
1.3.1 Inherent optical properties ……. 37
1.3.2 Variability in phytoplankton light absorption ……... 39
(a) Pigment composition ……. 39
(b) Pigment packaging …… 40

1.4 Phytoplankton Photosynthesis ……. 43
1.4.1 Photosynthetic apparatus ……... 43
1.4.2 Photosystems and photosynthetic unit …….. 47
1.4.3 The photosynthesis-irradiance (*PE*) curve …… 52

1.5 Presentation of Thesis ……. 54

Chapter 2 : Variation in Pigment Composition and Bio-optical Properties of Phytoplankton in the Atlantic Basin …… 56

2.1 Introduction ……. 56

2.2 Materials and Methods …… 60
2.2.1 Dataset ……... 60
2.2.2 Phytoplankton pigment composition ……. 60
2.2.3 Pigment-based determination of phytoplankton size structure 63
2.2.4 Phytoplankton light absorption ……. 64

2.2.5 Data quality assurance ……... 66
2.2.6 Estimation of light absorption by non-photosynthetic Pigments (NPPs) ……... 67

2.3 Results ……. 68
2.3.1 Variation in the chlorophyll *a*-specific absorption coefficient of phytoplankton ……... 68
2.3.2 Variation in cell size and photoacclimatory status of phytoplankton ……. 69
2.3.3 Effect of NPPs on phytoplankton absorption …… 74
2.3.4 The role of *Prochlorococcus* in governing the relationship between NPPs and phytoplankton absorption ……..... 79

2.4 Discussion ……... 81
2.4.1 Variation in phytoplankton absorption …….. 81
2.4.2 Relationship between trophic status, community structure, and photoacclimation ……... 83
2.4.3 Domain-specific changes in photophysiology and their relevance to pigment composition and light absorption …….. 85
2.4.4 Effects of NPPs on phytoplankton absorption …….. 93

2.5 Concluding Remarks ……... 97

Chapter 3 : Photoacclimatory Characteristics of Marine Picocyanobacteria ……. 99

3.1 Introduction ……. 99

3.2 Materials and Methods …… 103
3.2.1 Data ……... 103
(1) Phytoplankton pigment analysis …… 103
(2) Estimation of picocyanobacteria abundance ……. 109
3.2.2 Computation of mixed-layer and euphotic depths …… 110

3.3 Results and Discussion …… 112
3.3.1 Vertical and spatio-temporal distributions of NPPs …….. 112
3.3.2 Photoacclimatory characteristics of picocyanobacteria …… 122
3.3.3 Carbon-to-chlorophyll *a* ratios …….. 134
(1) Estimation of the carbon-to-divinyl chlorophyll *a* ratio of *Prochlorococcus* (θ_{Pro}) …….. 135
(2) Constraining the variability in the estimated θ_{Pro} …….. 137
(3) Comparison with eukaryotic phytoplankton ……. 139

3.4 Concluding Remarks ……... 142

Chapter 4 : Relationship between Pigment Composition and Photophysiology of Marine Phytoplankton …….. 144

4.1 Introduction ……. 144

4.2 Materials and Methods …… 148
4.2.1 Datasets ……. 148
4.2.2 Phytoplankton pigment composition ……. 150
4.2.3 *Prochlorococcus* abundance ……. 151
4.2.4 Phytoplankton light absorption ……. 151
4.2.5 Photosynthesis-irradiance (*PE*) parameters …….. 152

4.3 Results 155
4.3.1 Distribution of the photosynthetic parameters …….. 155
4.3.2 Relationship between the photosynthetic parameters and NPPs 162
4.3.3 Relationship between θ_{Pro} and the NPP index ……... 165
4.3.4 Relationship between θ_{Pro} and the spectral slope of total phytoplankton absorption …… 170
4.3.5 Estimation of the maximum growth rates of *Prochlorococcus* 172

4.4 Discussion 175
4.4.1 Vertical structure of the photosynthetic parameters …….. 175
4.4.2 Relationships between the NPP index and the photosynthetic parameters in the oligotrophic domain …….. 179
4.4.3 Relationship between θ_{Pro} and the NPP index ……... 183
4.4.4 *Prochlorococcus* growth rates ……... 188

4.5 Concluding Remarks ……... 192

Chapter 5 : Summary and Future Work …… 195

5.1 Summary ……. 195
5.2 Future work ……. 199

References …… 202
Appendix …….. 233
List of the original sources of oceanographic data included in this thesis ….. 234

List of Figures

Chapter 1

Figure 1.1 Electron (TEM and SEM) micrographs of picocyanobacteria and diverse picoeukaryotes 23

Figure 1.2 Vertical profiles of (a) carbon biomass of *Prochlorococcus*, *Synechococcus*, and photosynthetic picoeukaryotes and (b) cell abundances of *Prochlorococcus* ecotypes MED4 and SS120 27

Figure 1.3 Schematic of HPLC analysis approach for characterising phytoplankton community structure on the basis of pigment composition 32

Figure 1.4 Schematic representation of a flow cytometer 34

Figure 1.5 Example cytograms obtained from a sample collected in oligotrophic surface waters of the Pacific Ocean containing *Prochlorococcus*, *Synechococcus*, and photosynthetic picoeukaryotes 36

Figure 1.6 Total absorption spectrum of an idealized, productive oceanic water, together with spectra of the individual absorbing component 39

Figure 1.7 Weight-specific absorption spectra of different pigment groups measured in solution 40

Figure 1.8 Absorption spectra of a *Chlorella* (green alga) suspension and a quantitative methanol extract 41

Figure 1.9 Schematic representation of an increase in pigment packaging caused by an increase in either (a) cell diameter or (b) the intracellular pigment concentration 42

Figure 1.10 (a) Illustration of a chloroplast of typical eukaryotic cells and (b-e) transmission electron micrographs of the thylakoids of (b) higher plants, (c) the green alga *Dunaliella tertiolecta*, (d) *Synechococcus* PCC7942, and (e) *Prochlorococcus* MIT9313 45

Figure 1.11 The architecture of the photosynthetic apparatus of (a) *Synechococcus* spp. and (b) *Prochlorococcus* spp. 46

Figure 1.12 Diagrammatic representation of (a) the basic structure and function of a photosystem, and (b) the distribution of pigments among the pigment-protein complexes of the photosystems including the light-harvesting complexes, peripheral complexes, and the reaction-centre complexes 49

Figure 1.13 Relationship between the mean daily photosynthetically available radiation (PAR) and the NPP index for the upper mixed layer at three sampling sites in the subtropical North Atlantic visited using the French EUMELI cruise 51

Figure 1.14 The photosynthesis-light curve fitted to data obtained from an idealised *PE* experiment 53

Chapter 2

Figure 2.1 Map of sampling stations …… 61

Figure 2.2 Chlorophyll *a*-specific absorption coefficients of phytoplankton at 440 nm ($a^*_{ph}(440)$) plotted against the total chlorophyll *a* concentration (TChl-*a*) ……..... 68

Figure 2.3 (a) The average cell diameter of phytoplankton populations calculated using the pigment-based method of Bricaud *et al*. (2004) and (b) the NPP index plotted against TChl-*a*. (c) The NPP index plotted against pigment-based estimates of the average cell diameter ……... 70

Figure 2.4 Estimates of percent absorption by non-photosynthetic pigments (NPP) at 440 nm plotted against TChl-*a* …… 72

Figure 2.5 The weight-to-weight ratio of (a) zeaxanthin and (b) the sum of diadinoxanthin and diatoxanthin to total pigment concentration plotted against TChl-*a* …… 73

Figure 2.6 $a^*_{ph}(440)$ plotted against the NPP index …….. 75

Figure 2.7 $a^*_{ph}(440)$ plotted against the NPP index for sampling sites located within (a) the South Atlantic Gyral Province (Trades) and (b) the South Subtropical Convergence Province (Westerlies Biome) …….. 76

Figure 2.8 Average phytoplankton absorption spectra ($a_{ph}(\lambda)$) at various intervals of TChl-*a*: (a) oligotrophic (TChl-*a* < 0.2 mg Chl-*a* m^{-3}), (b) mesotrophic (0.2 ≤ TChl-*a* ≤ 2.0), and (c) eutrophic condition (TChl-*a* > 0.2) ……. 77

Figure 2.9 The spectral slopes of phytoplankton absorption in the blue-green region of the spectrum from 443 nm to 510 nm normalised to 676 nm ($S_{443\text{-}510}$) plotted against the NPP index …… 79

Figure 2.10 The weight-to-weight ratio of zeaxanthin to total pigment concentration plotted against the weight-to-weight ratio of divinyl chlorophyll *a* to TChl-*a* …… 80

Chapter 3

Figure 3.1 Map of sampling stations …… 106

Figure 3.2 The NPP index plotted as a function of the depth of sampling divided by the depth of the euphotic zone (z/z_e) as an index of the underwater light availability for each oceanographic dataset: (a) BIOSOPE, (b) AMT, (c) DCM, (d) HOT, and (e-h) BATS ……. 113

Figure 3.3 Frequency distributions of the percent contribution (a) zeaxanthin and (b) diadinoxanthin + diatoxanthin to the total concentration of non-photosynthetic carotenoids, and the percent contribution of (c) fucoxanthin, (d) 19'-butanoyloxyfucoxanthin, and (e) 19'-hexanoyloxyfucoxanthin to the total concentration of photosynthetic carotenoids, and (f) the estimated nitracline depth for different trophic domains encountered during the BIOSOPE transect …….. 114

Figure 3.4 Frequency distributions of the percent contribution (a) zeaxanthin and (b) diadinoxanthin + diatoxanthin to the total concentration of non-photosynthetic carotenoids, and the percent contribution of (c) fucoxanthin, (d) 19'-butanoyloxyfucoxanthin, and (e) 19'-hexanoyl-oxyfucoxanthin to the total concentration of photosynthetic carote-noids measured over an annual cycle in surface water ($z/z_e \leq 0.1$) of BATS stations ……. 121

Figure 3.5 The intracellular concentration of zeaxanthin for picocyanobacteria plotted as a function of the ratio z/z_e ……... 124

Figure 3.6 The intracellular concentration of divinyl chlorophyll *a* for *Pro-chlorococcus* plotted as a function of the ratio z/z_e …… 124

Figure 3.7 Relationship between cell abundance of picocyanobacteria and the concentration of zeaxanthin …… 125

Figure 3.8 (a) Relationship between *Prochlorococcus* cell abundance and the concentration of divinyl chlorophyll *a*. (b) As in Figure 3.8a with symbols coloured according to the weight-to-weight ratio of divinyl chlorophyll *b* to divinyl chlorophyll *a* (B/A ratio) ……..... 127

Figure 3.9 The cell carbon biomass of *Prochlorococcus* plotted against the con-centration of divinyl chlorophyll *a* …….. 136

Chapter 4

Figure 4.1 Map of sampling stations …… 149

Figure 4.2 Density plots showing the vertical variation in the maximum chloro-phyll *a*-normalised photosynthetic rate (P_m^B) for eutrophic, meso-trophic, and oligotrophic domains ……... 157

Figure 4.3 As Figure 4.2 for the chlorophyll *a*-normalised initial slope (α^B) ….. 158

Figure 4.4 As Figure 4.2 for the photoadaptation parameter (E_k) …… 159

Figure 4.5 As Figure 4.2 for the maximum quantum yield of photosynthesis (ϕ_m) ……. 161

Figure 4.6 The photosynthetic parameters plotted against the NPP index for the oligotrophic domain …… 163

Figure 4.7 The carbon-to-divinyl chlorophyll *a* ratio for *Prochlorococcus* (θ_{Pro}) plotted against the NPP index measured in the oligotrophic domain for (a) the BIOSOPE, DCM, and EUMELI cruises and (b) the AMT cruises (no. 3, 4, 13-15) …….. 168

Figure 4.8 Hawaii Ocean Time-series (HOT) observations of (a) sea surface temperature and (b) the NPP index, both of which collected between 1988 and 2014, and (c) θ_{Pro} collected between 1994 and 1995 …….. 169

Figure 4.9 θ_{Pro} plotted as a function of the 676 nm-normalised spectral slope of phytoplankton absorption coefficient between 443 nm and 550 nm ($S_{443\text{-}550}$) ……... 171

Figure 4.10 Frequency distributions of estimates of θ_{Pro} from the NPP index for all pigment samples taken on the AMT, BIOSOPE, DCM, and EUMELI cruises ……. 173

Figure 4.11 Frequency distributions of estimates of the maximum growth rates of *Prochlorococcus* populations in the ocean surface …….. 175

List of Tables

Chapter 1

Table 1.1 Comparative characteristics of the picocyanobacterial genera *Prochlorococcus* and *Synechococcus* ……... 24

Table 1.2 Common phytoplankton pigment markers and their associated size classes ……. 33

Chapter 2

Table 2.1 List of oceanographic cruises included in Chapter 2 analysis …… 62

Table 2.2 Summary of the filtration volume, organic solvent, and reference for each method used for HPLC pigment analysis for each oceanographic campaign ……. 63

Table 2.3 Summary of the filtration volume, equipment, and β-correction algorithms used to measure phytoplankton absorption for each oceanographic campaign …… 66

Chapter 3

Table 3.1 List of oceanographic cruises included in Chapter 3 analysis …… 104

Table 3.2 Summary of the filtration volume, organic solvent, and reference for each method used for HPLC pigment analysis for each oceanographic campaign ……. 107

Table 3.3 List of HPLC-detected pigments during each oceanographic campaign ……... 108

Table 3.4 Published estimates of carbon-to-(DV)Chl-*a* ratio for *Prochlorococcus* and photosynthetic picoeukaryotes …….. 139

Chapter 4

Table 4.1 List of oceanographic cruises included in Chapter 4 analysis …… 150

Table 4.2 Summary of the light sources and incubation conditions for photosynthesis-irradiance (*PE*) experiments and the non-linear model used to fit the experimental data to obtain *PE* parameters for each oceanographic campaign …… 154

List of Abbreviations

1. Pigments and pigment-related variables

Abbreviation	Description [Unit]
HPLC	High Performance Liquid Chromatography
PSP	Photosynthetic pigments [mg m^{-3}]
TChl-*a*	Total chlorophyll *a* (monovinyl + divinyl) [mg Chl-*a* m^{-3}]
DVChl-*a*	Divinyl chlorophyll *a* [mg DVChl-*a* m^{-3}]
TChl-*b*	Total chlorophyll *b* (monovinyl + divinyl) [mg m^{-3}]
DVChl-*b*	Divinyl chlorophyll *b* [mg m^{-3}]
B/A ratio	Relative concentration of DVChl-*b* to DVChl-*a* in *Prochlorococcus* [dimensionless]
Chl-$c_{1,2}$	Chlorophyll $c_{1,2}$ [mg m^{-3}]
Chl-c_3	Chlorophyll c_3 [mg m^{-3}]
FUCO	Fucoxanthin [mg m^{-3}]
19'-BUT	19'-Butanoyloxyfucoxanthin [mg m^{-3}]
19'-HEX	19'-Hexanoyloxyfucoxanthin [mg m^{-3}]
PERID	Peridinin [mg m^{-3}]
PRAS	Prasinoxanthin [mg m^{-3}]
NPP	Non-photosynthetic or photoprotective pigments [mg m^{-3}]
NPP index	Relative concentration of non-photosynthetic pigments to total pigments [dimensionless]
ALLO	Alloxanthin [mg m^{-3}]
CARO	Carotene (α-CARO + β-CARO) [mg m^{-3}]
DIAD	Diadinoxanthin [mg m^{-3}]
DIAT	Diatoxanthin [mg m^{-3}]
LUT	Lutein [mg m^{-3}]
NEOX	Neoxanthin [mg m^{-3}]
VIOL	Violaxanthin [mg m^{-3}]
ZEA	Zeaxanthin [mg m^{-3}]
SI	Size index [μm]
S_μ	Percent contribution of microphytoplankton to TCh-*a* biomass
S_n	Percent contribution of nanophytoplankton to TChl-*a* biomass
S_p	Percent contribution of picophytoplankton to TChl-*a* biomass

2. Photophysiological properties and growth

Abbreviation	Description [Unit]
PSI	Photosystem I
PSII	Photosystem II
σ_{PSII}	Functional absorption cross section of PS II [m^2 (mol photons)$^{-1}$]
PE parameters	Photosynthesis-irradiance parameters
α^B	Chlorophyll *a*-normalised initial slope of the *PE* curve [mg C (mg Chl-*a*)$^{-1}$ h^{-1} (μmol photons m^{-2} s^{-1})$^{-1}$]
E	Irradiance [μmol photons m^{-2} s^{-1}]
E_k	Photoadaptation parameter calculated as the ratio of P_m^B to α^B [μmol photons m^{-2} s^{-1}]
P_m^B	The maximum chlorophyll *a*-normalised photosynthetic rate or the assimilation number [mg C (mg Chl-*a*)$^{-1}$ h^{-1}]
$P_{m,\,\mathrm{Pro}}^B$	P_m^B for *Prochlorococcus* [mg C (mg DVChl-*a*)$^{-1}$ h^{-1}]
$P_{m,\,\mathrm{Pro}}^{\mathrm{cell}}$	The maximum cell-specific photosynthetic rate for *Prochlorococcus* [fg C cell^{-1} h^{-1}]
ϕ_m	The maximum quantum yield of photosynthesis [mol C (mol photons)$^{-1}$]
θ	Carbon-to-chlorophyll *a* ratio [g C (g Chl-*a*)$^{-1}$)]
θ_{Pro}	Carbon-to-divinyl chlorophyll *a* ratio for *Prochlorococcus* [g C (g DVChl-*a*)$^{-1}$)]
μ_m	Maximum growth rates of phytoplankton [d^{-1}]
$\mu_{m,\,\mathrm{Pro}}$	Maximum growth rates of *Prochlorococcus* [d^{-1}]

3. Optical properties and measurements

Abbreviation	Description [Unit]
$a(\lambda)$	Absorption coefficient at wavelength λ [m^{-1}]
$A(\lambda)$	Absorptance at wavelength λ [dimensionless]
$a_c(\lambda)$	Absorption coefficient of coloured dissolved organic matter (CDOM) at wavelength λ [m^{-1}]
$a_d(\lambda)$	Absorption coefficient of extracted detrital materials at wavelength λ [m^{-1}]
$a_{ph}(\lambda)$	Absorption coefficient of phytoplankton at wavelength λ [m^{-1}]
$a_p(\lambda)$	Absorption coefficient of total particulates retained on the sample filter at wavelength λ [m^{-1}]
$a_n(\lambda)$	Absorption coefficient of non-algal particulate materials at wavelength λ [m^{-1}]
$a_{NPP}(\lambda)$	Absorption coefficient of non-photosynthetic pigments at wavelength λ [m^{-1}]
$a_T(\lambda)$	Total absorption coefficient of seawater at wavelength λ [m^{-1}]

3. Optical properties and measurements (continued)

Abbreviation	Description [Unit]
$a_w(\lambda)$	Absorption coefficient of pure water at wavelength λ [m^{-1}]
$a^*_{ph}(\lambda)$	Chlorophyll *a*-specific absorption coefficient of phytoplankton at wavelength λ [m^2 (mg Chl-*a*)$^{-1}$]
$\overline{a}^*_{ph}$	Spectrally averaged chlorophyll *a*-specific absorption coefficient of phytoplankton [m^2 (mg Chl-*a*)$^{-1}$]
$a^*_{sol}(\lambda)$	Weight-specific absorption coefficients of individual pigments dispersed in solution at wavelength λ [m^2 mg^{-1}]
$D(\lambda)$	Absorbance at wavelength λ [dimensionless]
I_s	Geometric pathlength [m]
$O_d(\lambda)$	Optical density of extracted detrital material at wavelength λ [dimensionless]
$O_p(\lambda)$	Optical density of total particulates retained on the sample filter at wavelength λ [dimensionless]
K_d(PAR)	Vertical attenuation coefficient for PAR [m^{-1}]
$K_d(\lambda)$	Vertical attenuation coefficient at wavelength λ [m^{-1}]
$K_w(\lambda)$	Vertical attenuation coefficient for pure water at wavelength λ [m^{-1}]
PAR	Photosynthetically available radiation (400-700 nm)
S	Clearance area of the sample filter [mm^2]
$S_{\lambda_1-\lambda_2}$	Spectral slope of $a_{ph}(\lambda)$ between λ_1 and λ_2 normalised to 676 nm [nm^{-1}]
V	Volume of seawater filtered [m^3]
z_e	Euphotic depth [m]
β	Optical pathlength amplification factor [dimensionless]
ζ	Optical depth obtain by multiplying K_d(PAR) by depth [dimensionless]
Φ_0	Radiant flux incident on the medium [Energy or quanta per unit time]
Φ_a	Absorbed radiant flux [Energy or quanta per unit time]
Φ_s	Scattered radiant flux [Energy or quanta per unit time]
Φ_t	Transmitted radiant flux [Energy or quanta per unit time]

4. Physical properties of the water column

Abbreviation	Description [Unit]
z	Depth [m]
z_m	Mixed-layer depth [m]
σ_θ	Potential density of seawater [kg m^{-3}]

Chapter 1

General Introduction

This chapter provides background and context for the work presented. It is divided into four sections. The first section describes the general characteristics and the ecological and biogeochemical significances of marine phytoplankton of different size classes. A particular emphasis is placed on the smallest size class, the picophytoplankton, which is the focus of the second and third research chapters. The second section provides an overview of the various techniques used to assess the oceanographic distribution of phytoplankton size classes. The third section introduces the concept of the inherent optical properties of marine phytoplankton and how they can be quantified. It also briefly explains the factors known to modify the light absorptive characteristics of phytoplankton including pigment composition and pigment packaging. The final section summarises the process of algal photosynthesis, including the cellular structures involved in the harvesting of light, and the mathematical representation of the photosynthetic response of phytoplankton to the forcing irradiance described by the light saturation or photosynthesis-irradiance (*PE*) curve.

1.1 Marine Phytoplankton

Marine phytoplankton are a diverse group of unicellular photoautotrophic organisms, including both microalgae and cyanobacteria, which play central roles in ocean ecosystems and global biogeochemical cycles. They are responsible for the production of approximately 50 billion metric tonnes of organic carbon per annum through photosynthesis, accounting for nearly half of the total primary production on Earth (Falkowski, 1994; Field *et al.*, 1998). The fixed organic carbon is generally transferred to consumers at higher trophic levels through grazing and ultimately to the entire food web. Roughly a third of organic carbon produced by phytoplankton

is exported from the surface ocean to the deep ocean and sediment (Falkowski *et al.*, 1998), either through vertical mixing or the sinking of particles. This so-called biological carbon pump not only sustains marine benthic communities, but also influences the ocean-atmosphere carbon exchange and the way the ocean regulates the atmospheric concentrations of carbon dioxide (Volk and Hoffert, 1985; Moore *et al.*, 2013). Also, the absorption of solar irradiance by phytoplankton can contribute significantly to the heating of the surface ocean and, therefore, influence the heat exchange between ocean and atmosphere and the global radiation budget (Sathyendranath *et al.*, 1991; Frouin and Iacobellis, 2002; Park *et al.*, 2015). These integral roles of phytoplankton in modulating the Earth's climate and the cycling of carbon and other elements between the atmosphere, hydrosphere, and geosphere underscore their significance as a fundamental component of the Earth system. Hence, an understanding of the dynamics of marine phytoplankton and photosynthesis and the processes by which they are governed is a key aspect to understanding and predicting future effects of global climate change (Falkowski *et al.*, 2000; Jonkers *et al.*, 2019).

Phytoplankton are diverse not only taxonomically, but also functionally in terms of both their ecological and biogeochemical roles, and such differences are attributable in part to their size (Finkel *et al.*, 2010; Acevedo-Trejos *et al.*, 2015). For example, cell size influences sinking rates, and thus the export of production by phytoplankton. Due to the relevance of cell size to various metabolic and biogeochemical processes (Chisholm, 1992; Nair *et al.*, 2008; Marañón, 2015), it is one of the fundamental traits that have been used widely in biogeochemical and ecological modelling of the ocean (Acevedo-Trejos *et al.*, 2015 and references therein). Phytoplankton sizes are typically classified into the micro-, nano-, and picophytoplankton classes with size ranges of 20-200 μm, 2-20 μm, and < 2 μm, respectively (Sieburth *et al.*, 1978; Finkel *et al.*, 2010). Representative members of each size class are briefly described below.

1.1.1 Microphytoplankton

The two major groups of phytoplankton belonging to the microphytoplankton size class include diatoms and dinoflagellates, both of which are ubiquitously distributed throughout the world's oceans (Taylor *et al.*, 2008; Agustí *et al.*, 2015). Due to the ability to rapidly grow and reproduce, diatoms frequently dominate phytoplankton communities during bloom conditions and may contribute up to half of the marine primary production during bloom events (Le Quéré *et al.*, 2005). They are also considered to be the most significant marine silicifying organisms (Nair *et al.*, 2008; Agustí *et al.*, 2015), and are important contributors to global export production to the deep ocean (Williams and Follows, 2011). Unlike diatoms that are exclusively photoautotrophic (Barton *et al.*, 2013), dinoflagellates comprise both photoautotrophic and heterotrophic species in relatively equal proportions (Taylor *et al.*, 2008). Some dinoflagellates can both manufacture their own food through photosynthesis and prey on other microorganisms using their flagella, and are described to undergo a 'mixotrophic' mode of living, which helps to supplement their nutrition particularly in light- or nutrient-limited environments (Hammer and Pitchford, 2005). Dinoflagellates usually dominate the phytoplankton community in the summer to fall months following diatom blooms (Kremp *et al.*, 2008). Some dinoflagellates produce various kinds of natural toxins that may lead to large-scale mortality of fish and shellfish and have adverse effects on public health. Intense dinoflagellate blooms have been monitored through the use of *in situ* optical measurements and remotely-sensed imagery (IOCCG, 2014) as they visibly colour the surface waters through the formation of red tides.

1.1.2 Nanophytoplankton

The nanophytoplankton size class comprises various groups of haptophytes (including the coccolithophores) and cryptophytes (Jeffrey *et al.*, 2011). Coccolithophores, including the well-known *Emiliania huxleyi*, are characterised by their unique ability to produce the exoskeleton

consisting of small calcite plates called coccoliths. In temperate and subpolar regions, this nanophytoplanker occasionally forms intensive blooms (Taylor *et al.*, 2016), which can turn the surface ocean milky-turquoise in colour (as a result of light scattering by the coccoliths) visible from space (IOCCG, 2014). Coccolithophores are key players in the ocean's carbon (organic and inorganic) and sulphur cycles. As major marine calcifiers, they utilise dissolved bicarbonate ions in the surface waters to construct their coccoliths and account for up to half of the global pelagic calcite production (Balch *et al.*, 2007). During coccolith formation, carbon dioxide is also released to the surface ocean and the atmosphere. After the death of these organisms, their coccoliths can dissolve in the water column or be deposited as sediments on the seafloor. Certain species of coccolithophores and haptophytes, in particular *Phaeocystis* spp. (Shen *et al.*, 2011), as well as some dinoflagellates (microphytoplankton) (Turner *et al.*, 1988) can also produce an organic compound called dimethylsulfoniopropionate (DMSP) which undergoes bacteria-mediated transformations into a dimethylsulfide (DMS) gas (Yoch, 2002). When released to the atmosphere, this gas has the potential to induce the formation of clouds (Charlson *et al.*, 1987; Yoch, 2002).

1.1.3 Picophytoplankton

Phytoplankton in the pico-sized fraction are composed of prokaryotic picocyanobacteria and eukaryotic microalgae, which are commonly referred to by microbial ecologists as photosynthetic picoeukaryotes. Each group is described below.

(1) Picocyanobacteria

The two cyanobacterial genera which typically dominate the tropical and temperate oceans are *Prochlorococcus* and *Synechococcus* (Figure 1.1). *Prochlorococcus* was discovered in the mid-1980s with the aid of shipboard flow cytometers (Chisholm *et al.*, 1988) and, with average cell

diameter of *ca* 0.5-0.95 μm (Smyth *et al.*, 2019), have been described as the smallest known photoautotrophic microorganism (Partensky, Hess, *et al.*, 1999). Both *Prochlorococcus* and its sister genus *Synechococcus* have been intensively studied, and their significance to total phytoplankton biomass and primary production in the oligotrophic open ocean is widely known (Li *et al.*, 1992; Partensky, Blanchot, *et al.*, 1999; Lange *et al.*, 2018). Our current comparative understanding of some aspects of the biology, physiology, and ecology of these two marine cyanobacteria is summarised in Table 1.1.

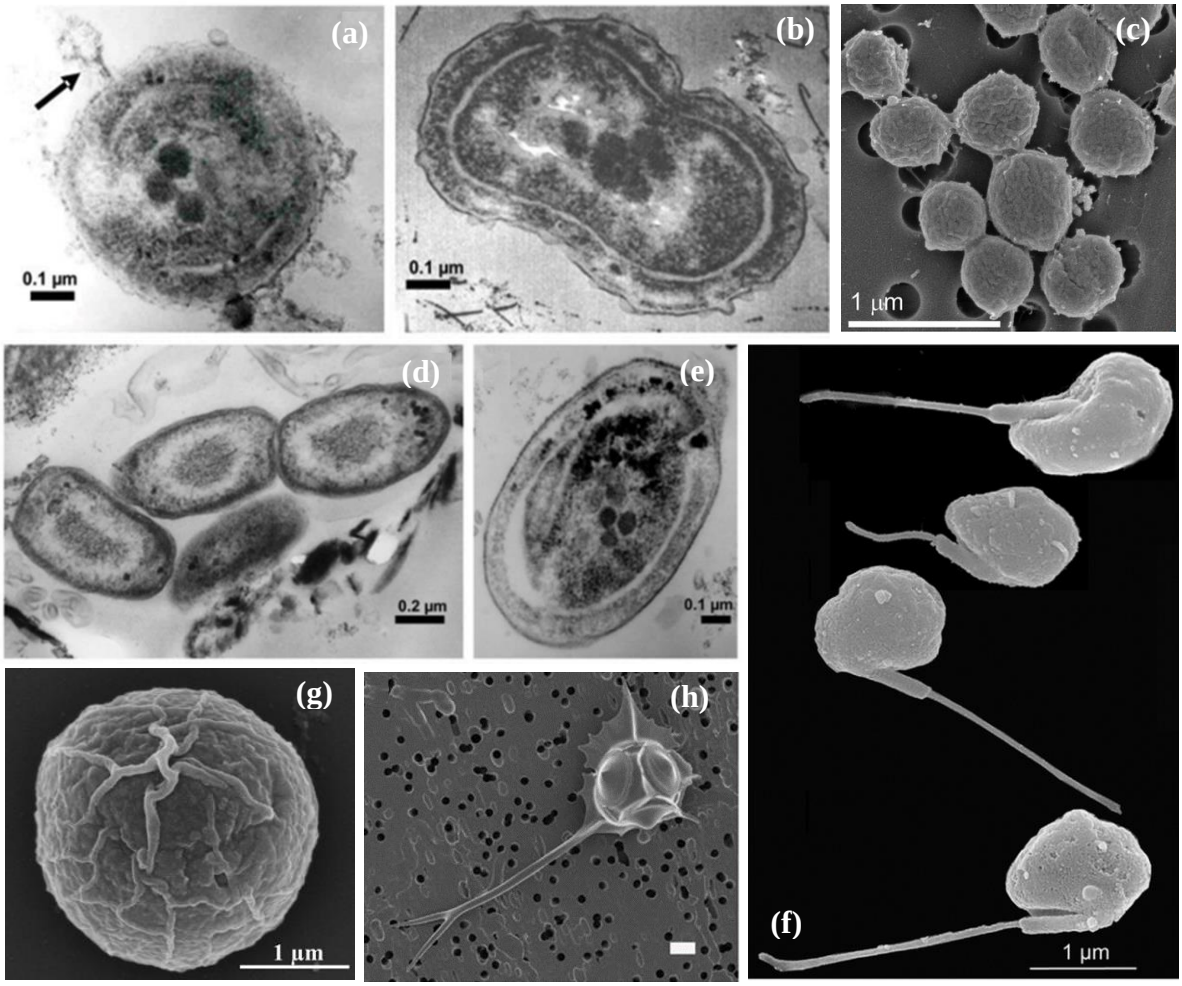


Figure 1.1: Electron (TEM and SEM) micrographs of picocyanobacteria and diverse picoeukaryotes: (a-c) *Prochlorococcus* (with one virus attached, arrow), (d, e) *Synechococcus*, (g, h) *Micromonas* spp. and (i) *Triparma laevis*. From (a, b, d, e) Aquino-Cruz *et al.* (2013), (c) Johnson and Lin (2009), (f) Simon *et al.* (2017), (g) Vaulot *et al.* (2008) and (h) Ichinomiya *et al.* (2016).

Table 1.1: Comparative characteristics of the picocyanobacterial genera *Prochlorococcus* and *Synechococcus*.

	Prochlorococcus	***Synechococcus***
Geographic distribution	Generally restricted to warm, nutrient-limited regions of the (sub)tropical oceans covering a latitudinal range of around 40˚S to 40˚N [1].	Ubiquitously distributed from the poles to the tropics and is particularly abundant in more productive waters, including coastal regions [1].
Vertical distribution [2] (tropical North Atlantic)	Present throughout the euphotic zone with subsurface abundance/biomass maxima [3,4,5] and can sometimes be found in abundance at depths up to 150-200 m [5] (Figure 1.2).	Often occupies the upper part of the euphotic zone with no clear subsurface maxima [3,4,5] (Figure 1.2).
Cell size and shape	Smaller, more elongated [1] (Figure 1.1), Estimated diameter: 0.5-0.7 μm (in culture [6]) and 0.65-0.95 μm (in the field [7])	Larger, more spherical [1] (Figure 1.1), Estimated diameter: 0.8-1.2 μm (in culture [6]) and 1.5-2.5 μm (in the field [7])
Genome size	Approximately 1.6-2.7 Mbp and 2000-3000 genes (the smallest genome of all oxygenic photoautotrophs) [8]	Larger and more variable genome size (e.g. 2.42 Mbp, 2426 genes in *Synechococcus* WH8102 [9] and 5.07 Mbp, 5093 genes in the PCC7335 isolate [10])
Nitrogen assimilation capacity		
(1) Nitrate	Lacking in most strains due to the absence of the nitrate uptake and reduction genes [11]. Strains reported to be capable of growth on nitrate include PAC1, SB, and MIT0604 [12].	Present in all strains examined to date [9] except isolates MIT S9220 (from the equatorial Pacific) [11] and RS9913, RS9914, and RS9917 (Red Sea) [13]
(2) Nitrite	Present in several strains, particularly the low light-adapted, possessing genes that are homologous to the nitrite utilisation genes in *Synechococcus* [11]	Present in virtually all strains [11,14,15]

Table 1.1 (continued)

	Prochlorococcus	*Synechococcus*
Nitrogen assimilation capacity (continued)		
(3) Reduced nitrogen (e.g. urea and ammonium)	Present in all strains [9,11] as evidenced by the activity of the urease enzyme [16] and the expression of the ammonium transport gene [17]	Most strains can grow on ammonium [11,15], and some strains (e.g. MIT S9220 [11], WH8103 [11], and WH7805 [18]) have also been reported to be able to utilise urea.
Pigment composition		
(1) Chlorophyll *a*	Divinyl chlorophyll *a* [19,20,21]	Monovinyl (normal) chlorophyll *a* [20,22]
(2) Chlorophyll *b*	Divinyl chlorophyll *b*. There are some strains (e.g. MIT9302, MIT9312, and SS120) also known to synthesise monovinyl chlorophyll *b*, especially when grown at high light [20,21].	Not present [20,22]
(3) Chlorophyll *c*	The presence of the HPLC-detected 'chlorophyll *c*-like' pigment (with an elution time identical to that of chlorophyll c_1 [19]) has been reported in several strains (e.g. MED4 and NATL1) [21].	Not present [20,22]
(4) α-carotene	Present [19,20,21]	Not present [20,22]
(5) β-carotene	Present in a small amount [19,20]	Present [20,22]
(6) Zeaxanthin	Present [19,20,21]	Present [20,22]
(7) Phycobiliproteins	Phycoerythrin (type III)* has been found in some low light-adapted strains (e.g. SS120, PAC1, PAC2, MIT9313, and MIT9303), although it is not certain whether it is integrated into phycobilisomes [1,23].	There are three types of phycobiliproteins: phycocyanin, phycoerythrin I, and phycoerythrin II, integrated into phycobilisomes, which act as the main light-harvesting apparatus [24,25].

Notes to Table 1.1

[1] Partensky, Hess, *et al.* (1999)

[2] Generalising the vertical distribution patterns for *Prochlorococcus* and *Synechococcus* is not always straightforward as they have been observed to vary dramatically on both spatial and seasonal scales as well as with hydrological conditions of the water column (Partensky, Blanchot, *et al.*, 1999; Partensky, Hess, *et al.*, 1999). Here I describe typical vertical profiles of the two picocyanobacteria in the tropical North Atlantic.

[3] Olson *et al.* (1990)

[4] Veldhuis and Kraay (2004)

[5] Hickman *et al.* (2010)

[6] Morel *et al.* (1993) used a Coulter counter to estimate cell sizes of various strains of *Prochlorococcus* and *Synechococcus* cultured at low irradiances.

[7] Smyth *et al.* (2019) determined the size distribution and refractive index of *Prochlorococcus* and *Synechococcus* using an intensive dataset of flow cytometric measurements made over a large latitudinal gradient of the Atlantic Ocean.

[8] Partensky and Garczarek (2010)

[9] Scanlan and West (2002)

[10] Coutinho *et al.* (2016)

[11] Moore *et al.* (2002)

[12] Berube *et al.* (2015)

[13] Fuller *et al.* (2003)

[14] Bird and Wyman (2003)

[15] Maeda *et al.* (2015)

[16] Lindell *et al.* (2002)

[17] Palinska *et al.* (2000)

[18] Collier *et al.* (1999)

[19] Goericke and Repeta (1992)

[20] Moore *et al.* (1995)

[21] Partensky *et al.* (1993)

[22] Six *et al.* (2004)

[23] Hess *et al.* (2001)

[24] Mahmoud *et al.* (2017)

[25] Grébert *et al.* (2018)

* Detailed discussion on different types of cyanobacterial phycoerythrin may be found in a review by Ting *et al.* (2002).

Several strains of *Prochlorococcus* (e.g. MED4, SS120, NATL1A, and MIT9312) and *Synechococcus* (e.g. WH8103, WH8113, and WH8018) (van Mooy *et al.*, 2006) have cell membranes made primarily of sulfolipids (e.g. sulfoquinovosyldiacylglycerol) instead of phospholipids as normally found in eukaryotic phytoplankton and heterotrophic bacteria. This striking

cellular feature results in a significant decrease in phosphorus demand, placing picocyanobacteria at an advantage over the rest of the bacterioplanktonic community in the nutrient-depleted (sub)tropical gyres.

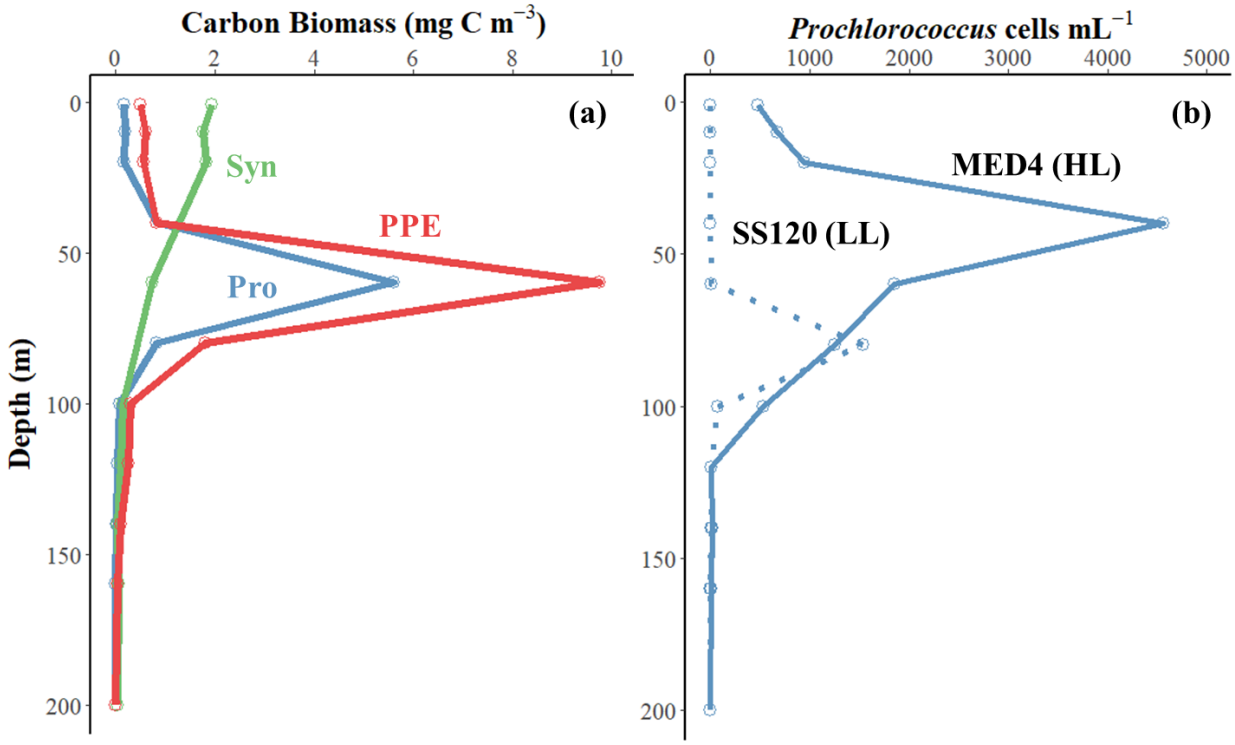


Figure 1.2: Vertical profiles of (a) carbon biomass of *Prochlorococcus* (Pro), *Synechococcus* (Syn), and photosynthetic picoeukaryotes (PPE) and (b) cell abundances of *Prochlorococcus* ecotypes MED4 (high light-adapted, HL, solid line) and SS120 (low light-adapted, LL, dotted line). Plots are generated using data obtained from the Bermuda Atlantic Time-series (BATS; cruise number 175, April 2003). Carbon biomass is converted from cell abundance determined by analytical flow cytometry using conversion factors reported in Buitenhuis *et al.* (2012).

The broad depth distribution of *Prochlorococcus* (Figure 1.2) across light levels spanning up to four orders of magnitude (Moore *et al.*, 1998) can be largely explained by the co-existence of distinct sub-populations, now widely referred to as ecotypes, that are genetically and physiologically adapted to grow at low- and high-light conditions (Moore *et al.*, 1998; Biller *et al.*, 2015). For a more comprehensive review of the historical background and the use of the term

'ecotype', see Coleman and Chisholm (2007). Compared to their high light-adapted (HL) counterparts, low light-adapted (LL) *Prochlorococcus* ecotypes tend to exhibit maximal growth rates at lower light intensities and contain relatively high ratios of divinyl chlorophyll *b* (DVChl-*b*) to divinyl chlorophyll *a* (DVChl-*a*), resulting in higher spectrally-weighted average DVChl-*a*-specific light absorption coefficient and DVChl-*a*-specific photosynthetic rate, especially when grown under low light (Moore *et al.*, 1998; Moore and Chisholm, 1999). These photophysiological characteristics confer a competitive advantage on members of the LL ecotypes to thrive in the light-limited portion of the water column compared to HL strains which tend to be more restricted to the surface layer (Partensky, Hess, *et al.*, 1999) (Figure 1.2b). *Prochlorococcus* are also able to absorb more photons than they scatter owing to their minute size and the increased amount of pigments per cell, which gives these cells a selective advantage to outcompete other phytoplankton taxa at extremely low light intensities that are found towards the bottom of the euphotic zone (Morel *et al.*, 1993; Biller *et al.*, 2015). Molecular studies (e.g. Moore *et al*., 1998; Rocap *et al.*, 2002) have suggested that the physiological discrepancies between HL and LL ecotypes are strongly consistent with the phylogenetic partitioning. HL strains show substantially high similarities in 16S ribosomal RNA (rRNA) (Moore *et al.*, 1998) and 16S-23S ribosomal DNA internal transcribed spencer (ITS) (Rocap *et al.*, 2002) sequences and form a monophyletic group that comprises at least six clades (Biller *et al.*, 2015). Isolates of the LL ecotype, on the other hand, are polyphyletic and can be partitioned based on 16S rRNA and ITS phylogenies into at least six distinct clades (Biller *et al.*, 2015). Whole-genome comparisons (Hess *et al.*, 2001; Rocap *et al.*, 2003) have shown that the *Prochlorococcus* ecotypes differ significantly in genome size and the number of genes involved in light harvesting and photoprotective processes. Differentiation of HL and LL ecotypes is further discussed in Chapter 3.

(2) Photosynthetic picoeukaryotes

Photosynthetic picoeukaryotes (PPE) of typical size ≤ 3 μm comprise a large number of taxa including the classes Prasinophyceae, Cryptophyceae, Prymnesiophyceae, and Pelagophyceae (Vaulot *et al.*, 2008; Kirkham *et al.*, 2011; Massana, 2011). While PPEs and other picophytoplankers in the prokaryotic component have been grouped together into one functional type (Le Quéré *et al.*, 2005), they differ in many aspects. PPEs are normally larger than picocyanobacteria, although the marine PPE *Ostreococcus* can be as small as 0.8-0.9 μm in diameter (Raven, 1984; Vaulot *et al.*, 2008). Also, their cellular structures are more complex: they possess a true nucleus, one mitochondrion, one chloroplast, one Golgi apparatus, and in some species, a flagellum (Massana, 2011). By means of its flagellum, the well-known picoprasinophyte *Micromonas pusilla* (Butcher, 1952) is capable of movement and has been reported to vertically migrate over a diel cycle, potentially to access light and nutrient resources (Corhlan and Harrison, 1991; Halsey *et al.*, 2014). Many flagellated PPEs, such as *Ollicolla vangoorii* (Chrysophyceae; Vaulot *et al.*, 2008), *Micromonas* CCMP2099 (Prasinophyceae; McKie-Krisberg and Sanders, 2014), and certain marine *Chrysochromulina* species (Prymnesiophyceae; Jones *et al.*, 1993), are mixotrophic, exemplifying metabolic diversity and highly complicated ecological nature of this group of picophytoplankton. PPEs are also diverse in terms of their pigment composition, possessing all three main types of chlorophylls (Chls *a*, *b*, and *c*) and a variety of carotenoids (Fogg, 1986; Six *et al.*, 2008; Dimier *et al.*, 2009). Regarding their geographical distribution, whereas picocyanobacteria tend to be abundant in tropical and temperate oligotrophic and mesotrophic waters, PPEs are ubiquitously distributed throughout the global ocean, with the prymnesiophytes and chrysophytes tending to be dominant within and below the deep-chlorophyll maximum in the subtropical gyres (Moon-van der Staay *et al.*, 2000; Not *et al.*, 2007; Kirkham *et al.*, 2011) and the cryptophytes and prasinophytes

being common in more productive coastal ecosystems and polar regions (Lovejoy *et al.*, 2007; Kirkham *et al.*, 2011).

1.2 Methods Used to Identify Phytoplankton Taxa and Size Classes

Various techniques are used for both qualitative and quantitative analyses of natural phytoplankton assemblages. Light microscopy is the most commonly-used technique which is easily accessible and has a minimal maintenance cost. This method enables identification of phytoplankton to the species level, although to do so accurately requires a high level of expertise and can be highly time-consuming. In addition, it is challenging to view small pico- and nanophytoplankton cells which lack well-defined morphologies, and, therefore, these cells are frequently misidentified or excluded from microscopic cell counts (Vaulot *et al.*, 2008; IOCCG, 2014). Epifluorescence and electron microscopes allow visualisation and enumeration of small picophytoplankton cells, but these instruments demand highly skilled users and are expensive to maintain, and epifluorescence microscopy sometimes unable to detect HL *Prochlorococcus* cells that dimly fluoresce (Marie *et al.*, 2005). Molecular techniques, such as the quantitative polymerase chain reaction (qPCR), fluorescent *in situ* hybridisation (FISH), and dot-blot hybridisation, offer faster and more accurate means of detecting phytoplankton taxa, especially those in the nano- and pico-sized fractions lacking distinct morphological markers. These techniques, however, require very expensive equipment and reagents which can be prohibitive to many laboratories. Due to these potential limitations, oceanographers have sought to use alternative tools, including phytoplankton diagnostic pigments and various optical properties, to glean information on the taxonomic and size structure of phytoplankton communities. Here, the two important methods that have been constantly used throughout this work are introduced: (1) pigment biomarkers determined using the High-Performance Liquid Chromatography (HPLC) technique, and (2) analytical flow cytometry.

1.2.1 Pigment biomarkers (HPLC method)

Phytoplankton possess a suite of pigments which can be categorised into three structurally-distinct groups: the chlorophylls (mainly Chls *a*, *b*, and *c*), the carotenoids, and the biliproteins (Kirk, 2011). For many years, studies of phytoplankton pigments involved only the routine measurement of Chl-*a* using conventional fluorometric methods (Holm-Hansen *et al.*, 1965). The development of the HPLC technique in the 1970s allowed the separation, identification, and quantification (Figure 1.3) of a vast array of accessory pigments (pigments other than Chl-*a*) of phytoplankton from both field samples and laboratory cultures (Jeffrey and Mantoura, 1997). In the HPLC system, a sample mixture of phytoplankton pigments extracted in an organic solvent is pumped, under high pressures, through a column filled with a solid adsorbent material. Depending on how well each pigment in solvent gradient interacts with the adsorbent material (largely a function of size and charge), they will each have characteristic retention times, resulting in the separation of the pigment components as they flow out of the column to a set of detectors that measure the absorbance and fluorescence at specific wavelengths.

HPLC not only supplies information on Chl-*a* (both monovinyl and divinyl derivatives) concentration which is a commonly-used proxy for phytoplankton biomass (Platt *et al.*, 2005), the detected accessory pigments are also particularly useful for phytoplankton identification (chemotaxonomy) as some pigments are unique to certain phytoplankton taxa (Table 1.2). Further, by linking taxa to their corresponding size classes (Table 1.2), the relative contribution of each size class to total phytoplankton pigment biomass can be estimated (Claustre, 1994).

One of the major limitations of HPLC analysis is that it relies on the extraction of pigments in a non-aqueous organic solvent (Garrido *et al.*, 2011). Therefore, it does not allow for water-soluble biliproteins to be detected. Other disadvantages of this technology include the prime

requirement of large sample volumes in order to avoid missing minor accessory pigments (Bidigare *et al.*, 2005) and difficulties in interpretation of pigment data arising when pigment markers are common to several phytoplankton classes and/or when a given class contain multiple pigment signatures (Uitz *et al.*, 2006; Vaulot *et al.*, 2008). Moreover, within a phytoplankton group, pigment composition and concentration can vary significantly in response to growth conditions, which can further complicate attempts to use pigment indices for analysing the large-scale distribution of phytoplankton groups or size classes in the ocean. For instance, variation in the pigment index for the contribution of the picophytoplankton size class to Chl-*a* standing stock is largely driven by changes in the relative concentration of zeaxanthin (photoprotective pigment) (Table 1.2) which depend not only on variation in the abundance of picocyanobacteria but the photoacclimatory status of the assemblage (Chapter 2).

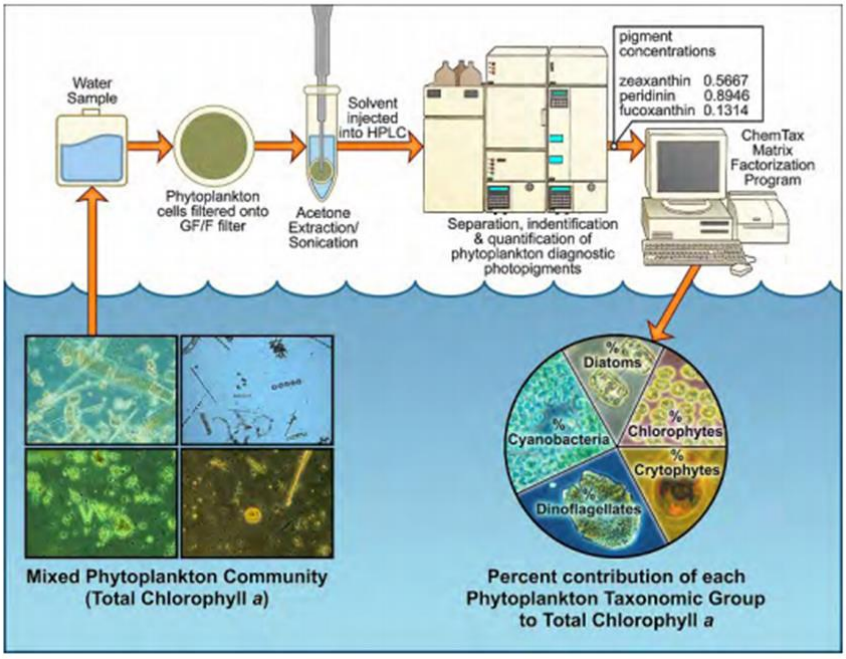


Figure 1.3: Schematic of the HPLC analysis method for characterising phytoplankton community structure on the basis of pigment composition. Natural samples consisting of a mixture of species are filtered, then extracted and injected into the HPLC system, where individual pigments are separated and quantified. From IOCCG (2014).

Table 1.2: Common phytoplankton pigment markers and their associated size classes. Modified from Vidussi *et al.* (2001) and Uitz *et al.* (2006). Pico, nano, and micro refer to picophytoplankton, nanophytoplankton, and microphytoplankton size class, respectively.

Pigment	Taxonomic significance	Size class
Chlorophylls		
Divinyl chlorophyll *a*	*Prochlorococcus*	Pico
Chlorophyll *b*	Chlorophytes, *Prochlorococcus*	Pico, Nano
Divinyl chlorophyll *b*	*Prochlorococcus*	Pico
Carotenoids		
Zeaxanthin	*Prochlorococcus*, *Synechococcus*	Pico
19′-Hexanoyloxyfucoxanthin	Prymnesiophytes	Nano, Pico
19′-Butanoyloxyfucoxanthin	Pelagophytes, Prymnesiophytes	Nano, Pico
Alloxanthin	Cryptophytes	Nano
Fucoxanthin	Diatoms, Prymnesiophytes	Micro, Nano
Peridinin	Dinoflagellates	Micro

1.2.2 Analytical flow cytometry

Flow cytometry is a method used to detect, count, and characterise some physical properties of single particles (including cells) by measuring light scattered and fluoresced from those particles as they flow through a fluid stream and are excited by a beam of light (Sosik *et al.*, 2010). This technique was initially developed for clinical uses in the late 1970s and later introduced into oceanographic research in the early 1980s (Olson *et al.*, 1983). The subsequent development of shipboard flow cytometry (Olson *et al.*, 1985; Li, 1989) provided microbial oceanographers a unique opportunity to study natural communities of marine phytoplankton, especially those in the smaller nano- and pico-sized fractions and contributed fundamentally to the discovery of the previously undetected *Prochlorococcus* (Chisholm *et al.*, 1988). With its ability to accurately evaluate a large number of cells in a very short time, flow cytometry has become a popular tool used in various aspects of phytoplankton studies (Veldhuis and Kraay, 2000; Sosik *et al.*, 2010), and there have been ongoing efforts to improve the sensitivity of flow cytometric measurements or to combine them with other analytical techniques to increase the observational capacities (Sosik *et al.*, 2010).

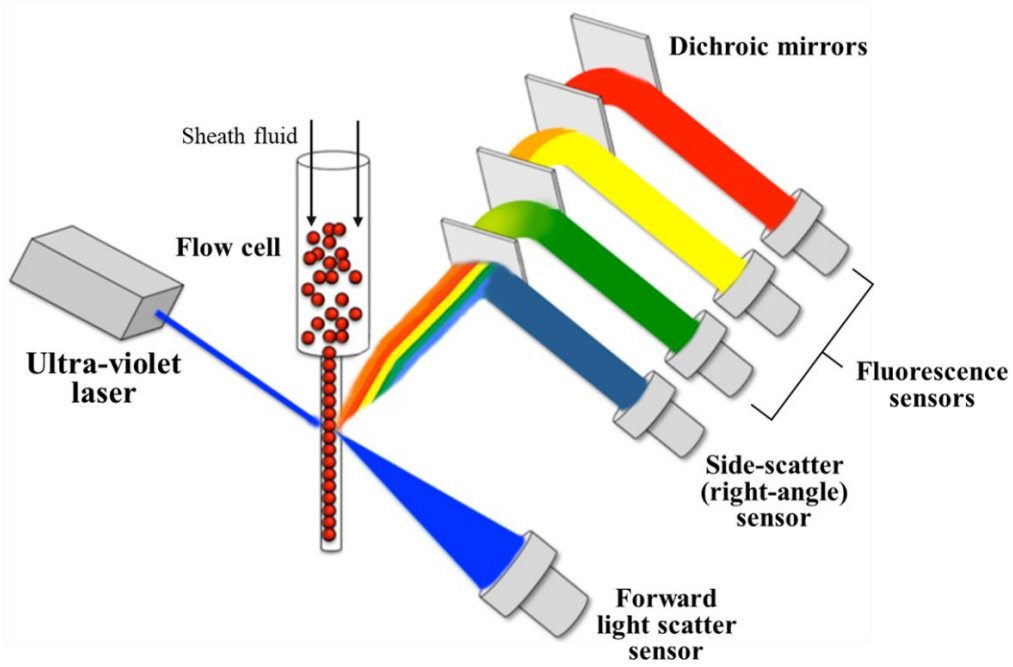


Figure 1.4: Schematic representation of a flow cytometer. Phytoplankton cells are hydrodynamically focused with sheath fluid to flow in single file through a focused laser beam. The optical signals emitted from the cell are collected by a forward angle light scatter sensor, a side-scatter (right-angle) sensor, and multiple fluorescence sensors. Modified from Brown and Wittwer (2000) and de Grazia (2015).

A flow cytometer consists of a flow chamber (called a flow cell in case of a benchtop flow cytometer) where particles (cells) in a sample are injected into a stream created by surrounding sheath fluid (Figure 1.4) that would force (hydrodynamically focus; Brown and Wittwer, 2000) the particles to flow through an interrogation point one particle at a time. At this point, the particle is illuminated by a beam of monochromatic light (usually from a laser), and the light scattered and fluoresced from the particle are collected by a forward angle light scatter sensor, a side-scatter (right angle) sensor, and several fluorescence emission sensors (Brown and Wittwer, 2000). The detected light signals are then converted into electronic signals that can be processed and displayed on a computer screen as mono-parametric histograms or bi-parametric cytograms (Marie *et al.*, 2005) (Figure 1.5). Flow cytometers designed for picophytoplankton analyses are typically equipped with sensors for the red fluorescence emitted by

(DV)Chl-*a* molecules, and the orange fluorescence which is due to the presence of phycoerythrin found in *Synechococcus*.

Apart from providing information on abundance and distribution patterns of picophytoplankton in the natural environment, flow cytometry also provides information on the physiological status of individual cells. For example, flow cytometric measurements of *Prochlorococcus* single-cell fluorescence have been shown to strongly vary with changes in light intensity induced by vertical mixing (Dusenberry *et al.*, 1999), indicating photoacclimation with deeply mixed cells having a stronger DVChl-*a* fluorescence signal than surface cells. HL-acclimated *Prochlorococcus* populations in the surface layers characterised by dim fluorescence are difficult to detect using natural fluorescence and tend to be overlooked, especially in the early days of shipboard flow cytometry (Olson *et al.*, 1985). To overcome this problem, the sensitivity of flow cytometric analyses has been improved through modifications of the flow cytometer set-up to improve excitation energy (Olson *et al.*, 1990; DuRand *et al.*, 2001) or cell staining with fluorescent dyes prior to analysis (Zubkov *et al.*, 1998; Veldhuis and Kraay, 2004) (Chapter 3).

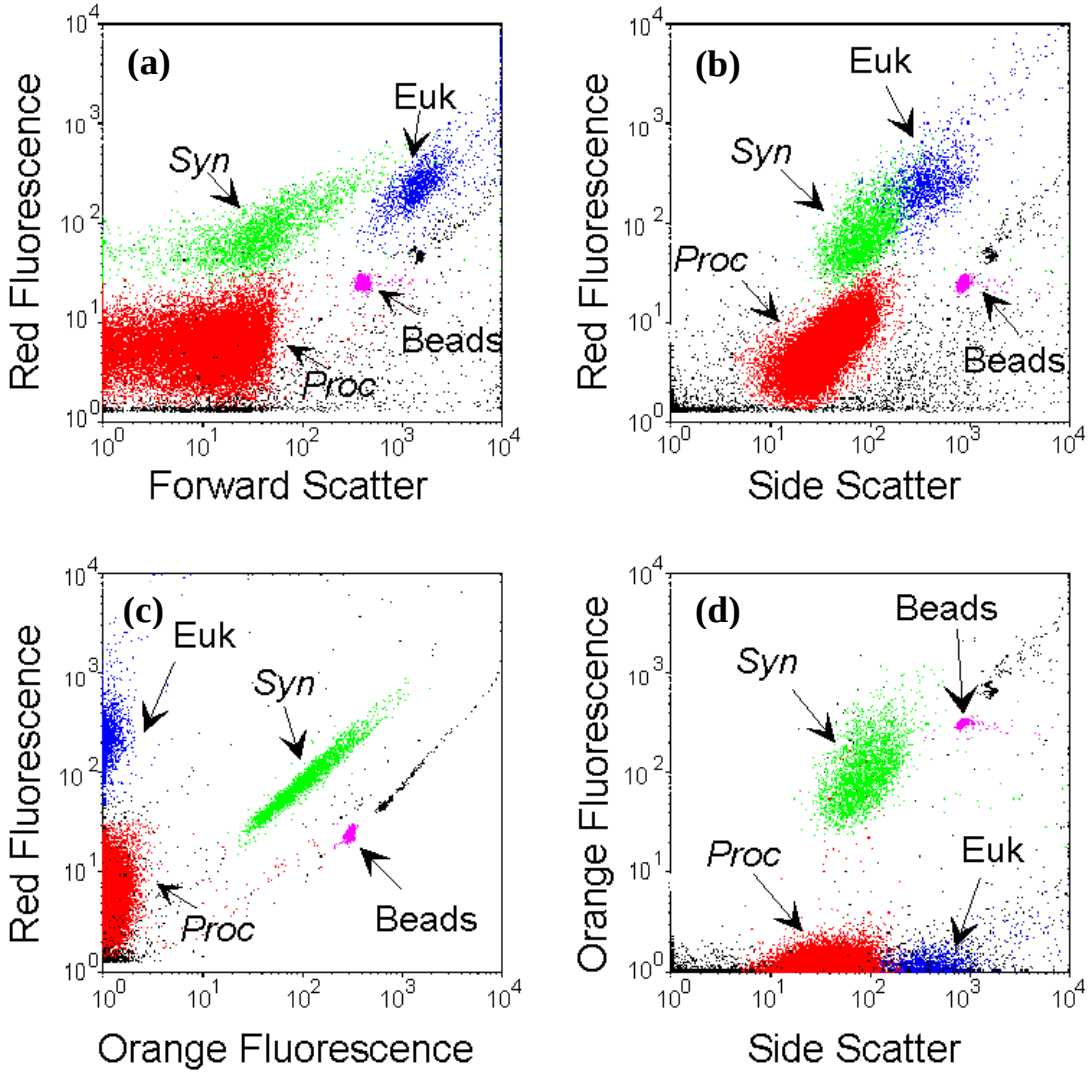


Figure 1.5: Example cytograms obtained from a sample collected in oligotrophic surface waters of the Pacific Ocean containing *Prochlorococcus* (Proc, red), *Synechococcus* (Syn, green) and photosynthetic picoeukaryotes (Euk, blue). *Prochlorococcus* cells that are smaller and less fluorescent are distinguished from picoeukaryotes based on the bivariate distribution of the forward and side scatters (as a function of size) versus red fluorescence (a and b). The *Synechococcus* population is discriminated from other picophytoplankters by its orange fluorescence associated with phycoerythrin on the orange versus red fluorescences cytogram (c). Fluorescent microspheres (0.95 µm beads) are added as an internal reference. All other particles are non-photosynthetic detrital particles. From Marie *et al*. (available online at http://www.cyto.pudue.edu/achive/flowcyt/research/micrflow/marie/dmfcm.htm, accessed on 30 December 2019).

1.3 Phytoplankton Optical Properties

Phytoplankton cells both absorb and scatter light, and these two inherent optical properties harbour information on taxonomic and size structures of phytoplankton communities (IOCCG, 2014). The following section provides background information regarding the concept of the inherent optical properties of marine phytoplankton and other seawater constituents and the main factors governing absorptive properties of phytoplankton cells.

1.2.1 Inherent optical properties

When light, or more precisely a flux of photons, penetrates a medium (e.g. water or phytoplankton cell), it can be absorbed or scattered (Kirk, 2011). The absorptive and scattering properties of the medium are described as the inherent optical properties (Preisendorfer, 1961; Morel and Bricaud, 1986; Kirk, 2011) since they are characteristic of the medium itself; in other words, they depend only on the composition of the medium and not on the geometric structure of the ambient light fields within it. The ability of the medium to absorb light can be measured in terms of the spectral absorption coefficient $a(\lambda)$ [m^{-1}], where λ represents wavelength, which is defined as the ratio of the proportion of incident light absorbed (termed the spectral absorptance, $A(\lambda)$ [dimensionless]) to the thickness of the medium (Δr [m]) (Mobley, 1994; Kirk, 2011):

$$a(\lambda) = \lim_{\Delta r \to 0} \frac{A(\lambda)}{\Delta r}, \tag{1.1}$$

$$A(\lambda) = \Phi_a / \Phi_0, \tag{1.2}$$

where Φ_0 is the radiant flux (energy or quanta per unit time) incident on the medium and Φ_a is the radiant flux absorbed by the medium. It must be noted that, in practice, $A(\lambda)$ is indirectly derived from the absorbance or optical density, $D(\lambda)$, an optical parameter that is actually measured in a spectrophotometer. $D(\lambda)$ can be defined as the logarithm to the base 10 of the

ratio of the radiant flux (Φ_0) incident on the medium to the re-emerged radiant flux, which includes both the scattered flux (Φ_s) and the transmitted flux with no change in direction (Φ_t) (Mobley, 1994; Kirk, 2011):

$$D(\lambda) = \log_{10} \frac{\Phi_0}{\Phi_s + \Phi_t} = -\log_{10} [1 - A(\lambda)]. \quad (1.3)$$

In oceanic waters, there are four major components contributing to light absorption (Prieur and Sathyendranath, 1981): (1) the water itself, (2) phytoplankton, (3) coloured dissolved organic matter (CDOM), and (4) non-algal particulate materials (sometimes referred to as detritus; Mobley, 1994). The total absorption coefficient of seawater ($a_T(\lambda)$) is a linear combination of the absorption coefficients of the four light-absorbing components:

$$a_T(\lambda) = a_w(\lambda) + a_{ph}(\lambda) + a_c(\lambda) + a_n(\lambda), \quad (1.4)$$

where the subscripts *w*, *ph*, *c*, and *n* represent water, phytoplankton, CDOM, and non-algal particulate materials, respectively. The absorption spectra of the optical components and the total absorption spectrum of seawater are shown in Figure 1.6.

For phytoplankton, it is a common practice to normalise the absorption coefficient of phytoplankton ($a_{ph}(\lambda)$ [m^{-1}]), to the concentration of Chl-*a* [mg Chl-*a* m^{-3}] to derive the chlorophyll *a*-specific absorption coefficient of phytoplankton ($a^*_{ph}(\lambda)$ [m^2 (mg Chl-*a*)$^{-1}$]):

$$a^*_{ph}(\lambda) = \frac{a_{ph}(\lambda)}{\text{Chl-}a}, \quad (1.5)$$

which can be considered as a measure of the absorptive efficiency of phytoplankton cells.

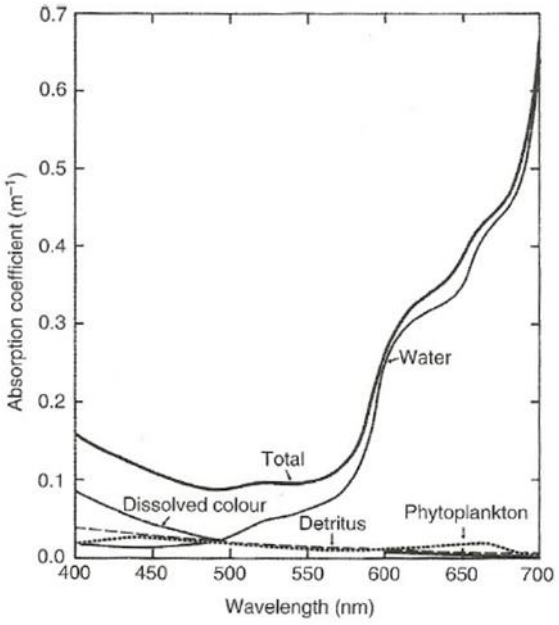


Figure 1.6: Total absorption spectrum of an idealized, productive (1 mg Chl-*a* m^{-3}) oceanic water, together with spectra of the individual absorbing component. From Kirk (2011).

1.3.2 Variability in phytoplankton light absorption

The spectral shape and magnitude of phytoplankton absorption spectrum are modulated predominately by two main factors: (1) intracellular pigment composition (Bidigare *et al.*, 1990; Hoepffner and Sathyendranath, 1991), and (2) pigment packaging (Kirk, 1975; Morel and Bricaud, 1981). Both factors are strongly influenced by photoacclimation, a process by which phytoplankton cells physiologically respond to varying growth irradiances (Richardson *et al.*, 1983; Falkowski and LaRoche, 1991).

(1) Pigment composition

Phytoplankton pigments, as detected using HPLC, can be grouped into two functional categories (Bouman, Platt, Kraay, *et al.*, 2000): photosynthetic (PSP) and non-photosynthetic or photoprotective (NPP) pigments. These pigments have different spectral absorption characteristics (Bidigare *et al.*, 1990) as illustrated in Figure 1.7, and thus the total absorption spectrum of phytoplankton cells heavily depends on the relative abundance of individual pigments present

in the cell (Hoepffner and Sathyendranath, 1991). Pigment composition is known to vary among phytoplankton taxa (Jeffrey and Vesk, 1997; Ras *et al.*, 2008), and the intracellular concentration of each group of pigments is affected by photoacclimation (Moore *et al.*, 1995; MacIntyre *et al.*, 2002; Letelier *et al.*, 2017). In the subtropical open ocean, the NPP zeaxanthin associated with picocyanobacteria has been shown to be responsible for much of the variability in light absorptive properties of phytoplankton (Babin *et al.*, 1996; Bouman, Platt, Kraay, *et al.*, 2000; Letelier *et al.*, 2017). Within picocyanobacterial populations, the relative abundance of zeaxanthin has been shown to be positively correlated with growth light intensities (Barlow *et al.*, 2002).

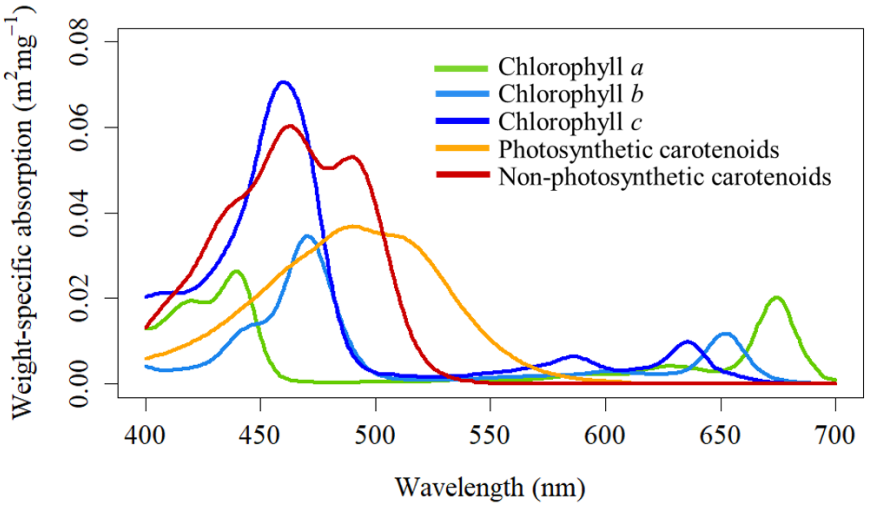


Figure 1.7: Weight-specific absorption spectra of different groups of pigment measured in solution. Replotted using absorption coefficients derived by Bidigare *et al.* (1990).

(2) Pigment packaging

Pigments absorb light most efficiently when uniformly distributed in a solution. However, when pigment molecules are aggregated into discrete packages such as within pigment-protein complexes in photsynthetic cells, their light absorptive efficiency decreases (Duyens, 1956; Kirk, 1975; Morel and Bricaud, 1981) (Figure 1.8). This optical phenomenon is referred to as the pigment-packaging or flattening effect. The degree of pigment packaging is proportional to cell size and the concentration of pigment per cell (Duyens, 1956).

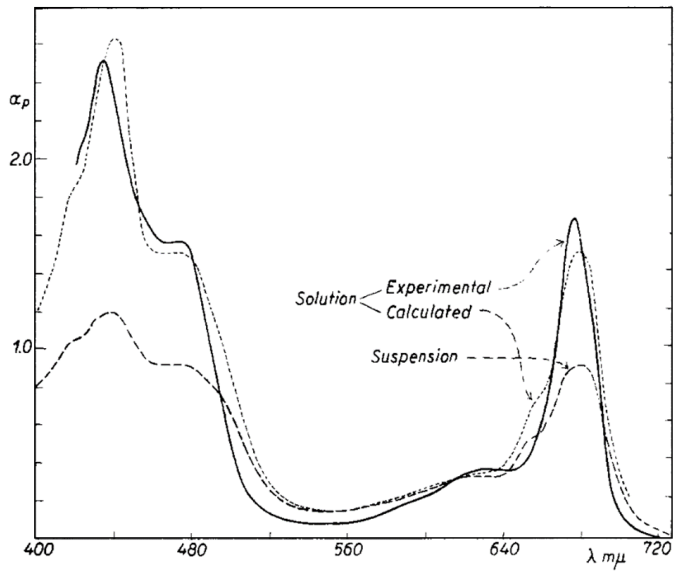


Figure 1.8: Absorption spectra of a *Chlorella* (green alga) suspension and a quantitative methanol extract. Also shown is a calculated spectrum of cell pigments in solution based on optical theory. From Duyens (1956).

As the diameter of a cell increases, pigment packaging becomes proportionately more pronounced (Figure 1.9a) and is greatest at the peaks of the spectra where absorption is strongest (Bricaud *et al.*, 2004; Kirk, 2011). This is consistent with field observations that absorption spectra for samples dominated by large microphytoplankton appear flatter than those of smaller size classes (Lutz *et al.*, 1996; Ciotti *et al.*, 2002; Hirata *et al.*, 2008). Changes in the intracellular pigment concentration can also cause the intensity of pigment packaging to vary (Figure 1.9b). In marine environments where light is strongly attenuated, such as in coastal environment or during an intense bloom, phytoplankton deeper in the water column photoacclimate to the reduced light intensities by increasing their pigment concentration, resulting in enhanced pigment packaging and a corresponding flattening of the absorption spectrum (Berner *et al.*, 1989; Stuart *et al.*, 1998). Previous studies have revealed that modification of the number and transparency of thylakoid membranes due to photoacclimation may also cause increased levels of pigment packaging (Berner *et al.*, 1989; Falkowski and LaRoche, 1991) (Chapter 2). These effects of photoacclimation (i.e. intracellular pigment concentration and arrangement) and cell

size on the magnitude of pigment packaging are highly interconnected and difficult to examine separately on natural samples containing mixed populations without independent measures of cell size, which are difficult to obtain as no single method is able to measure phytoplankton cell diameters across the entire size spectrum. Therefore, the impact of photoacclimation through pigment packaging on light absorption by phytoplankton is poorly known.

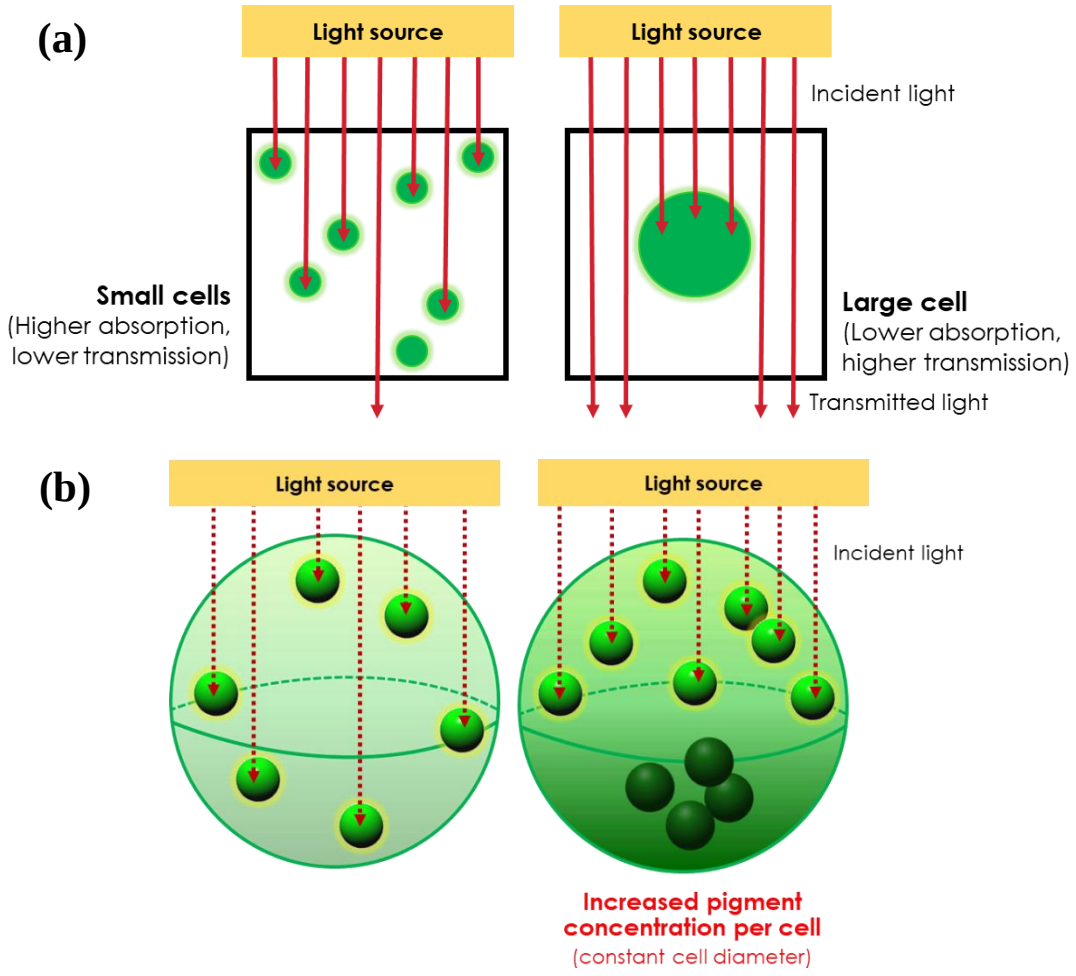


Figure 1.9: Schematic representation of an increase in pigment packaging caused by an increase in either (a) cell diameter or (b) the intracellular pigment concentration. If the same biovolume in many small cells is combined within a single large cell, it is less likely to intercept incident photons. Similarly, as the intracellular pigment concentration increases, pigment particles located at the surface can prevent the incident light from reaching the inner part of the cell.

1.4 Phytoplankton Photosynthesis

The process of photosynthesis can be simplistically divided into two major stages, each with a very complex series of photochemical reactions. These two stages are (1) the light reactions (the 'photo' part of photosynthesis; Urry *et al.*, 2013) that involve collection and transfer of excitation energy through the photosynthetic machinery to form chemical energy (Falkowski and Raven, 2007), and (2) the Calvin cycle which incorporates CO_2 and synthesises organic compounds by reduction of the fixed carbon (the 'synthesis' part of photosynthesis). The Calvin cycle is frequently referred to as the light-independent reactions to reflect that it is a process where light is not directly required.

1.4.1 Photosynthetic apparatus

The light reactions occur in intracellular photosynthetic membranes, while the light-independent reactions are carried out in a fluid-filled space outside the membranes. The ensemble of these biochemical elements where all photosynthetic processes take place are collectively referred to as a cellular photosynthetic apparatus (Falkowski and Raven, 2007). In eukaryotes (including higher plants and eukaryotic phytoplankton), the photosynthetic apparatus is compartmentalised within the chloroplasts (Figures 1.10a-c), a specialised organelle characterised by two to four (depending on taxa; Falkowski and Raven, 2007; Kirk, 2011) envelope lipoprotein membranes (Weier and Benson, 1967) and a dense fluid surrounded by the membranes called the stroma. Suspended within the stroma is another membrane system consisting of an array of membranous sacs called thylakoids whose morphology and arrangement are observed to be highly variable among algal classes (Kirk, 2011; Rochaix, 2016; Mareš *et al.*, 2019). In plants and most eukaryotic algae, the thylakoids are vertically stacked with each stack of thylakoids, commonly known as a granum, being interconnected, by the stroma lamella, into a continuous thylakoid network (Mareš *et al.*, 2019). The thylakoids serve as photosynthetic

membranes where the proteins and pigments involving in the light reactions of photosynthesis are embedded. Surrounding the thylakoids, various enzymes and chemical reductants required to carry out the Calvin cycle are dispersed in the stroma of the chloroplast (Falkowski and Raven, 2007).

In cyanobacteria, the photosynthetic apparatus is not organised in the chloroplast but lies freely in the cytoplasm (Kirk, 2011). Also, although they are sites of the photosynthetic light reactions as in eukaryotes, the cyanobacterial thylakoid membranes do not form grana (Nevo *et al.*, 2009; Mareš *et al.*, 2019). Instead, they typically occur as parallel layers (Falkowski and Raven, 2007; Liberton *et al.*, 2011) that run along the cell membrane as evident, for instance, in various strains of *Synechococcus* and *Prochlorococcus* (Figures 1.10d, e) (Lichtlé *et al.*, 1995; Partensky, Hess, *et al.*, 1999; Nevo *et al.*, 2009; Mareš *et al.*, 2019). It is important to note when examining Figures 1.10d, e that the thylakoid layers in *Prochlorococcus* are generally much more closely appressed than in *Synechococcus* (Partensky, Hess, *et al.*, 1999). Most cyanobacteria (except *Prochlorococcus*), as well as members of the Rhodophyta and Cryptophyta (Kirk, 2011), also have water-soluble pigment-protein complexes called the phycobilisomes anchored to their thylakoid membranes to serve as the main light-harvesting complex of photosystem II (Fujita *et al.*, 1985). The ultrastructure and composition of phycobilisomes vary between cyanobacterial groups and with environmental conditions at which the cells are grown (Grossman *et al.*, 1993). Figure 1.11 illustrates the basic structure of a phycobilisome contained within the photosynthetic apparatus of *Synechococcus* as opposed to the photosynthetic apparatus of *Prochlorococcus* lacking phycobilisomes (Hess *et al.*, 2001).

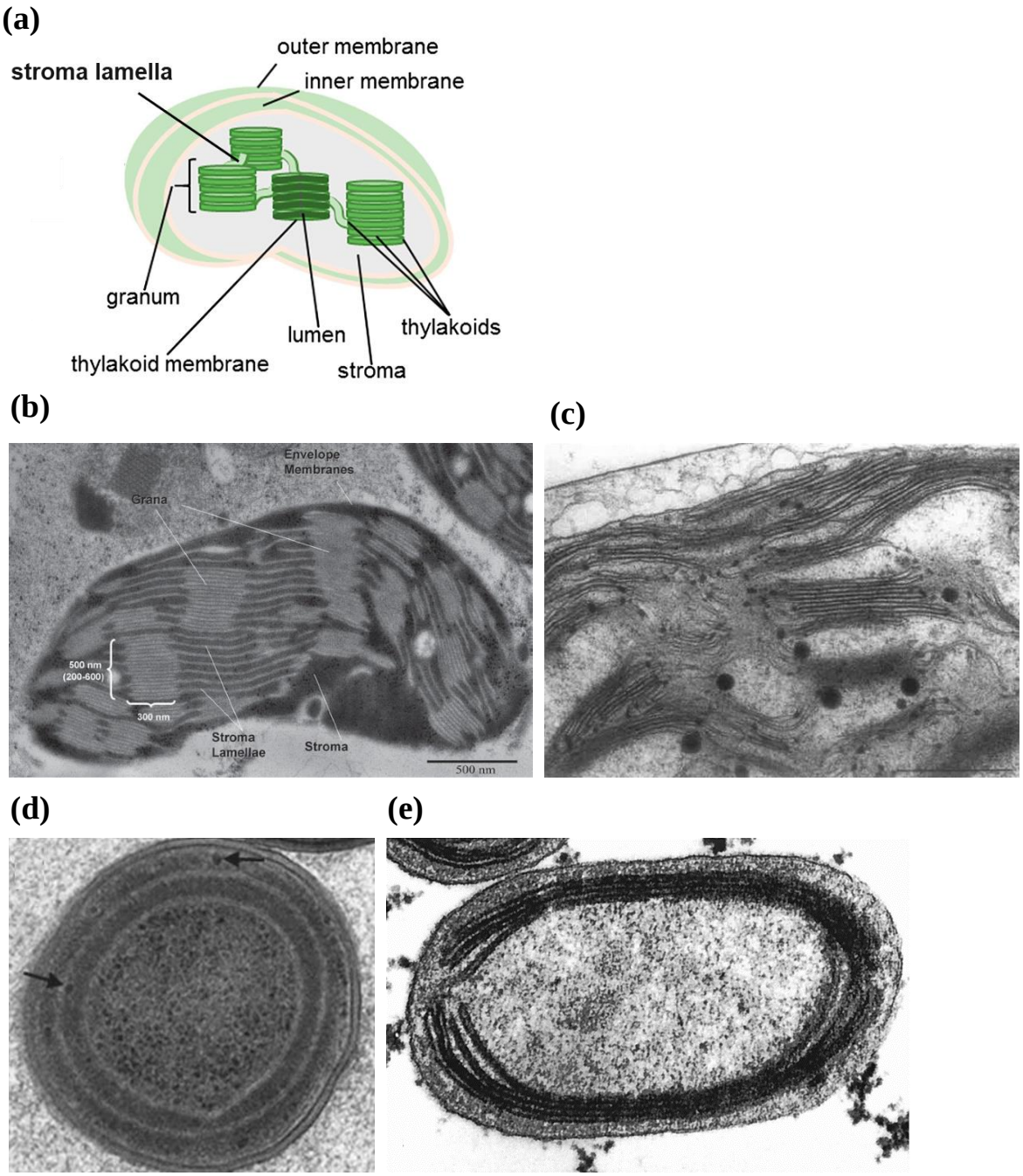


Figure 1.10: (a) Illustration of a chloroplast of typical eukaryotic cells (modified from Lehmuskero *et al.*, 2018). (b-e) Transmission electron micrographs of the thylakoids of (b) higher plants showing grana and stroma lamellae (from Nevo *et al.*, 2009), (c) the green alga *Dunaliella tertiolecta* showing the irregular stacking of thylakoids to form rudimentary grana (from Kirk, 2011), (d) *Synechococcus* PCC7942 showing phycobilisome complexes (arrows) alternately arranged on adjacent layers of the thylakoids (from Nevo *et al.*, 2009), and (e) *Prochlorococcus* MIT9313 (from Partensky, Hess, *et al.*, 1999).

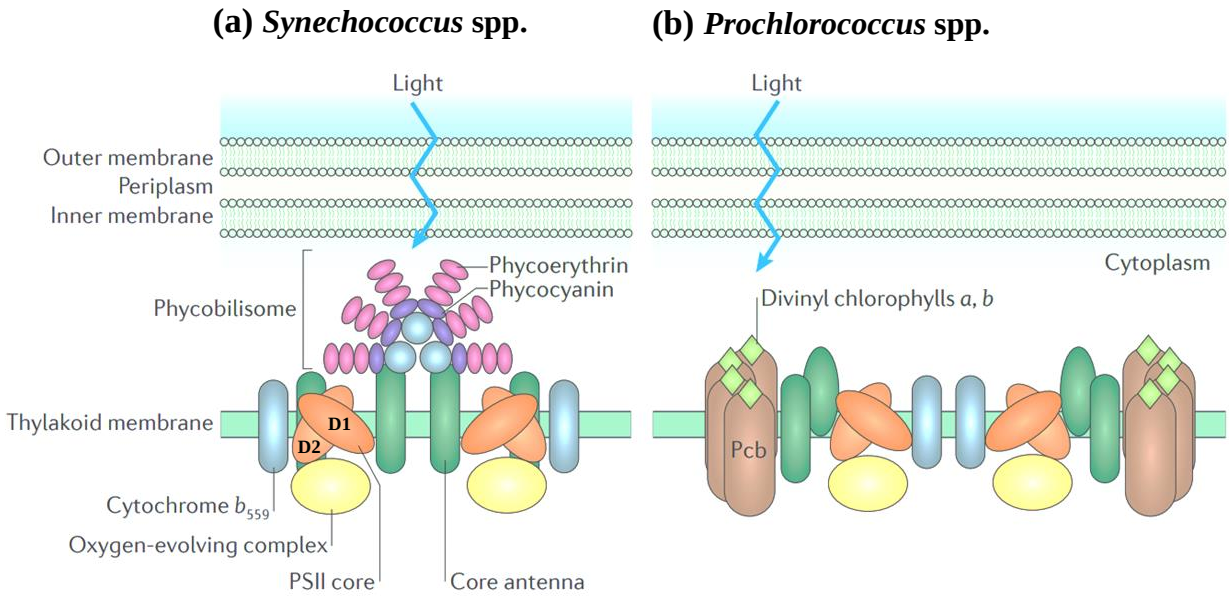


Figure 1.11: The architecture of the photosynthetic apparatus of (a) *Synechococcus* spp. containing a phycobilisome as the main light-harvesting complex in photosystem II (PSII) compared with that of (b) *Prochlorococcus* spp. without the phycobilisome. From Biller *et al.* (2015). Each phycobilisome is composed of phycobiliproteins, which can be categorised into four classes: phycoerythrin, phycoerythrocyanin, phycocyanin, and allophycocyanin (Kirk, 2011). The colour and spectral properties of phycobiliproteins are determined by light-absorbing chromophores called phycobilins which are covalently bound to them. There are four types of phycobilins: phycocyanobilin (blue phycobilin), phycoerythrobilin (red), phycoviolobilin (purple), and phycourobilin (yellow) (Kirk, 2011). A central core of the phycobilisome consists of three molecules of allophycocyanin, which, in turn, bind at least six radiating rods made of other types of phycobiliproteins (Grébert *et al.*, 2018). In marine *Synechococcus*, they can be either phycocyanin or phycoerythrin or both (Grébert *et al.*, 2018). *Prochlorococcus* (as well as *Prochloron* and *Prochlorothrix*) lacks phycobilisomes. Instead, their light-harvesting complex contains prochlorophyte chlorophyll-binding protein (Pcb) which binds DVChl-*a* and DVChl-*b*. In both *Synechococcus* and *Prochlorococcus*, light energy collected by the light-harvesting complex is transferred to the PSII core antenna proteins and then to the reaction centre of PSII which consists of core protein subunits D1 and D2, and cytochrome b_{559} (Ting *et al.*, 2002).

The relatively simple photosynthetic apparatus of *Prochlorococcus* compared to that of *Synechococcus* (Figure 1.11) results in more rapid degradation and replacement of components of the photosynthetic apparatus (Hartmann *et al.*, 2014), which can be particularly beneficial for *Prochlorococcus* in coping with photodamage caused by extremely high light characteristic of the subtropical ocean.

1.4.2 Photosystems and photosynthetic unit

Pigments and proteins (and other organic molecules) in the thylakoid membranes, are organised into two distinct types of pigment-protein complexes, a reaction-centre complex and a light-harvesting (or antenna) complex, which together constitute a photosystem (Alberts *et al.*, 2015) (Figure 1.12a). The reaction-centre complex contains a special pair of Chl-*a* molecules bound to a specific protein and is surrounded by a cluster of several light-harvesting complexes. In addition to Chl-*a*, each light-harvesting complex, depending on the algal taxa, contains different types of accessory chlorophylls and carotenoids (e.g. Chl-*b* in green algae, Chl-*c* and fucoxanthin in diatoms, and peridinin in dinoflagellates) (Figure 1.12b) (MacIntyre *et al.*, 2002) or phycobilisomes in cyanobacteria and red algae (Figure 1.11a). The function of light-harvesting complexes is to collect photons and then pass on the absorbed energy from one pigment molecule to another and eventually to the reaction-centre complex where Chl-*a* molecules (the special pair) are excited, releasing an excited electron which is then fed to an electron-transport chain.

There are two types of photosystems referred to as photosystem I (PSI) and photosystem II (PSII) (named in order of their discovery), each of which differs primarily in the spectral characteristics of the special Chl-*a* at the reaction-centre complex. The reaction-centre Chl-*a* of

PSII, commonly known as P_{680}, absorbs photons most efficiently at 680 nm, whereas the reaction-centre Chl-*a* of PSI, called P_{700}, has an absorption maximum at a slightly longer wavelength of 700 nm (Thornber, 1975). The different absorptive properties of P_{700} and P_{680} are due primarily to the different proteins to which the pigments are bound, not the molecular properties of the pigments themselves as they are nearly identical (Urry *et al.*, 2013).

The reaction centre of PSII consists of two protein subunits, designated D1 and D2 (encoded by the genes psbA and psbD, respectively), and two subunits of cytochrome b_{559} (psbE and psbF) (Nanba and Satoh, 1987; Zouni *et al.*, 2001) (Figure 1.11a). The D1 protein has been shown to be highly subjected to photoinactivation (Geider *et al.*, 1993; Telfer, 2002; Six *et al.*, 2004, 2007; Key *et al.*, 2010; Wu *et al.*, 2011, 2012), which explains its much higher turnover rates when compared to other proteins found in the chloroplast (Aro *et al.*, 1993; Telfer, 2002). As shown in Figure 1.12b, the reaction-centre complexes of both PSI and PSII comprise not only Chl-*a*, but also some NPPs, notably β-carotenes (Searle and Wessels, 1978; Kana *et al.*, 1988; Telfer, 2002). Rather than participating in photochemistry, NPPs play a primary role in protecting the reaction centres from photo-oxidative stress caused by excess excitation energy. For example, two β-carotene molecules located proximal to the PSII reaction-centre Chl-*a* have been found to quench highly reactive (harmful) singlet oxygen produced when excited Chl-*a* triplets are formed (Telfer, 2002).

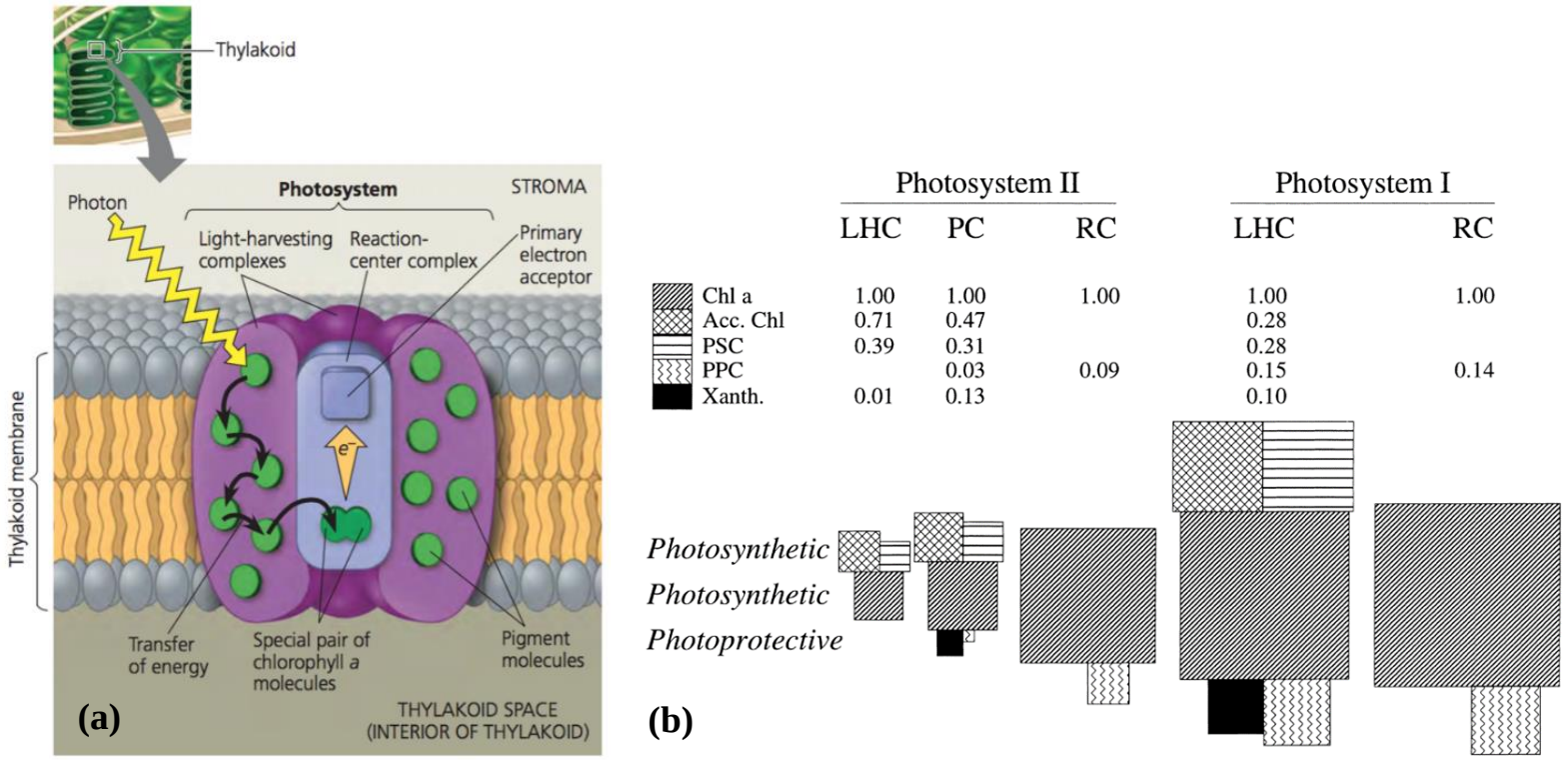


Figure 1.12: Diagrammatic representation of (a) the basic structure and function of a photosystem, and (b) the distribution of pigments among the pigment-protein complexes of the photosystems (PS) including the light-harvesting complexes (LHC), peripheral complexes (PC), and the reaction-centre complexes (RC). Tabulated data are given as ratios of molecules per polypeptide within each complex and are grouped as Chl-*a*, photosynthetic accessory chlorophylls (Acc. Chl), photosynthetic accessory carotenoids (PSC), photoprotective carotenoids (PPC), and xanthophylls (Xanth). The area of each square in the diagram is proportional to the abundance of pigments per unit of the pigment-protein complex and shows the ratios both between and within complexes. Note that the relative numbers of each complex also vary. The peripheral complex of PSII comprises the CP29, CP26, and CP24 subunits. The PSII reaction centre comprises the D1/D2 heterodimer and CP47 and CP43. From (a) Urry *et al.* (2013) and (b) MacIntyre *et al.* (2002).

In the light-harvesting complexes, there is also another group of NPPs collectively known as xanthophylls that, through the xanthophyll cycle, can quench singlet-excited Chl-*a* and harmlessly dissipate excitation energy in excess as heat. This photoprotective process is also described as non-photochemical quenching to reflect that it reduces (quenches) fluorescence emission in a non-photochemical manner (i.e. as heat) (Müller *et al.,* 2001). In higher plants and some green and brown algae (Brunet *et al.,* 2011), the xanthophyll cycle involves the enzymatic de-epoxidation of violaxanthin (non-quenching) to antheraxanthin and ultimately to zeaxanthin (quenching) under high-light conditions and the reverse epoxidation at low light. In diatoms and most other eukaryotic phytoplankton (Lavaud, 2007), the xanthophyll cycle consists of the de-epoxidation/epoxidation of diadinoxanthin (non-quenching) and diatoxanthin (quenching). In cyanobacteria, however, photoprotection does not depend on non-photochemical quenching via the xanthophyll cycle (Brunet *et al.,* 2011) but the accumulation of zeaxanthin in the cytoplasm at high light (Post *et al.,* 1993; Brunet *et al.,* 2011). For natural phytoplankton assemblages, the ratio of the sum of NPPs to the sum of all pigments, commonly referred to as the NPP index, has been shown to be strongly correlated with growth irradiances and can therefore be considered as an index of the photoacclimatory status of phytoplankton (Babin *et al.,* 1996) (Figure 1.13).

When PSI and PSII, including both of their light-harvesting and reaction-centre complexes, are described together as a single entity, this functional unit is commonly referred to as a photosynthetic unit (Kirk, 2011). The ‘size’ of the photosynthetic unit is defined as the number of Chl-*a* molecules that are contained in that photosynthetic unit (Mauzerall and Greenbaum, 1989; Dubinsky and Stambler, 2009). In the course of photoacclimation to low-light intensity, it has been found that phytoplankton cells can increase either the number or the size of the photosynthetic unit or both (Falkowski and Owens, 1980; Perry *et al.,* 1981; Richardson *et al.,*

1983). Both of these photoacclimatory strategies imply an overall increase in the intracellular pigment concentration in phytoplankton cells (Prézelin, 1981) which can lead to an intensification of the pigment-packaging effect and a corresponding reduction in the specific absorption coefficient as discussed in section 1.3.2 (Figure 1.9). Oppositely, the reverse processes occur upon exposure to high-light intensity, decreasing the total amount of pigments to reduce light energy captured. Photoacclimation by means of changes in the number and size of the photosynthetic unit occurs on longer time scales (hours to days) than that accomplished by the xanthophyll cycle (seconds to minutes) (Falkowski and LaRoche, 1991).

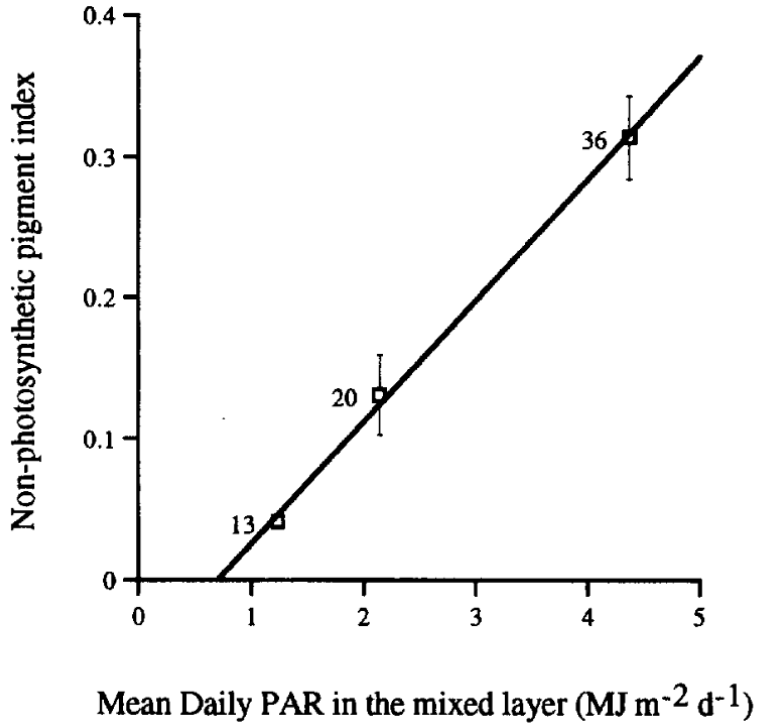


Figure 1.13: Relationship between the mean daily photosynthetically available radiation (PAR) and the NPP index for the upper mixed layer at three sampling sites in the subtropical North Atlantic visited during the French EUMELI cruise. From Babin *et al*. (1996).

1.4.3 The photosynthesis-irradiance (*PE*) curve

The rate of photosynthesis, equivalent to the primary production, may be measured either as the rate of carbon assimilation or as the rate of oxygen evolution (Sakshaug *et al.*, 1997). The photosynthetic rates of phytoplankton are related to available light (Smith, 1936; Jassby and Platt, 1976), and the relationship between the two variables can be determined empirically using the photosynthesis - irradiance (*PE*) experiment. In these experiments, samples of phytoplankton cells inoculated with a tracer for either carbon or oxygen are exposed to a range of light intensities (typically from near zero to the near surface-light intensities; Bouman *et al.*, 2018) for a certain time period. Data obtained from the *PE* experiment can be fitted by a smooth curve commonly known as the light-saturation curve or the *PE* curve (Figure 1.14).

At low irradiances, the photosynthetic rate is almost directly proportional to irradiance with the curve being quasi-linear with the initial slope denoted as α^B (where the subscript *B* indicates normalisation to biomass, typically considered as the Chl-*a* concentration). In other words, α^B can be thought of as a parameter that describes the photosynthetic efficiency under light limitation (Sakshaug *et al.*, 1997; Bouman *et al.*, 2018). As irradiance increases, the photosynthetic rate continues to increase, although non-linearly, until it reaches the maximal level, P_m^B (the plateau of the curve). After P_m^B is reached, photosynthesis is no longer dependent on irradiance and is said to be light-saturated (Kirk, 2011). P_m^B is also referred to as the assimilation number (Jassby and Platt, 1976) or the photosynthetic capacity (Kirk, 2011). Also shown in Figure 1.14, the photoadaptation or light saturation parameter, E_k is the irradiance which corresponds to the intersection point between the initial slope and the plateau of the curve. Hence, E_k can be defined by the relationship (Jassby and Platt, 1976):

$$E_k = \frac{P_m^B}{\alpha^B} . \qquad (1.6)$$

In natural environments, the photosynthetic rate in the upper part (light-saturated) and the lower part (light-limited) of the water column is governed primarily by P_m^B and α^B, respectively, and E_k represents the transition zone between the two regimes (Sakshaug *et al.*, 1997). Although the *PE* curve can be represented by various mathematical functions, in the absence of photoinhibition (i.e. the high light-induced reduction in the photosynthetic efficiency associated with a decrease in functional PSII reaction centres; Kulk *et al*. 2011), it can be described sufficiently using only two parameters: P_m^B and α^B (Jassby and Platt, 1976; Platt *et al.*, 1980).

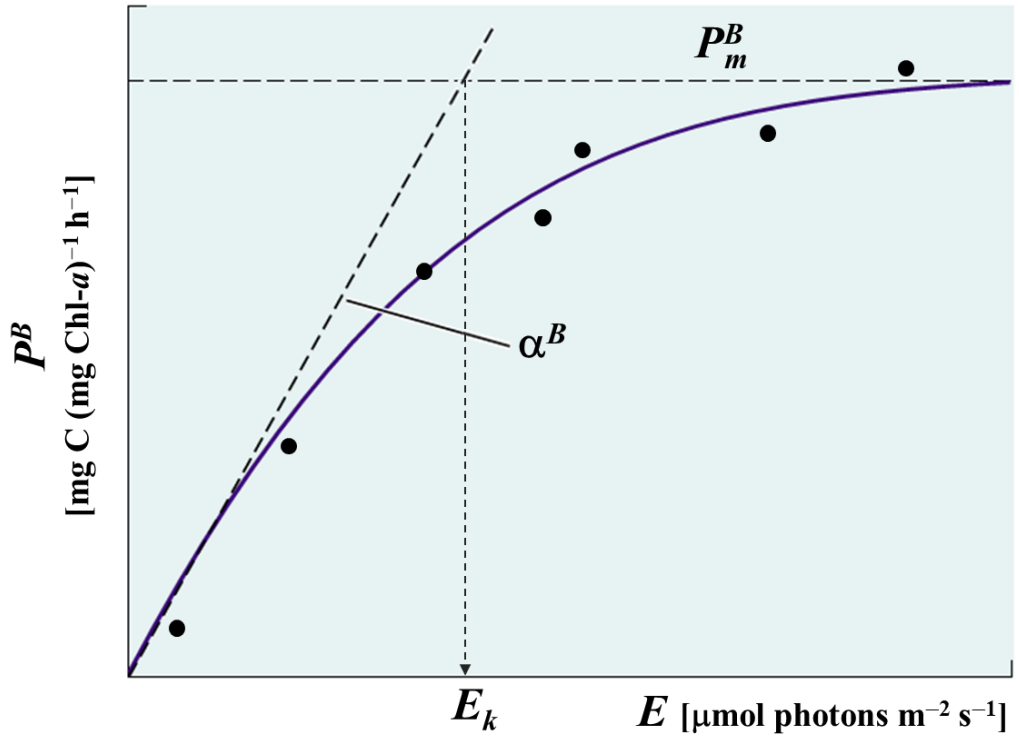


Figure 1.14: The photosynthesis-light curve (solid line) fitted to data obtained from an idealised *PE* experiment (solid circles). The broken lines are constructed to show the biomass-normalised initial slope (α^B), the maximum biomass-normalised photosynthetic rate (P_m^B) and the photoadaptation parameter (E_k). Redrawn after Bouman *et al.* (2018).

The magnitude of α^B depends on the proportion of incident photons absorbed and is thus affected by the factors known to influence the light absorptive properties of phytoplankton, including photoacclimation. Also, in response to changes in light history, phytoplankton adjust

the intracellular concentration of NPPs relative to PSPs (particularly Chl-*a*), which can, in turn, affect their photosynthetic performance since NPPs absorb photons without transferring excitation energy to photosynthetic machinery. The adjustment of the cellular content Chl-*a*, relative to that of carbon (Sathyendranath *et al.*, 2020) due to photoacclimation also results in variation in the carbon-to-Chl-*a* ratio (θ). θ represents the algal photophysiological status (Geider, 1987; Sathyendranath *et al.*, 2020) in phytoplankton growth models and is required to derive phytoplankton growth rates (μ) from P^B values (i.e. $\mu = P^B / \theta$) (Marañón, 2005). In addition, θ is also critical when fields of phytoplankton carbon computed in numerical models of ocean biogeochemistry are to be converted to fields of Chl-*a*, especially in order to compare model predictions with satellite data for validation purposes (Sathyendranath *et al.*, 2009, 2020).

.

1.5 Thesis Objectives

Based on the background described in the previous sections, the overall objective of the work presented in this thesis is to assess the effect of pigment-related photoacclimation on the bio-optical and photosynthetic properties of marine phytoplankton. The following chapters aim to contribute towards this goal.

Chapter 2 investigates the relationship between the photoacclimatory status as indicated by the concentration of NPPs relative to total pigments (NPP index; Babin *et al.*, 1996), the size structure estimated using diagnostic pigment markers (Bricaud *et al.*, 2004), and light absorptive properties of surface phytoplankton populations using *in situ* data of pigment concentrations and $a_{ph}(\lambda)$ collected from across different ecological biomes (Longhurst, 1998) of the Atlantic Basin. It will specifically examine the roles of NPPs in governing the basin-scale variations in $a^*_{ph}(440)$, which indicates the light absorptive efficiency of phytoplankton, and the shape of $a_{ph}(\lambda)$ represented by a spectral slope index. It will also explore the eco-physiological factors

underlying the close relationship between phytoplankton light absorption, photoacclimation, and community structure.

Chapter 3 aims to assess vertical and seasonal variations in the NPP index in relation to photoacclimation and changes in phytoplankton community structure. Using picocyanobacteria as a case study, it will then proceed to examine variations in the cellular quotas of PSPs and NPPs along vertical gradients of available light in order to better understand the relative roles of the two pigment groups in governing changes in the NPP index. Picocyanobacteria, in particular *Prochlorococcus*, are chosen to investigate vertical shifts in photoacclimation since they are unique in terms of their intracellular pigment complement and are routinely identified and enumerated by analytical flow cytometry. Using cell abundance and pigment datasets obtained on oceanographic cruises focused on the (subtropical) ocean, the carbon-to-DVChl-*a* ratio for *Prochlorococcus* (θ_{Pro}) is estimated and variability is examined in relation to environmental forcing.

Using a global dataset of *PE* parameters, Chapter 4 aims to examine the vertical structure of the photosynthetic properties of phytoplankton in contrasting trophic regimes and how variation in *PE* parameters is related to changes in the NPP index. It will then explore and discuss the physiological basis for the relationship between the NPP index and *PE* parameters. This chapter will also assess the correlation between θ_{Pro}, which is calculated using the same approach used in the previous chapter, and both the NPP index and the spectral slope in order to assess the utility of these pigment and absorption indices to predict θ_{Pro}. Finally, I will demonstrate how estimates of θ_{Pro} derived based on the NPP-θ_{Pro} relationship can be used alongside information on the photosynthetic rates at light saturation to calculate the maximum growth rates of *Prochlorococcus*.

Chapter 2

Variation in Pigment Composition and Bio-optical Properties of Phytoplankton in the Atlantic Basin

2.1 Introduction

Light absorptive characteristics of marine phytoplankton depend largely on the properties of the phytoplankton cells, including their size and their intracellular pigment composition and concentration (Kirk, 2011). The commonly-held view that cell size primarily governs changes in the shape of the *in vivo* phytoplankton absorption spectra ($a_{ph}(\lambda)$) has resulted in its wide-spread use to predict the size and taxonomic structure of surface phytoplankton communities (Ciotti *et al.*, 2002; Sathyendranath *et al.*, 2004; Hirata *et al.*, 2008; Devred *et al.*, 2011; Brewin *et al.*, 2015). Yet, each algal pigment has its own absorptive characteristics (Bidigare *et al.*, 1990), and thus the variation in the shape and magnitude of $a_{ph}(\lambda)$ must also depend heavily on the relative concentrations of individual pigments present in the cells (Hoepffner and Sathyendranath, 1991). Moreover, the arrangement of pigment molecules within the cell needs to be considered. As pigment molecules are aggregated into chloroplasts, which in turn are contained within the algal cell, their efficiency for light absorption becomes lower than if they are uniformly dispersed in solution (Duyens, 1956). This is commonly referred to as the pig-ment-packaging effect. Consequently, an increase in either the cell size or the intracellular pig-ment concentration will intensify pigment packaging, resulting in a flattening of the absorption spectrum (Duyens, 1956; Morel and Bricaud, 1981). In addition to an overall flattening in the *in vivo* absorption by phytoplankton, the shape of the absorption spectrum of pigments is al-tered as pigment molecules interact with proteins in which they are embedded (Johnsen *et al.*, 1994).

Light absorption by phytoplankton has an impact on the optical properties of the open-ocean waters (Morel, 1988). It can affect vertical attenuation of light through the water column and thus the amount of photosynthetically-available light within the surface ocean (Sathyendranath and Platt, 1988). The light harvested by phytoplankton pigments also primarily governs the photosynthetic efficiency of phytoplankton under light-limited conditions (Platt and Sathyendranath, 1988; Geider, 1993). Furthermore, changes in phytoplankton absorption efficiency can lead to errors in the estimation of phytoplankton pigment biomass by remote sensing since this inherent optical property has a strong impact on the reflectance signal measured by ocean-colour satellites (Platt and Sathyendranath, 1988). For these reasons, knowledge of the spectral characteristics of phytoplankton absorption is required in the computation of marine primary production. In addition, absorption of solar radiation by phytoplankton pigments affects the heating of the surface ocean which can in turn influence the stability of the water column and heat exchange between ocean and atmosphere (Sathyendranath *et al.*, 1991; Ueyoshi *et al.*, 2005). Therefore, information on phytoplankton absorption coefficient is critical for improving our understanding of the biological impacts on global ocean physics (Lutz *et al.*, 1996).

Light harvesting pigments of phytoplankton collect light incident upon the cells, and the photon energy absorbed in the photosystem can either be (1) used for photosynthesis, or (2) re-emitted as fluorescence, or (3) lost as heat (Johnsen and Sakshaug, 1996). Consequently, based on their functional roles, phytoplankton pigments can be divided into two main categories (Bidigare *et al.*, 1990; Bouman, Platt, Kraay, *et al.*, 2000): photosynthetic pigments (PSPs) which serve to provide light energy for photosynthesis, and non-photosynthetic (or photoprotective) pigments (NPPs) which protect the cells against photodamage at excessively high light intensities. The

fraction of energy absorbed by NPPs is thermally dissipated and is therefore not active in photosynthesis. The intracellular concentration of the two classes of pigments is known to be regulated through responses of phytoplankton to variable environmental factors, in particular the underwater light conditions (Kirk, 2011). Although pigments have distinct absorptive characteristics, their *in vivo* absorption peaks, particularly for the carotenoids, which is a class of pigments that contains both PSPs and NPPs, overlap greatly in the blue and green parts of the visible spectrum (Bidigare *et al.*, 1990).

Essentially, all phytoplankton can temporarily acclimate to fluctuations in the intensity and/or spectral composition of the underwater light field (Richardson *et al.*, 1983; Falkowski and LaRoche, 1991). This process, termed photoacclimation (Falkowski and LaRoche, 1991; MacIntyre *et al.*, 2002), encompasses a suite of mechanisms operating over a broad range of time scales from seconds to days and ensures that cells are able to achieve optimal photosynthetic and growth rates under the prevailing light conditions (Falkowski and LaRoche, 1991; van de Poll *et al.*, 2007; Ross *et al.*, 2008). On longer time scales (hours to days), photoacclimation is typically manifested in the variation of the intracellular proportion of chlorophyll *a* and accessory pigments present in the cells (Geider *et al.*, 1993; MacIntyre *et al.*, 2002; Kirk, 2011). As the light intensity at which phytoplankton grow becomes limiting, the cells increase the total concentration of pigments and/or the relative content of PSPs through an increase either in the number or the average size of photosynthetic units (Prézelin, 1981; Falkowski and LaRoche, 1991; Kirk, 2011). This is accompanied by a corresponding reduction in $a_{ph}(\lambda)$ due to the intensified pigment packaging. On the other hand, if phytoplankton are exposed to an increase in growth irradiances, cells will reduce the relative abundance of PSPs and increase the relative concentration of NPPs (Kana and Glibert, 1987; Johnsen and Sakshaug, 1996). Positive correlations between the relative proportion of NPPs and light intensities have been

widely documented in experimental studies on both eukaryotic and prokaryotic taxa (intensively reviewed in MacIntyre *et al*. 2002) and in field studies (Babin *et al.*, 1996; Bouman, Platt, Kraay, *et al.*, 2000; Lutz *et al.*, 2003). Changes in ratios of NPPs to PSPs as well as the total amount of pigment per cell due to photoacclimation can influence both the spectral shape and magnitude of $a_{ph}(\lambda)$ and offer another explanation, in addition to the impact of cell size, for the observed variability in absorptive properties of phytoplankton over the global ocean (Hoepffner and Sathyendranath, 1991; Sosik and Mitchell, 1995; Stuart *et al.*, 1998, 2000; Bouman, Platt, Kraay, *et al.*, 2000; Eisner *et al.*, 2003; Lohrenz *et al.*, 2003; Lutz *et al.*, 2003; Ferreira *et al.*, 2017). Moreover, photoacclimatory variation in pigment ratios and its impact on the shape of $a_{ph}(\lambda)$ may also provide important insight into phytoplankton photophysiology (SooHoo *et al.*, 1986; Johnsen *et al.*, 1994; Eisner *et al.*, 2003) and have been used as tracers for the degree of turbulent mixing in the surface ocean (Falkowski, 1983; Claustre *et al.*, 1994; Matsumoto and Ando, 2009).

Over the past few decades, biological oceanographers have examined patterns and sources of natural variation of $a_{ph}(\lambda)$ for different regions of the Atlantic Basin (Bricaud *et al.*, 1995, 2004; Lazzara *et al.*, 1996; Lutz *et al.*, 1996, 2003; Bouman, Platt, Kraay, *et al.*, 2000; Gibb *et al.*, 2000; Stuart *et al.*, 2000; Barlow *et al.*, 2002, 2004). However, most of these published studies focused on local or regional scales. In this study, a large *in situ* dataset of simultaneous measurements of $a_{ph}(\lambda)$ and pigment concentrations collected over a wide range of oceanographic regimes across the Atlantic Basin, including the undersampled Arctic Ocean and high nutrient-low chlorophyll (HNLC) regions of the Southern Ocean, is used to examine how changes in both the spectral shape and magnitude of $a_{ph}(\lambda)$ are related to changes in pigment composition. It then examines how these pigment-related changes correspond with pigment proxies of photoacclimation and size structure. While the relationship between pigment indices

of size and $a_{ph}(\lambda)$ has been fairly well described in previous investigations (Ciotti *et al.*, 2002; Bricaud *et al.*, 2004), the results of this study point to variation in NPPs which is the combined result of basin-scale photoacclimatory and taxonomic shifts in community structure as a key factor governing large-scale changes in absorptive properties of phytoplankton across trophic domains. The eco-physiological factors that govern the close relationship between phytoplankton light absorption, photoacclimatory status, and size structure are also explored.

2.2 Materials and Methods

2.2.1 Dataset

A database of phytoplankton absorption spectra and HPLC pigment concentrations was assembled from observations made on oceanographic cruises covering the four ecological biomes in the Atlantic Basin as defined by Longhurst (1998) (Figure 2.1 and Table 2.1). Since the principal motivation behind this study is to develop relationships between the optical properties of surface phytoplankton communities and their pigments that could be used for remote sensing applications, data collected from the optically-complex Coastal Biome were excluded. Analyses were also restricted to the top 20 m of the water column since satellite-borne sensors are unable to detect signals of ocean colour below the first attenuation length (Platt *et al.*, 2005).

2.2.2 Phytoplankton pigment composition

Phytoplankton pigment composition was determined using high-performance liquid chromatography (HPLC). Seawater samples were vacuum filtered onto GF/F (glass-fibre) filters, flash frozen in liquid nitrogen, and stored in a -60°C or -80°C freezer until analysis. Pigments were subsequently extracted in organic solvent and were analysed using a reverse-phase HPLC system. The filtration volume, organic solvents, and corresponding reference for each dataset are

summarised in Table 2.2. Pigment identification was based on comparison of retention times and spectral absorption of individual pigments determined with known standards.

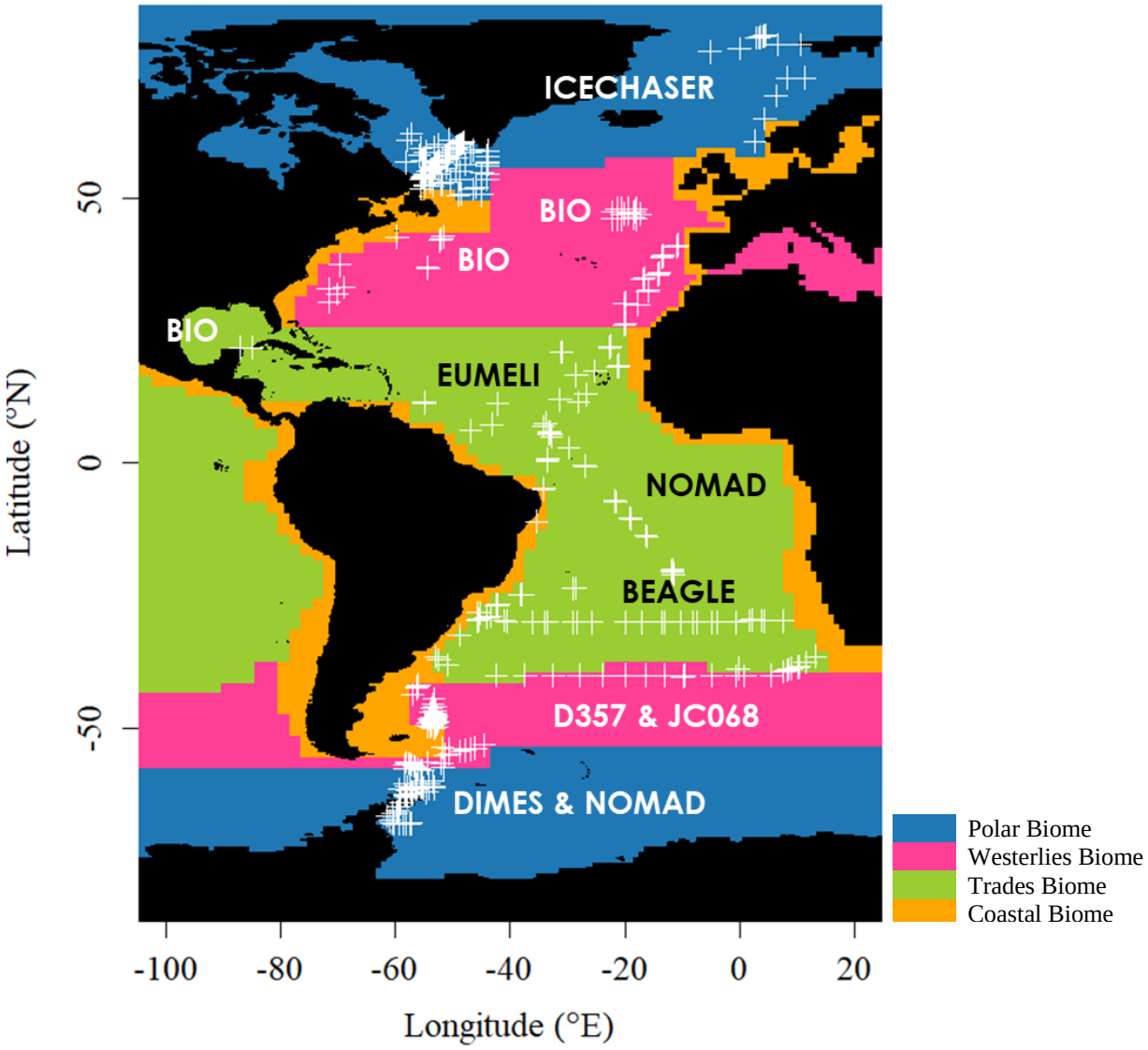


Figure 2.1: Map of sampling stations where phytoplankton absorption and pigment concentrations were measured simultaneously. The Polar, Westerlies, Trades, and Coastal Biomes defined according to Longhurst (1988) are shaded in blue, magenta, green, and orange, respectively. Note that stations located within the Coastal Biome were excluded from the database.

Table 2.1: Oceanographic data included in the database. *N* is the number of samples collected from each campaign after the data were quality controlled. Sampling depth was restricted to the upper 20 m of the water column.

Campaign	**Biome covered**	**Year**	***N***	**Reference**
BEAGLE [I]	Trades	2003	26	Bouman *et al*. (2006)
BIO [II]	Polar, Trades, Westerlies	1997-2003	177	Stuart *et al.* (2000)
D357 [III]	Trades, Westerlies	Oct-Nov 2010	18	Browning *et al*. (2014)
EUMELI-3 [IV]	Trades	Oct 1991	10	Bricaud *et al*. (1995, 2004)
ICE-CHASER [V]	Polar	Jun 2010	29	Jackson (2013)
JC068 [III]	Polar, Trades, Westerlies	Dec 2011-Jan 2012	24	Browning *et al*. (2014)
JC069/DIMES [III]	Polar, Westerlies	Feb-Mar 2013	45	Browning *et al*. (2014)
NOMAD [VI]	Polar, Trades, Westerlies	2000-02	125	Werdell and Bailey (2005); Hirata *et al.* (2008)
		Total	454	

I: The Blue EArth GLobal Expedition (BEAGLE)
(Japan Agency for Marine-Earth Science and Technology)

II: Bedford Institute of Oceanography, Canada

III: UK-GEOTRACES

IV: EUtrophy, MEsotrophy, oLigotrophy programme (EUMELI)
(The French Research Institute for Exploitation of the Sea)

V: ICE CHASER (CHAnging Sea-ice Ecosystem Response) expedition
(The Scottish Association for Marine Science)

VI: NASA bio-Optical Marine Algorithm Dataset (version 1.3.h, Feb 2007)
NOMAD is a large, publicly available dataset that combines optical and phytoplankton pigment observations collected across the global ocean (Werdell and Bailey, 2005). The dataset was part of the SeaWiFS Bio-optical Archive and Storage System (SeaBASS) maintained by the NASA Ocean Biology Processing Group. Subsets of the NOMAD dataset that was used in our analyses were obtained during the following oceanographic cruises (Werdell and Bailey, 2005):

(1) Antarctic Marine Living Resources (AMLR), NOAA, Weddell Sea, 2000-2002 (contributor: Dr B G Mitchell, *https://seabass.gsfc.nasa.gov/cruise/amlr2000* (AMLR2000), *https://seabass.gsfc.nasa.gov/cruise/amlr2001* (AMLR2001), and *https://seabass.gsfc.nasa.gov/cruise/amlr2002* (AMLR2002));
(2) EN355 cruise (WHOI Active Fluorescence Experiment), NW Atlantic, 2001 (contributor: Dr R Morrison, *https://seabass.gsfc.nasa.gov/cruise/en355*);
(3) Measurements on board the *Akademik Ioffe* Russian vessel along a Meridional Transect of the Atlantic Ocean, 2001 (contributor: Dr O Kopelevich, *https://seabass.gsfc.nasa.gov/cruise/ioffe01*);
(4) MANTRA-PIRANA, West Equatorial Atlantic, Jan-Feb 2001 (contributor: Dr A Subramaniam, *https://seabass.gsfc.nasa.gov/cruise/jan01sj*)

Table 2.2: Summary of the filtration volume (V), organic solvent, and reference for each method used for HPLC pigment analysis for each oceanographic campaign.

Campaign	HPLC pigment analysis			Reference
	Methodology	V	Solvent	
BEAGLE BIO	Head and Horne (1993)	1 L	90% acetone	Bouman *et al*. (2006) Stuart *et al*. (2000)
EUMELI-3	Claustre and Marty (1995)	4 L	Methanol	Claustre and Marty (1995)
ICE-CHASER	Barlow *et al*. (1997)	0.2-1 L	90% acetone	Jackson (2013)
D357 JC068 JC069	Gibb *et al*. (2000)	0.5-2 L	90% acetone	Browning *et al*. (2014)

Detailed procedures for HPLC pigment analysis for the NOMAD dataset are described in the work of Bidigare *et al.* (2003).

2.2.3 Pigment-based determination of phytoplankton size structure

Accessory pigments are useful for analysing the taxonomic composition of phytoplankton communities, provided that the pigment in question is a distinct marker for a particular phytoplankton class or group. Diagnostic pigments used in this study include fucoxanthin (FUCO), peridinin (PERID), alloxanthin (ALLO), 19′-hexanoyloxyfucoxanthin (19′-HEX), 19′-butanoyloxyfucoxanthin (19′-BUT), zeaxanthin (ZEA), and total chlorophyll *b* (TChl-*b*).

Vidussi *et al*. (2001) and Uitz *et al*. (2006) grouped phytoplankton taxa and their associated diagnostic pigments into three distinguish size classes: picophytoplankton (0.2-2 μm), nanophytoplankton (2-20 μm), and microphytoplankton (20-200 μm). From concentrations of diagnostic pigments, the relative contributions (percent) of the three size classes to TChl-*a* biomass, denoted as S_p, S_n, and S_μ for pico-, nano-, and microphytoplankton, respectively, can be computed as follows (Bricaud *et al.*, 2004):

$$S_p = \frac{0.86[\text{ZEA}] + 1.01[\text{TChl-}b]}{\text{DP}} \times 100, \quad (2.1)$$

$$S_n = \frac{0.60[\text{ALLO}] + 0.35[19'\text{-BUT}] + 1.27[19'\text{-HEX}]}{\text{DP}} \times 100, \quad (2.2)$$

$$S_\mu = \frac{1.41[\text{FUCO}] + 1.41[\text{PERID}]}{\text{DP}} \times 100, \quad (2.3)$$

where DP is the sum of the weighted concentrations of all diagnostic pigments:

$$\text{DP} = 1.41[\text{FUCO}] + 1.41[\text{PERID}] + 0.60[\text{ALLO}] + 0.35[19'\text{-BUT}] + 1.27[19'\text{- HEX}] + 0.86[\text{ZEA}] + 1.01[\text{TChl-}b]. \quad (2.4)$$

The numerical coefficients (weights) used in these equations were derived by conducting multiple linear regression analyses on a global HPLC-pigment database (Uitz *et al.*, 2006).

As a pigment-based proxy to represent the average cell size of a given phytoplankton sample for analysing the relationships between phytoplankton size and other variables of interest, the size index (SI), as proposed by Bricaud *et al*. (2004), was computed for each HPLC sample by assigning an average cell diameter to each size class (1, 5, and 50 μm for pico-, nano-, and microphytoplankton, respectively) and scaling to the value by the relative contribution of each size class determined using equations 2.1-2.4. The SI is expressed as:

$$\text{SI}\ (\mu\text{m}) = \frac{S_p + 5\,S_n + 50\,S_\mu}{100}. \quad (2.5)$$

Values of the SI vary from 1 μm for the pigment sample that is completely dominated by picophytoplankton to 50 μm by microphytoplankton (Bricaud *et al.*, 2004).

2.2.4 Phytoplankton light absorption

Seawater was filtered through GF/F filters, flash frozen in liquid nitrogen, and transferred to a -60°C or -80°C freezer until analysis. Optical densities of total particulates retained on the

filters, $O_p(\lambda)$, were measured over the visible wavelengths (350-750 nm) using a dual-beam spectrophotometer (model details see Table 2.3) equipped with an integrating sphere. The optical densities of the total particulates were then converted to absorption coefficients, $a_p(\lambda)$ [m^{-1}], by dividing by the geometrical path length, I_s, which is the ratio of the volume of seawater filtered, V [m^3], and the clearance area of the filter, S [mm^2], and applying a correction for optical path-length amplification (β-correction factor) resulting from scattering by the filter (Bouman, Platt, Kraay, *et al.*, 2000; Stuart *et al.*, 2000). The absorption coefficient for total particulates, $a_p(\lambda)$, was calculated using the following equation:

$$a_p(\lambda) = \frac{2.3\ O_p(\lambda)}{\beta\ I_s}, \tag{2.6}$$

where 2.3 is the conversion factor for transforming common (base 10) logarithms to natural logarithms, and β is the β-correction factor which converts the spectrophotometric data of optical density to the absorption coefficient and it is important to note that different laboratories applied different β factors to obtain estimates of $a_p(\lambda)$ (see Table 2.3 for details). The optical density of detrital material, $O_d(\lambda)$, was measured after extracting both the sample and the blank filters with hot methanol as described in Kishino *et al*. (1985). By subtracting the detrital absorption spectra, $a_d(\lambda)$, from the total absorption spectra, phytoplankton absorption coefficients, $a_{ph}(\lambda)$, were then obtained (Bouman, Platt, Kraay, *et al.*, 2000):

$$a_{ph}(\lambda) = a_p(\lambda) - a_d(\lambda). \tag{2.7}$$

The chlorophyll *a*-specific absorption coefficient of phytoplankton at wavelength λ, $a^*_{ph}(\lambda)$ [m^2 (mg Chl-*a*)$^{-1}$], can then be derived by normalising $a_{ph}(\lambda)$ [m^{-1}] to the HPLC-determined total chlorophyll *a* concentration (TChl-*a*) [mg Chl-*a* m^{-3}], which is the sum of concentrations of monovinyl chlorophyll *a* and divinyl chlorophyll *a*.

Table 2.3: Summary of the filtration volume (V), equipment, and β-correction algorithms (β) used to measure phytoplankton absorption for each oceanographic campaign.

Campaign	Absorption measurement			Reference
	V	Equipment	β	
BEAGLE BIO	1 L	Shimadzu UV-2101 PC spectrophotometer	Hoepffner and Sathyendranath (1992)	Bouman *et al*. (2006) Stuart *et al*. (2000)
EUMELI-3	4 L	LICOR 1800 UW spectro-radiometer	Bricaud and Stramski (1990)	Claustre and Marty (1995)
ICE-CHASER	0.5-l L	Perkin-Elmer Lambda 800 spectrophotometer	Hoepffner and Sathyendranath (1992)	Jackson (2013)
D357 JC068 JC069	0.5-1 L	Shimadzu UV-2550 spec-trophotometer	Cleveland and Weidemann (1993)	Browning *et al*. (2014)
AMLR*		Varian Cary-1 spectropho-tometer	Mitchell (1990)	Mitchell (2002)
EN355*		Perkin-Elmer Lambda 18 spectrophotometer	Mitchell (1990)	
IOFFE*	1-5 L	Cary-50 spectrophotometer	Mitchell *et al*. (2000)	Rudorff *et al*. (2007)
MANTRA-PIRANA*	3.15 L	Shimadzu 2401-PC spec-trophotometer	Mitchell *et al*. (2002)	del Vecchio and Subramaniam (2004)

* NOMAD dataset

2.2.5 Data quality assurance

Given that our Atlantic database was constructed from different subsets of data provided by various institutions and laboratories (Table 2.1), phytoplankton pigment and absorption data were quality controlled independently using a variety of published criteria. Only samples with a minimum of four detected accessory pigments were included in the pigment database as previously suggested by Trees *et al*. (2000). Using a global dataset, Trees and colleagues (2000) also demonstrated that $\log_{10}$ transformed accessory pigment concentrations strongly covary with TChl-*a* in a near-linear fashion, with the regression slope of 0.93. Similarly, I conducted log-log regressions of total accessory pigment concentration on TChl-*a* and observed the overall slope of 0.94 ($R^2 = 0.95$). A few outliers (N = 9), whose calculated standard deviations (SD)

were larger than 3 in absolute value (Uitz *et al.*, 2006), were then removed, leaving 872 surface samples in the pigment database (final slope = 0.94, R^2 = 0.96). For the absorption database, spectra were removed if they contained negative values (N = 26) in the visible (400-700 nm) region of the spectrum or they were potentially overestimated (N = 7) due to the interference by phaeopigments using the criterion $a^*_{ph}(420) > a^*_{ph}(440)$ (Bricaud *et al.*, 1995). The quality of the absorption data was also ensured by the regression of $a_{ph}(440)$ on $a_{ph}(490)$ (Hirata *et al.*, 2008) and outlier removal (|SD| > 3; N = 7) (final R^2 = 0.99). The absorption database was overall reduced to 468 observations, which was 92% of the original data. The final merged database consisted of 454 simultaneous measurements of $a_{ph}(\lambda)$ and pigment concentration.

2.2.6 Estimation of light absorption by non-photosynthetic pigments

The relative contribution of non-photosynthetic pigments (NPP) to total phytoplankton light absorption (due to all pigments), denoted as $c_{np}(\lambda)$, was estimated using the following expression described in Babin *et al*. (1996):

$$c_{np}(\lambda) = \frac{\sum_{m=1}^{np} c_m \, a^*_m(\lambda)}{\sum_{m=1}^{n} c_m \, a^*_m(\lambda)} \quad , \tag{2.8}$$

where $a^*_m(\lambda)$ is the weight-specific absorption coefficient of the *m*th pigment in solvent at wavelength λ provided by Bidigare *et al*. (1990), c_m is the concentration of the *m*th pigment, *np* is the total number of NPPs in the sample, and *n* is the total number of all pigments in the sample. The *in vivo* absorption coefficient of NPPs, $a_{NPP}(\lambda)$, could then be derived through multiplying the quantity $c_{np}(\lambda)$ by the measured *in vivo* absorption coefficient of phytoplankton ($a_{ph}(\lambda)$):

$$a_{NPP}(\lambda) = c_{np}(\lambda) \, a_{ph}(\lambda). \tag{2.9}$$

2.3 Results

2.3.1 Variation in the chlorophyll *a*-specific absorption coefficient of phytoplankton

In this study, the chlorophyll *a*-specific absorption coefficient of phytoplankton at 440 nm (a^*_{ph}(440)) was used as an indicator of the absorptive efficiency of phytoplankton in the blue region of the spectrum since the 440-nm waveband corresponds to the absorption peak of chlorophyll *a* (Chl-*a*) and is commonly used in various bio-optical and remote sensing algorithms. For our Atlantic dataset, a^*_{ph}(440) ranged from *ca* 0.01 to 0.26 m^2 (mg Chl-*a*)$^{-1}$ for samples collected from the Subantarctic Province in the Westerlies Biome and the Caribbean Province in the Trades Biome, respectively.

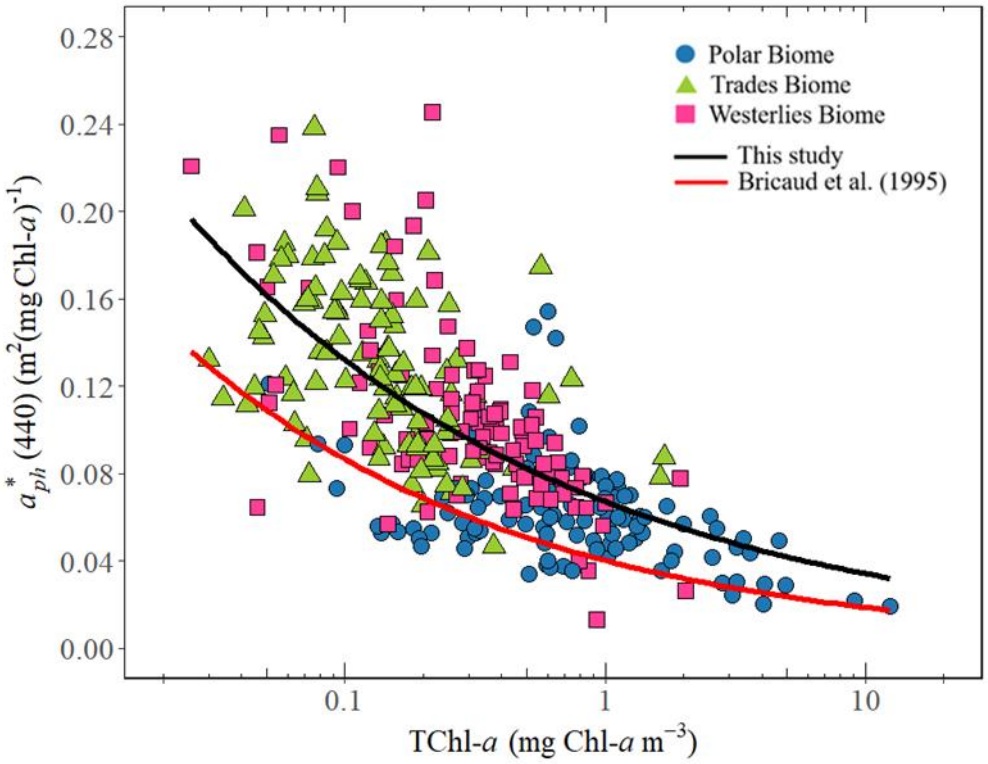


Figure 2.2: Chlorophyll *a*-specific absorption coefficients of phytoplankton at 440 nm (a^*_{ph}(440)) plotted against the total chlorophyll *a* concentration (TChl-*a*). A power regression line ($a^*_{ph}(440) = 0.067\,[\text{TChl-}a]^{-0.293}$, black line) fitted to the entire dataset is shown along with the equation used in the study of Bricaud et al. (1995) ($a^*_{ph}(440) = 0.0403\,[\text{TChl-}a]^{-0.332}$, red line). The blue circle, green triangle, and magenta square correspond to data collected from the Polar, Trades, and Westerlies Biomes (Longhurst, 1998), respectively.

Figure 2.2 illustrates that, to a first order, $a^*_{ph}(440)$ decreased with increasing total chlorophyll *a* concentration (TChl-*a*) ($R^2 = 0.53$, $p < 0.01$). TChl-*a* varied from 0.03 mg Chl-*a* m^{-3} in the North Atlantic subtropical gyres (Westerlies Biome) to 12.5 mg Chl-*a* m^{-3} in the Arctic region (Polar Biome). Marked differences in absorptive properties of phytoplankton were observed for the Polar and Trades Biomes: while samples collected from the polar seas showed consistently low $a^*_{ph}(440)$ over a broad range of TChl-*a*, the Trades Biome samples were mostly confined to waters of low surface TChl-*a* of less than 0.1 mg Chl-*a* m^{-3} and exhibited elevated values of $a^*_{ph}(440)$ that were more variable. The majority of data taken from the Westerlies Biome were restricted to between TChl-*a* values of 0.1 and 1.0 mg Chl-*a* m^{-3}, yet this particular biome showed the largest range of $a^*_{ph}(440)$ (0.01 m^2 (mg Chl- *a*)$^{-1}$ recorded in the Southern Ocean compared to over 0.24 m^2 (mg Chl-*a*)$^{-1}$ in the subtropical gyres). The dependence of $a^*_{ph}(440)$ on TChl-*a* observed in this study could be described using a power function and followed a similar trend to that obtained in the work of Bricaud and colleagues (1995) (Figure 2.2), which used bio-optical data collected in different (Case I) waters of the global ocean. Our data, however, showed somewhat higher $a^*_{ph}(440)$ values for comparable ranges in TChl-*a*.

2.3.2 Variation in cell size and photoacclimatory status of phytoplankton

The inverse relationship between $a^*_{ph}(440)$ and TChl-*a* in the surface ocean has been widely observed in previous published studies (Yentsch and Phinney, 1989; Bricaud *et al.*, 1995, 2004) and attributed to a progressive increase in the dominant cell size of phytoplankton assemblages, and thus pigment packaging, as one moves from oligotrophic (i.e. low TChl-*a*, < 0.2 mg Chl-*a* m^{-3}; Bricaud *et al*. 2004) open-ocean conditions dominated by picocyanobacteria to more eutrophic (i.e. high TChl-*a*) coastal regions where large-celled eukaryotic phytoplankton of the micro- and nano-size classes typically thrive (Chisholm, 1992; Bricaud *et al.*, 2004; Brewin *et al.*, 2011). For this dataset, a positive correlation between surface TChl-*a* and gross estimates

for the average cell diameter of phytoplankton populations (Bricaud *et al.*, 2004) determined using the diagnostic pigment-based approach (Claustre, 1994; Vidussi *et al.*, 2001; Uitz *et al.*, 2006) (R^2 = 0.48, $p < 0.01$; Figure 2.3a) was observed, although the size index was weakly correlated with $a^*_{ph}(440)$ (R^2 = 0.29, $p < 0.01$, data not shown).

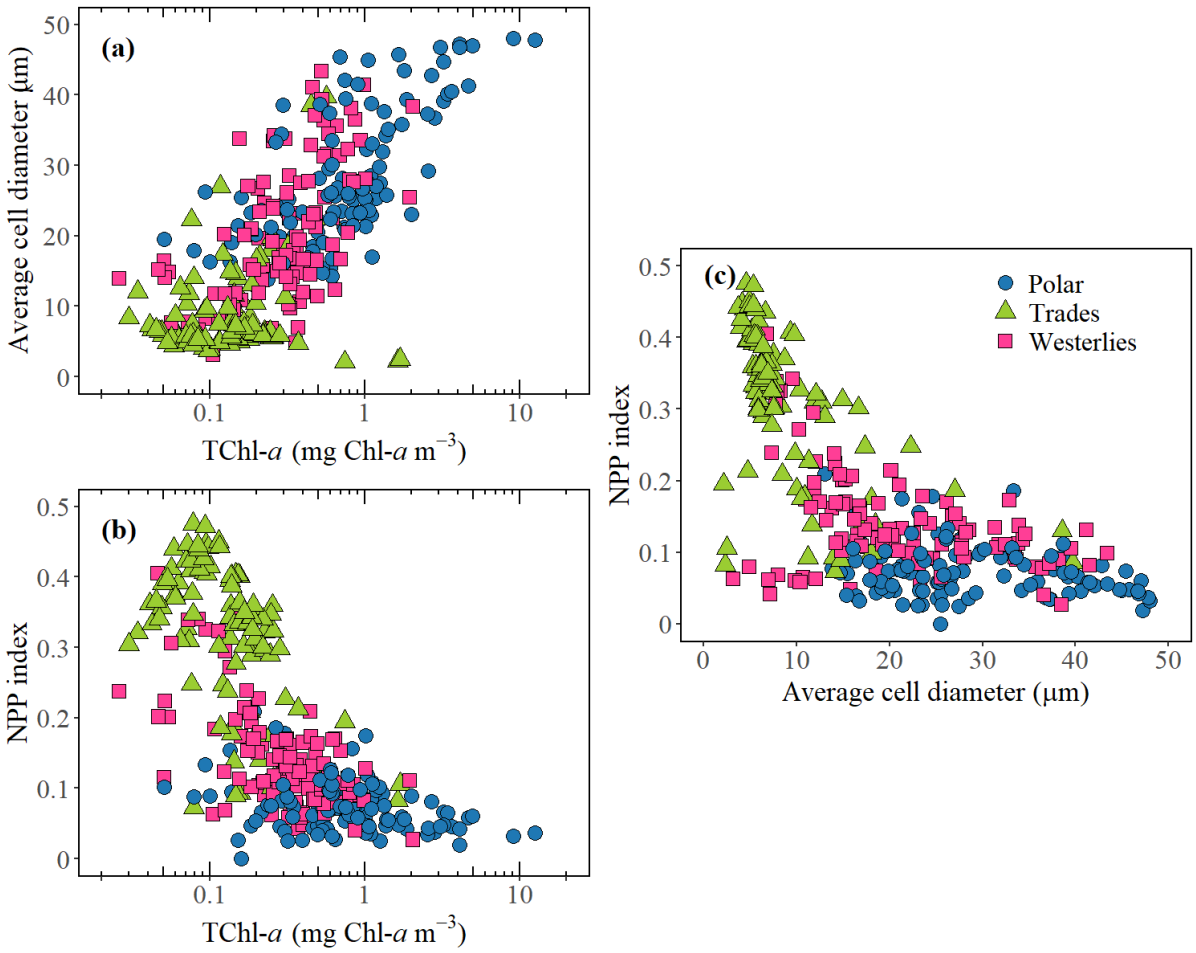


Figure 2.3: (a) The average cell diameter of phytoplankton populations calculated using the pigment-based method of Bricaud *et al*. (2004) and (b) the NPP index plotted against the total chlorophyll *a* concentration (TChl-*a*). (c) The NPP index plotted against pigment-based estimates of the average cell diameter. Colour and shape are assigned according to oceanic biomes. Note that the average cell size of 50 µm and 1 µm can be interpreted as the complete dominances of microphytoplankton and picophytoplankton, respectively.

In the open ocean, an increase in surface TChl-*a* may also indicate a reduction in the light available for phytoplankton (Morel and Maritorena, 2001; Kirk, 2011). It can therefore be anticipated that a decrease in growth irradiance would lead to an overall decrease in the proportion of non-photosynthetic or photoprotective pigments (NPPs: zeaxanthin, diadinoxanthin, diatoxanthin, alloxanthin, β-carotene) relative to total pigments (i.e. chlorophylls and both photosynthetic and non-photosynthetic carotenoids) or the NPP index, given that this pigment index has been shown to be a robust indicator of photoacclimatory status of phytoplankton (Babin *et al*. 1996) and this was clearly evident in Figure 2.3b ($R^2 = 0.52$, $p < 0.01$). The oligotrophic gyres in the Trades and Westerlies Biomes showed markedly high values of the NPP index, indicating that small picocyanobacteria dominating in these waters are acclimated to high growth irradiances. In contrast, in the Polar Biome, which tends to be dominated by larger eukaryotes, the NPP index was consistently low across a large range of TChl-*a* (Figure 2.3b). The overall inverse relationship between the NPP index and the size structure of phytoplankton communities is illustrated in Figure 2.3c ($R^2 = 0.53$, $p < 0.01$).

To quantify the relative significance of NPPs to phytoplankton absorption in the oligotrophic open ocean, the spectral reconstruction technique of Babin and colleagues (1996) was used (equations 2.8-2.9). NPP absorption at 440 nm, $a_{NPP}(440)$, accounted for up to 60% of total absorption by phytoplankton whereas in meso- and eutrophic waters in the Westerlies and Polar Biomes, $a_{NPP}(440)/a_{ph}(440)$ was generally low (Figure 2.4). However, there were a few Arctic Ocean samples collected at the ice or under-ice stations that showed relatively high percent contribution of NPPs to phytoplankton absorption. Yet, despite the presence of anomalously high NPP in some samples, the mean value of the estimated percent absorption by NPPs for the Arctic Ocean samples was significantly lower than that for those collected from the Antarctic provinces (*t*-test, 95% confidence interval, $p < 0.05$).

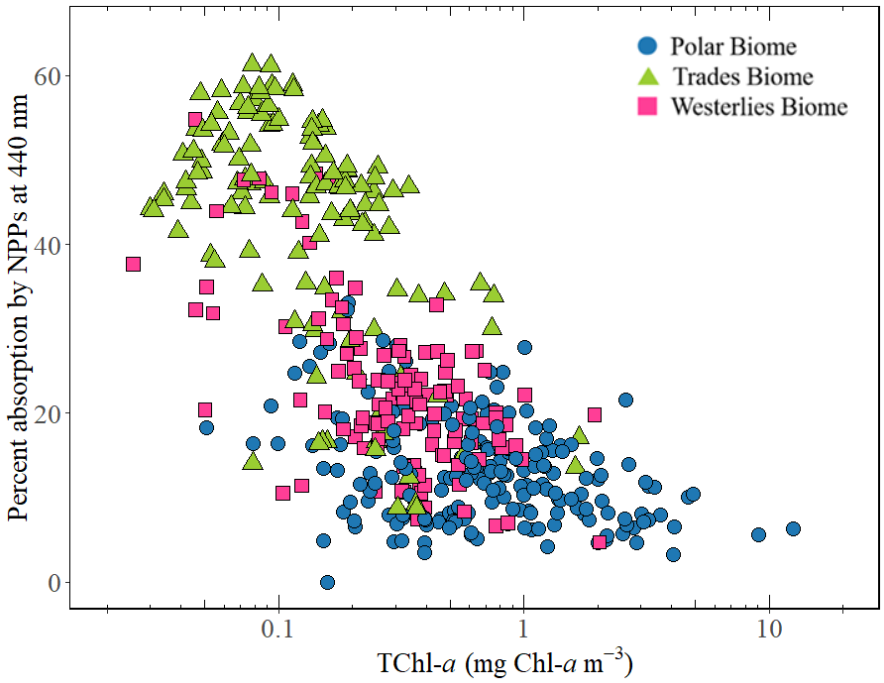


Figure 2.4: Estimates of percent absorption by non-photosynthetic pigments (NPPs) at 440 nm plotted against the total chlorophyll *a* concentration (TChl-*a*). Absorption by NPPs was determined using the modified spectral reconstruction method of Babin *et al*. (1996).

Zeaxanthin, a diagnostic pigment maker for the picocyanobacteria genera *Synechococcus* and *Prochlorococcus* (Vidussi *et al.*, 2001; Uitz *et al.*, 2006), was the most abundant NPP in oligotrophic waters in the Trades and Westerlies Biomes (Figure 2.5a). Therefore, this abundant photoprotective carotenoid (Gieskes *et al.*, 1988) primarily governs relationships between NPPs and other variables of interest, including phytoplankton absorption, in mid- and low-latitude open waters. These results are consistent with other studies (Sosik and Mitchell, 1995; Allali *et al.*, 1997; Barlow *et al.*, 2002; Bouman *et al.*, 2006, 2011) that reported high relative concentrations of zeaxanthin in the surface waters of the tropical and subtropical waters. The fractional contribution of zeaxanthin to total pigment concentration substantially decreased as TChl-*a* increased ($R^2 = 0.48$, $p < 0.01$; Figure 2.5a). The pigment was present at low concentrations in the Arctic Ocean (Polar Biome) and was barely detectable over a gradient of TChl-*a* in the subantarctic (Westerlies Biome) and austral polar (Polar Biome) regions in the Southern Ocean.

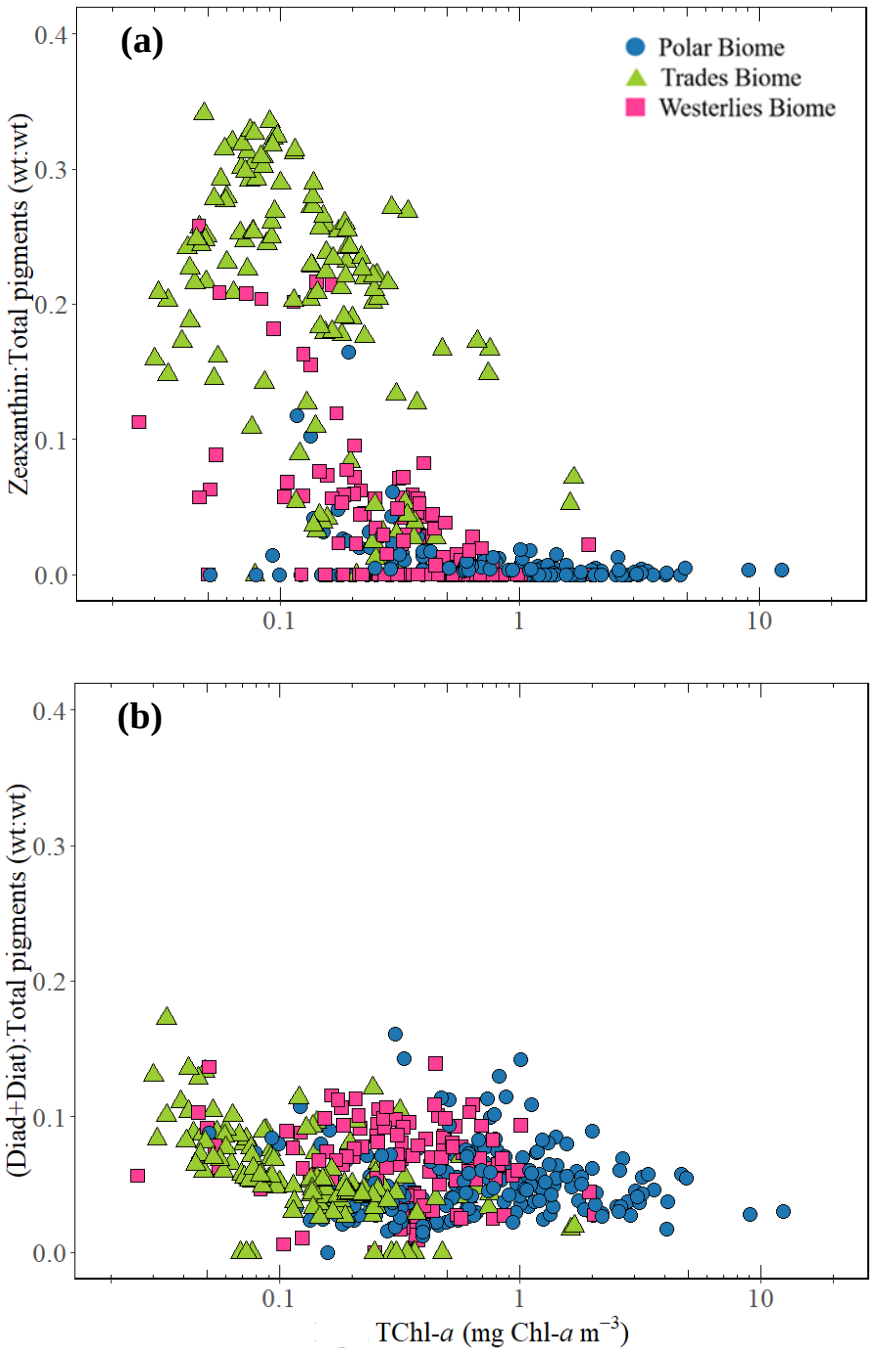


Figure 2.5: The weight-to-weight ratio of (a) zeaxanthin and (b) the sum of diadinoxanthin (Diad) and diatoxanthin (Diat) to total pigment concentration plotted against the total chlorophyll *a* concentration (TChl-*a*).

In the Arctic and Southern Ocean samples, diadinoxanthin and diatoxanthin were dominant NPPs (Figures 2.5b). However, in contrast to zeaxanthin that showed a strong inverse relationship with TChl-*a* (Figure 2.5a), the summed concentration of diadinoxanthin and diatoxanthin relative to total pigments (Diad+Diat) was overall poorly correlated with TChl-*a* ($R^2 = 0.07$, $p < 0.01$; Figure 2.5b) with values of Diad+Diat typically falling below 10%. While Diad+Diat measured in the Westerlies and Polar Biomes appeared to remain relatively unchanged over a gradient of TChl-*a*, data collected from the Trades Biome, when exclusively analysed, exhibited a distinctively stronger correlation between Diad+Diat and TChl-*a* ($R^2 = 0.35$, $p < 0.01$). It should be noted by summing both diadinoxanthin and diatoxanthin, the light-induced, short-term interconversion between the two pigments (Fujiki *et al.*, 2003) that might arise at any stage of sample processing is accounted for, which is likely the reason for the higher correlation coefficient.

2.3.3 Effect of non-photosynthetic pigments on phytoplankton absorption

Given that both $a^*_{ph}(440)$ and the NPP index were negatively correlated with TChl-*a* (Figures 2.2 and 2.3b), and that NPPs absorb very strongly in the blue-green (*ca* 420-510 nm) region of the visible spectrum (Bidigare *et al.*, 1990), NPPs govern a significant fraction of the overall variability in the absorption of blue photons. The strong dependence of phytoplankton absorption on NPPs is clear when $a^*_{ph}(440)$ is plotted against the NPP index (Figure 2.6), revealing a positive correlation ($R^2 = 0.39$, $p < 0.01$). This pattern appeared to be particularly strong for stations located within the Trades Biome where NPPs contributed more than 20% to total pigment concentration. There were, however, several pigment samples collected from the Trades and Westerlies Biomes that had the NPP index of less than 0.2 yet exhibited relatively high $a^*_{ph}(440)$ values (> 0.16 m^2 (mg Chl-*a*)$^{-1}$). Since the data points were sampled in the South Atlantic Gyral Province (Trades Biome) (Longhurst, 1998) and the South Subtropical Convergence

Province (Westerlies Biomes), the relationships between $a^*_{ph}(440)$ and NPPs in these provinces were examined separately (Figure 2.7).

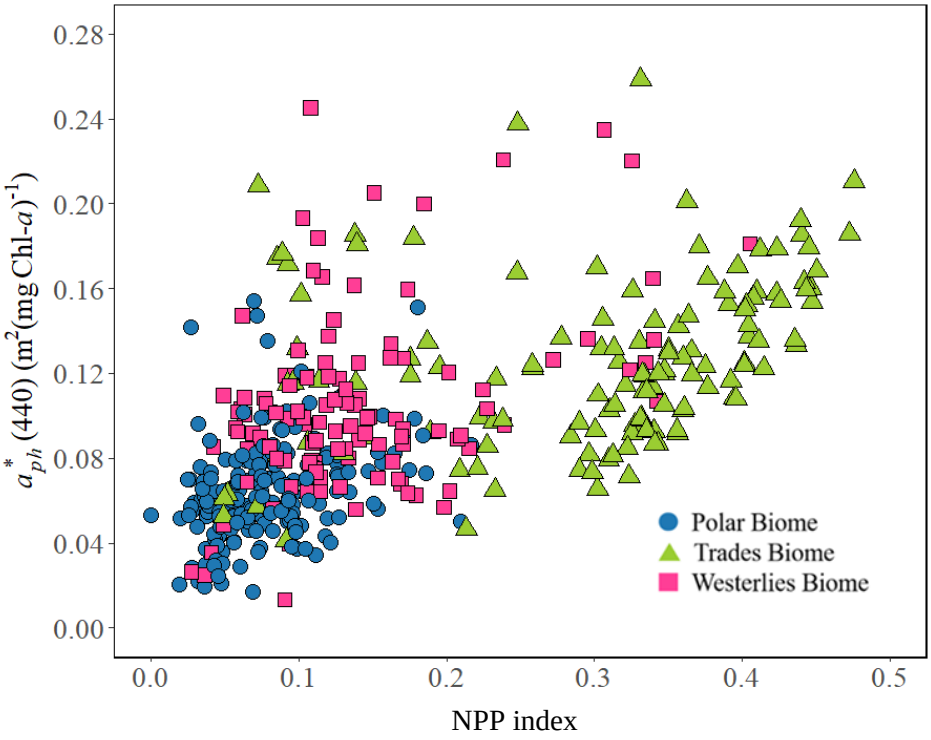


Figure 2.6: Chlorophyll *a*-specific absorption coefficients of phytoplankton at 440 nm ($a^*_{ph}(440)$) plotted against the NPP index.

Overall, there was no statistically significant correlation between $a^*_{ph}(440)$ and the NPP index for both provinces (Figures 2.7a, b). A high degree of scatter in the relationship observed in the South Atlantic Gyral Province appeared to originate from the cluster of points with the NPP index of lower than 0.3 (Figure 2.7a). If these samples were removed from the analysis, some 36% ($p < 0.01$) of the variance in $a^*_{ph}(440)$ measured in this province could be explained by changes in the NPP index. Removal of this cluster of points also improved the R^2 value for the relationship observed in the Trades Biome from approximately 0.09 to 0.44 ($p < 0.01$).

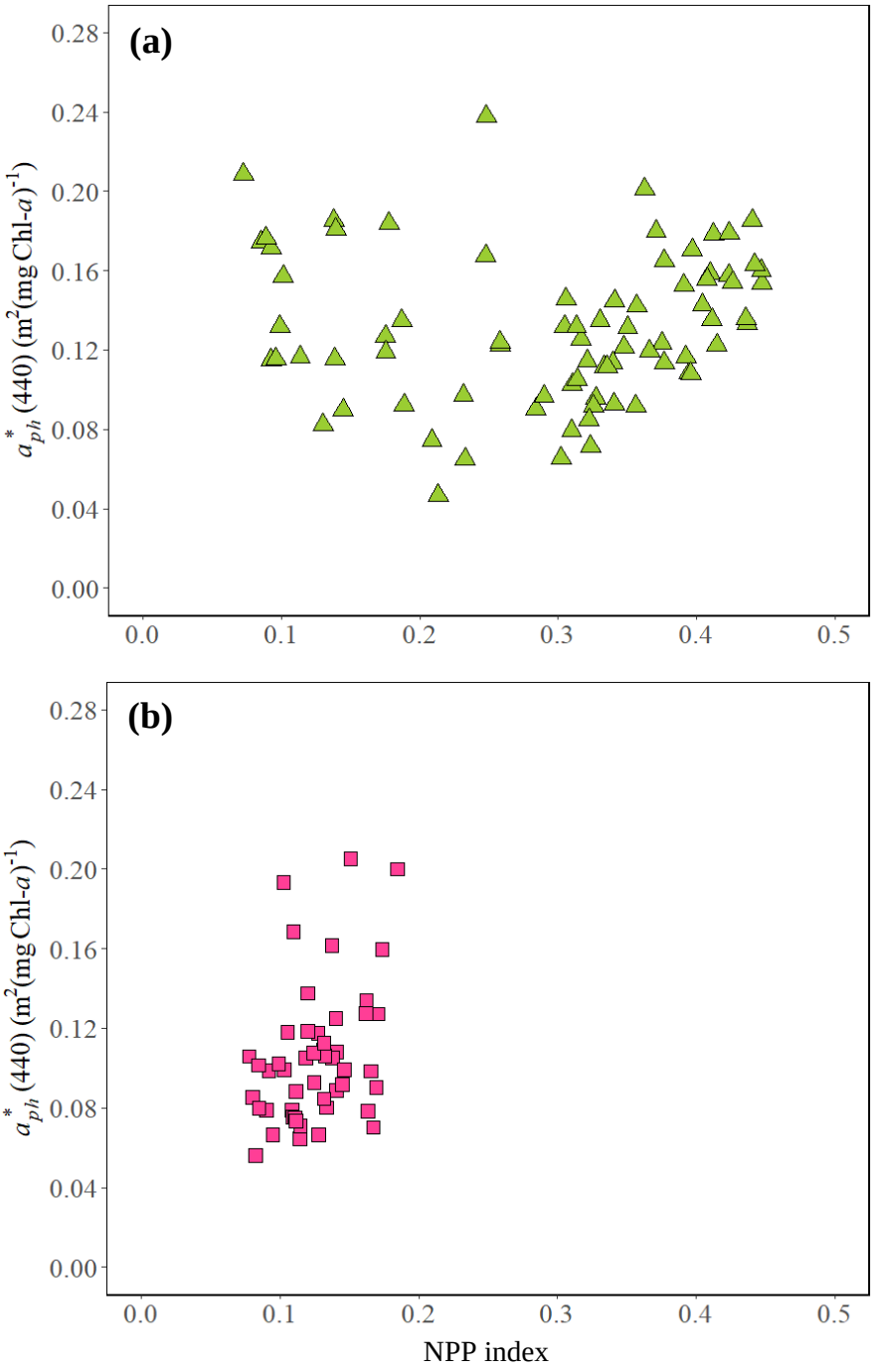


Figure 2.7: Chlorophyll *a*-specific absorption coefficients of phytoplankton at 440 nm ($a^*_{ph}(440)$) plotted against the NPP index for sampling sites located within (a) the South Atlantic Gyral Province (Trades) and (b) the South Subtropical Convergence Province (Westerlies Biome).

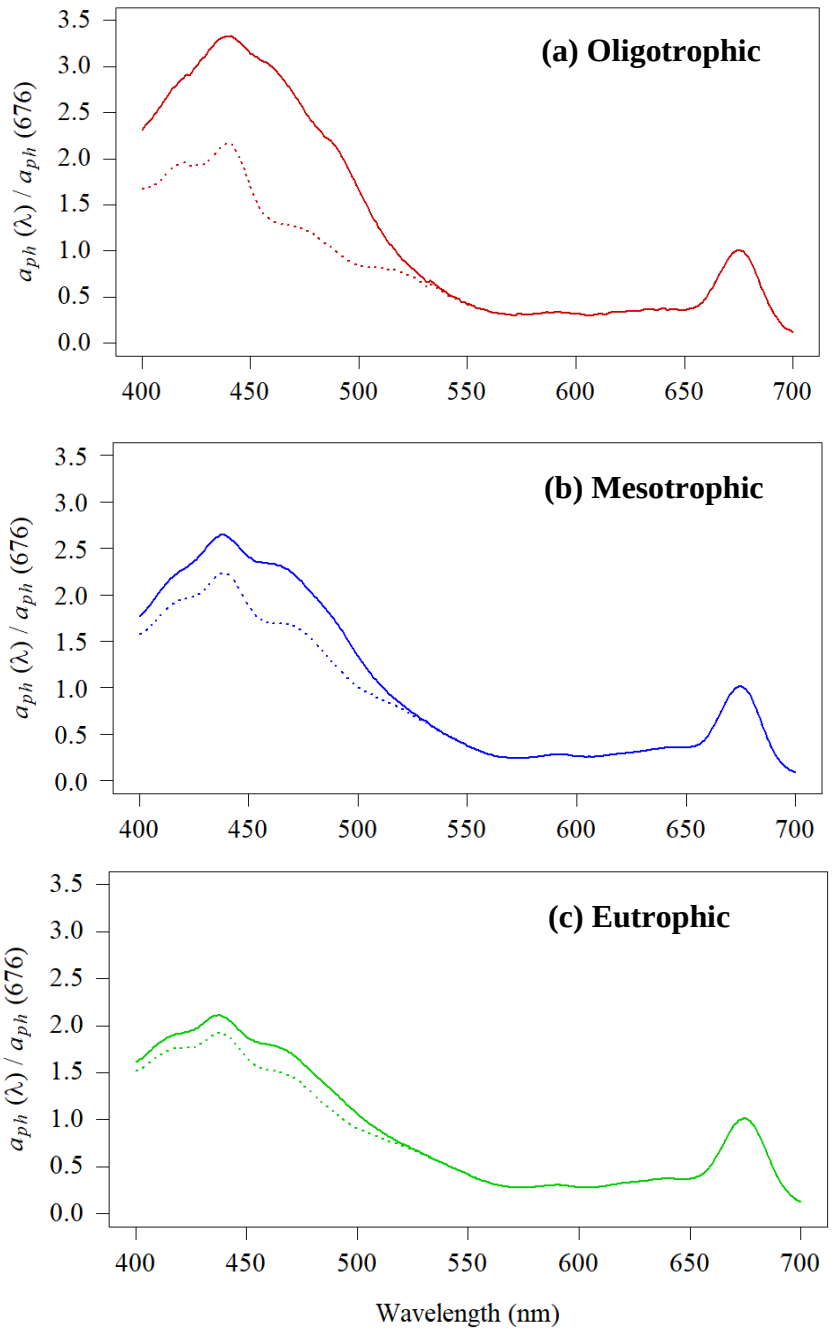


Figure 2.8: Average phytoplankton absorption spectra ($a_{ph}(\lambda)$) at various intervals of total chlorophyll *a* concentration (TChl-*a*): (a) oligotrophic (TChl-*a* < 0.2 mg Chl-*a* m^{-3}), (b) mesotrophic (TChl-*a* = 0.2-2.0 mg Chl-*a* m^{-3}), and (c) eutrophic condition (TChl-*a* > 2.0 mg Chl-*a* m^{-3}). Spectra were normalised to 676 nm ($a_{ph}(676)$) prior to averaging. Solid lines represent total absorption of phytoplankton, and dotted lines represent phytoplankton absorption with the contribution of non-photosynthetic pigments (NPPs) removed.

Next, to examine the variability in the shape of phytoplankton absorption spectra, absorption coefficients of phytoplankton at each wavelength, $a_{ph}(\lambda)$, were normalised with respect to the absorption coefficient at 676 nm, $a_{ph}(676)$. The normalised absorption spectra for surface samples were then averaged over different intervals of TChl-*a* as shown in Figure 2.8.

A progressive flattening of the averaged absorption spectra with increasing TChl-*a* likely resulted from an increase in pigment packaging from oligotrophic to more productive conditions as previously described in Section 2.3.1. To directly illustrate that NPPs were an important additional factor responsible for the observed variation in the spectral shape of phytoplankton absorption, the contribution of NPPs was removed using the spectral reconstruction method. The resulting spectra of phytoplankton absorption due solely to photosynthetic pigments were subsequently compared with the measured total absorption spectra (Figures 2.8a-c).

The amplitude of the 440-nm absorption peaks of all the three phytoplankton absorption spectra were systematically reduced after the absorption by NPPs were removed, with the largest difference seen at low TChl-*a* where NPPs were abundant (Figure 2.8a) (reduction of *ca* 35.3% compared to 16.7% and 9.5% for meso-, and eutrophic conditions, respectively). Differences in the spectral shape between the measured and reconstructed spectra were also most noticeable at the oligotrophic condition: the blue absorption peak became much narrower, and there was a dramatic reduction (*ca* 41.7% compared to 23.9% and 16.7% for meso- and eutrophic conditions, respectively) in absorption at approximately 450-470 nm (Figure 2.8a), the spectral region corresponding to the blue absorption peak of the NPP zeaxanthin (Bricaud *et al.*, 2004). At higher TChl-*a* (meso- and eutrophic conditions; Figures 2.8b, c), the spectral shapes of phytoplankton absorption converged, reflecting similarities in the taxonomic structure of phytoplankton communities, and there appeared to be no major alteration of the shapes of absorption spectra after the removal of the contribution of NPPs to phytoplankton absorption.

The slope of phytoplankton absorption spectra in the blue-green region was also strongly influenced by the varying proportion of NPPs. When the spectral slope from 443 to 510 nm (Hirata *et al.*, 2008) normalised to 676 nm was plotted against the NPP index (Figure 2.9), it was clear that an increase in the NPP index resulted in steeper slopes ($R^2 = 0.55$, $p < 0.01$).

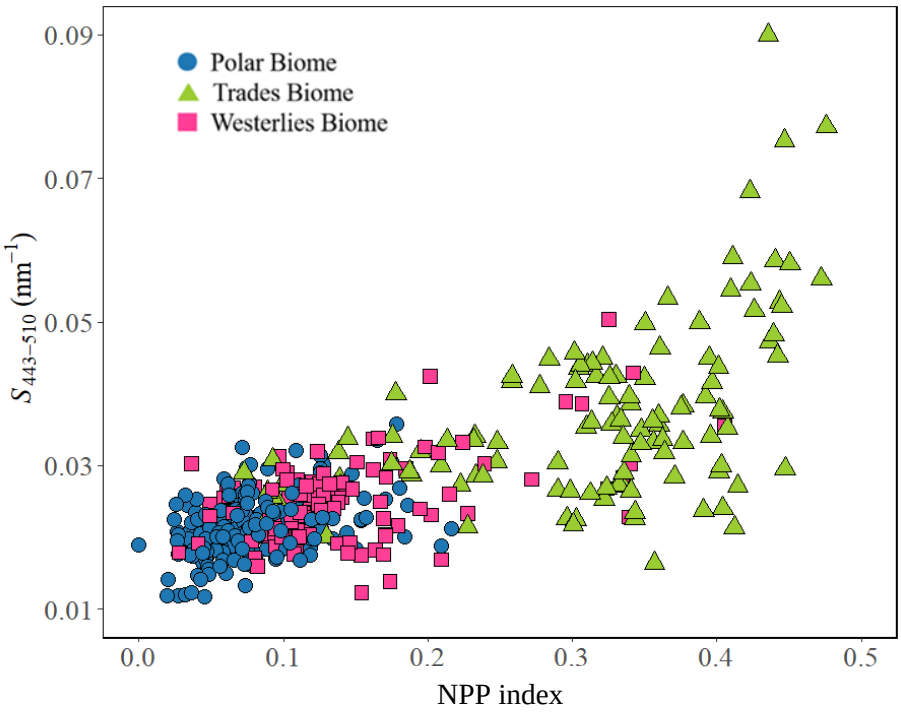


Figure 2.9: The spectral slopes of phytoplankton absorption in the blue-green region of the spectrum from 443 nm to 510 nm normalised to 676 nm ($S_{443-510}$) plotted against the NPP index.

2.3.4 The role of *Prochlorococcus* in governing the relationship between NPPs and phytoplankton absorption

It has been shown throughout this study that relationships between TChl-*a*, phytoplankton absorption, and the significance of NPPs as an index of phytoplankton photoacclimation (Sections 2.3.1-2.3.3) were most prevalent in the oligotrophic tropical and temperate gyres (Trades and Westerlies Biomes) where picocyanobacteria, which contain zeaxanthin (Section 2.3.2),

are known to dominate. *Prochlorococcus* was found to contribute significantly to the zeaxanthin pool measured in the gyral regions as was evident by a strong positive correlation between the relative concentration of zeaxanthin to total pigments and the TChl-*a*-normalised concentration of divinyl chlorophyll *a* which has been widely used as a pigment marker for *Prochlorococcus* (Bouman *et al.*, 2006; Uitz *et al.*, 2006) ($R^2 = 0.80$, $p < 0.01$; Figure 2.10).

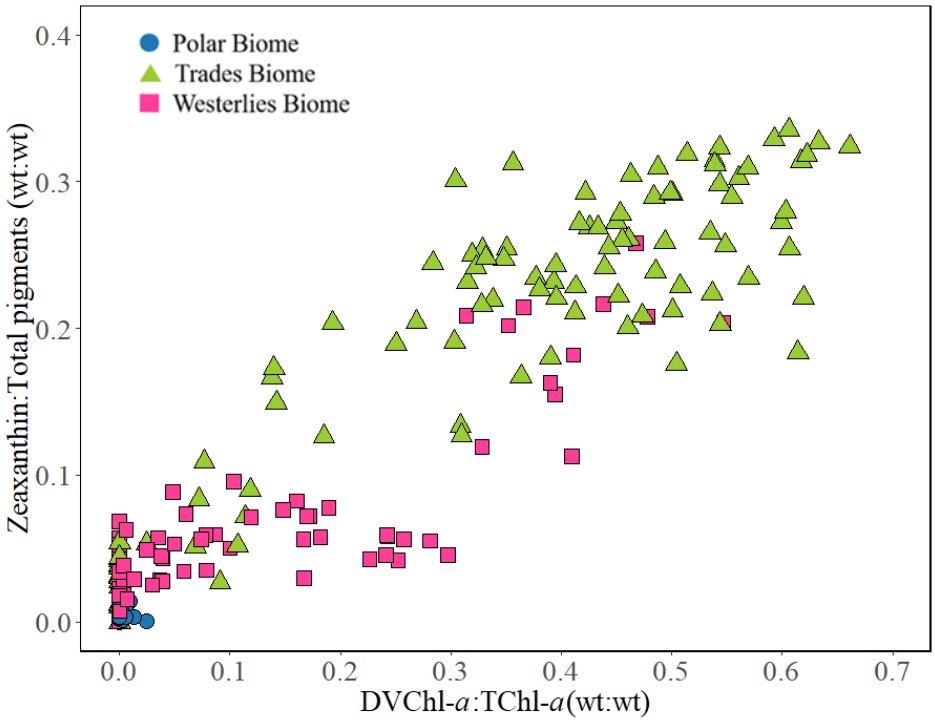


Figure 2.10: The weight-to-weight ratio of zeaxanthin to total pigment concentration plotted against the weight-to-weight ratio of divinyl chlorophyll *a* (DVChl-*a*) to total chlorophyll *a* concentration (TChl-*a*).

2.4 Discussion

2.4.1 Variation in phytoplankton absorption

Phytoplankton light absorption is an inherent optical property which has been used to monitor the large-scale distribution of phytoplankton functional types and size classes in the surface ocean using remote sensing, and is an essential input variable in bio-optical models of marine primary production. It is therefore critical to understand the sources of its natural variability and how much of the absorbed light is available for photosynthesis (Bouman, Platt, Kraay, *et al.*, 2000). The light absorption efficiency of phytoplankton cells is normally measured in terms of the chlorophyll *a* (Chl-*a*)-specific absorption coefficient, $a^*_{ph}(\lambda)$, particularly in the blue region of the spectrum (*ca* 440 nm) corresponding to the major absorption peak of Chl-*a*. In this study, $a^*_{ph}(440)$ was found to be inversely correlated with TChl-*a*, which is consistent with other studies (Yentsch and Phinney, 1989; Bricaud *et al.*, 1995, 2004; Sathyendranath *et al.*, 1996; Allali *et al.*, 1997; Stuart *et al.*, 2004; Ferreira *et al.*, 2013). However, our measured $a^*_{ph}(440)$ values appeared higher, especially at low ambient TChl-*a* (Figure 2.2) when compared to the study of Bricaud *et al*. (1995). One explanation for this difference is that for this Atlantic Basin dataset, samples from the oligotrophic waters tended to have higher relative abundance of blue light-absorbing non-photosynthetic pigments (NPPs). While the NPP:TChl-*a* ratio for surface samples in the Bricaud *et al*. (1995) study never exceeded the value of 1.0, in our dataset, samples with TChl-a < 0.2 mg Chl-*a* m^{-3} had the NPP:TChl-*a* ratio of up to 1.5 (data not shown). Also, as pointed out in Bricaud and Stramski (1990) and Bricaud *et al*. (1995), the presence of nonalgal particulate material, which also absorbs strongly in the blue wavebands, if not completely removed from the total particulate spectrum, could result in an overestimation of $a^*_{ph}(440)$ at low TChl-*a*. Yet the plot of $a_{ph}(440)$ against TChl-*a* shows no vertical intercept, implying that absorption by non-algal material was an unlikely cause of the high $a^*_{ph}(440)$ values (Bricaud *et al.*, 1995). Moreover, in contrast to our Atlantic dataset, which consisted

mostly of data obtained from oligotrophic and mesotrophic environments, a relatively large fraction of observations in the Bricaud's global dataset was confined to very productive regions, such as the upwelling system off Peru and the Gulf of St Lawrence, where TChl-*a* reached *ca* 25 mg Chl-*a* m^{-3}. Thus, another possibility is that the samples from the Bricaud *et al*. (1995) study consisted of larger cells with higher levels of pigment packaging, leading to lower values of $a^*_{ph}(440)$ at TChl-*a* > 2 mg Chl-*a* m^{-3}.

In general, changes in $a^*_{ph}(440)$ of natural phytoplankton communities as a function of TChl-*a* are driven by two main factors: pigment packaging and pigment composition (Morel and Bricaud, 1981; Hoepffner and Sathyendranath, 1991; Stuart *et al.*, 1998). The degree of pigment packaging is proportional to the cell size and intracellular pigment concentration (Morel and Bricaud, 1981), although for phytoplankton in the surface ocean, cell size is considered to be the dominant factor (Bricaud *et al.*, 2004). Since $a^*_{ph}(440)$ is normalised to Chl-*a* rather than total pigment concentration, the presence of accessory pigments (pigments other than Chl-*a*) in varying proportions can modify the magnitude of $a^*_{ph}(440)$. Accessory pigment composition varies with taxa, and the intracellular concentration of each pigment varies due to photoacclimatory changes with growth irradiances. In the following section, impacts of both sources (cell size and pigment composition) on the absorption coefficient of marine phytoplankton across trophic regimes are discussed from both ecological and physiological points of view.

2.4.2 Relationship between trophic status, phytoplankton community structure, and photoacclimation

There is a progressive increase in the dominant cell size, and thus a decrease in $a^*_{ph}(440)$, of phytoplankton assemblages as one moves from oligotrophic (i.e. low TChl-*a*) open-ocean conditions to more eutrophic (i.e. higher TChl-*a*) regions (Yentsch and Phinney, 1989; Chisholm, 1992). In the oligotrophic regions, such as (sub)tropical waters in the Trades Biome, strong water-column stratification caused by intense solar heating of surface waters reduces the vertical flux of new nitrogen from the depth to the surface (Platt *et al.*, 2005). This surface depletion in nutrients frequently leads to an increase in the relative abundance of picocyanobacteria (< 2 μm), including the dominant genera *Synechococcus* and *Prochlorococcus*, whose large surface-area-to-volume ratio (Partensky, Hess, *et al.*, 1999) and preference for reduced forms of nitrogen (Claustre, 1994; Bertilsson *et al.*, 2003), allow these picocyanobacteria to outcompete larger cells under nutrient-limited conditions. On the other hand, productive waters are typically associated with stronger surface mixing, allowing the entrainment of deep, nutrient-rich water to the surface and thus tend to favour the dominance of larger eukaryotic cells in the upper water column (Yentsch and Phinney, 1989; Claustre, 1994).

Although this dataset shows a positive correlation between TChl-*a* and the average cell diameter of phytoplankton samples based on pigment indices (Figure 2.3a), the relationship exhibited a considerable degree of scatter. Our pigment index of cell size is at best a proxy of phytoplankton size structure. Many diagnostic pigments are shared amongst more than one phytoplankton group and most taxa can fall within different size classes. For instance, fucoxanthin, which is a marker pigment for diatoms (microphytoplankton), can also be found in prymnesiophytes (nanophytoplankton) (Ras *et al.*, 2008). Diatoms are also typically classified into the microphytoplankton, but many species can fall within the nano-size range (Uitz *et al.*, 2009).

Another shortcoming of pigment indices of cell size is that, although zeaxanthin and divinyl chlorophyll *b* are normally used to estimate the abundance of picocyanobacteria, they do not account for a diverse community of picoeukaryotes, which have been increasingly recognised as abundant primary producers using molecular techniques (Bouman *et al.*, 2011; Massana, 2011). Moreover, zeaxanthin is not confined only to picocyanobacteria, but can also be found in the colonial marine cyanobacterium *Trichodesmium*, which, for the Atlantic Basin, has been reported to be far more abundant in the North Atlantic than the South Atlantic gyres (Fernández *et al.*, 2010). Thus, fluctuations in the occurrence of *Trichodesmium* colonies between samples could be a significant cause of variability in the relationship between pigment indices of phytoplankton size and absorption since the aggregation of cells into large colonies of *Trichodesmium* could enhance pigment packaging and hence result in an abnormally reduced $a^*_{ph}(\lambda)$ for samples classified into the small picophytoplankton size class (i.e. high relative concentration of zeaxanthin). Assigning a fixed mean cell diameter to each size class to obtain the gross size index (Bricaud *et al.*, 2004) may also be prone to errors, especially for the larger nano- and microphytoplankton with very broad size distributions (Agustí *et al.*, 2015). Hence, pigment indices should be considered rough proxies of the phytoplankton size structure and the widely-observed relationship between pigment-based indicators of size and phytoplankton *in vivo* absorption is the combined result of photoacclimatory and community-based responses of marine phytoplankton to environmental forcing that are registered in a range of cellular properties, of which cell size is only one.

Changes in surface TChl-*a* in the open ocean impact the intensity and quality of the underwater light field (Morel and Maritorena, 2001; Kirk, 2011) and consequently the photoacclimatory status of phytoplankton cells. In the oligotrophic (sub)tropical gyres, a relatively shallow and stable mixed layer constrains phytoplankton in the mixed layer to the surface waters where

they are continuously exposed to high levels of irradiance. However, as one moves to more eutrophic environments, the average daily growth irradiance may decrease as high concentrations of particulate (including algal cells) and dissolved materials can lead to an increase in the vertical attenuation of light with depth (Kirk, 2011). Moreover, an increase in turbulent mixing, typically associated with more productive regions, can also reduce the average light intensity for phytoplankton growth (Margalef, 1978). Therefore, it is important to bear in mind the physical factors that increase the phytoplankton standing stock by enhancing nutrient supply also tend to reduce the light available to marine phytoplankton and this, in turn, will lead to a community-wide photoacclimatory response.

2.4.3 Domain-specific changes in photophysiology and their relevance to pigment composition and light absorption

The relationship between phytoplankton size, taxonomic structure, and photoacclimatory status (Figure 2.3b) may stem from the inherent cellular properties and photophysiologies of the dominant primary producers in each trophic regime. Nutrients have often been invoked as a key factor governing the size structure of phytoplankton communities, yet one must keep in mind that nutrient supply also tends to be inversely correlated with light availability. While being small is advantageous in enabling picocyanobacteria to cope with nutrient limitation in oligotrophic gyres, it can also put the cells at risk of photodamage at high-light intensities that are characteristic of these environments. Thus as one moves from eukaryote-dominated communities in more productive, well-mixed regions to picocyanobacterial communities in more oligotrophic, stratified environments, it can be anticipated that there would also be a corresponding shift in the photoacclimatory status of phytoplankton.

One of the most commonly-known mechanisms by which intense blue-light may harm phytoplankton cells is the photoinactivation of photosystem II (PSII) (Six *et al.*, 2007; Key *et al.*, 2010), which is a specialised pigment-protein complex located in the thylakoid membrane of the cells and is where the light-dependent reactions of photosynthesis take place (Kirk, 2011). The PSII photoinactivation involves degradation of protein subunits (D1 and D2) associated with the reaction centre (P680) of PSII, particularly the D1 protein (Latifi *et al.*, 2009; Key *et al.*, 2010). The cells counteract this photodamage through rapid metabolic removal of the inactivated D1 subunit and replacement by a newly synthesised copy (Six *et al.*, 2007). Inefficient PSII repair can result in an overall reduction in cellular photosynthetic capacity and potentially lead to cell death. Typically, the sensitivity of phytoplankton cells to photodamage is quantified in terms of the fluorescence-based measurements of the effective target size for PSII inactivation, denoted as σ_i (Six *et al.*, 2007; Key *et al.*, 2010; Wu *et al.*, 2012). Picocyanobacteria, which dominate in the oligotrophic (sub)tropical gyres, have been demonstrated to be intrinsically more susceptible to photodamage (i.e. higher σ_i) than eukaryotic phytoplankton (Six *et al.*, 2007; Key *et al.*, 2010; Kulk *et al.*, 2011). Key and colleagues (2010) reported the negative correlation between cell size and σ_i within the marine diatoms and suggested that σ_i values measured amongst the smallest diatoms were still lower than those found in picocyanobacteria under similar environmental conditions. Owing to their extremely minute size, picocyanobacterial cells are less affected by pigment packaging (Morel *et al.*, 1993) which means that, compared to larger eukaryotic cells at a similar intracellular concentration of light-absorbing pigments, they are able to absorb light more efficiently (i.e. higher pigment-specific absorption coefficient) (Raven, 1998). Moreover, higher risk of photodamage for the photosynthetic apparatus of picocyanobacteria may also result from their thylakoid membranes being situated in close proximity to the cell membrane. In cyanobacterial cells *Synechocystis*, *Synechococcus*

and *Prochlorococcus* (Partensky, Hess, *et al.*, 1999; Liberton *et al.*, 2011), the thylakoid membranes are found to run parallel to the cell membrane and, unlike their eukaryotic counterparts, are not differentiated into grana stacks and stroma lamellae contained within chloroplasts (Richardson *et al.*, 1983).

In order to cope with deleterious effects of high UV and visible radiation that is encountered in the surface waters of oligotrophic regions, picocyanobacteria employ various photoprotective strategies such as the production of UV-screening compounds and the cellular repair of photosystems as described earlier. However, these specific strategies have been shown to be not as effective as the similar mechanisms observed in eukaryotic species. Raven (1991) demonstrated that it would require picophytoplankton (< 3 μm) to synthesise more UVB-absorbing compounds and thus more energy investment to achieve a similar degree of photoprotection than it would for larger cells. Studies have also pointed to the conclusion that picocyanobacteria tend to have relatively slow rates of cellular PSII repair compared to marine diatoms (Six *et al.*, 2007; Key *et al.*, 2010) and show lower potential for photoacclimation to high light than eukaryotic phytoplankton, including picoeukaryotes (Kulk *et al.*, 2011). Six and colleagues (2007) also noted that the number of PSII D1 proteins in *Prochlorococcus* strains (PCC9511 and SS120) was so large that cells might not be able to afford the high metabolic cost of maintaining their photosystems during the fast PSII photoinactivation. Therefore, under long-term exposures to high irradiance, which are expected in tropical and subtropical oceans, picocyanobacteria must develop other mechanisms for additional photoprotection since their cellular repair may not be sufficient to outcompete photoinactivation. Among those mechanisms is the adjustment of the relative intracellular concentration of photoprotective and photosynthetic pigments.

Under excessively high growth irradiances, picocyanobacteria typically decrease the intracellular content of PSPs (chlorophylls and photosynthetic carotenoids) to minimise the fraction of light energy absorbed and thereby increase the relative abundance of NPPs in their cells to enhance the thermal dissipation of absorbed energy (MacIntyre *et al.*, 2002). This explains the increased NPP index, and thus the percent absorption of NPPs at 440 nm, in oligotrophic surface waters observed in this study (Figures 2.3b-2.4). Zeaxanthin is the dominant NPP in *Synechococcus* and *Prochlorococcus* (Moore *et al.*, 1995) and was found to contribute significantly to the total NPP concentration for pigment samples collected from the oligotrophic gyres (Figure 2.5a). In higher plants and certain groups of eukaryotic algae (e.g. chlorophytes; Dubinsky and Stambler 2009), zeaxanthin has been suggested to play an important photoprotective role by the non-photochemical quenching of the excitation energy via the high light-induced, enzymatic conversion of the xanthophyll violaxanthin (non-quenching) ultimately to zeaxanthin (quenching), a process known as the xanthophyll cycle (Brunet *et al.*, 2011). However, since picocyanobacteria lack a xanthophyll cycle (Latifi *et al.*, 2009), they are thought to produce zeaxanthin by a different biosynthesis pathway (Masamoto *et al.*, 1999), and it is not clear how zeaxanthin serves in photoprotection in *Synechococcus* and *Prochlorococcus* (Veldhuis and Kraay, 1990; Kulk *et al.*, 2011). An intriguing hypothesis on the functional role of picocyanobacterial zeaxanthin stems from the observation that the pigment is located primarily in the cytoplasm or the outer cell wall (Siefermann-Harms, 1985; Kana *et al.*, 1988). In such a location, zeaxanthin is spatially disconnected to photosystems in the thylakoid membranes, and thus the fraction of light energy it absorbs will not be transferred to the reaction centres (Kana *et al.*, 1988), reducing the potential risk of overexcitation. The increased concentration of zeaxanthin relative to total pigments (PSPs + NPPs) in the picocyanobacteria-dominated environments (Figure 2.5a), which could be considered as an indicator of high light-acclimated cells, could partly result either from an increase in the absolute concentration of

zeaxanthin (Kulk *et al.*, 2011; Mella-Flores *et al.*, 2012), or a reduction in the content of PSPs, particularly Chl-*a* (Kana *et al.*, 1988; Moore *et al.*, 1995). However, the latter tends to be more commonly observed both in field (Veldhuis and Kraay, 1990, 2004; Matsumoto and Ando, 2009) and culture studies (Kana *et al.*, 1988; Moore *et al.*, 1995; Six *et al.*, 2004): the amount of Chl-*a* per cell decreases significantly with increasing growth irradiance, while the intracellular content of zeaxanthin tends to remain relatively stable.

For a given growth irradiance, *Prochlorococcus* could have up to 3 times lower intracellular concentration of zeaxanthin than *Synechococcus* (Moore *et al.*, 1995), and the amount of DVChl-*a* per cell of *Prochlorococcus* could be as low as *ca* 0.1 fg DVChl-*a* $cell^{-1}$ (Moore *et al.*, 1995; Bouman *et al.*, 2006), which is 2 to 6 times lower than the Chl-*a* per cell of *Synechococcus* (Moore *et al.*, 1995). Correspondingly, *Prochlorococcus* has the carbon-to-chlorophyll ratios that are markedly higher than those of *Synechococcus* and photosynthetic picoeukaryotes (e.g. 93-122 compared to 38-58 g C g Chl-a^{-1}; Hartmann *et al*. 2014). This suggests that *Synechococcus* are likely to invest a considerable fraction of their energy on the synthesis of NPPs (Raven, 1991). This may also invite speculation as to how *Prochlorococcus* can maintain optimal photosynthesis and growth with extremely reduced intracellular concentration of PSPs. A recent molecular study by Mella-Flores *et al*. (2012) suggests that, rather than intensively inducing a variety of photoprotective mechanisms (including the production of zeaxanthin) as observed in *Synechococcus*, high light-acclimated *Prochlorococcus* reduces their energy demand by temporarily down-regulating the main metabolic processes, such as the synthesis of light-harvesting pigment proteins, ATP formation, and the light-independent reactions of photosynthesis (Calvin cycle). This is not only to avoid photodamage during a period of high irradiance (Hartmann *et al.*, 2014), but also to allow *Prochlorococcus* cells to generate the energy from photosynthesis that is sufficient to satisfy their minimised energy requirement despite

having only a low amount of PSPs to carry out light absorption for photochemistry. The unique capacity to withstand photodamage at high light whilst being able to optimise photosynthesis has in part enabled *Prochlorococcus* to thrive and frequently outnumber *Synechococcus* in the vast (sub)tropical regions of the global ocean (Morel *et al.*, 1993).

In contrast, eukaryotic phytoplankton inhabiting productive and high-latitude waters respond to decreasing light intensities by increasing the total amount of pigment per cell, or increasing the proportion of PSPs, or both (Richardson *et al.*, 1983; MacIntyre *et al.*, 2002; Kirk, 2011) in order to increase their light-harvesting capacity and maintain optimal growth rates (Falkowski and LaRoche, 1991). The resulting fraction of NPPs would thus remain low as photoprotection is not required, and this explains the decrease in the relative concentration of NPPs and their percentage absorption at 440 nm from oligotrophic to productive systems as observed in our dataset (Figures 2.3b-2.5).

The absence of picocyanobacteria in higher latitude (polar) seas implies that there are less likely to be domain (prokaryotic to eukaryotic) shifts across TChl-*a* gradients as typically observed in tropical and temperate regions and this is supported by NPP pigments tending to be dominated by diadinoxanthin and diatoxanthin associated with eukaryotic algae. In the Polar Biome, despite exhibiting a broad range of surface TChl-*a*, the NPP index was consistently low. Vertical density profiles showed that, in general, the polar waters were more deeply mixed, reducing the light availability for surface phytoplankton communities. It is also important to note that polar phytoplankton communities are typically dominated by larger diatoms. Compared to cyanobacteria and other eukaryotic taxa, such as dinoflagellates, prymnesiophytes, and chlorophytes, photosynthetic and growth rates of diatoms appear to be less affected by fluctuating growth irradiances (Claustre *et al.*, 1994; Lavaud, 2007; van de Poll *et*

al., 2007). Also, in contrast to the picocyanobacteria (Six *et al.*, 2007) and green algae species examined to date (Six *et al.*, 2009), diatoms are less vulnerable to the photoinactivation of PSII (i.e. low σ_i), possibly due to their large cell size (Key *et al.*, 2010; Wu *et al.*, 2012). Therefore, when they are subjected to rapid and dramatic fluctuations in irradiance in a more turbulent surface ocean layer, their cellular PSII repair mechanism is sufficient to counteract their intrinsically low susceptibility to photodamage (Wu *et al.*, 2012), so the cells may not need to significantly adjust their NPP pools for extra photoprotection as observed in picocyanobacteria. By maintaining the relative concentrations of NPPs to PSPs (i.e. the fraction of absorbed energy lost as heat compared to that is used in photochemistry), the cells reduce the risk of light limitation when they are subsequently mixed down to the dim portion of the mixed layer (Polimene *et al.*, 2014).

The notion that the thermal dissipation of excitation energy is perhaps more significant in prokaryotic/small cells than eukaryotic/large cells is supported by a fair number of studies. A culture experiment by Kulk *et al*. (2011) showed that although there was a general tendency for the diatom *Thalassiosira oceanica* to increase the intracellular concentration of the xanthophyll-cycle pigments diadinoxanthin (non-quenching) + diatoxanthin (quenching) relative to Chl-*a* with increasing irradiance, this photoacclimatory change in pigment composition was not as marked as the increase in the zeaxanthin/Chl-*a* ratio in picocyanobacteria. Moreover, the NPP-to-Chl-*a* ratios for eukaryotes were almost five times lower than those of picocyanobacterial strains. Size has also been shown to be an important factor governing photoacclimation. Wu *et al*. (2012) found that larger diatoms accumulated much lower amount of diatoxanthin upon an exposure to high light than smaller diatoms. Likewise, in a comparative experimental study using a range of chlorophyll *c*-containing pico- and nanophytoplankton species, Dimier *et al*. (2009) observed a negative correlation between cell size and the ratio of diatoxanthin to

Chl-*a*, and suggested that this might be related to smaller cells having a lower intracellular Chl-*a* concentration.

In the Arctic and Subarctic regions within the Polar Biome, sampling stations displaying elevated NPP indices were typically in open, well-lit waters. Yet, the highest NPP abundance (i.e. NPP:TChl-*a* ratios > 0.3) was recorded in ice or under-ice stations. Johnsen and colleagues (2018), in their recent study in the Chukchi Sea, suggested that blooms consisting of high light-acclimated phytoplankton cells (NPP:TChl-*a* > 0.2) found in the water column beneath the sea ice might be, in fact, advected in from the adjacent ice-free waters, or alternatively, cells growing initially in open water were later covered by sea ice drifting from elsewhere. Also, as incident solar irradiances increase in the spring and summer, the formation of ice melt ponds allows a greater proportion of light to penetrate the sea ice (2-3 times compared to bare ice or snow) (Scharien *et al.*, 2017) which may trigger high-light photoacclimation of phytoplankton constrained to near-surface waters of the shallow and stable mixed layer produced by salinity-driven water-column stratification due to an increase in freshwater input (Matsuoka *et al.*, 2009).

In general, within the Polar Biome, the contribution of NPPs to the total pigment pool and phytoplankton absorption tended to be higher for stations sampled in the Southern Ocean than those in the Arctic Ocean. Experiments conducted on these Southern Ocean stations used in the present study showed clear evidence of iron limitation associated with high residual nitrate + nitrite concentrations (Browning *et al.*, 2014). In eukaryotic marine phytoplankton, iron stress has been found to associate with a reduction in the cellular synthesis of the D1 protein subunit of PSII (Greene *et al.*, 1992) which, as mentioned earlier, is a critical process to counteract the PSII photoinactivation. Consequently, since the reduced rates of PSII repair of iron-stressed cells are not likely to keep up with photodamage (Alderkamp *et al.*, 2010), the cells

would have to increase the dissipation of excess energy by a rapid xanthophyll cycle for extra protection when mixed up to the upper water column. This could result in iron-limited cells increasing the proportion of xanthophyll-cycle pigments (i.e. diadinoxanthin and diatoxanthin) as widely observed in experimental (Geider *et al.*, 1993; Petrou *et al.*, 2014) and field investigations (Alderkamp *et al.*, 2010; Cheah *et al.*, 2013).

2.4.4 Effects of non-photosynthetic pigments on phytoplankton absorption

This large basin-scale dataset clearly shows that $a^*_{ph}(440)$ was significantly influenced by the NPP index which was, in turn, inversely correlated with TChl-*a*. As the NPP index increased, there was a corresponding increase in $a^*_{ph}(440)$ (Figure 2.6). This is consistent with several studies: Bricaud *et al*. (1995) for tropical and temperate waters in the North Atlantic, Sosik and Mitchell (1995) for the California Current System, Stuart *et al*. (2000) for the Labrador Sea, Barlow *et al*. (2002) for the eastern boundary of the North and South Atlantic, and Ferreira *et al*. (2013) for the Patagonian subantarctic waters. In the North Pacific Subtropical Gyre, Letelier *et al*. (2017) suggested that the variability in $a^*_{ph}(\lambda)$ observed in the upper water column was controlled solely by NPPs as the relative abundance of PSPs was nearly constant due to the chronic nutrient-limiting conditions. The contribution of zeaxanthin to phytoplankton absorption in the blue part of the spectrum has been demonstrated both in laboratory and field studies. In culture experiments on *Prochlorococcus* SS120 strain isolated from the deep waters of the Sargasso Sea and *Prochlorococcus* MED4 strain from the surface waters of the Mediterranean Sea, Moore and colleagues (1995) reported that, at high light, zeaxanthin contributed approximately 40% to the reconstructed total absorption by phytoplankton at 449 nm for the SS120 strain, and 50% at 443 nm for the MED4 strain. The authors also concluded that the observed variation of $a^*_{ph}(\lambda)$ in the blue spectral range at different growth irradiances was due primarily to photoacclimatory changes in the intracellular pigment composition rather than

pigment packaging. In a study by Stuart *et al*. (1998) in the Arabian Sea, zeaxanthin was found to account for 68% of variation in phytoplankton absorption at the 490 nm waveband.

A high degree of scatter in the relationship between the NPP index and phytoplankton absorption was observed in the South Subtropical Convergence Province (SSTC; Westerlies Biome) and near the southeastern boundary of the South Atlantic Gyral Province (SATL; Trades Biome) just to the north of the SSTC (JC068 and D357 transects; Figure 2.1), with phytoplankton samples collected from low TChl-*a* waters of these regions possessing a low contribution of NPPs, yet still expressing a high $a^*_{ph}(440)$ (Figure 2.7). Diagnostic pigment markers (low zeaxanthin coinciding with elevated 19′-hexanoyloxyfucoxanthin + 19′-butanoyloxyfucoxanthin relative to total pigment concentration) indicate that these specific samples were dominated by prymnesiophytes belonging to the nanophytoplankton size class. However, molecular data (Liu *et al.*, 2009; Cuvelier *et al.*, 2010) suggest that, in the southern subtropical convergence zone across major oceanic basins, it is actually small, non-calcifying prymnesiophytes within the picophytoplankton size range that contribute significantly to phytoplankton pigment biomass. Therefore, the small cell size may explain the higher light absorption efficiencies of surface phytoplankton in the SSTC and the adjacent southern portion of the SATL that could not be accounted for by NPPs. It should also be noted that as pigments associated with prymnesiophytes may also represent cells less than 2-3 μm, a different set of pigment indices need to be derived for the SSTC in order to relate phytoplankton size structure to pigment markers.

In the polar seas, although there was a general tendency for pigment samples with high values of the NPP index to exhibit higher $a^*_{ph}(440)$, the correlation was rather weak when compared with other biomes. This could due in part to relatively low and invariant values of $a^*_{ph}(440)$ and that pigment packaging (i.e. cell size and intracellular pigment concentration) may be more

important in governing the variability in $a^*_{ph}(\lambda)$ in these regions. In the Atlantic sector of the Arctic Ocean, a group of samples having abnormally high $a^*_{ph}(440)$ of more than 0.13 m^2 (mg Chl-*a*)$^{-1}$ was estimated using the pigment-based approach (Bricaud *et al.*, 2004) to have the smallest dominant cell size (< 16 μm). Note that in the Polar Biome, samples contained the highest relative proportion of (monovinyl) chlorophyll *b*, a bio-marker for small chlorophytes in the pico-size class (Ras *et al.*, 2008). Therefore, it is likely that the increased relative importance of this pigment, combined with the small cell size, was responsible for the high $a^*_{ph}(440)$ observed in the Arctic Ocean dataset. However, when the entire Polar Biome was considered, variation in size structure turned out to be able to explain only *ca* 10% of variance of $a^*_{ph}(440)$ with many samples dominated by small cells showing absorption efficiencies that were atypically low and similar to those dominated by large cells (data not shown). A possible explanation for similarities in the magnitude of $a^*_{ph}(440)$ across communities of varying size structure is that many phytoplankton cells may acclimate to low-light conditions, particularly when residing underneath the sea ice, by increasing the total amount of pigments per cell and/or increasing the number of thylakoid membranes in the chloroplast, both of which can lead to enhanced pigment packaging (Berner *et al.*, 1989; Falkowski and LaRoche, 1991). This may offset the effect of cell size on pigment packaging, resulting in samples dominated by small cells having low $a^*_{ph}(440)$. In a study by Berner *et al*. (1989), it was shown that for the marine chlorophyte *Dunaliella teriolecta*, 40% and 50% of the variation in pigment packaging can be explained by photoacclimatory changes in the arrangement and the transparency of thylakoid membranes, respectively, whereas changes in the size of the cell do not affect packaging. Thus, a large number of studies support the view that photoacclimation of phytoplankton cells to growth light intensities can play a significant role in determining the absorptive characteristics

of natural phytoplankton communities as it can affect both the intracellular pigment composition and pigment packaging, the two predominant factors widely known to influence $a^*_{ph}(\lambda)$, especially at shorter wavelengths.

Variation in the relative proportions of NPPs to PSPs can alter the shape of phytoplankton absorption spectrum, particularly in the blue-green (400-550 nm) spectral region where most accessory pigments have their major absorption peaks (Lutz *et al.*, 1996). It has been widely documented that the height of the blue peak (*ca* 440 nm) relative to that of the red peak (*ca* 676 nm) of $a_{ph}(\lambda)$ spectra varies significantly with the varying proportions of NPPs (Bouman, Platt, Kraay, *et al.*, 2000; Lutz *et al.*, 2003; Ferreira *et al.*, 2017).

As a complement to examining ratios of $a_{ph}(440):a_{ph}(676)$, following Hirata *et al*. (2008), the spectral slope between absorption peaks at 443 and 510 nm was used to represent the spectral shape of phytoplankton absorption. Again the significance of NPPs on the variation in this optical property was clear (Figure 2.9). In their original study, Hirata and colleagues (2008) utilised a tight covariation between the magnitude of $a_{ph}(443)$, retrievable from the normalised water-leaving reflectance, and the spectral slope from 443 to 510 nm to determine phytoplankton size classes using satellite observations. Our results may add to the Hirata *et al*. (2008) study by providing evidence that the observed robust relationship between $a_{ph}(443)$ and the spectral slope exists not only because, as noted by the authors, both optical variables are characteristic of phytoplankton size classes, but also because they are similarly influenced by changes in the photoacclimatory status of phytoplankton.

Given the substantial contribution of NPPs to phytoplankton absorption in the blue region of the spectrum in oligotrophic waters (Figure 2.8a), one must consider whether it is appropriate

to use $a_{ph}(\lambda)$, which includes the light absorption that would not be used for photosynthesis (Sosik and Mitchell, 1995), to represent the shape of the photosynthetic action spectrum in spectral models of primary production, and that a spectrum that only includes absorption by photosynthetic pigments (i.e. $a_{ps}(\lambda)$) should be used instead (Sosik and Mitchell, 1995; Bouman, Platt, Sathyendranath, *et al.*, 2000). In addition, NPPs may also introduce a bias to estimates of quantum yields of photosynthesis (ϕ) (Falkowski and LaRoche, 1991; MacIntyre *et al.*, 2002; Dubinsky and Stambler, 2009) which represents the ratio of the moles of carbon fixed to the moles of quanta absorbed (Sosik and Mitchell, 1995). An increase in $a^*_{ph}(\lambda)$ and a corresponding decrease in the fraction of excitation energy transferred to reaction centres caused by an increase in NPPs would be accompanied by a reduction in ϕ (Dubinsky *et al.*, 1986; Babin *et al.*, 1996).

2.5 Concluding Remarks

Pigment and absorption data collected from surface waters across the Atlantic Basin were used to examine how pigment indices of size structure and photoacclimation relate to the spatial variability in absorptive properties of natural phytoplankton communities. By dividing a large dataset into the four primary biomes of the upper ocean (Longhurst, 1998), the relationships were examined over a range of chlorophyll concentrations in oceanic zones with fundamental differences in physical forcing.

Variation of $a^*_{ph}(440)$ was tightly linked to variation in the NPP index, an indicator of photoacclimatory status of phytoplankton communities, from oligotrophic, high-light environments dominated by picocyanobacteria to more productive, low-light regions abundant with large-celled eukaryotic algae. In oligotrophic gyres (Trades Biome), more than half of the total absorption by phytoplankton at 440 nm was due to NPPs. The spectral shape (indexed by the

spectral slope) of phytoplankton absorption was demonstrated to be influenced strongly by the presence of NPPs, particularly zeaxanthin. The strong relationship between NPPs and phytoplankton absorption efficiency ($a^*_{ph}(440)$) reported here is consistent with other regional studies which together covered a range of hydrographic conditions (Bricaud *et al.*, 1995; Lazzara *et al.*, 1996; Stuart *et al.*, 2000; Barlow *et al.*, 2002). Zeaxanthin, a pigment marker for picocyanobacteria, was found to be the most abundant NPP and the primary driver of the relationship between NPPs and phytoplankton light absorption in the oligotrophic gyres. In such regions, changes in zeaxanthin concentration were strongly linked to the presence of the picocyanobacterium *Prochlorococcus*, as revealed by a genus-specific pigment marker divinyl chlorophyll *a*. The results also showed a much weaker correlation between $a^*_{ph}(440)$ and pigment indices of phytoplankton size, with a general tendency for larger cells to exhibit lower $a^*_{ph}(440)$. Hence, one can view that the apparent robust nature of pigment indices of the gross phytoplankton size structure in part stems from the concomitant photoacclimatory changes in the relative concentrations of NPPs.

Understanding the role NPPs play in governing the variability in phytoplankton light absorption is critical when using the absorptive characteristics to glean important information on the size and taxonomic composition of natural phytoplankton communities. Our ability to detect changes in the relative concentrations of NPPs and PSPs will improve our understanding of the cellular mechanisms governing fluctuations in quantum yield of photosynthesis and fluorescence, and will aid in improving remote-sensing algorithms used for chlorophyll retrieval by reducing potential errors associated with variation in phytoplankton absorption in the blue-to-green region of the spectrum due to large-scale changes in accessory pigment composition. The results obtained from this work also sheds some light on the relationship between the bio-optical and ecophysiological properties of marine phytoplankton, which warrants further study.

Chapter 3

Photoacclimatory Characteristics of Marine Picocyanobacteria

3.1 Introduction

Picophytoplankton (cell diameter < 2-3 μm; Raven, 1998) are the dominant primary producers in the expansive subtropical gyres. This size class consists of picocyanobacteria of the two sister genera *Prochlorococcus* and *Synechococcus*, and a diverse group of photosynthetic picoeukaryotes (Li *et al.*, 1992). *Prochlorococcus* is believed to be the smallest and the most abundant photosynthetic organism in the ocean (Partensky, Hess, *et al.*, 1999). It has been estimated that picophytoplankton can fix up to *ca* 1 Pg C, accounting for *ca* 30% of global phytoplankton carbon biomass (Le Quéré *et al.*, 2005; Buitenhuis *et al.*, 2012) and 24% of annual marine primary production (Uitz *et al.*, 2010). The contribution of picophytoplankton, specifically *Prochlorococcus*, to the global primary production is expected to increase (Partensky and Garczarek, 2010; Flombaum *et al.*, 2013) as their oligotrophic habitats are expanding, presumably as a result of global warming (Polovina *et al.*, 2008). A number of studies (e.g. Li *et al.*, 2009; Morán *et al.*, 2010; Ward, 2015; Paulsen *et al.*, 2016) have reported a community structure shift towards small picophytoplankton in polar habitats due to rising temperatures and freshening of surface waters.

The community structure of picophytoplankton has been shown to vary according to the strength of water-column stability, with a general tendency of picocyanobacteria to dominate in highly stratified waters with lower nutrient availability, and picoeukaryotes being favoured in more dynamic, nutrient-replete environments (Karl, 1999; Bouman *et al.*, 2011). Interestingly, picophytoplankton also differ in their vertical distribution: while *Synechococcus* often

occupies the upper part of the euphotic zone, *Prochlorococcus* and picoeukaryotes can be found throughout the water column typically with biomass maxima at depth (Hickman *et al.*, 2010). The ability of *Prochlorococcus* to grow at the base of the euphotic zone has been ascribed to increased light absorption efficiency resulting from its minute cell size (Morel *et al.*, 1993) and enhanced by the presence of divinyl chlorophyll *b* (DVChl-*b*) allowing the cells to harvest extremely low levels of blue light at depth (Moore *et al.*, 1995). The co-existence of high light and low light-adapted ecotypes with variable ratios of DVChl-*b* to divinyl chlorophyll *a* (DVChl-*a*) (Moore *et al.*, 1998) can also explain the observed large depth distribution of this genus (Campbell *et al.*, 1994; Hickman *et al.*, 2010; Karl and Church, 2014). Similarly, accessory chlorophylls *b* and *c* and a variety of photosynthetic carotenoids with distinct light absorptive properties (Bidigare *et al.*, 1990) enable picoeukaryotes to exploit a broad range of light niches and ensure sufficient photosynthesis in the deep euphotic zone (Fogg, 1986). The dominance of picoeukaryotes at depth is also linked to their high efficiency in the assimilation of newly upwelled nitrogen (Fawcett *et al.*, 2011). Many strains of *Synechococcus* contain photosynthetic apparatuses rich in phycoerythrin and phycoerythrobilin which allow them to utilise orange-green photons abundant particularly near the surface of more mesotrophic waters where blue light is strongly attenuated due to the presence of dissolved organic materials, including algal cells (Grébert *et al.*, 2018).

To derive information on the biomass, taxonomic composition, and productivity of picophytoplankton over larger spatio-temporal scales, various empirical models exploiting satellite observations of ocean colour have been proposed (Hirata *et al.*, 2008; Pan *et al.*, 2013; Lange *et al.*, 2018). Since the sea-surface reflectance signal is a function of light absorption by phytoplankton, any factors that potentially cause variability in phytoplankton absorption would also have an impact on the established relationship between remote sensing reflectance and other

variables in question. Moreover, variation in the intracellular chlorophyll *a* (Chl-*a*) concentration induced by changes in environmental factors, such as light and vertical mixing (Dusenberry *et al*., 1999), would complicate the conversion of Chl-*a* concentration measured by remote sensing into phytoplankton biomass (Karl, 1999; Behrenfeld *et al.*, 2005).

Non-photosynthetic pigments (NPP) have been shown to play a very important role in governing the regional- and basin-scale variability in light absorptive properties of phytoplankton in the surface ocean (Babin *et al.*, 1996; Bouman, Platt, Kraay, *et al.*, 2000; Lutz *et al.*, 2003; Ferreira *et al.*, 2017; Letelier *et al.*, 2017). Variation in NPPs is closely linked with the taxonomic structure of phytoplankton communities: the NPP zeaxanthin associated with picocyanobacteria can contribute up to 60% (Chapter 2) of total pigment concentration in warmer, oligotrophic waters, whereas in temperate and polar regions, NPPs associated with eukaryotic cells (e.g. diadinoxanthin and diatoxanthin) tend to be more important. Within a phytoplankton community or biogeochemical province, fractional contributions of phytoplankton pigments, including NPPs, could also vary as cells physiologically respond to seasonal and/or vertical variation in available light (Uitz *et al.*, 2008) and such light-dependent changes in pigment composition have been widely observed in culture (Kulk *et al.*, 2011; Stawiarski *et al.*, 2018).

Following from the points raised above, the first part of this study examines how variations in both the taxonomic composition and photoacclimatory status of phytoplankton may influence the variability in the relative abundance of NPPs observed across various marine systems. Using a combination of *in situ* pigment data and flow cytometric measurements of cell abundance, the second part of this study examines the photoacclimatory characteristics of picocyanobacteria given that picocyanobacteria-dominated systems are known to display strong changes in the ratio of NPPs to total pigments in response to changes in light conditions. The unique pigment

composition of picocyanobacteria, particularly *Prochlorococcus*, is used to observe how this genus regulates the intracellular concentrations of photosynthetic and non-photosynthetic pigments in response to changes in available light. By converting cell abundances to carbon biomass using carbon conversion factors obtained from the literature, the carbon-to-(DV)Chl-*a* ratio (θ) of *Prochlorococcus* is estimated and compared to those obtained from both bulk estimates obtained in field measurements and from laboratory cultures. The photoacclimatory properties of *Prochlorococcus*, in terms of both the intracellular concentrations of pigments and θ, are compared to those of eukaryotic (pico)phytoplankton in order to assess whether the photoacclimatory strategies employed by *Prochlorococcus* and other phytoplankton groups are comparable and whether this globally-important picocyanobacterium can serve as an indicator of photoacclimatory status for the phytoplankton community as a whole.

3.2 Materials and Methods

3.2.1 Data

Measurements of phytoplankton pigment concentrations and picocyanobacteria cell abundance used in this study were compiled from measurements carried out during various oceanographic campaigns, most of which focused primarily on the tropical and subtropical gyres of the Atlantic and Pacific Basins (Table 3.1 and Figure 3.1). Seawater samples were collected using a conductivity-temperature-depth (CTD) profiler equipped with a rosette of Niskin bottles. Further details on sampling strategies for individual oceanographic datasets can be found in the references provided in Table 3.1.

(1) Phytoplankton pigment analysis

Phytoplankton pigments were identified and quantified using high-performance liquid chromatography (HPLC). For each of the datasets, the filtration volumes, organic solvents used for pigment extraction, and corresponding references are summarised in Table 3.2, and the HPLC pigments detected are listed in Table 3.3. It is important to note that data on the concentration of the pigments DVChl-*a* and DVChl-*b*, unique to *Prochlorococcus*, are not available for the BATS programme as the HPLC method employed did not allow for these pigments to be completely separated from their normal monovinyl derivatives (Steinberg *et al.*, 2001). To minimise the variability introduced by differences in methodology between laboratories, a quality check on the HPLC-determined pigment data (Trees *et al.*, 2000) was conducted using linear regressions of total accessory pigment concentration on total chlorophyll *a* concentration (TChl-*a*). Outliers with estimated standard deviations greater than 3 in absolute value (Uitz *et al.*, 2006) were removed (final slope = 0.82, $R^2 = 0.90$), reducing the pigment database to 2,960 observations, which was 83% of the original data.

Table 3.1: Summary of oceanographic campaigns included in the database. *N* is the number of samples collected from each campaign for determination of pigment concentration using HPLC analysis (HPLC) and cell enumeration using flow cytometry (FCM). Biogeochemical provinces are defined according to Longhurst (1998).

Dataset	**Dates**	***N***		**Regions**	**Relevant publications**
		HPLC	**FCM**		
Atlantic Meridional Transect (AMT)		1856	2684	North Atlantic Drift Province, South Atlantic Subtropical Convergence Province, North and South Atlantic Subtropical Gyres, Eastern and Western Tropical Atlantic Provinces, Canary Coastal Province, Benguela Current Coastal Province (upwelling system)	
AMT-3	22 Sep – 25 Oct 1996	298	209		Zubkov *et al.* (1998, 2000); Barlow *et al.* (2002)
AMT-4	27 Apr – 21 May 1997	219	232		Gibb *et al.* (2000); Zubkov *et al.* (2000)
AMT-6	15 May – 16 Jun 1998	508	170		Barlow *et al.* (2004); Heywood *et al.* (2006)
AMT-12	12 May – 17 Jun 2003	236	371		Heywood *et al.* (2006); Poulton *et al.* (2006); Lange *et al.* (2018)
AMT-13	8 Sep – 13 Oct 2003	172	277		Heywood *et al.* (2006); Johnson *et al.* (2006); Poulton *et al.* (2006); Tarran *et al*. (2006); Lange *et al.* (2018)
AMT-14	28 Apr – 1 Jun 2004	208	942		Heywood *et al.* (2006); Poulton *et al.* (2006); Tarran *et al*. (2006); Lange *et al.* (2018)
AMT-15	17 Sep – 29 Oct 2004	215	483		Poulton *et al.* (2006); Zwirglmaier *et al.* (2007; Hickman *et al.* (2010); Lange *et al.* (2018)

Table 3.1 (continued)

Dataset	Dates	*N*		Regions	Relevant publications
		HPLC	FCM		
Bermuda Atlantic Time-series Study (BATS)	2002 – 2007	698	761	Western North Atlantic Subtropical Gyre	Steinberg *et al.* (2001); Casey *et al.* (2007); Malmstrom *et al.* (2010)
BIogeochemistry and Optics SOuth Pacific Experiment (BIOSOPE)	26 Oct – 11 Dec 2004	615	1170	Transect from Marquesas Islands to the Coast of Chile (South Pacific Subtropical Gyre and Humboldt Current Coastal Province)	Grob, Ulloa, Claustre, *et al.* (2007); Claustre *et al.* (2008); Raimbault *et al.* (2008); Ras *et al.* (2008); West *et al.* (2011)
Deep Chlorophyll Maximum Study (DCM)	Jul – Aug 1996	75	75	North Atlantic Subtropical Gyre	Bouman, Platt, Kraay, *et al.* (2000); Bouman, Platt, Sathyendranath, *et al.* (2000); Veldhuis and Kraay (2004)
Hawaii Ocean Time-series (HOT)	2002 – 2008	301	138	North Pacific Subtropical Gyre	Malmstrom *et al.* (2010); Karl and Church, (2014); Letelier *et al.* (2017); Thompson *et al.* (2018)

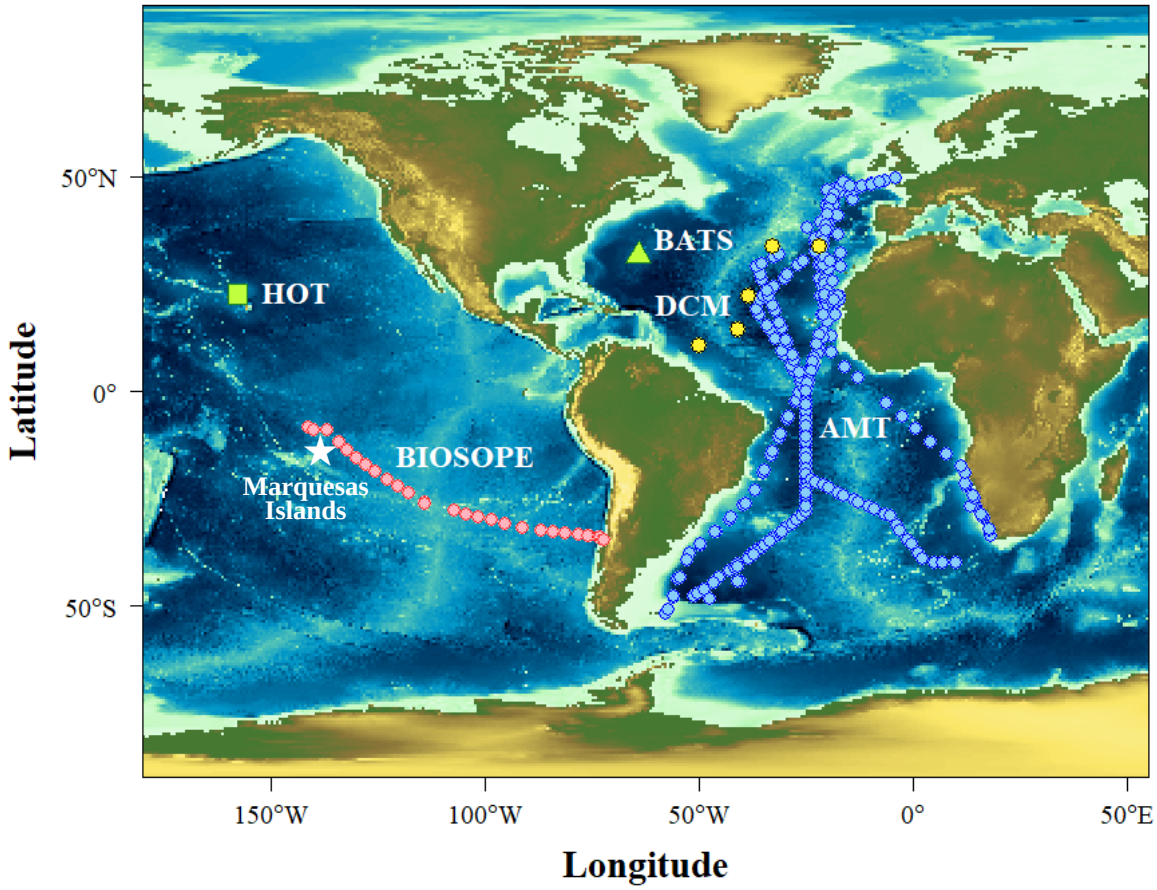


Figure 3.1: Map showing the distribution of oceanographic datasets of simultaneous measurements of phytoplankton pigment and picocyanobacteria abundance that passed quality assurance (N = 1,934).

Table 3.2: Summary of the filtration volume (V), organic solvent used for pigment extraction, and reference for each method used for HPLC pigment analysis for each oceanographic campaign.

Campaign	HPLC pigment analysis			Reference
	Methodology	V	Solvent	
AMT-3	Barlow *et al.* (1997)	0.5-2 L	90% acetone	Gibb *et al.* (2000); Barlow *et al.* (2002); Aiken *et al.* (2009)
AMT-4	Barlow *et al.* (1997)	2 L	90% acetone	Gibb *et al.* (2000); Aiken *et al.* (2009)
AMT-6	Barlow *et al.* (1997)	0.5-4 L	90% acetone	Barlow *et al.* (2002, 2004); Aiken *et al.* (2009)
AMT 12-15	Barlow *et al.* (1997)	1-4.2 L	90% acetone	Poulton *et al.* (2006); Aiken *et al.* (2009)
BATS	Bidigare (1991); Wright *et al.* (1991)	4 L	90% acetone	Steinberg *et al.* (2001)
BIOSOPE	van Heukelem and Thomas (2001)	1-5.6 L	100% methanol	Ras *et al.* (2008)
DCM	Veldhuis and Kraay (1990); Kraay *et al.* (1992)	20 L	100% methanol	Bouman, Platt, Kraay, *et al.* (2000); Veldhuis and Kraay (2004)
HOT	Bidigare *et al.* (2005)	4-10 L	100% acetone	Letelier *et al.* (2017)

Table 3.3: List of HPLC-detected pigments during each oceanographic campaign.

Pigments	Campaign				
	AMT	**BATS**	**BIOSOPE**	**DCM**	**HOT**
Photosynthetic pigments (PSP)					
Total chlorophyll *a* (TChl-*a*; monovinyl + divinyl)	X	X	X	X	X
Divinyl chlorophyll *a* (DVChl-*a*)	X	–	X	X	X
Total chlorophyll *b* (TChl-*b*; monovinyl + divinyl)	X	X	X	X	X
Divinyl chlorophyll *b* (DVChl-*b*)	X	–	X	X	–
Chlorophyll $c_{1,2}$ (Chl-$c_{1,2}$)	X	X	X	X	X
Chlorophyll c_3 (Chl-c_3)	X	X	X	X	X
Fucoxanthin (FUCO)	X	X	X	X	X
Peridinin (PERID)	X	X	X	X	X
19'-Hexanoyloxyfucoxanthin (19'-HEX)	X	X	X	X	X
19'-Butanoyloxyfucoxanthin (19'-BUT)	X	X	X	X	X
Prasinoxanthin (PRAS)	X	X	X	X	X
Non-photosynthetic pigments (NPP)					
Alloxanthin (ALLO)	X	X	X	X	–
Diadinoxanthin (DIAD)	X	X	X	X	X
Diatoxanthin (DIAT)	X	X	X	X	X
Zeaxanthin (ZEA)	X	X	X	X	X
Lutein (LUT)	X	X	X	X	X
Violaxanthin (VIOL)	X	–	X	X	X
Neoxanthin (NEOX)	–	–	X	X	–
Carotene (CARO; α-CARO + β-CARO)	X	X	X	X	X

(2) Estimation of picocyanobacteria abundance

Cell abundances of the picocyanobacteria *Prochlorococcus* and *Synechococcus* were determined by flow cytometry (Chapter 1, also in Olson *et al*., 1993; Li, 1995; Marie *et al*., 2005) on either freshly-collected or preserved samples. *Synechococcus* populations were identified from the orange fluorescence emitted by their characteristic phycoerythrin pigment-protein complex (Moore *et al.*, 1995), and *Prochlorococcus* populations were distinguished based on their red fluorescence associated with DVChl-*a* and right-angle light scattering properties (Olson *et al.*, 1993; Zubkov *et al.*, 1998). However, *Prochlorococcus* cells collected from the surface layer of the (sub)tropical gyres typically contain a very low concentration of DVChl-*a*, which makes it difficult to enumerate the cells accurately using their natural fluorescence signal (Zubkov *et al.*, 1998; Grob, Ulloa, Claustre, *et al.*, 2007). Therefore, alternative approaches have been developed at different laboratories to estimate the abundance of *Prochlorococcus* populations that are weakly fluorescent as summarised below.

For the BIOSOPE project, Grob, Ulloa, Claustre, *et al.* (2007) determined the concentration of *Prochlorococcus* cells with low fluorescence by using the software Cytowin to fit a normal curve to the signal distribution plot. In cases where the fluorescence signal was too dim, the cell number was derived from the pigment DVChl-*a* assuming an average cell-specific concentration of 0.23 fg DVChl-*a* $cell^{-1}$ which was intracellular pigment concentration collected within the surface layer above the 5% level of the incident light and corresponded to the lowest possible values reported in Blanchot and Rodier (1996) and Partensky, Hess, *et al.* (1999) for surface, high light-acclimated *Prochlorococcus* populations.

For the AMT (Zubkov *et al.*, 1998, 2000; Hartmann *et al.*, 2014; Lange *et al.*, 2018) and DCM datasets (Veldhuis and Kraay, 2004), *Prochlorococcus* in surface water samples were DNA-

stained with fluorescent dyes, such as TOTO-1 iodide (Li *et al.*, 1995; Zubkov *et al.*, 1998), or SYBR Green I (Marie *et al.*, 1997; Zubkov *et al.*, 2007; Hartmann *et al.*, 2014), or PicoGreen (Veldhuis *et al.*, 1997; Veldhuis and Kraay, 2004), prior to analysis by flow cytometry. The staining technique allows for better visualisation of the dim *Prochlorococcus* cells (Zubkov *et al.*, 1998; Veldhuis and Kraay, 2004) based on the green fluorescence originating from the DNA-binding dyes in addition to their chlorophyll (red) fluorescence and scatter signals.

Flow cytometric measurements for the HOT programme between 1990 and 2005, which corresponds to the time period when most of the HOT data used in this study were collected (Fujieki *et al.*, 2016), were carried out routinely using a flow cytometer fitted with a 1-W 488-nm laser as described in Campbell and Vaulot (1993). However, the authors noted that the flow cytometer configuration often failed to detect surface populations of *Prochlorococcus*. Thus, under these circumstances, a laser that generates an excitation beam in the range 457-515 nm was used instead (Olson *et al.*, 1990) so that the excitation energy better matches with absorption bands of the DVChl-*a* and DVChl-*b* pigments of *Prochlorococcus* (Olson *et al.*, 1990). This flow cytometer set-up (Olson *et al.*, 1990) was also optimised to increase the sensitivity of the instrument to detect surface assemblages of *Prochlorococcus* at the BATS station (DuRand *et al.*, 2001).

3.2.2 Computation of mixed-layer and euphotic depths

For each of the datasets, the depth of the mixed-layer (z_m) was calculated from vertical profiles of the potential density (σ_θ) [kg m^{-3}] obtained from online data repositories. When the online information of σ_θ was not readily available, the σ_θ was calculated from temperature and salinity profiles using the R statistical package '*oce*' (Kelly, 2018; https://dankelley.github.io/oce). The

z_m was defined as the depth at which the σ_θ was offset from the surface (10 m) reference value by a threshold value of 0.125 kg m^{-3} (Bouman *et al.*, 2006).

The euphotic depth (z_e) is the maximum depth in the water column where significant phyto-plankton photosynthesis takes place, which typically corresponds to the depth at which the downwelling irradiance of the photosynthetically-available radiation (PAR) decreases to 1% of its surface value (Kirk, 2011). Assuming that the vertical attenuation coefficient for PAR, K_d(PAR) [m^{-1}], is constant with depth, the z_e can be estimated from K_d(PAR) using the relation (Kirk, 2011):

$$z_e = \frac{4.6}{K_d(\mathrm{PAR})}. \tag{3.1}$$

K_d(PAR) was converted from the attenuation coefficient at 490 nm, K_d(490) [m^{-1}], using the relationship reported in Morel *et al.* (2007) for open-ocean (Case I) waters:

$$K_d(\mathrm{PAR}) = 0.0665 + 0.874\,K_d(490) - \frac{0.00121}{K_d(490)}. \tag{3.2}$$

The K_d(490) was calculated from the HPLC total chlorophyll *a* concentration (TChl-*a*) based on an empirical relationship derived by Morel and Maritorena (2001):

$$K_d(490) = K_w(490) + 0.07242\,\mathrm{Chl}^{0.68955}, \tag{3.3}$$

where K_w(490) = 0.0166 m^{-1} is the attenuation coefficient for pure water at 490 nm, and Chl is the average TChl-*a* [mg Chl-*a* m^{-3}] in the mixed layer (Grébert *et al.*, 2018).

3.3 Results and Discussion

3.3.1 Vertical and spatio-temporal distributions of non-photosynthetic pigments

Clear patterns in the vertical distributions of non-photosynthetic pigments (NPPs) were evident across the oceanographic datasets (Figure 3.2). The ratio of the sum of NPPs (ZEA, DIAD, DIAT, VIOL, ALLO, and CARO; Table 3.3) to the sum of all pigments (so-called the NPP index as in Babin *et al.*, 1996) decreased vertically with a reduction in the relative availability of light in the water column as indexed by the ratio of the sampling depth to the euphotic depth (z/z_e; Uitz *et al.*, 2008), which is consistent with the findings of other studies (Babin *et al.*, 1996; Bouman, Platt, Kraay, *et al.*, 2000; MacIntyre *et al.*, 2002). The advantages of using the z/z_e index rather than nominal depths are two folds. First, it provides an approximation of ambient light conditions at a given depth when *in situ* vertically-resolved measurements of irradiance were not available for many of the samples in the database (Uitz *et al.*, 2008). Second, as pointed out in Lange *et al.* (2018), it implicitly carries information about attenuation of light through the water column, which has been shown to be a more effective predictor of long-term changes in phytoplankton pigments and cell abundance in the open ocean than does the instantaneous variation of light intensity expressed in absolute units. For many of the datasets, the magnitude of the NPP index varied appreciably within the surface layer (i.e. $z/z_e < 0.5$), and the values appeared to converge to the minimum at below the ~$1.5z_e$ depth, where light is too low to sustain phytoplankton growth.

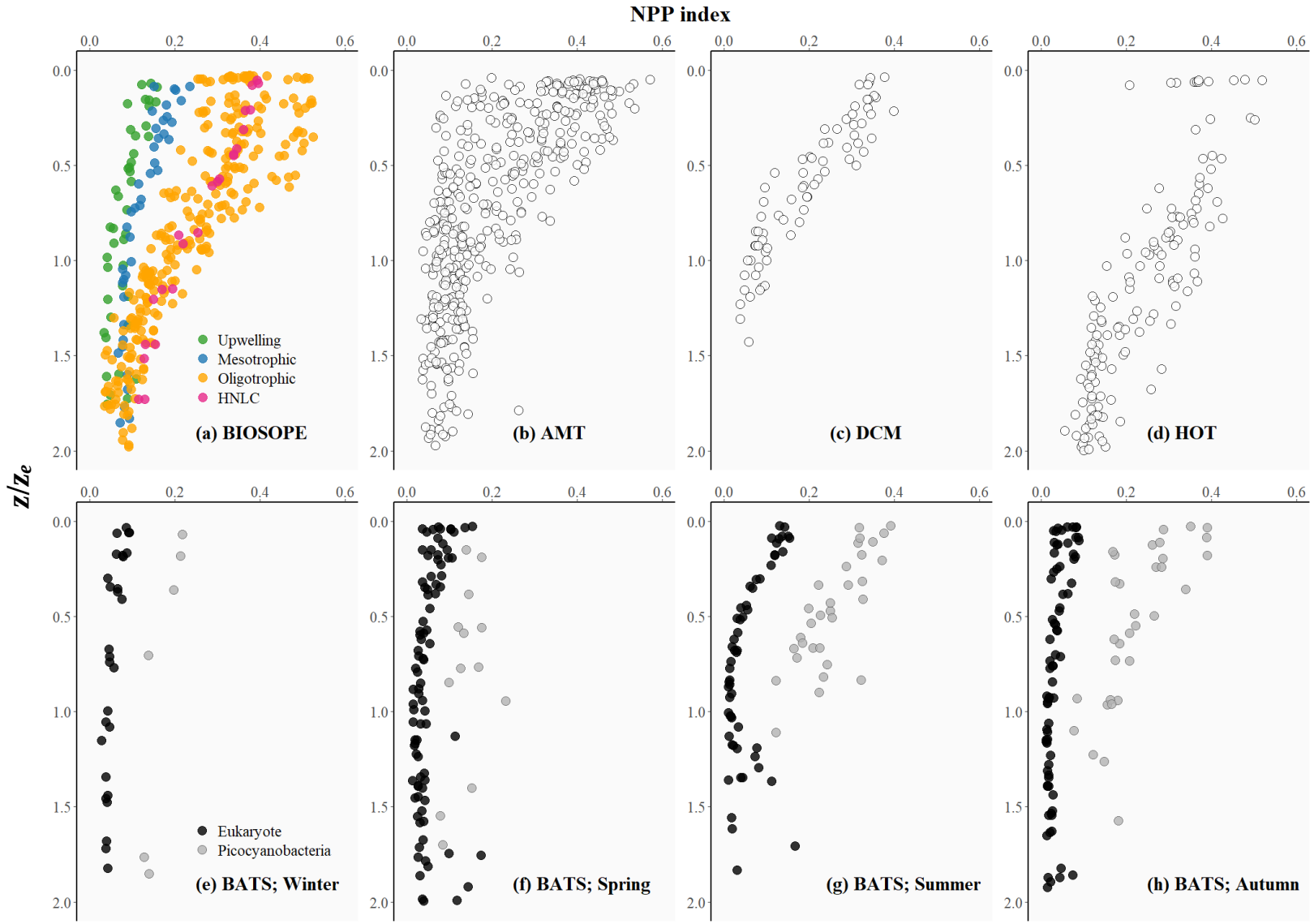

NPP index
z/Ze
Upwelling
Mesotrophic
Oligotrophic
HNLC
(a) BIOSOPE
(b) AMT
(c) DCM
(d) HOT
Eukaryote
Picocyanobacteria
(e) BATS; Winter
(f) BATS; Spring
(g) BATS; Summer
(h) BATS; Autumn

Figure 3.2.

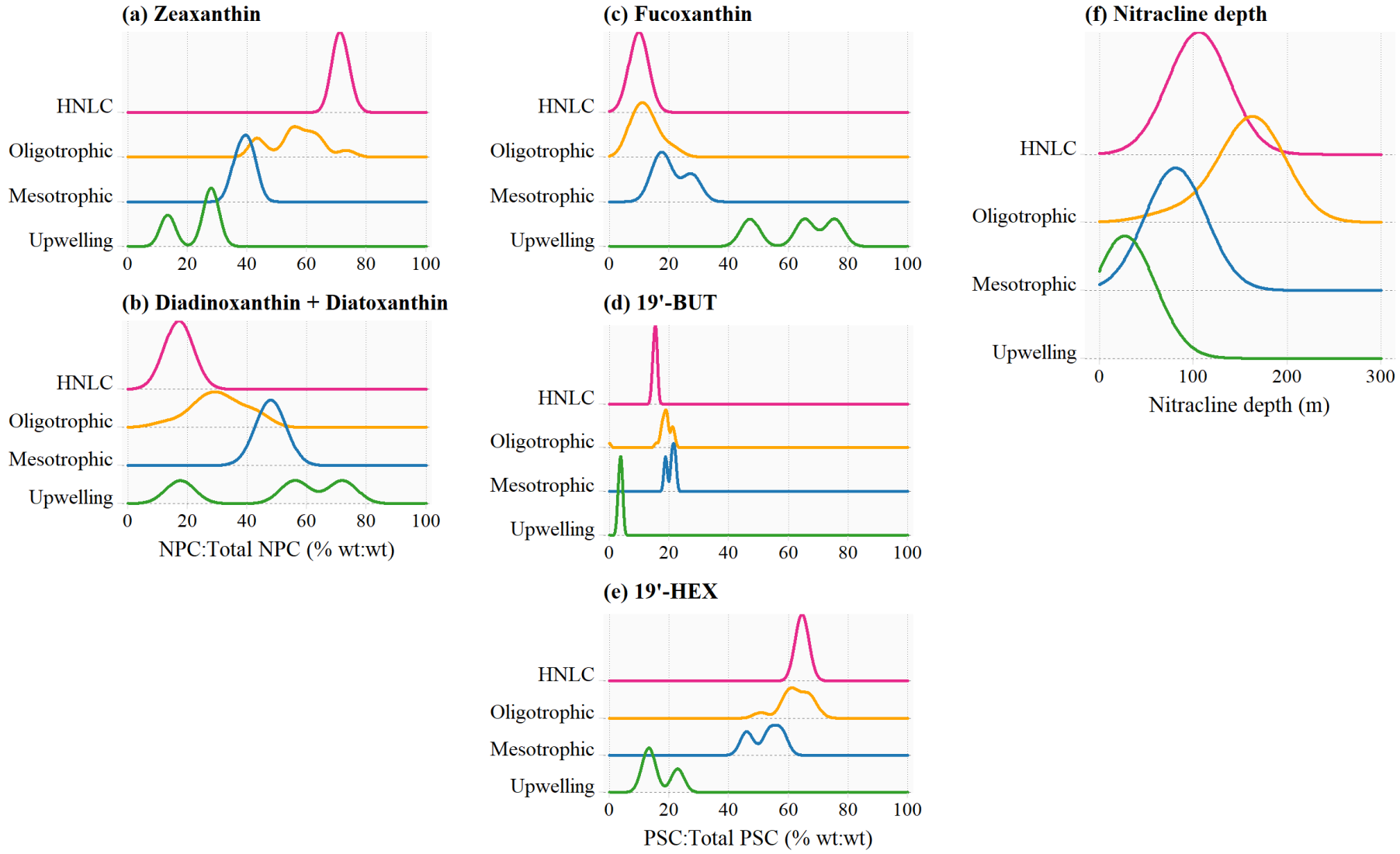

(a) Zeaxanthin
HNLC
Oligotrophic
Mesotrophic
Upwelling
0
20
40
60
80
100
(b) Diadinoxanthin + Diatoxanthin
HNLC
Oligotrophic
Mesotrophic
Upwelling
0
20
40
60
80
100
NPC:Total NPC (% wt:wt)
(c) Fucoxanthin
HNLC
Oligotrophic
Mesotrophic
Upwelling
0
20
40
60
80
100
(d) 19'-BUT
HNLC
Oligotrophic
Mesotrophic
Upwelling
0
20
40
60
80
100
(e) 19'-HEX
HNLC
Oligotrophic
Mesotrophic
Upwelling
0
20
40
60
80
100
PSC:Total PSC (% wt:wt)
(f) Nitracline depth
HNLC
Oligotrophic
Mesotrophic
Upwelling
0
100
200
300
Nitracline depth (m)

Figure 3.3.

Figure 3.2: The non-photosynthetic pigment index (NPP index: the ratio of NPPs to the sum of all pigments) plotted as a function of the depth of sampling divided by the depth of the euphotic zone (z/z_e) as an index of the underwater light availability for each oceanographic dataset included in this study: (a) BIOSOPE, (b) AMT, (c) DCM, (d) HOT, and (e-h) BATS (see the Methods section for details of each cruise). The BIOSOPE dataset was partitioned into the coastal upwelling, mesotrophic, oligotrophic, and high-nutrient, low-chlorophyll (HNLC) regions as described in Grob, Ulloa, Claustre, *et al.* (2007). The BATS time series was roughly divided into seasons: (e) winter (21 December – 20 March), (f) spring (21 March – 20 June), (g) summer (21 June – 20 September), and (h) autumn (21 September – 20 December). For each season, phytoplankton communities were classified into those dominated by eukaryotic taxa (no detectable zeaxanthin; black circles) and those dominated by picocyanobacteria (ratio of zeaxanthin to the sum of all NPPs ≥ 0.6; grey circles).

Figure 3.3: Frequency distributions of the percent contribution (a) zeaxanthin and (b) diadinoxanthin + diatoxanthin to the total concentration of non-photosynthetic carotenoids (NPC), and the percent contribution of (c) fucoxanthin, (d) 19'-butanoyloxyfucoxanthin (19'-BUT), and (e) 19'-hexanoyloxyfucoxanthin (19'-HEX) to the total concentration of photosynthetic carotenoids (PSC), and (f) the estimated nitracline depth for different trophic domains encountered during the BIOSOPE transect. Pigment contributions were measured in surface waters where $z/z_e \leq 0.1$.

Observed variations in surface values of the NPP index had both a spatial and temporal component. For the BIOSOPE transect in the South Pacific, the NPP index increased systematically as one moved from productive, upwelling stations to mesotrophic conditions, and eventually to the high-nutrient, low-chlorophyll (HNLC) regions and the (hyper)oligotrophic central gyres (Figure 3.2a). The possible explanation for these trophic-dependent changes could be a result of corresponding shifts in both the photoacclimatory status and the taxonomic composition of phytoplankton communities. Given that the BIOSOPE data were all collected within a restricted time period and latitudinal range, seasonal and geographical variation in incident solar radiation should be minimal and thus would not be a likely source of large differences in the photoacclimatory characteristics of phytoplankton at the surface ocean.

The importance of phytoplankton taxonomic composition in driving the spatial variation in the NPP index observed at the sea surface during the BIOSOPE cruise was verified using diagnostic pigments (Ras *et al.*, 2008) as summarised in Figure 3.3. In the HNLC and oligotrophic stations, ZEA, a diagnostic pigment of picocyanobacteria *Synechococcus* and *Prochlorococcus* (Ras *et al.*, 2008), accounted for more than 50% of the total NPP concentration (Figure 3.3a). On the other hand, DIAD and DIAT, associated with eukaryotic phytoplankton (Gibb *et al.*, 2000) including photosynthetic picoeukaryotes (Dimier *et al.*, 2009), contributed a low percentage (*ca* < 30%) to the total NPP budget in these regions (Figure 3.3b). The relative abundance of ZEA decreased, while that of DIAD + DIAT increased as trophic conditions progressed toward a more productive state, indicating a domain-shift (Karl, 1999; Karl *et al.*, 2001; Bouman *et al.*, 2011) from a prokaryote-dominated to a eukaryote-dominated surface phytoplankton community. This domain shift was also reflected in a progressive increase in the proportion of the diagnostic pigment FUCO for diatoms to total PSPs from the oligotrophic open-ocean region to the coastal upwelling zone (Figure 3.3c). The PSPs Chl-*b* and PRAS along

with the NPPs VIOL and NEOX were in significant quantities at several upwelling sites (data not shown) and indicated the presence of picoeukaryotic green algae (Ras *et al.*, 2008), such as those in the genus *Ostreococcus* (Six *et al.*, 2009) which has been reported to thrive in various coastal environments (Tragin and Vaulot, 2019). VIOL is involved in the non-photochemical quenching of Chl-*a* through the xanthophyll cycle (conversion of VIOL to ZEA) which is a photoprotective mechanism typical of higher plants and eukaryotic green algae, yet absent in picocyanobacteria (Dubinsky and Stambler, 2009). The near ubiquity of 19'-HEX throughout the transect (Figure 3.3d) reflects the cosmopolitan nature of prymnesiophytes (Gibb *et al.*, 2000; Ras *et al.*, 2008), and the elevated fraction of this carotenoid observed both under oligotrophic conditions and in HNLC waters suggested that some of these cells may fall within the picophytoplankton size fraction (Ras *et al.*, 2008; Liu *et al.*, 2009). It is interesting to note that despite having surface TChl-*a* values (0.2-2 mg Chl-*a* m^{-3}) similar to those of the mesotrophic sites (i.e. near the Marquises Islands), the HNLC stations exhibited a markedly higher abundance of picocyanobacteria, especially *Prochlorococcus* (average of *ca* 200 *Prochlorococcus* cells mL^{-1} in surface waters (0-80 m) of the HNLC region compared to *ca* 60 cells mL^{-1} at other mesotrophic stations; see also Grob, Ulloa, Claustre, *et al.* (2007)) and this is clearly reflected by a markedly higher relative proportion of ZEA (Figure 3.3a). The numerical dominance of *Prochlorococcus* in these low-latitude HNLC waters was associated with highly stable water columns which were likely influenced by the South Pacific Tropical Water (Ras *et al.*, 2008). Molecular studies (Rusch *et al.*, 2010; Malmstrom *et al.*, 2013) have revealed that *Prochlorococcus* isolated from HNLC regions of the tropical Pacific and Indian Oceans are evolutionarily adapted to iron limitation by reducing their iron requirements through the loss of several genes encoding iron-containing proteins which are mostly involved in the electron transport chain. These HNLC isolates are also found to possess genes that enable them to efficiently acquire iron bound to organic ligands in seawater (Malmstrom *et al.*, 2013).

Field experiments conducted by Claustre and colleagues (1994) in the tropical Atlantic Ocean showed that phytoplankton populations inhabiting eutrophic frontal waters were less affected by changes in irradiance than those in the adjacent oligotrophic regions, and in particular diatoms showed relatively high tolerance to high-light stress. This may in part offer an explanation as to why, for the BIOSOPE dataset, the NPP index was observed to decrease systematically from the oligotrophic and HNLC areas to the productive upwelling zone.

The taxonomic composition of phytoplankton communities is governed largely by the intensity of turbulence and its corresponding impact on nutrient availability (Margalef, 1978; Yentsch and Phinney, 1989; Cullen *et al.*, 2002; Platt *et al.*, 2005). In general, turbulence or episodic upwelling is responsible for the physical entrainment of deep, nutrient-rich water to the surface euphotic layer, enhancing the growth of large eukaryotic cells. Highly-stable water columns, on the other hand, are often associated with the reduced supply of new nutrients, which typically leads to the increased abundance of small picophytoplankton which are more efficient in acquiring regenerated forms of nutrients (Raven, 1998; Moore *et al.*, 2002) allowing them to outcompete large-celled eukaryotes under extreme nutrient-limited conditions (Chisholm, 1992; Raven, 1998; Cullen *et al.*, 2002). The region in the water column where there is a sharp increase in nitrate concentration is commonly referred to as the nitracline, and its depth, termed the nitracline depth, is widely regarded as an indicator of the supply of the deep-ocean nitrate to the upper mixed layer (Cullen *et al.*, 1983; Cermeño *et al.*, 2008). The nitracline depth has been demonstrated to be an effective predictor of the geographical distribution of marine phytoplankton taxa, such as diatoms and coccolithophores (Cermeño *et al.*, 2008), and variability in phytoplankton production (Eppley *et al.*, 1979; McGillicuddy *et al.*, 1998; Aksnes *et al.*, 2007; Omand *et al.*, 2012).

Along the BIOSOPE transect, the depth of the nitracline was found to increase steadily from the productive upwelling system nearshore to the more oligotrophic open ocean (Figure 3.3f). In the gyres, the deep nitracline and the corresponding reduced nutrient supply to surface waters resulted in a high abundance of picocyanobacteria indicated by higher values of ZEA:Total NPPs (Figure 3.3a) and NPP index (Figure 3.2a). As the nitracline shoaled, the surface phytoplankton community structure shifted toward a eukaryote-dominated ecosystem (i.e. higher relative contributions of DIAD + DIAD and FUCO (Figures 3.3b-c), and lower NPP index values (Figure 3.2a)) supported by entrainment of new nutrients from depth. These findings are consistent with the results of early investigations showing a link between shifts in phytoplankton community structure and variation of proxies of new nutrient supply in different marine ecosystems (Cleveland *et al.*, 1989; Olson *et al.*, 1990; Sosik and Mitchell, 1995).

HPLC data from the BATS time series revealed that the NPP index at the sea surface varied seasonally with consistently low and less variable values in the winter and spring, and higher and more variable NPP index values observed during the summer-autumn months (Figures 3.2e-h). The uniformly low NPP index observed during winter (late December to mid-March) (Figure 3.2e) could be attributed to the combined effect of deep vertical mixing typical of the Sargasso Sea (Steinberg *et al.*, 2001) and a seasonal reduction in incident solar radiation leading to a weakly-stratified water column. These conditions resulted in a surface mixed layer characterised by nutrient and light conditions that were favourable to low light-acclimated eukaryotic cells as revealed by the higher relative contribution of DIAD + DIAT to the total NPP pool compared to that of ZEA (Figures 3.4a, b). Nutrient-replete conditions established previously by deep winter mixing allowed eukaryotic phytoplankton to dominate within the surface layer to the early spring (late March to mid-April). The relative similarities in the ambient nutrient and light conditions during the winter and spring likely resulted in surface populations dominated by low light-acclimated cells and thus were reflected in the NPP indices for both

seasons falling within a relatively similar range of values (Figures 3.2e, f). As the upper water column became thermally stratified due to intense solar heating, and the intensity of the wind-driven surface mixing was weakened during the late spring and summer months (late June to mid-September), the mixed layer shoaled such that phytoplankton were confined within the upper mixed layer and thereby continuously exposed to high UV and visible radiation. Photoacclimation of phytoplankton to high-light conditions resulted in an overall increase in the NPP index observed for both eukaryote-dominated and picocyanobacteria-dominated populations (Figure 3.2g), although for the picocyanobacterial population, higher NPP index values could also be due in part to an increase in the relative abundance of these cells. Picocyanobacterial cells continued to dominate the surface phytoplankton as surface waters became more nutrient-limited during the early autumn (late September to early October) when the sea-surface temperature remained relatively high (> 25^{o}C) and the water-column was strong stratified (Bouman *et al.*, 2003). However, as the autumn progressed, surface cooling and a deepening of the mixed layer allowed for the upper water column to be replenished with nutrients and resulted in a phytoplankton community dominated by larger eukaryotic cells acclimated to low-light intensities. This prokaryote-to-eukaryote domain shift occurring intraseasonally between early and late autumn was supported by pigment analyses which showed bimodal frequency distributions for the relative abundance of ZEA and DIAD + DIAT (Figures 3.4a, b), and delineating profiles of the NPP index (Figure 3.2h).

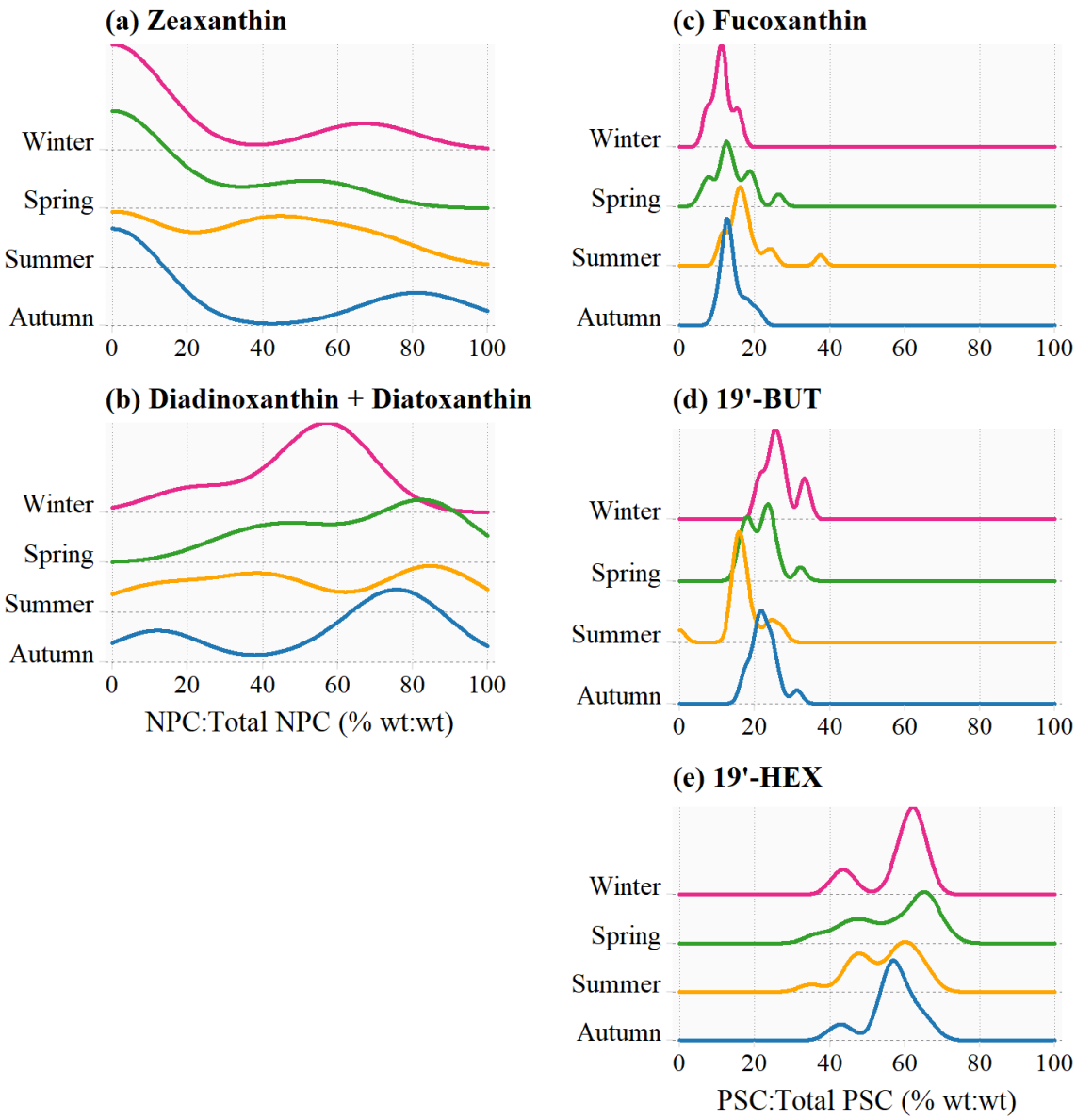


Figure 3.4: Frequency distributions of the percent contribution (a) zeaxanthin and (b) diadinoxanthin + diatoxanthin to the total concentration of non-photosynthetic carotenoids (NPC), and the percent contribution of (c) fucoxanthin, (d) 19'-butanoyloxyfucoxanthin (19'-BUT), and (e) 19'-hexanoyloxyfucoxanthin (19'-HEX) to the total concentration of photosynthetic carotenoids (PSC) measured over an annual cycle in surface water ($z/z_e \leq 0.1$) of BATS stations.

3.3.2 Photoacclimatory characteristics of picocyanobacteria

Picocyanobacteria-dominated populations have been shown to exhibit an extremely large degree of variation in their pigment composition in response to both seasonal and vertical variation in growth irradiances (Figure 3.2; see also Chapter 2). In this section, the photoacclimatory characteristics of this group were examined at the cellular level by virtue of their diagnostic pigment markers. Analyses were focused primarily on the picocyanobacterial-dominated waters of the (sub)tropical oligotrophic gyres where simultaneous measurements of cell abundance determined by flow cytometry and pigment concentrations measured using the HPLC method were available.

In picocyanobacteria, photoacclimatory changes in the magnitude of the NPP index could be attributed to variation in the intracellular concentration of either photoprotective (Kulk *et al.*, 2011; Mella-Flores *et al.*, 2012), or photosynthetic pigments (Kana *et al.*, 1988; Moore *et al.*, 1995), or both. To assess the relative influences that each of these two major pigment groups has on variation in the NPP index, intracellular concentrations of ZEA (Figure 3.5) found in both picocyanobacterial genera *Synechococcus* and *Prochlorococcus* and DVChl-*a*, which is the major photosynthetic pigment for the genus *Prochlorococcus* (Figure 3.6) were plotted against the z/z_e index as a proxy for the available light. When calculating the intracellular concentration of ZEA, one must consider that *Synechococcus* has been shown in culture to be approximately 3-times higher in the amount of ZEA per cell than *Prochlorococcus* when grown over a range of light intensities (Moore *et al.*, 1995).

The intracellular concentration of ZEA tended to remain relatively uniform from the well-lit surface layer down to the bottom of the euphotic zone (Figure 3.5), whereas the amount of DVChl-*a* per cell gradually increased with depth (Figure 3.6). However, for the BIOSOPE

dataset, the calculated DVChl-*a* per cell was relatively constant within the top 0-0.5z_e layer with most values falling between 0.2-0.3. This is likely the result of the authors estimating *Prochlorococcus* abundance based on pigment data assuming 0.23 fg DVChl-*a* cell^{-1} for surface samples where the natural fluorescence of these cells was too low to detect them using flow cytometry (Grob, Ulloa, Li, *et al.*, 2007). In addition, mesotrophic stations sampled during the BIOSOPE cruise off the Marquesas Islands (Grob, Ulloa, Claustre, *et al.*, 2007; Claustre *et al.*, 2008) exhibited intracellular concentrations of DVChl-*a* that were substantially higher (nearly 1.0 fg DVChl-*a* cell^{-1}) and less variable than the rest of the transect (Figure 3.6, blue circles). Vertical density profiles revealed that these stations were more deeply mixed (mixed layer depths of *ca* 70-100 m compared to < 50 m typically observed at other stations), which would reduce the average daily mixed-layer irradiance for phytoplankton communities. If we assume that *Prochlorococcus* cells were uniformly mixed throughout the mixed layer, the reduction in the average mixed-layer irradiance would result in an increase in the intracellular concentration of their major light-harvesting pigments and therefore explain the relatively high DVChl-*a* per cell and low NPP index (Figure 3.2a, blue circles) measured throughout the water column at these stations.

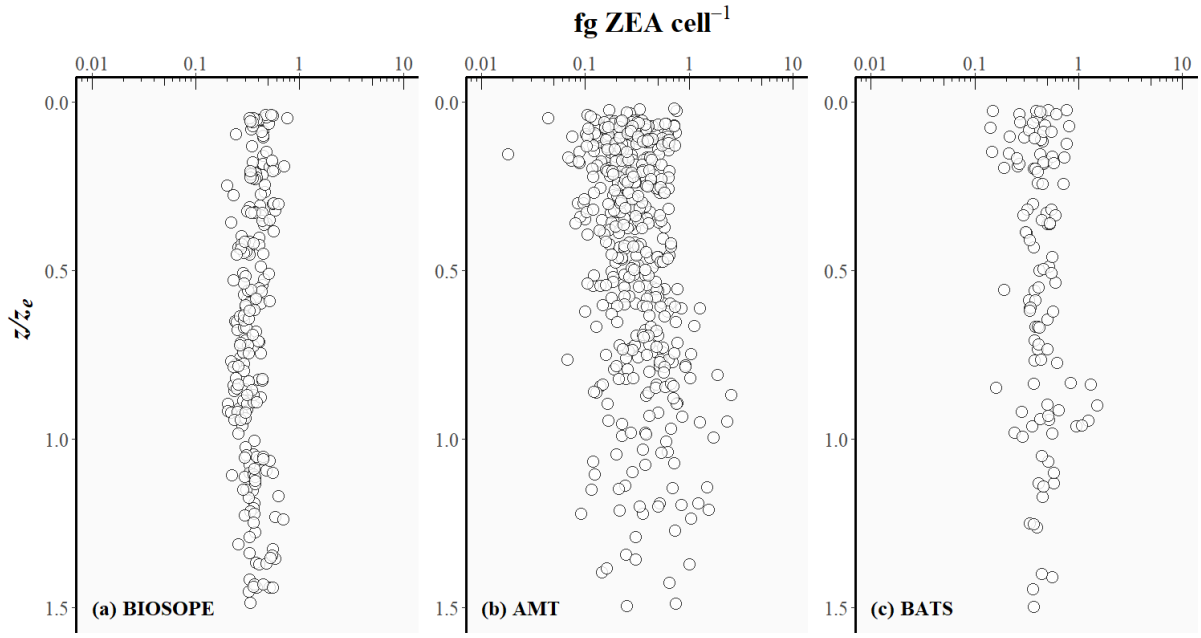


Figure 3.5: The intracellular concentration of zeaxanthin (fg ZEA cell^{-1}) for picocyanobacteria plotted as a function of the depth of sampling divided by the depth of the euphotic zone (z/z_e).

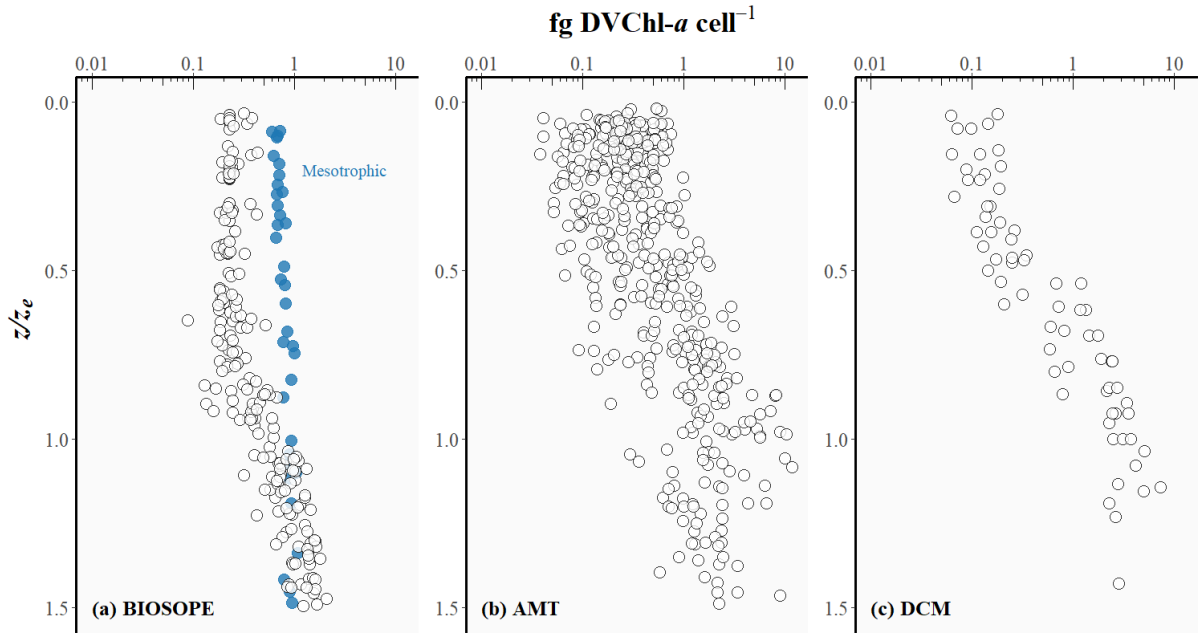


Figure 3.6: The intracellular concentration of divinyl chlorophyll *a* (fg DVChl-*a* cell^{-1}) for *Prochlorococcus* plotted as a function of the depth of sampling divided by the depth of the euphotic zone (z/z_e).

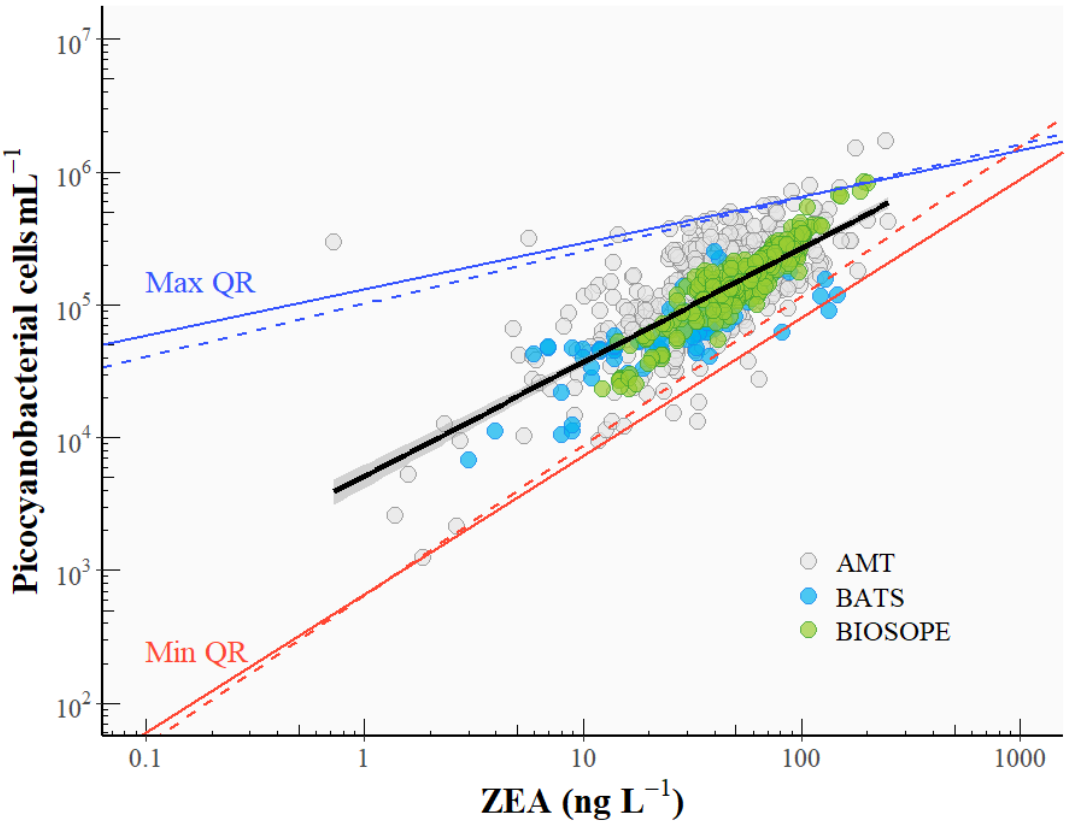


Figure 3.7: Relationship between cell abundance of picocyanobacteria and the concentration of zeaxanthin (ZEA). A linear regression was performed (black line), and the 95% confidence interval for the linear regression line is shaded in grey. The upper (solid blue line) and lower (solid red line) boundaries correspond to the maximum (99th) and minimum (1st) quantiles, respectively (see text for the calculation). Dashed lines represent the re-fitted quantile regressions after identified outliers were excluded.

Uniform ZEA cell^{-1} values over a range of z/z_e values (Figure 3.5) is reflected in the linear relationship between bulk ZEA concentration and the number of picocyanobacterial cells (Pico) depicted in Figure 3.7 ($\log_{10}$ Pico = 0.90 $\log_{10}$ ZEA + 3.65, R^2 = 0.61). Upper and lower envelopes shown in Figure 3.7 correspond, respectively, to the maximum (q_{max}) and minimum (q_{min}) quantiles (Koenker and Bassett, 1978; Sathyendranath *et al.*, 2009). Based on the criteria originally described by Rogers (1992) and later used in the work of Sathyendranath *et al.* (2009), q_{min} and q_{max} should satisfy the conditions $q_{min} > \frac{5}{N}$ and $q_{max} < 1 - \frac{5}{N}$, where N is the total number of observations. Given that our datasets comprised more than 800 observations, q_{min} and q_{max} regression lines could be fitted at the first (q_{min} = 0.01) and the 99th (q_{max} = 0.99)

quantiles, respectively. Quantile regression facilitated constraining the variability in values of ZEA cell^{-1} by allowing outliers that fell outside the computed maximum and minimum quantiles to be identified and removed (Rogers, 1992). The lower and upper boundaries could be viewed as being representatives of extremely high-light (surface) and low-light (bottom of the euphotic zone) conditions, respectively. Note that higher ZEA cell^{-1} values could be the result of the presence of other cyanobacterial populations not accounted for in the flow cytometry counts, in particular the colonial diazotroph *Trichodesmium* that is known to be abundant in the North Atlantic Subtropical Gyre.

Quantile regressions were also fitted to the plot of DVChl-*a* concentration against *Prochlorococcus* cell abundance (Pro) (Figure 3.8a; $\log_{10}$ Pro = 0.82 $\log_{10}$ DVChl-*a* + 3.53, R^2 = 0.40). In this case, the physiological interpretation of the upper and lower envelopes are the opposite to that for the ZEA-cell abundance relationship (Figure 3.7): the lower boundary (q_{min} = 0.01) corresponds to the upper limit of DVChl-*a* cell^{-1} for *Prochlorococcus* cells acclimated to extremely low light, whereas the upper boundary (q_{max} = 0.99) represents the lower limit of DVChl-*a* cell^{-1} resulting from cells photoacclimated to maximum surface irradiances. The overall variability in the relationship between DVChl-*a* and cell abundance (Figure 3.8a) was far greater than that of ZEA and cell abundance (Figure 3.7). This highlights the significance of variation in the cellular content of (DV)Chl-*a* in driving changes in the NPP index in picocyanobacterial-dominated systems.

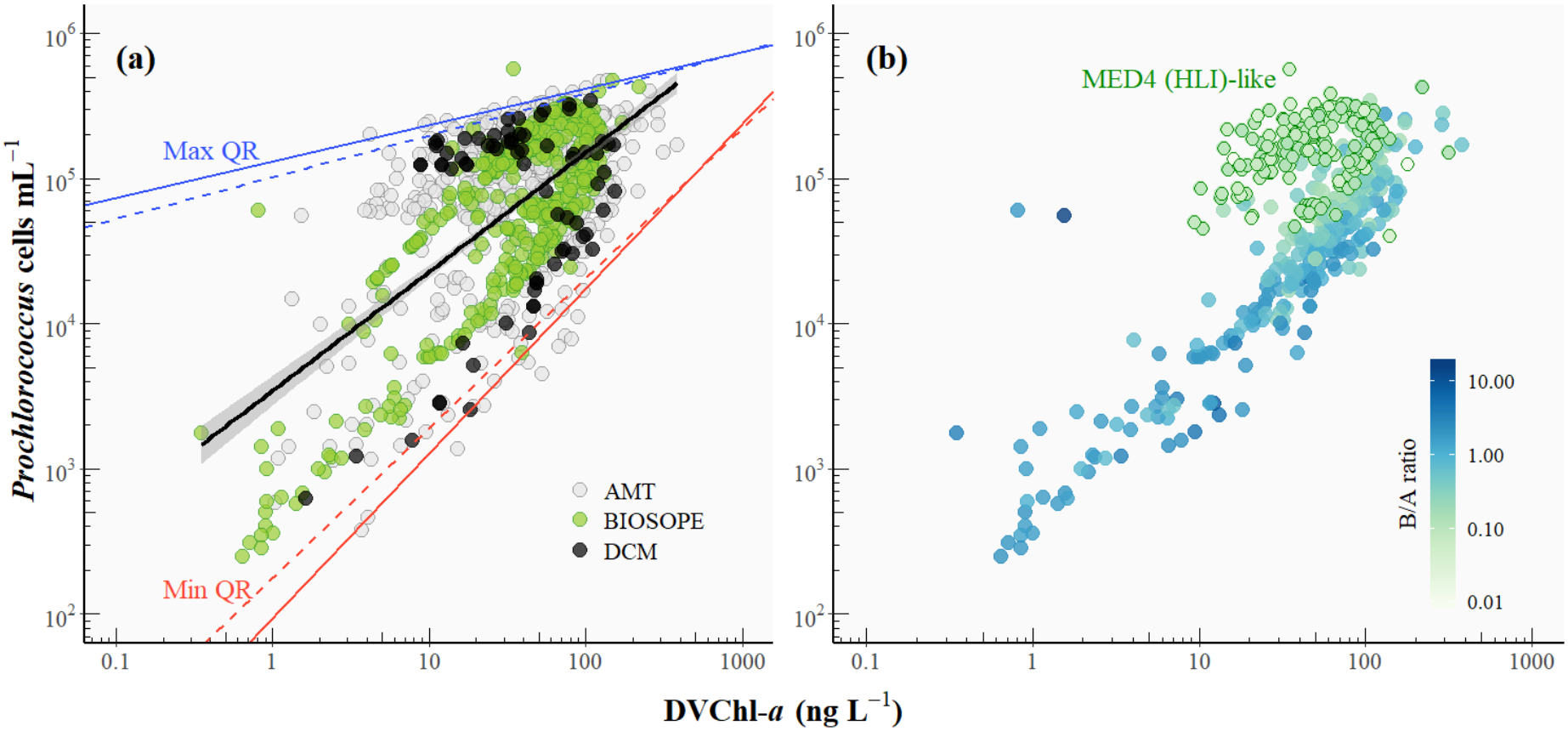


Figure 3.8: (a) Relationship between *Prochlorococcus* cell abundance and the concentration of divinyl chlorophyll *a* (DVChl-*a*). The black line represents the line of best fit, and the grey shaded area indicates the 95% confidence interval. The upper (solid blue line) and lower (solid red line) boundaries correspond to the maximum (99th) and minimum (1st) quantiles, respectively. Dashed lines represent the re-fitted quantile regressions after outliers were removed. (b) As in Figure 3.8a with symbols coloured according to the weight-to-weight ratio of divinyl chlorophyll *b* to divinyl chlorophyll *a* (B/A ratio). *Prochlorococcus* samples with B/A ratios of ≤ 0.14 were classified as the MED4 (HLI)-like populations. Note that only a subset of the HPLC dataset could be used for this analysis since for some datasets DVChl-*b* was not separated from monovinyl Chl-*b*.

These results are consistent with those obtained by Matsumoto and Ando (2009) who examined vertical profiles of picocyanobacterial pigments in the nutrient-limited western Pacific and found a steady vertical increase in the intracellular Chl-*a* concentration but no obvious variation in ZEA content. Our findings are also supported by the culture experiments. Kana and colleagues (1988) were amongst the first to observe the constant ZEA cell^{-1} in nutrient-replete batch cultures of *Synechococcus* WH7803 grown under different irradiance levels. Similarly, Moore *et al.* (1995) found that *Synechococcus* WH8103 and *Prochlorococcus* MED4 maintained relatively constant cellular content of ZEA under varying irradiances, although for the *Prochlorococcus* SS120 strain, there was a slight increase with the increased light level. In contrast, the intracellular concentration of (DV)Chl-*a* was found to decrease significantly at high light for all picocyanobacterial isolates, with the DVChl-*a* cell^{-1} of *Prochlorococcus* being up to 6 times lower than the Chl-*a* cell^{-1} of *Synechococcus*.

The large dynamic range of DVChl-*a* cell^{-1} values observed in our dataset demonstrates the ability of *Prochlorococcus* to acclimate to a broad range of light conditions (Falkowski and LaRoche, 1991; Bouman *et al.*, 2006; Kirk, 2011). Yet, culture experiments by Moore and colleagues (1995) on *Prochlorococcus* strains MED4 and SS120 suggested that plasticity in the intracellular content of DVChl-*a* in different ecotypes may be restricted to a range of light levels not greater than *ca* 2.5 orders of magnitude (Moore *et al.*, 1995; Partensky, Hess, *et al.*, 1999). This therefore suggests that these changes in the DVChl-*a* cell^{-1} are likely the combined result of both photoacclimation and a vertical shift in dominant ecotypes. *Prochlorococcus* strains fall into two broad ecotypes that are differentially adapted to high-light (HL-adapted ecotype) and low-light conditions (LL-ecotype) (Moore *et al.*, 1998).

Figure 3.8a shows that data points tended to separate into two clusters: one above a line of best fit corresponding to lower cell-specific DVChl-*a* concentration, and another below the line of best fit which corresponded to samples exhibiting higher DVChl-*a* content per cell. These clusters represent two distinct populations of *Prochlorococcus* cells occupying different vertical niches in the water column. The occurrence of a double or bimodal population is a common feature in flow cytometric studies of *Prochlorococcus* (Campbell and Vaulot, 1993; Blanchot and Rodier, 1996; Partensky *et al.*, 1996; Zubkov *et al.*, 2000; Thompson *et al.*, 2018) which examine the intensity of cellular fluorescence in the red due to DVChl-*a*. Dim populations have a lower intracellular concentration of DVChl-*a* and thus lower cellular fluorescence, and tend to be found within the surface mixed layer. On the other hand, bright populations have markedly higher DVChl-*a* cell^{-1} and thus a much stronger fluorescence signal, and typically dominate near the bottom of the euphotic zone. Previous studies (Moore *et al.*, 1998; Moore and Chisholm, 1999) on cultured isolates distinguished the dim and bright *Prochlorococcus* as HL- and LL-adapted ecotypes, respectively, according to the observation that the dim isolates have lower ratios of DVChl-*b* to DVChl-*a* (B/A ratios) than the bright ones over a range of growth irradiances. Molecular studies (Moore *et al.*, 1998; Urbach *et al.*, 1998; Hess *et al.*, 2001; Partensky and Garczarek, 2010) later confirmed that the two ecotypes differentiated by B/A ratios are, in several ways, genetically distinct.

Various physiological and genetic properties have been shown to govern the vertical partitioning of *Prochlorococcus* ecotypes in the water column (West and Scanlan, 1999). In laboratory studies, HL-adapted strains have been observed to grow optimally at much higher growth irradiances than their LL counterparts (Moore and Chisholm, 1999). HL ecotypes, such as the MED4 strain, have evolved to withstand light stress by possessing more genes associated with the production of both high light-inducible proteins, which have been suggested to be involved

in excess energy dissipation (He *et al.*, 2001; Hess *et al.*, 2001), and enzyme photolyases used by the cells to repair ultraviolet-induced DNA damage (Rocap *et al.*, 2003). In contrast, LL ecotypes lack the photolyase gene (Rocap *et al.*, 2003), yet they possess multiple genes encoding the Chl-*a*/*b*-binding proteins (Garczarek *et al.*, 2000), a characteristic that helps maximise chlorophyll synthesis and photosynthesis (Hess *et al.*, 2001) and ensure viability of the cells at extremely low irradiances. The higher intracellular concentration of chlorophylls in LL ecotypes does not lead to a significant reduction in their light absorptive efficiency as the pigment-packaging effect is compensated for by their minute cell size (Morel *et al.*, 1993). Yet, it could be another potential factor preventing LL ecotypes from outnumbering HL-adapted strains at the sea surface as it would make them relatively easy to detect by visual grazers compared to optically transparent HL ecotypes (Reckermann and Veldhuis, 1997; Partensky, Hess, *et al.*, 1999). Additionally, in terms of nutrient utilisation, while HL ecotypes are generally unable to use nitrate as a nitrogen source due to the loss of the nitrate uptake genes during their evolution (Moore *et al.*, 2002; Rocap *et al.*, 2002; Johnson and Lin, 2009), certain strains of the LL ecotype have been shown, both in laboratory studies and by genomic analysis, to be capable of nitrite assimilation owing to the presence of the genes that are virtually identical to those found in *Synechococcus* that are associated with the production of the nitrite reductase enzyme and its co-factors (Moore *et al.*, 2002). This may give LL ecotypes a selective advantage over their HL counterparts for growth in deeper waters where new nitrogen is abundant.

Figure 3.8b illustrates that ecotype differentiation in *Prochlorococcus* could account for variation in the intracellular DVChl-*a* concentration measured in this study. In the absence of genetic information for most of our datasets, ratios of DVChl-*b* to DVChl-*a* (B/A ratios) (Moore and Chisholm, 1999; Rocap *et al.*, 2002) were used instead to distinguish ecotypes in *Prochlorococcus* assemblages, with an increase in B/A ratios indicating a shift from HL ecotype-

dominated populations toward populations dominated by LL-adapted strains. Note that only a subset of the HPLC dataset could be used for this analysis since for some datasets DVChl-*b* was not separated from monovinyl Chl-*b*.

Figures 3.8a, b show a clear separation of HL (lower B/A ratios) and LL ecotypes (higher B/A ratios) based on their DVChl-*a* per cell^{-1}, highlighting the robust relationship between the two *Prochlorococcus* ecotypes and the intracellular pigment concentration. Note however that this rather crude pigment criteria for classifying HL and LL ecotype-dominated populations does not reflect the fact that both ecotypes can co-exist. A recent study by Thompson and colleagues (2018) conducted at station ALOHA reported the presence of the LL-adapted strain NATL (with relatively high B/A ratios; Rocap *et al.*, 2002) in the surface *Prochlorococcus* populations characterised by low intracellular chlorophyll concentrations. This was likely to be the result of deep vertical mixing of the water column that brought LL ecotypes into the surface layer (Bouman *et al.*, 2006; Thompson *et al.*, 2018). The physiological and genetic characteristics that are intermediate between HL and LL ecotypes (Partensky and Garczarek, 2010) and the ability to be better acclimated to high light relatively to other members of the same LL ecotype (Rocap *et al.*, 2002; Malmstrom *et al.*, 2010) allow the *Prochlorococcus* NATL to occupy a larger depth range than other clades (Partensky and Garczarek, 2010; Biller *et al.*, 2015).

To examine the impact of shifts in ecotype diversity on variation in DVChl-*a* cell^{-1} requires that ecotype abundances were measured using molecular methods for each sample. Since this information was not available for many of the datasets, the B/A ratios were used to assist in the identification of certain *Prochlorococcus* strains. Comparative culture experiments by Partensky and colleagues (1993) on the isolates MED4 (HLI), SARG (LLI), and NATL1 (LLI) grown at different irradiance levels (*ca* 7.5-133.0 μmol quanta (white light) m^{-2} s^{-1}) showed that the

relationship between intracellular concentrations of DVChl-*a* and DVChl-*b* (Figure 2 in Partensky *et al.*, 1993) for the MED4 strain had the regression slope that was markedly different from those for SARG and NATL1 strains. Also, although B/A ratios for all strains exhibited a general trend to decrease with increasing growth irradiances, the B/A ratio of the MED4 strain was always less than 0.14, while those of the SARG and NATL1 strains were never found to fall below this value. The range of B/A ratios of the MED4 isolate reported in Partensky *et al.* (1993) is comparable to the results of more recent studies such as the work by Moore *et al.*, (1995) who observed the range between 0.05 and 0.20 (growth irradiances >10-400 μmol quanta (white light) $m^{-2}\,s^{-1}$), and the work by Rocap and colleagues (2002) reporting that the MED4 strain acclimating to low light at 18 μmol quanta (white light) $m^{-2}\,s^{-1}$ (*ca* 1% of typical surface irradiance at subtropical gyres) has the B/A ratio of 0.20, which is the lowest among the 32 *Prochlorococcus* strains examined.

Based on the culture study of Partensky *et al.* (1993), *Prochlorococcus* samples which were likely to be dominated by the MED4 strain (B/A ratio < 0.14) were identified. As shown in Figure 3.8b (green outline circles), populations dominated by the MED4-like cells exhibited very low intracellular concentrations of DVChl-*a*, typical of HLI ecotypes, although the values were somewhat variable. Vertical profiles (data not shown) showed that DVChl-*a* $cell^{-1}$ for samples identified as resembling *Prochlorococcus* HLI populations increased from approximately 0.1 near the well-lit surface to up to 1.0 fg DVChl-*a* $cell^{-1}$ below the euphotic depth (z/z_e > 1). This increase was within the similar range previously observed in culture studies (Moore *et al.*, 1995; Moore and Chisholm, 1999) and suggested photoacclimation in this ecotype. It is interesting to note that the occurrence of the HLI ecotype indicated by the (low) B/A ratio throughout the euphotic layer was consistent with observations from various regions of the Atlantic and Pacific Oceans (Zinser *et al.*, 2007; Zwirglmaier *et al.*, 2007; Malmstrom *et al.*,

2010; Thompson *et al.*, 2018) where the HLI ecotype identified using quantitative polymerase chain reaction (qPCR) and dot blots was found in both the population of the high light-acclimated (low DVChl-*a* cell^{-1}) cells in surface waters and the high-chlorophyll cells acclimated to low light at the base of the euphotic zone. These observations illustrate the high degree of physiological plasticity of wild HL-*Prochlorococcus* strains which are able to upregulate the amount of DVChl-*a* cell^{-1} in response to decreasing irradiances, potentially to the same extent as LL ecotypes (Thompson *et al.*, 2018).

The results presented in this study show that variability in DVChl-*a* cell^{-1} is likely to be the result of (1) changes in vertical distribution of genetically distinct HL and LL-adapted *Prochlorococcus* ecotypes, and (2) photoacclimation of each ecotype to the local light environment through regulation of the intracellular concentration of the major light-harvesting pigment. The apparent link between genetic diversity and the inherent photophysiological characteristics of *Prochlorococcus* provides important insight to its ecological success. *Prochlorococcus* is able to occupy a broad range of ocean niches from the sea surface to the bottom of the euphotic zone (Coleman and Chisholm, 2007; Partensky and Garczarek, 2010), and, as a result, is a significant contributor to global marine primary production (Goericke and Welschmeyer, 1993; Vaulot *et al.*, 1995; Lange *et al.*, 2018). Because of its small and highly-sequenced genome, unique pigmentation, and its rapid identification based on its unique optical signature (Coleman and Chisholm, 2007), *Prochlorococcus* has been heavily used as a model organism for understanding relationships between environmental forcing and microbial processes across vast scales of organisation, from genomes to biomes (Coleman and Chisholm, 2007; Partensky and Garczarek, 2010; Biller *et al.*, 2015). However, several studies have pointed to differences in photoprotective mechanisms amongst picocyanobacterial taxa as well as when compared to other eukaryotic phytoplankton (e.g. Six *et al.*, 2007; Key *et al.*, 2010; Kulk *et al.*, 2011; Mella-

Flores *et al.*, 2012; see also Chapter 2). The question then arises whether *Prochlorococcus* can serve as a useful model for elucidating phytoplankton photoacclimation in general. In other words, are photoacclimatory characteristics of *Prochlorococcus* similar or different from those of eukaryotic species, including photosynthetic picoeukaryotes? Since, in many global ocean biogeochemical models, *Prochlorococcus* is normally classified together with *Synechococcus* and picoeukaryotes as a 'pico-autotroph' functional type (Le Quéré *et al.*, 2005; Nair *et al.*, 2008) based on their shared characteristics of playing a key role in regenerative production and being highly effective in nutrient and photon acquisition (Raven, 1998; Le Quéré *et al.*, 2005), it is important to be able to compare photoacclimatory properties of picophytoplankton groups so that it can be justified, from a physiological point of view, whether it is appropriate to combine them into one distinct biogeochemical functional type. I attempt to address this problem in the next section through examining how the carbon-to-(DV)Chl-*a* ratio varies in natural populations of *Prochlorococcus*.

3.3.3 Carbon-to-Chl-*a* ratios

The carbon-to-Chl-*a* ratio (θ) is widely used in phytoplankton growth models to represent the photophysiological status of microalgae (Geider, 1987; Geider *et al.*, 1996; Graff *et al.*, 2016) and to convert Chl-*a* concentration to estimates of carbon standing stock. Studies (Geider, 1987; MacIntyre *et al.*, 2002) have shown that, for various phytoplankton species grown under constant temperature and nutrient-replete conditions, θ increases linearly with increasing light level. Light-dependent variability in θ is the result of photophysiological mechanisms used by the cell to avoid the harmful overexcitation of photosystems under high light by lowering the cellular content of Chl-*a* and accumulating more carbon reflecting the increase in the photosynthetic utilisation of the absorbed light energy (Geider, 1987; Jakobsen and Markager, 2016).

However, when cultures are maintained under constant light levels, θ decreases significantly with increased temperature (Geider, 1987), suggesting that high temperature may inhibit phytoplankton growth and thus reduce the demand for energy in the form of fixed carbon (Geider *et al.*, 1997). Variation in θ is also regulated strongly by the availability of nutrients, particularly nitrogen which is a major component of the light-harvesting apparatus (Halsey and Jones, 2015). In addition, since the cellular quota of Chl-*a* differs widely between phytoplankton taxa (MacIntyre *et al.*, 2002), it can be expected that θ also varies across taxa.

(1) Estimation of the carbon-to-DVChl-*a* ratio of *Prochlorococcus*

The carbon-to-DVChl-*a* ratio of *Prochlorococcus* (θ_{Pro}) was estimated based on simultaneous measurements of cell abundance and the concentration of DVChl-*a* illustrated in Figure 3.9. *Prochlorococcus* cell carbon was estimated from abundances (determined by flow cytometry) using a conversion factor of 49 fg C cell^{-1} (Cailliau *et al.*, 1996) based on the assumption that both high light-adapted (HL) and low light-adapted (LL) ecotypes have similar carbon contents. In non-axenic cultures of a *Prochlorococcus* strain, Cailliau and colleagues (1996) derived the cellular carbon contents from flow cytometric cell counts and measurements of particulate organic carbon (POC) that were corrected for the presence of heterotrophic bacteria. Their study found that the values obtained for *Prochlorococcus* under low and high light were not statistically different, suggesting that this value may be applied to both HL and LL cells. The carbon content of *Prochlorococcus* directly determined by Cailliau and colleagues from culture experiments are comparable to other published estimates based on indirect conversions of cell volume to carbon (e.g. 59 fg C cell^{-1} reported in Li *et al.* (1992); 54 fg C cell^{-1} in DuRand *et al*. (2001); 53 fg C cell^{-1} in Campbell *et al*. (1994) and Grob, Ulloa, Li, *et al.* (2007)), although it is important to stress that determination of the carbon content from cell volume has a

significant degree of uncertainty since, as pointed out in Bertilsson *et al.* (2003), the amount of carbon per unit cell volume observed in marine bacteria can vary widely both between and within species in response to changes in growth conditions. Our choice of conversion factor is therefore based on the robustness of using estimates of *Prochlorococcus* cellular carbon content derived from direct measurements of POC (Partensky, Hess, *et al.*, 1999; Bertilsson *et al.*, 2003) and its agreement with other estimates from the literature.

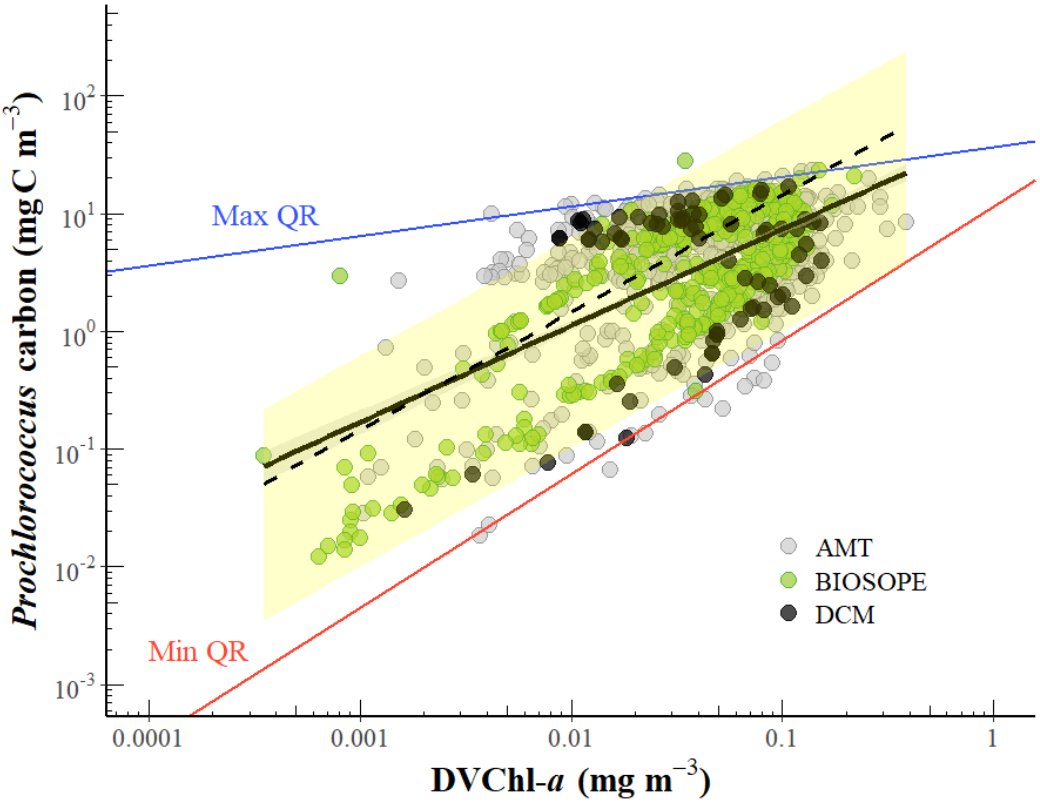


Figure 3.9: The cell carbon biomass of *Prochlorococcus* plotted against the concentration of divinyl chlorophyll *a* (DVChl-*a*). Carbon content was converted from cell abundances using the conversion factor of 49 fg C cell^{-1} (Cailliau *et al.*, 1996). The black line represents the line of best fit, and the grey shaded area indicates the 95% confidence interval. The upper (solid blue line) and lower (solid red line) boundaries correspond to the maximum (99th) and minimum (1st) quantiles, respectively. The black dashed line corresponds to the carbon-to-DVChl-*a* of *Prochlorococcus* (θ_{Pro}) of 145 g C (g DVChl-*a*)$^{-1}$ reported in Sathyendranath *et al.* (2009). The yellow-shaded area represents the possible range of θ_{Pro} values reported in the literature.

(2) Constraining the variability in the estimated θ_{Pro}

When samples collected from below the $1.5z_e$ depth and potential outliers (Figure 3.9) were removed, our estimates of θ_{Pro} varied from 8 to 396 g C (g DVChl-*a*)$^{-1}$ with a mean surface (≤ 20 m) θ_{Pro} of 168 (60-342), 170 (66-342), 145 (60-257), and 266 (258-273) g C (g DVChl-*a*)$^{-1}$ for the entire dataset, the AMT, the BIOSOPE, and the DCM cruises, respectively. To assess whether the extent of the observed variability in θ_{Pro} was reasonable, I compared these results with θ_{Pro} measured in various culture experiments and field studies using an approach outlined in Marañón (2005). Given that (1) the intracellular carbon content of *Prochlorococcus* previously reported in the literature ranged from about 40 to 124 fg C cell^{-1} (Veldhuis and Kraay, 1990, 2004; Cailliau *et al.*, 1996; Veldhuis *et al.*, 1997; DuRand *et al.*, 2001; Claustre *et al.*, 2002; Bertilsson *et al.*, 2003; Grob, Ulloa, Li, *et al.*, 2007), and (2) the intracellular content of DVChl-*a* of *Prochlorococcus* cells subject to extremely high irradiances typical of the subtropical surface ocean (e.g. > 1,000 μmol quanta m^{-2} s^{-1}) can be as low as *ca* 0.2 fg DVChl-*a* cell^{-1} (Blanchot and Rodier, 1996; Gibb *et al.*, 2001; Grob, Ulloa, Claustre, *et al.*, 2007) and that of *Prochlorococcus* cells growing under very low irradiances (e.g. 7 μmol quanta m^{-2} s^{-1}) is up to *ca* 4.0 fg DVChl-*a* cell^{-1} (Partensky *et al.*, 1993; Blanchot *et al.*, 2001), the resulting upper boundary of θ_{Pro} values should be in the range of 200-620 g C (g DVChl-*a*)$^{-1}$ and the lower boundary in range of 10-31 g C (g DVChl-*a*)$^{-1}$. In general, our estimated values of θ_{Pro} fell within these derived upper and lower limits.

Using open-ocean samples collected from the Northwest Atlantic and the Arabian Sea, Sathyendranath and colleagues (2009) indirectly estimated θ for different groups of phytoplankton in the field based on linear regressions of POC and Chl-*a* concentration and obtained an average θ_{Pro} value of 145 g C (g DVChl-*a*)$^{-1}$ for stations classified as *Prochlorococcus*-dominated.

When this average value was superimposed on the scatterplot of *Prochlorococcus* cell carbon content and DVChl-*a* concentration (Figure 3.9), the slope of the line tended towards HL *Prochlorococcus* samples. It should be noted that most of the data used in Sathyendranath *et al.* (2009) were from samples collected within the top 40 m of the water column. The estimated value of θ_{Pro} obtained in the Sathyendranath *et al.* (2009) study was much higher than the average θ_{Pro} values reported by Blanchot and colleagues (2001) for surface (0-40 m) *Prochlorococcus* samples from the oligotrophic (66 g C (g DVChl-*a*)$^{-1}$) and HNLC (93 g C (g DVChl-*a*)$^{-1}$) regions of the equatorial Pacific (Table 3.4). It has been shown that *Prochlorococcus* samples from mesotrophic regions contain more carbon biomass relative to chlorophyll pigment than samples associated with oligotrophic environments (Wei *et al.*, 2019) and this may explain the higher θ_{Pro} values in the Sathyendranath *et al.* (2009) study.

The choices of the carbon conversion factor used to convert phytoplankton cell density to carbon biomass could introduce significant bias to our estimates of θ_{Pro}. Our conversion factor of 49 fg C cell^{-1} (Cailliau *et al.*, 1996) was directly measured on cultures, whereas Grob, Ulloa, Claustre, *et al.* (2007) independently derived the cellular content of *Prochlorococcus* from total particle beam attenuation coefficient measurements conducted in the South Pacific Subtropical Gyre and obtained a much lower value of 29 fg C cell^{-1} which is in line with that determined by Zubkov and colleagues (2000) based on cell volume (by size fractionating filtration) on samples collected during the AMT-3 cruise. This illustrates that there is no universal carbon conversion factor (Veldhuis and Kraay, 2004) and shows that such conversion factors vary widely depending on the method as well as the natural and experimental growth conditions of the cells. Attempts have been made, particularly in culture studies on axenic strains (Claustre

et al., 2002; Bertilsson *et al.*, 2003), to refine taxon-specific conversion factors to aid the assessment of the contribution of the phytoplankton standing stock to the ocean carbon pool. Independent information including the genome size and optical properties (Veldhuis *et al.*, 1997; Veldhuis and Kraay, 2004) will also help to improve phytoplankton carbon conversion factors for use in marine biogeochemical studies.

Table 3.4 Published estimates of carbon-to-(DV)Chl-*a* ratio (θ) for *Prochlorococcus* (Pro) and photosynthetic picoeukaryotes (PPE)

Reference	**Study area (sampling depth)**	**θ (g C (g Chl-*a*)$^{-1}$)**	
		Pro[I]	**PPE**
Blanchot *et al*. (2001)	Equatorial Pacific (0-50 m)		
	- Oligotrophic (warm pool) region	67	43
	- HNLC region	93	84
Kulk *et al*. (2011)	Culture experiments (light intensities: 50-125 μmol quanta m^{-2} s^{-1})	14-43 (HLI)	39-40[II]
Sathyendranath *et al*. (2009)	Northwest Atlantic and the Arabian Sea (0-40 m)	143-147	
Stawiarski *et al*. (2018)	Culture experiments (13-150 μmol quanta m^{-2} s^{-1})	12-36 (HLII) 15-56 (LLII)	19-24[III] 19-28[IV]
Veldhuis and Kraay (2004)	Subtropical North Atlantic (0-150 m)	15-450	30-80
This study		8-396	

[I] HL and LL = High light and low light-adapted ecotypes
[II] *Ostreococcus* sp., [III] *Micromonas pusilla*, [IV] *Nannochloropsis granulata*

(3) Comparison with eukaryotic phytoplankton

The high and variable values of θ_{Pro} observed in this study clearly demonstrate that *Prochlorococcus* has a tremendous physiological capacity to acclimate to changes in the wide range of environmental conditions in which it lives. In general, picocyanobacteria tend to have higher and more variable θ than eukaryotic micro- and nanophytoplankton (i.e. diatoms, dinoflagellates, and nano-prymnesiophytes) (Veldhuis and Kraay, 2004; Sathyendranath *et al.*, 2009).

Larger eukaryotes, notably diatoms which are known to be successful in fluctuating light environments (more deeply mixed waters) (Claustre *et al.*, 1994), have been shown to be intrinsically less sensitive to photodamage not only owing to their large cell size and corresponding high pigment packaging (Key *et al.*, 2010; Wu *et al.*, 2012), but also because they are able to maintain their constitutive resource investments in photoprotection under varying light regimes (Talmy *et al.*, 2013; Halsey and Jones, 2015), which in turn reflects in the relatively stable θ. In contrast, small picocyanobacteria, which are adapted to more stable water columns, can adjust the proportion of cellular resources allocated to light-harvesting apparatus in response to shifts in irradiance (Talmy *et al.*, 2013), resulting in highly variable intracellular concentration of photosynthetic pigments (Moore *et al.*, 1995) and thus θ. However, within the picoplankton size range, it remains unclear whether cyanobacteria significantly differ from photosynthetic eukaryotes with respect to variation in θ since studies that directly compare θ values of the two picophytoplankton groups are rare (Table 3.4).

In comparison to picocyanobacteria, picoeukaryotes have been found to be better adapted to grow in ocean habitats characterised by more extreme physical dynamics (Bouman *et al.*, 2011). Laboratory studies (Kulk *et al.*, 2011; Stawiarski *et al.*, 2018) have demonstrated that photosynthetic picoeukaryotes are able to maintain the high growth rates over a wide range of irradiances and are less affected by photoinhibition at high light. Therefore, it is reasonable to anticipate that our estimates of θ_{Pro} should be higher and more variable than those of picoeukaryotes. This expectation is consistent with the findings of Veldhuis and Kraay (2004) that examined flow cytometry samples from oligotrophic subtropical waters of the North Atlantic using an independent approach for converting cellular DNA content to phytoplankton carbon biomass. The study showed that θ_{Pro} decreased substantially from a maximum of 450 at the surface to a minimum of 15 g C (g DVChl-*a*)$^{-1}$ at 150 m, whereas θ of the collective pico- and

nanoeukaryote communities also decreased with depth, although to a much lesser extent (3-7 fold variation) with surface values of 30-80 g C (g Chl-*a*)$^{-1}$. The reduced vertical variation in θ observed for photosynthetic eukaryotes was likely due in part to a co-variation of cell pigment content and size as reflected by the increases in both the intracellular concentration of Chl-*a* and the genome size (proportional to cell size) with depth. A culture experiment by Kulk and colleagues (2011) also showed that θ_{Pro} varied from 14 ± 1.27 to 43 ± 1.17 g C (g DVChl-*a*)$^{-1}$ under variable light intensities (50-125 μmol quanta m^{-2} s^{-1}), while the observed range for the picoeukaryote *Ostreococcus* sp. was only between 39 ± 1.89 and 40 ± 0.99 g C (g Chl-*a*)$^{-1}$.

Blanchot and colleagues (2001) measured vertical profiles of picophytoplankton abundance, cell size, and HPLC pigment concentrations, and using information on cell size estimated the cellular carbon content for both picocyanobacteria and photosynthetic picoeukaryotes in the oligotrophic and HNLC regions of the equatorial Pacific. Using their estimates of intracellular pigment concentration and carbon content (Tables 1-2 in Blanchot *et al.*, 2001), θ_{Pro} and θ for picoeukaryotes were computed for samples collected within the top 50 m of the water column. It was found that *Prochlorococcus* had significantly higher θ than picoeukaryotes in oligotrophic waters (means of 65.5 ± 9.87 g C (g DVChl-*a*)$^{-1}$ and 43.1 ± 4.89 g C (g Chl-*a*)$^{-1}$, *t*-test, 95% confidence interval, $p < 0.05$), whereas, in the HNLC region, the average surface θ values for the two algal groups (92.8 ± 11.5 g C (g DVChl-*a*)$^{-1}$ for *Prochlorococcus* and 84.1 ± 6.98 g C (g Chl-*a*)$^{-1}$ for picoeukaryotes) were not statistically different ($p = 0.24$). Note that θ for both *Prochlorococcus* and picoeukaryotes increased considerably under HNLC conditions as a result of an increase in cell diameter (and thus cellular carbon content estimated from cell biovolume) in both groups as well as a decline in the amount of Chl-*a* cell^{-1} (*ca* 2 fold in the surface layer) in photosynthetic picoeukaryotes.

Similarly, a recent laboratory study by Stawiarski *et al.* (2018) using three groups of picocyanobacteria (HL-*Prochlorococcus*, LL-*Prochlorococcus*, and *Synechococcus*) and four different strains of picoeukaryotes also showed that θ for all picophytoplankton groups exhibited similar light-dependent variation, although *Prochlorococcus* cultures reached higher θ values under high-light treatments, and the variability in θ_{Pro} appeared to be relatively large compared to other species. However, as a group, picocyanobacteria (including *Synechococcus*) were found to have the maximum θ that was not statistically higher than that of the eukaryotic picophytoplankton.

3.4 Concluding Remarks

The wealth of pigment and flow cytometry data obtained from a range of open-ocean environments allowed examination of the vertical variation in the NPP index and how it relates to photoacclimatory responses of individual phytoplankton cells in terms of changes in their intracellular pigment complement, in particular the relative concentrations of NPPs and PSPs.

The NPP index varied significantly in response to depth-dependent changes in the underwater light conditions (indexed by the ratio z/z_e), photoacclimatory status, and gross phytoplankton community structure (determined by pigment markers and cell counts). Vertical variability in the NPP index was especially pronounced in the subtropical gyres and low-latitude HNLC regions and observations from the BATS time series show that there is also a seasonal component to changes in the NPP index: the summer and early autumn surface communities dominated by high-light acclimated picocyanobacteria were characterised by higher NPP index, which was largely caused by the presence of a strongly stratified water column.

At the cellular level, variation in the NPP index in *Prochlorococcus* was found to be associated primarily with changes in the intracellular concentration of DVChl-*a* rather than NPPs. The marked increase in DVChl-*a* cell^{-1} with depth is the result of both a photoacclimatory response to low light through increasing the intracellular concentration of DVChl-*a* in order to harvest sufficient light to support net growth and a shift from HL to LL ecotypes which are inherently more pigmented as a result of evolutionary adaptation to low-light conditions (Moore *et al.*, 1998). The vertical partitioning of ecotypes allows this globally-significant marine picocyanobacterium to acclimate to a wide range of light and nutrient conditions which is also reflected by the observed variability in derived values of θ_{Pro} computed from flow cytometry counts, pigment data, and published conversion factors. Estimates of θ_{Pro} appeared to be far more variable than θ values for eukaryotic phytoplankton reported in the literature, implying that *Prochlorococcus* is more sensitive to changes in growth irradiance and must therefore regulate the cellular constituents involved in light harvesting and photoprotection, whereas microalgae have been shown to be more resilient to changes in light history (Claustre *et al.*, 1994) and less vulnerable to photodamage at high light (Six *et al.*, 2007; Key *et al.*, 2010).

These results serve to underscore the importance of considering the physiological plasticity of different phytoplankton groups when using pigments and cell counts as proxies of phytoplankton biomass or chemotaxonomic markers. The unique pigment signatures of *Prochlorococcus* can be used to not only map their distribution but also provide insight into the photoacclimatory status of the natural population in response to light history caused by seasonal changes in physical forcing. Developing a mechanistic understanding of how Chl-*a*, PSPs, and NPPs change relative to one another at the cellular level across different taxa is required if these pigments are to be used to derive estimates of phytoplankton carbon biomass, taxa, and θ from *in situ* and satellites observations (Karl, 1999; Behrenfeld *et al.*, 2005).

Chapter 4

Relationship between Pigment Composition and Photophysiology of Marine Phytoplankton

4.1 Introduction

Phytoplankton are responsible for the majority of carbon fixation occurring in marine environments (Field *et al.*, 1998; Falkowski and Raven, 2007), and the net primary production by phytoplankton fuels the marine food webs which sustains global fisheries (Field *et al.*, 1998). Recent advances in ocean-colour remote sensing have provided a synoptic view of the global distribution of near-surface phytoplankton biomass in the form of chlorophyll *a* (Chl-*a*) and the photosynthetically-available radiation incident on the sea surface. To estimate global marine primary production, these two fundamental variables must be coupled with additional information on the response of phytoplankton photosynthesis to available irradiance (Platt and Sathyendranath, 1988; Behrenfeld and Falkowski, 1997) which is not directly accessible to present-day satellite remote sensing. Thus, there is a pressing need to understand the environmental factors governing variability in phytoplankton photophysiology based on field observations.

The photosynthetic response of phytoplankton to the forcing irradiance is influenced by the structure of phytoplankton communities (Harrison and Platt, 1986; Bouman *et al.*, 2005; Uitz *et al.*, 2006, 2008; Xie *et al.*, 2015) and the physiological status of phytoplankton (Falkowski, 1981; Sakshaug *et al.*, 1997), both of which, in the subtropical oligotrophic ocean, are known to vary along vertical gradients of light, temperature, and nutrients that are characteristic of highly stratified water columns. The proportion of non-photosynthetic pigments relative to total phytoplankton pigments, commonly referred to as the NPP index (Babin *et al.*, 1996), also

varies in response to vertical changes in light conditions. The variation in the NPP index originates from a combination of vertical shifts in phytoplankton taxonomic groups or ecotypes with their distinct intracellular pigment complement and vertical changes in photoacclimatory status of the algal cells (Falkowski and LaRoche, 1991; Moore *et al.*, 1998, 2006). NPPs are well known to govern changes in the magnitude and shape of phytoplankton absorption spectra ($a_{ph}(\lambda)$) (Chapter 2). Consequently, there has been a growing interest in using the NPP index or the corresponding variability in the shape of $a_{ph}(\lambda)$ measured either in relative terms (i.e. absorption ratio) or in terms of absolute differences (i.e. spectral slope) in the blue-green region of the spectrum to characterise the physiological state of phytoplankton (SooHoo *et al.*, 1986; Johnsen *et al.*, 1994; Eisner *et al.*, 2003) and the physical properties of the water column in which they live (Matsumoto and Ando, 2009).

Changes in the NPP index resulting from photoacclimation also have a profound impact on the photosynthetic performance of phytoplankton since NPPs absorb light without delivering excitation energy to the reaction centre. As cells acclimate to high irradiances, an increase in the NPP index leads to a decrease in the functional absorption cross section of photosystem II (Falkowski and LaRoche, 1991) which is, in turn, associated with reductions in the efficiency of light utilisation represented by the initial slope of the photosynthesis-irradiance (*PE*) response and the maximum quantum yield of photosynthesis (Sakshaug *et al.*, 1997).

The primary factor that drives photoacclimatory changes in the NPP index is variance in the cellular quota of photosynthetic pigments, notably Chl-*a*, with the light history of the cell (MacIntyre *et al.*, 2002). Under varying growth irradiances, phytoplankton adjust the intracellular concentration of Chl-*a* relative to their cellular carbon content, reflecting differential allocation of resources (Halsey and Jones, 2015) to light-harvesting apparatus and the carbon

biomass pool (retained following carbon losses to respiration and excretion, Sathyendranath *et al.*, 2020). Therefore, similar to the NPP index, the resultant variation in the ratio of carbon to Chl-*a* (θ) can be viewed as an indicator of shifts in the photoacclimatory status in phytoplankton (Geider, 1987; Kirk, 2011) and is parameterised into models of phytoplankton growth and primary production (Sathyendranath *et al.*, 2020). Also, in primary production models, Chl-*a* has been commonly used as an index of phytoplankton biomass (Sathyendranath and Platt, 1993) since the pigment plays a central role in photosynthesis and can be measured unambiguously either in the laboratory, in the field, or by remote sensing. However, in numerical biogeochemical models aimed to assess the role of phytoplankton in the global carbon cycle, phytoplankton biomass is typically measured in carbon units, and θ has to be invoked to convert between the two currencies of biomass (Sathyendranath *et al.*, 2009). Knowledge of θ is also needed to relate the Chl-*a*-specific photosynthetic rates to phytoplankton growth rates (Marañón, 2005), which is considered a direct measure of the fitness of an algal species or group (Boyd *et al.*, 2013; Fanesi *et al.*, 2017).

A major challenge in assessing the natural variability in θ has been the determination of the concentration of phytoplankton carbon (Graff *et al.*, 2016). In contrast to Chl-*a* which can be quantified using standard methodologies, measuring phytoplankton carbon is far more complicated due primarily to an inability to physically separate phytoplankton cells from other particles (e.g. inorganic and detrital particles and heterotrophic organisms) (Laws, 2013; Graff *et al.*, 2015). Therefore, a range of indirect approaches have been developed to estimate phytoplankton carbon including conversions from cell counts and cell volume (Verity *et al.*, 1992), from intracellular contents of deoxyribonucleic acid (DNA) (Veldhuis *et al.*, 1997; Veldhuis and Kraay, 2004) and adenosine triphosphate (ATP) compounds (Sinclair *et al.*, 1979; Hunter and Laws, 1981), and from the concentration of particulate organic carbon (POC) based on a

linear relationship between POC and Chl-*a* (Buck *et al.*, 1996; Sathyendranath *et al.*, 2009). However, some complications may arise, for example, from difficulties in staining of DNA in some cell types (Veldhuis *et al.*, 1997) and variable contributions of organisms or seawater constituents other than phytoplankton to the ATP and POC pools in different trophic regimes (Sathyendranath *et al.*, 2009; Laws, 2013).

Behrenfeld and colleagues (Behrenfeld *et al.*, 2005; Behrenfeld and Boss, 2006) have proposed that particulate backscattering (b_{bp}) can be used to estimate POC, of which phytoplankton carbon is known to be a variable fraction. A linear relationship between b_{bp} and phytoplankton carbon can be expected as long as the contribution of non-phytoplankton particles to b_{bp} covaries with phytoplankton biomass (Behrenfeld *et al.*, 2005), which might not always be the case (IOCCG, 2008). Using b_{bp} to derive phytoplankton carbon can also be prone to errors, especially in case of the increased amount of bubbles and other highly reflective substances such as calcium carbonate plates during coccolithophore blooms, which can intensify the b_{bp} signal without a concomitant increase in phytoplankton biomass (Sathyendranath *et al.*, 2009). The methodological constraints discussed above suggest a need to develop alternative approaches to derive θ that exploit bio-optical and biochemical features unique to marine phytoplankton.

Based on the issues presented above, this chapter has four principal objectives. These are, (1) to examine the vertical structure of the photosynthetic properties of marine phytoplankton measured across different trophic regimes of the tropical and subtropical oceans, (2) to assess the extent to which the NPP index can explain the observed variation in photosynthetic parameters in the oligotrophic, open ocean regions where NPPs are found to contribute substantially to the algal pigment pool, (3) to explore the use of NPPs and the spectral slope of light absorp-

tion to predict the carbon-to-chlorophyll *a* ratio of the dominant picocyanobacterium *Prochlorococcus* (θ_{Pro}) in the oligotrophic domain, and (4) to incorporate data on the maximum photosynthetic rates and estimates of θ_{Pro} derived based on their relationship with NPPs to compute the maximum growth rates of *Prochlorococcus*.

4.2 Materials and Methods

4.2.1 Datasets

The data of phytoplankton pigment concentrations, picocyanobacterial cell counts, and photosynthesis-irradiance (*PE*) parameters used in this chapter (Figure 4.1, Table 4.1) originated from oceanographic programmes including (1) the Atlantic Meridional Transect (AMT; 1996-2004) (e.g. Zubkov *et al.*, 1998; Aiken *et al.*, 2009), (2) the BIogeochemistry and Optics SOuth Pacific Experiment (BIOSOPE; October-November 2004) (Claustre *et al.*, 2008; Uitz *et al.*, 2008), (3) the Deep Chlorophyll Maximum Study (DCM; July-August 1996) in the subtropical North Atlantic (Bouman, Platt, Kraay, *et al.*, 2000; Veldhuis and Kraay, 2004), and (4) the French Joint Global Ocean Flux Study (JGOFS) carried out at EUtrophic, MEsotrophic, and oLIgotrophic stations (EUMELI cruise number 4, hereafter referred to as EUMELI; May-June 1992) in the northeast Atlantic Ocean (Claustre and Marty, 1995; Babin *et al.*, 1996; Morel *et al.*, 1996). Data from the Hawaii Ocean Time-series (HOT; 1998-2014) (Karl and Church, 2014; Thompson *et al.*, 2018) were also used partly to illustrate seasonal coupling of the sea-surface temperature, the NPP index, and θ_{Pro}.

Sampling stations encountered during each research cruise were classified into different trophic domains based on the total chlorophyll *a* concentration (TChl-*a*: monovinyl + divinyl derivatives) measured at the sea surface according to a similar criterion proposed in a study of Bricaud *et al.* (2004) using a global HPLC dataset: oligotrophic, mesotrophic, and eutrophic stations

were those with surface TChl-*a* of < 0.2, between 0.2 and 2, and > 2 mg Chl-*a* m^{-3}, respectively. Note that samples collected during the DCM study were all classified as oligotrophic.

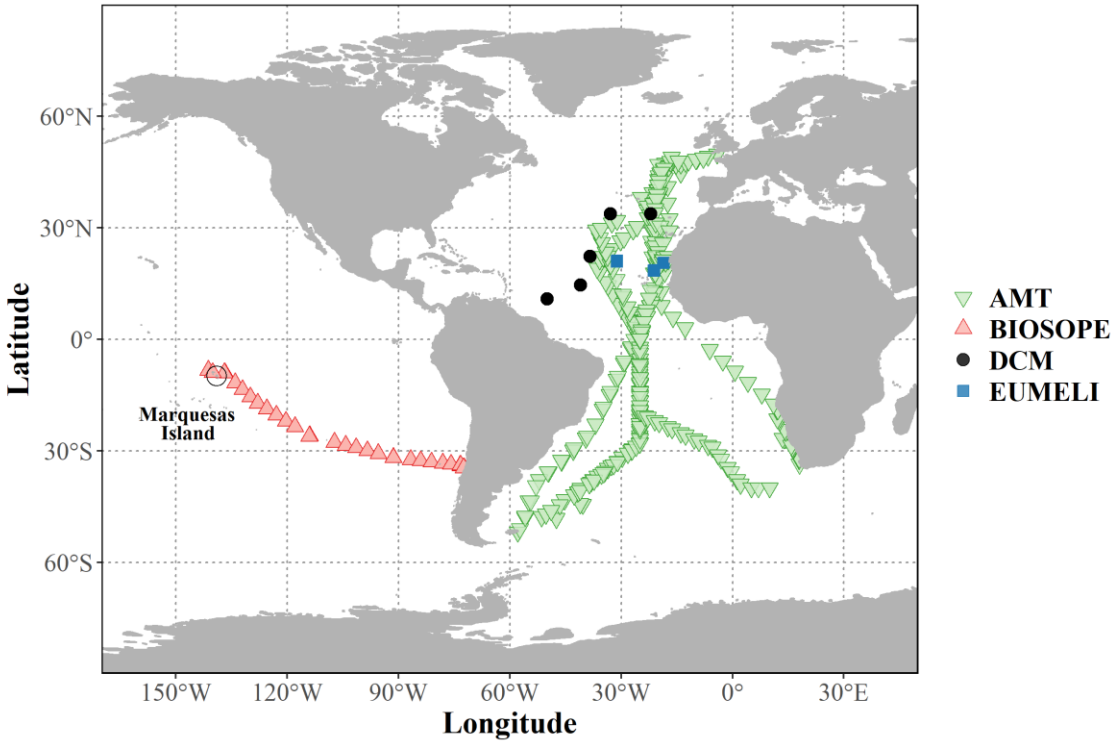


Figure 4.1: Map of sampling stations included in this study. Symbols are assigned according to different oceanographic campaigns.

Also, when calculating growth rates for *Prochlorococcus* populations, *Prochlorococcus*-dominated stations were identified using the pigment criteria modified from Sathyendranath *et al.* (2009): (1) the percent contribution of divinyl chlorophyll *a* (DVChl-*a*) to TChl-*a* ≥ 50%, (2) the relative concentration of fucoxanthin (FUCO) to TChl-*a* ≤ 0.02, (3) the relative concentration of 19′-hexanoylfucoxanthin (19′-HEX) to TChl-*a* ≤ 0.2, and (4) the relative concentration of chlorophyll c_3 (Chl-c_3) to TChl-*a* ≤ 0.02. Taxonomically, DVChl-*a* is a diagnostic pigment maker for *Prochlorococcus*, FUCO for diatoms and prymnesiophytes, 19′-HEX for prymnesiophytes (including those in the picophytoplankton, Kirkham *et al.*, 2013), and Chl-c_3 for prymnesiophytes and chrysophytes (Kraay *et al.*, 1992; Ras *et al.*, 2008; Jeffrey *et al.*, 2011). Ratios

of these diagnostic pigments with respect to TChl-*a* were used to exclude all samples containing mixed populations, which resulted in a considerable reduction in the size of the dataset.

Table 4.1: Summary of oceanographic cruises included in this study. *N* is the number of samples contained in the databases of pigment concentrations (HPLC), cell counts using flow cytometry (FCM), and photosynthesis-irradiance parameters (PE) that passed quality control.

Dataset	**Location**	**Date**				***N***		
						HPLC	**FCM**	**PE**
AMT-3	North-South Atlantic transect	Sep	–	Oct	1996	271	72	51
AMT-4		Apr	–	May	1997	27	21	12
AMT-6		May	–	Jun	1998	185	97	28
AMT-12		May	–	Jun	2003	224	119	-
AMT-13		Sep	–	Oct	2003	163	103	-
AMT-14		Apr	–	Jun	2004	137	114	-
AMT-15		Sep	–	Oct	2004	181	53	14
BIOSOPE	Subtropical South Pacific	Nov	–	Dec	2004	187	127	334
DCM	Subtropical North Atlantic	Jul	–	Aug	1996	75	75	72
EUMELI-4	Tropical North Atlantic	May	–	Jun	1992	158	107	192

4.2.2 Phytoplankton pigment composition

Measurements of pigment concentrations were carried out using high-performance liquid chromatography (HPLC) as previously described in Chapters 2-3. For further details on pigment extraction procedures and the corresponding references for the AMT, BIOSOPE, and DCM cruises, please refer to Section 3.2.2 of the previous chapter. For the EUMELI cruise, pigment analysis followed the method outlined in Claustre and Marty (1995) in which 2 litres of seawater samples were vacuum filtered onto 25 mm GF/F (glass-fibre) filters and pigments were extracted in 100% methanol. The quality of the pigment database was ensured using similar quality-control measures as described in Chapters 2-3 (Trees *et al.*, 2000; Uitz *et al.*, 2006).

4.2.3 *Prochlorococcus* abundance

Prochlorococcus cell concentrations were enumerated by flow cytometry (Olson *et al.*, 1993; Li, 1995). Methodological issues for the AMT, BIOSOPE, and DCM campaigns have been discussed in the previous chapter. Flow cytometric analysis for samples collected during the EUMELI cruise was carried out according to the protocol described in Partensky *et al.* (1996) using an EPICS® 541 flow cytometer (Coultronics, Hialeah, FL). The abundance of *Prochlorococcus* cells in the surface layer (0-60 m) with very low fluorescence was approximated by multiplying by two the cell number in the right part of the red-fluorescent distributions assumed to be log normal (Partensky *et al.*, 1996).

4.2.4 Phytoplankton light absorption

Phytoplankton absorption coefficients, $a_{ph}(\lambda)$, over the visible range (400-700 nm) for samples collected during the BIOSOPE and DCM cruises were measured using the filter-pad technique with pigment extraction generally following the standard method proposed by Kishino *et al.* (1985). The procedures are described in Section 2.2.4 of Chapter 2. For the DCM campaign (Bouman, Platt, Kraay, *et al.*, 2000), optical densities of total particulate and detrital materials were measured using a SPECTRONIC® GENESYS™ 2PC spectrophotometer with a split-beam, dual detector optical system and were corrected for optical pathlength amplification using the correction algorithms reported in Hoepffner and Sathyendranath (1992), Moore *et al.*, (1995), and Stuart *et al.* (1998). Pigments were extracted in a mixture of 90% acetone and dimethyl sulphoxide (DMSO) at a ratio of 6:4 (vo1:vol) (Stuart *et al.*, 1998; Bouman, Platt, Kraay, *et al.*, 2000). For the BIOSOPE cruise (Bricaud *et al.*, 2010), measurements of optical densities were made in a Perkin-Elmer Lambda-19 spectrophotometer equipped with an integrating sphere, and the correction algorithms of Bricaud and Stramski (1990) and Allali *et al.* (1997) were applied. Pigments were extracted in 100% hot methanol.

Following the approaches of Eisner *et al.* (2003) and Hirata *et al.* (2008), a normalised spectral slope between 443 nm and 550 nm ($S_{443\text{-}550}$) considered as an index for changes in the shape of $a_{ph}(\lambda)$ in the blue-green part of the spectrum was computed as follows:

$$S_{443\text{-}550} = \frac{a_{ph}(443) - a_{ph}(550)}{|443 - 550|\, a_{ph}(676)} \quad . \tag{4.1}$$

4.2.5 Photosynthesis-irradiance parameters

Photosynthesis-irradiance (*PE*) parameters were obtained by ^{14}C uptake experiments. In brief, light and dark bottles of seawater were inoculated with ^{14}C in the form of buffered sodium bicarbonate and incubated over a range of light intensities for 2-4 hours. After the incubation, samples were filtered onto GF/F filters under low-vacuum pressure (< 100 mm Hg) (Marañón *et al.*, 2001) and then exposed to concentrated HCl fumes to remove traces of inorganic radioactive carbon remaining on the filters. Samples were then immersed in scintillation cocktail and counted on a liquid scintillation counter. The recorded counts in the disintegration time per minute of ^{14}C were converted into units of carbon fixed per unit time (Bouman, Platt, Kraay, *et al.*, 2000) which were then normalised to phytoplankton biomass as indexed by fluorometrically-determined chlorophyll *a* concentrations. To derive the initial slope (α^B) and the photosynthetic rate at light saturation (P_m^B), these experimental data were then fitted to a *PE* model depending on the various laboratories concerned. Details on the light sources and incubation conditions used for *PE* experiments and the non-linear equation to which the experiment data were fit for each oceanographic dataset are summarised in Table 4.2.

The maximum quantum yield of photosynthesis (ϕ_m) can be computed from measurements of α^B and the spectrally averaged chlorophyll *a*-specific absorption coefficient of phytoplankton ($\bar{a}_{ph}^*$) using the relation (Bouman *et al.*, 2018):

$$\phi_m = 0.0231 \left(\frac{\alpha^B}{\bar{a}^*_{ph}} \right), \tag{4.2}$$

where 0.0231 is a factor converting milligrams to moles of carbon, micromoles to moles of photons, and hours to seconds. It is important to note that values of $\bar{a}^*_{ph}$ for the AMT samples were derived indirectly from a global relationship between TChl-*a* and $\bar{a}^*_{ph}$ (Bouman *et al.*, 2018). For the EUMELI dataset, due to a poor matchup between measurements of $a_{ph}(\lambda)$ and *PE* parameters, constant $\bar{a}^*_{ph}$ values of 0.011 and 0.0452 m^2 (mg Chl-*a*)$^{-1}$ were assigned to samples obtained from eutrophic and mesotrophic stations, respectively as suggested by Babin *et al.* (1996). However, for the oligotrophic domain, $\bar{a}^*_{ph}$ was derived based on its tight relationship with the optical depth (ζ) (Babin *et al.*, 1996):

$$\bar{a}^*_{ph} = -0.44 \tanh [\, 0.6 \, (\zeta - 4.9) \,] - 4.9, \tag{4.3}$$

where $\zeta = K_d$ (PAR) z. K_d (PAR) is the vertical attenuation coefficient for downward PAR (photosynthetically-available radiation; 400-700 nm) irradiance [m^{-1}], and z is the sampling depth. Note that the euphotic depth (z_e) is defined as the depth where PAR is *ca* 1% of its surface value, which corresponds to $\zeta = 4.6$ (Babin *et al.*, 1996).

Table 4.2: Summary of the light sources and incubation conditions for photosynthesis-irradiance (*PE*) experiments and the non-linear model used to fit the experimental data to obtain *PE* parameters for each oceanographic campaign.

Datasets	**Incubation procedure**			**Equation fitted to the experimental data**	**Reference**
	Lamp source	**Light Intensity [1]**	**Time (hr)**		
AMT-3	100-W halogen lamp	5-2,500	2.5	Platt *et al.* (1980)	Marañón *et al.* (2001); Marañón *et al.* (2007)
AMT-4	100-W halogen lamp	5-2,500	2.5	Platt *et al.* (1980)	Marañón *et al.* (2001)
AMT-6	200-W tungsten halogen lamp spectrally corrected	5-2,200	2.5-3.5	Platt *et al.* (1980)	Lawrenz *et al.* (2013); Tilstone *et al.* (2017)
AMT-15	Tungsten halogen lamp behind blue light filters		2	Jassby and Platt (1976)	Hickman (2007); Lawrenz *et al.* (2013)
BIOSOPE	250-W arc lamp (OSRAM, HQI-T 250 W/D)	5-2,000	2-3.5	Platt *et al.* (1980)	Huot *et al.* (2007)
DCM	Tungsten-halogen lamp	8-2,700	3	Platt *et al.* (1980)	Bouman, Platt, Sathyendranath, *et al.* (2000)
EUMELI-4	250-W arc lamp (OSRAM, HQI-T 250 W/D)	5-2,000	2-3.5	Platt *et al.* (1980)	Babin *et al.* (1994, 1996)

[1] Light intensities are in μmol photons m^{-2} s^{-1}

4.3 Results

4.3.1 Distribution of the photosynthetic parameters

Vertical profiles of the photosynthetic parameters are shown in Figures 4.2-4.5. Although the assimilation number (P_m^B) did not appear to vary significantly with depth within the eutrophic waters (Figure 4.2a), vertical variation was clear within mesotrophic and oligotrophic domains with both exhibiting a decrease in P_m^B with increasing depth (Figures 4.2b, c). A wide range of P_m^B values was observed within the surface layer (above 25 m) of the mesotrophic domain (Figure 4.2b), reaching values of up to *ca* 12-15 mg C (mg Chl-*a*)$^{-1}$ h^{-1}. Within the mesotrophic domain, surface P_m^B values varied between the three datasets: P_m^B values greater than *ca* 8 mg C (mg Chl-*a*)$^{-1}$ h^{-1} were almost exclusively from the EUMELI study, whereas a cluster of lower and less variable P_m^B values were observed for the AMT and BIOSOPE cruises. Similarly, the eutrophic domain also displayed P_m^B that was highly variable with depth (Figure 4.2a), with relatively high values (above *ca* 6 mg C (mg Chl-*a*)$^{-1}$ h^{-1}) associated with the EUMELI stations. The markedly increased surface values of P_m^B observed at the EUMELI mesotrophic stations (Figure 4.2b) appeared to be largely due to the significantly higher abundance of *Synechococcus* (i.e. average of *ca* 348,876 cells mL^{-1} within the upper (25 m) water column compared to *ca* 46,812 and 77,741 cells mL^{-1} at the BIOSOPE and AMT mesotrophic sites, respectively), which is supported by the results of a global study by Richardson and colleagues (2016) showing the highest P_m^B associated with *Synechococcus*-dominated communities. Methodological differences in *PE* experiments, on the other hand, are an unlikely explanation as to why the EUMELI data tended to be different from the other datasets particularly in terms of the magnitude of P_m^B given that the *PE* measurements during the EUMELI and BIOSOPE studies were carried out using the same experimental design (Babin *et al.*, 1994, 1996; Huot *et al.*, 2007)

and values of the *PE* parameters obtained from the BIOSOPE campaign appeared to fall within a relatively similar range to the AMT and DCM data.

The magnitude of the chlorophyll *a*-normalised initial slope (α^B) of the *PE* curve tended to remain relatively constant at *ca* 0.03 mg C (mg Chl-*a*)$^{-1}$ h^{-1} (μmol photons m^{-2} s^{-1})$^{-1}$ for the eutrophic domain with higher variability observed near the surface (Figure 4.3a) and showed no discernible depth dependence in the mesotrophic domain (Figures 4.3b). In contrast, α^B exhibited strong depth dependence within the oligotrophic domain, with values increasing from < 0.02 at the surface to up to *ca* 0.10 mg C (mg Chl-*a*)$^{-1}$ h^{-1} (μmol photons m^{-2} s^{-1})$^{-1}$ at depth (Figure 4.3c). A considerable degree of scatter recorded in the mesotrophic domain was observed over several of the AMT cruises. When each dataset was examined independently, both the EUMELI and BIOSOPE mesotrophic samples showed depth dependence in α^B.

Vertical profiles of the photoadaptation parameter (E_k) reflected similar patterns to those of P_m^B for the three trophic regimes: E_k was relatively uniform with depth at eutrophic stations (Figure 4.4a), whereas it decreased with depth in the mesotrophic and oligotrophic domains (Figures 4.4b, c). Depth-dependent reductions in E_k as much as *ca* 10-fold were observed for oligotrophic samples, with E_k values ranging from an average of about 300 μmol photons m^{-2} s^{-1} within the top 25 m of the water column to < 40 μmol photons m^{-2} s^{-1} below 100 m (Figure 4.4c). Within the surface layer, E_k tended to increase progressively as one moved from eutrophic to oligotrophic conditions (average E_k values of 130.7 (N=22), 196.2 (61), and 324.1 (67) μmol photons m^{-2} s^{-1} for the eutrophic, mesotrophic, and oligotrophic domains, respectively). Note that the higher E_k values (> 250 μmol photons m^{-2} s^{-1}) were observed within the top 50 m of the water column at the HNLC waters of the South Pacific sampled during the BIOSOPE cruise.

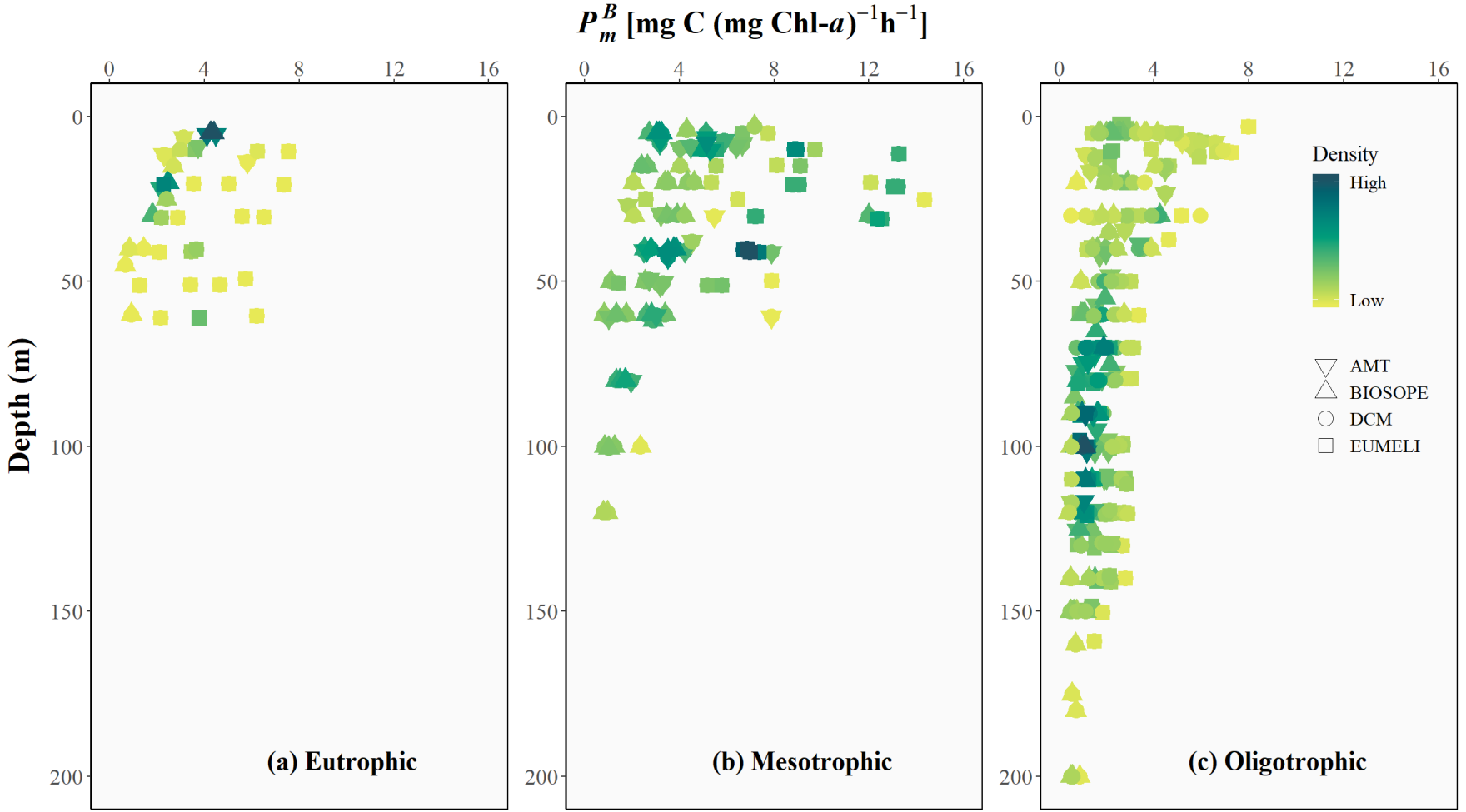


Figure 4.2: Density plots showing the vertical variation in the maximum chlorophyll *a*-normalised photosynthetic rate (P_m^B). Stations were categorised based on the surface total chlorophyll *a* concentration (TChl-*a*, mg Chl-*a* m^{-3}) (Bricaud *et al.*, 2004) into (a) the eutrophic (TChl-*a* > 2), (b) mesotrophic (0.2 ≤ TChl-*a* ≤ 2), and (c) oligotrophic domains (TChl-*a* < 0.2). Colour gradient represents probability density estimates. Symbols denote different oceanographic datasets included in this study.

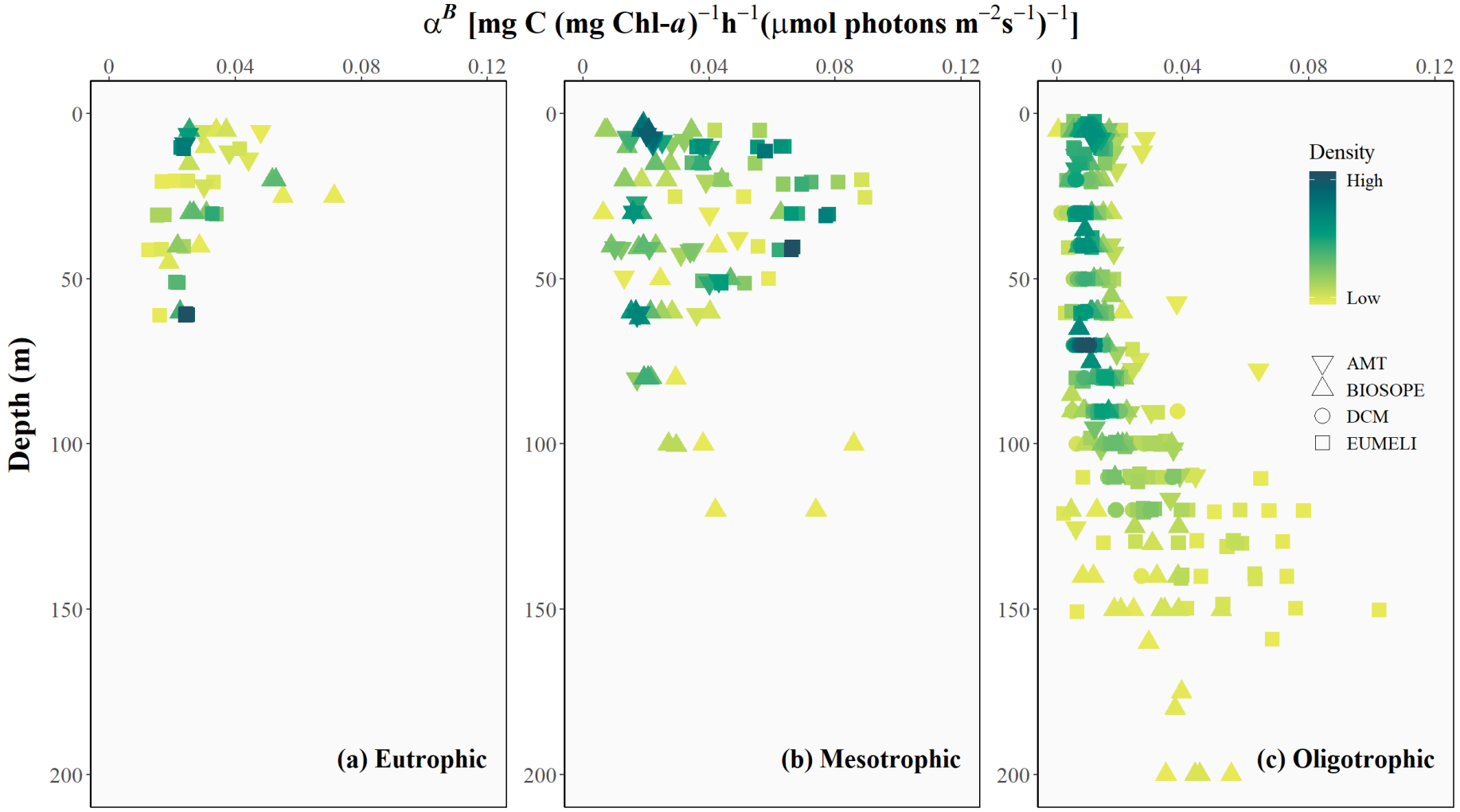


Figure 4.3: As Figure 4.2 for the chlorophyll *a*-normalised initial slope (α^B).

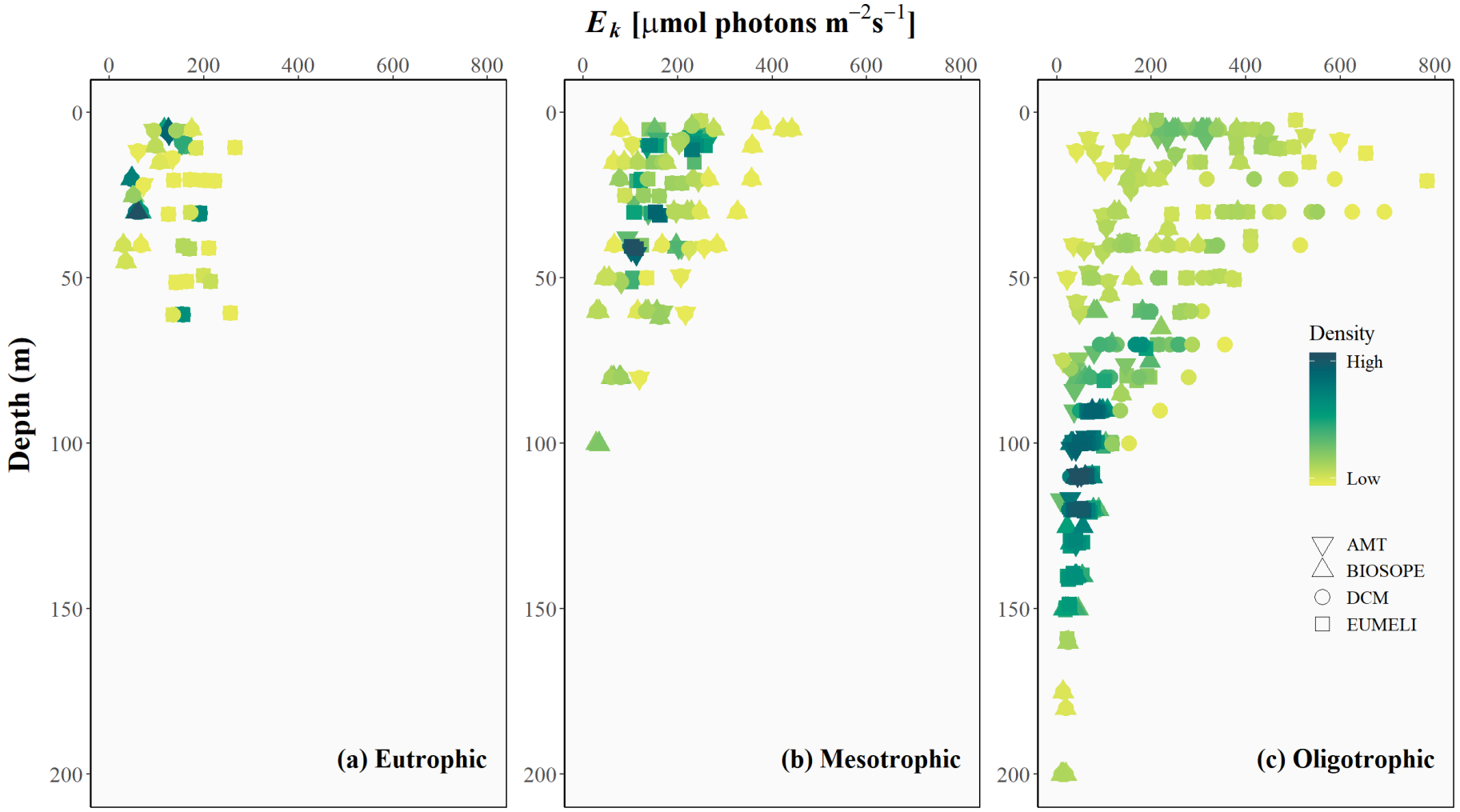


Figure 4.4: As Figure 4.2 for the photoadaptation parameter (E_k).

Depth-dependent variation in the maximum quantum yield of photosynthesis (ϕ_m) was observed for the oligotrophic domain (Figure 4.5c), although there was a considerable degree of scatter. This may be due, in part, to the uncertainty associated with the calculation of ϕ_m from measurements of α^B and the spectrally averaged chlorophyll *a*-specific absorption coefficient of phytoplankton ($\bar{a}^*_{ph}$) (Equation 4.2), especially in cases when $\bar{a}^*_{ph}$ was measured from samples from different CTD casts (Bouman, 1998) or when $\bar{a}^*_{ph}$ values were estimated using a global relationship between TChl-*a* and $\bar{a}^*_{ph}$ (Bouman *et al.*, 2018), which was the case for the AMT dataset. I explored using the relationship between $\bar{a}^*_{ph}$ and optical depth described in Babin *et al.* (1996) (Equation 4.3) to estimate ϕ_m from the AMT α^B values. However, it was found that estimates of ϕ_m calculated from $\bar{a}^*_{ph}$ obtained using optical depth were not significantly different from those using the global relationship between TChl-*a* and $\bar{a}^*_{ph}$. Although mesotrophic samples collected during the AMT and EUMELI cruises did not appear to show depth dependence, the BIOSOPE samples showed an increase in ϕ_m with depth. Within the BIOSOPE cruise data, there was also some marked differences in the depth-dependence of ϕ_m: the HNLC stations showed consistently low ϕ_m values throughout the water column with a mean of *ca* 0.005 mol C (mol photons)$^{-1}$ (N=4) in the surface (top 50m) waters compared to that of about 0.02 mol C (mol photons)$^{-1}$ for the other BIOSOPE mesotrophic stations (N=24).

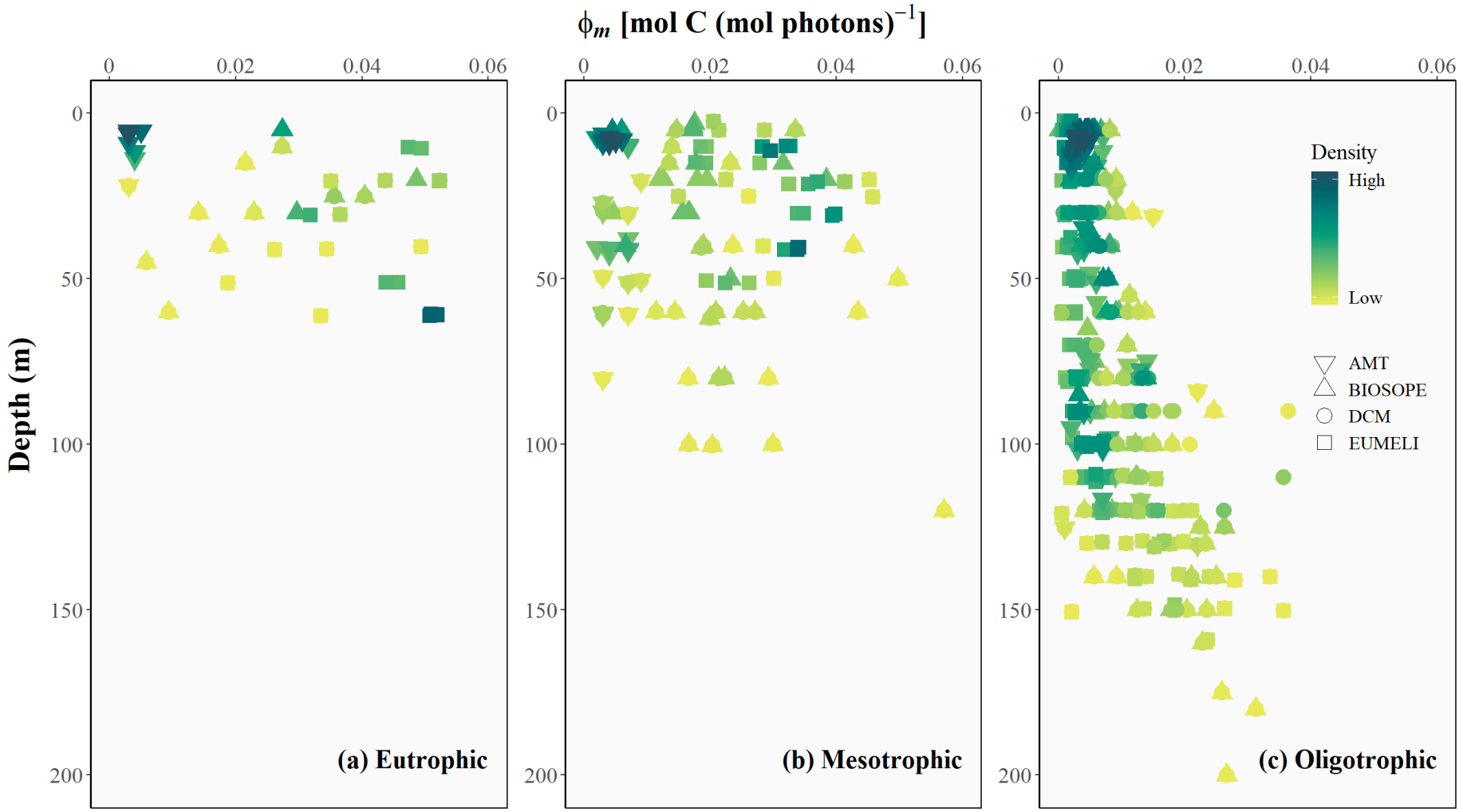


Figure 4.5: As Figure 4.2 for the maximum quantum yield of photosynthesis (ϕ_m).

4.3.2 Relationship between the photosynthetic parameters and non-photosynthetic pigments

In the oligotrophic domain, the NPP index varied from *ca* 0.02 (EUMELI, at the 200 m depth) to 0.57 (AMT, at 6 m), with the majority of samples (86%) falling below 0.4 (Figure 4.6) and mean values of *ca* 0.34 for the top 50 m of the water column and 0.15 for deeper samples. Overall, P_m^B was positively correlated with the NPP index (*NPP*) ($P_m^B = 6.59\,NPP + 0.57$, $R^2 = 0.34$, $p < 0.01$, $N = 308$) (Figure 4.6a), however, considerable scatter occurred in cases with relatively low P_m^B values (i.e. ≤ 2 mg C (mg Chl-*a*)$^{-1}$ h^{-1}) and very high NPP index (i.e. ≥ 0.4). Samples characterised by low P_m^B and high NPP index values were typically collected in the surface waters (≤ 30 m with one exception of 60 m) and tended to have a very high concentration of divinyl chlorophyll *a* (DVChl-*a*, the pigment maker for *Prochlorococcus*) relative to TChl-*a* (43-89%).

Interestingly, below the euphotic depth where values of the NPP index were greatly reduced (i.e. ≤ 0.09) and the relationship between P_m^B and the NPP index accordingly became less significant ($R^2 = 0.21$, $p = 0.02$), the eukaryotic pigments 19′-butanoyloxyfucoxanthin (19′-BUT) and 19′-hexanoylfucoxanthin (19′-HEX) became the significant predictors of the magnitude of P_m^B, with the relative concentrations of 19′-BUT and 19′-HEX to total pigments exhibiting inverse correlations with P_m^B ($R^2 = 0.45$, $p < 0.01$ for 19′-BUT and $R^2 = 0.29$, $p < 0.01$ for 19′-HEX). A weaker positive correlation was also observed between the relative proportion of fucoxanthin, another pigment indicator of larger eukaryotes, and P_m^B ($R^2 = 0.20$, $p = 0.02$).

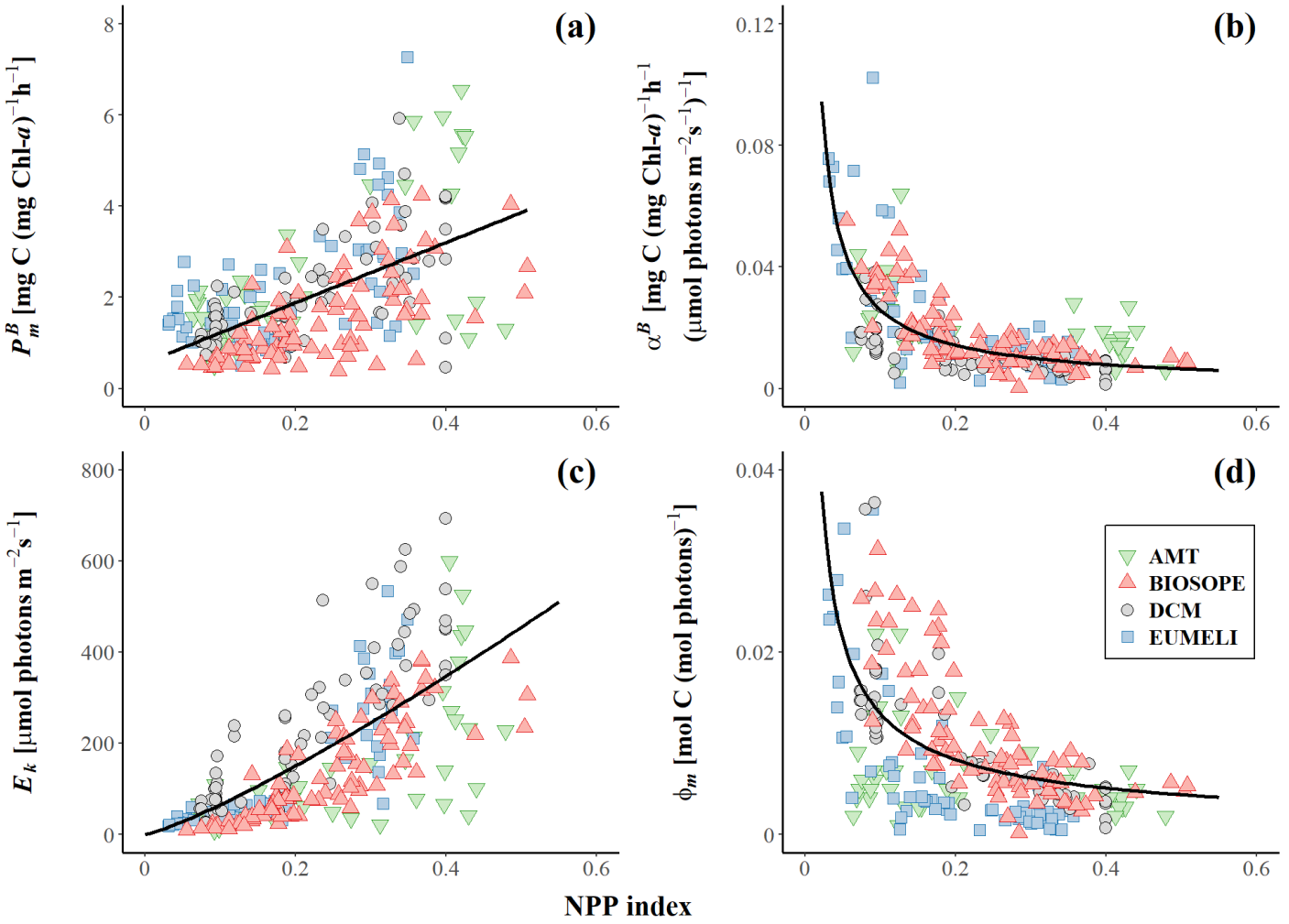


Figure 4.6: The photosynthetic parameters plotted against the NPP index for the oligotrophic domain: (a) the maximum photosynthetic rate (P_m^B), (b) the initial slope (α^B), (c) the photoadaptation parameter (E_k), and (d) the maximum quantum yield of photosynthesis (ϕ_m). Symbols denoted the different oceanographic cruises used in this study.

Results presented in Figure 4.6b show that α^B decreased significantly with increasing NPP index ($\alpha^B = 0.0035\,NPP^{-0.8}$, $R^2 = 0.41$, $p < 0.01$, $N = 305$), and this relationship was robust across cruises. A few outliers corresponding to samples deeper in the water column were observed with values α^B less than 0.01 mg C (mg Chl-*a*)$^{-1}$ h^{-1} (μmol photons m^{-2} s^{-1})$^{-1}$ coinciding with low NPP indices (i.e. < 0.1). Similar to P_m^B, other photosynthetic carotenoids were able to explain the observed variation in α^B in the deep ocean: the relative concentration of 19′-BUT exhibited the most significant positive correlation with α^B ($R^2 = 0.37$, $p < 0.01$).

E_k was positively correlated with the NPP index ($E_k = 995\,NPP^{1.31}$, $R^2 = 0.59$, $p < 0.01$, $N = 309$) (Figure 4.6c) and this is expected given that both E_k (Platt *et al.*, 1980; Sakshaug *et al.*, 1997) and the relative abundance of NPPs (Babin *et al.*, 1996; Johnsen and Sakshaug, 1996) have been shown to strongly vary in response to changes in light history. However, there is also a physiological basis for this finding: the quantity E_k can be expressed as a function of the absorption cross-section of photosystem II (σ_{PSII}) (Sakshaug *et al.*, 1997) which, in turn, has been widely shown to be affected by NPPs during photoacclimation (Six *et al.*, 2007; Suggett *et al.*, 2009; Brunet *et al.*, 2011).

A broad range of E_k values (from below 50 to up to 600 μmol photons m^{-2} s^{-1}) at the very narrow range of NPP indices of 0.4-0.42 was observed for the AMT dataset (Figure 4.6c). These observations were exclusively made on AMT-3 in (sub)tropical waters between 30°N and 30°S. The samples were collected daily within the surface layer (0-10 m) around noontime from late September to early October. Under these conditions, one would anticipate that the phytoplankton were acclimated to high surface irradiances and this is reflected by high and invariable NPP indices. Yet, despite the narrow range of values of the NPP index, there was a

large variation in the fractional contribution of DVChl-*a* to TChl-*a* (*ca* 30-80%), which is indicative of the relative contribution of *Prochlorococcus* to total pigment biomass, which increased progressively toward the equator. To examine whether the fractional contribution of *Prochlorococcus* to TChl-*a* may account for the large change in the values of E_k at high NPP indices, I plotted E_k against the DVChl-*a* to TChl-*a* ratio and found a strong correlation (R^2 = 0.73, $p < 0.01$, $N = 11$). These results suggest that within these highly-stratified oligotrophic waters, community structure must be considered when accounting for the large-scale variability of E_k within the surface ocean.

Several studies have examined the impact of NPPs on ϕ_m in marine phytoplankton (Bidigare *et al.*, 1989; Demmig-Adams, 1990; Lindley *et al.*, 1995; Sathyendranath *et al.*, 1996; Marra *et al.*, 2000). In this study, when values of ϕ_m were plotted against the NPP index, a clear trend was evident (Figure 4.6d): an increase in the NPP index resulted in a corresponding decrease in ϕ_m ($\phi_m = 0.0016\,NPP^{-0.84}$, $R^2 = 0.33$, $p < 0.01$, $N = 269$). The large amount of scatter of the data points presented in Figure 4.6d could be explained partially by uncertainties associated with the calculation of ϕ_m from α^B and $\bar{a}^*_{ph}$ values as discussed in the previous section.

4.3.3 Relationship between the carbon-to-DVChl-*a* ratio for *Prochlorococcus* populations and the NPP index

To estimate phytoplankton growth rates from P_m^B requires information on the carbon-to-chlorophyll *a* ratio (θ) (Geider, 1987; Marañón, 2005; Sathyendranath *et al.*, 2009). For *Prochlorococcus*, estimates of cell carbon may be obtained using information of cell abundances from analytical flow cytometry (AFC) and a cell-specific carbon conversion factor (Li *et al.*, 1992; Campbell *et al.*, 1994; Bertilsson *et al.*, 2003; Grob *et al.*, 2007; see also Chapter 3). Given that DVChl-*a* is exclusively found in *Prochlorococcus*, the ratio of AFC estimated cell carbon to

DVChl-*a* allows us to obtain a species-specific estimate of θ_{Pro} for this globally-significant marine picocyanobacterium. Since changes in the NPP index in *Prochlorococcus* are largely driven by changes in the intracellular concentration of photosynthetic rather than photoprotective pigments, one may anticipate that the NPP index could serve as a useful predictor of θ_{Pro} as both derived variables can be viewed as indices of photoacclimation.

To assess the extent to which the NPP index could explain variation in θ_{Pro}, measurements of *Prochlorococcus* cell abundance were combined with DVChl-*a* concentrations determined by HPLC. For observations made on the AMT, BIOSOPE, and EUMELI cruises, the conversion factor of 49 fg C cell^{-1} (Cailliau *et al.*, 1996) was used which was derived from particulate organic carbon measurements of *Prochlorococcus* cultures. For the DCM cruise, the average carbon content of a given *Prochlorococcus* sample was estimated based on the relative abundances of cells with (PE+) and without (PE–) detectable phycoerythrin (PE) fluorescence signal as described in Veldhuis and Kraay (2004). The conversion factors of 50 and 35 fg C cell^{-1} were applied to the PE+ and PE– populations, respectively.

θ_{Pro} was positively correlated with the NPP index and this trend was robust across all oceanographic datasets (Figure 4.7), although the AMT data points exhibited a relatively high degree of scatter with a markedly shallower slope. Hence, data points corresponding to samples from the BIOSOPE, DCM, and EUMELI cruises were separated from the AMT observations for linear regression analyses. The resulting linear regression fit was

$$\log_{10} \theta_{Pro} = 1.76 \log_{10} NPP + 3.25 \quad (4.4)$$

for the BIOSOPE, DCM, and EUMELI cruises ($R^2 = 0.83$, $p < 0.01$, $N = 212$, Figure 4.7a), and

$$\log_{10} \theta_{Pro} = 1.26 \log_{10} NPP + 2.89 \quad (4.5)$$

for the AMT cruises ($R^2 = 0.60$, $p < 0.01$, $N = 223$, Figure 4.7b). Note that, for the BIOSOPE cruise, samples collected in the surface waters of the oligotrophic gyres were excluded given that the cell fluorescence signal was too weak to be determined directly using analytical flow cytometry (Grob, Ulloa, Li, *et al.*, 2007).

To examine seasonal variability in the θ_{Pro}-NPP relationship, HPLC and flow cytometric measurements in the top 20 m of the water column were examined from the Hawaii Ocean Time-series (HOT) Station ALOHA in the North Pacific Subtropical Gyre (Figure 4.8). As the degree of water-column stratification due to solar heating gradually increased from winter to summer as reflected by an increase in the sea surface (0-20 m) temperature (Figure 4.8a), a corresponding domain shift (Karl *et al.*, 2001) in the surface phytoplankton community towards picocyanobacterial dominance occurred. This led to an increase in both the NPP index (Figure 4.8b) and θ_{Pro} (Figure 4.8c). Conversely, as the surface waters cooled in the autumn, the NPP index and θ_{Pro} declined due to the prevalence of the low light-acclimated larger eukaryotic phytoplankton. Due to the limited number of simultaneous measurements of *Prochlorococcus* cell counts and HPLC-determined pigment concentrations, Figure 4.8c showed only θ_{Pro} recorded in the year 1994-1995 when the seasonal fluctuation in θ_{Pro} tightly followed that of the NPP index as reflected in a strong positive correlation shown in Figure 4.8d ($R^2 = 0.57$, $p < 0.01$, $N = 15$). The results presented in Figures 4.7 and 4.8 illustrate the potential value of the NPP index as a predictor of θ_{Pro}, particularly in cases where flow cytometry data is absent or when HPLC method cannot separate DVChl-*a* from monovinyl Chl-*a*.

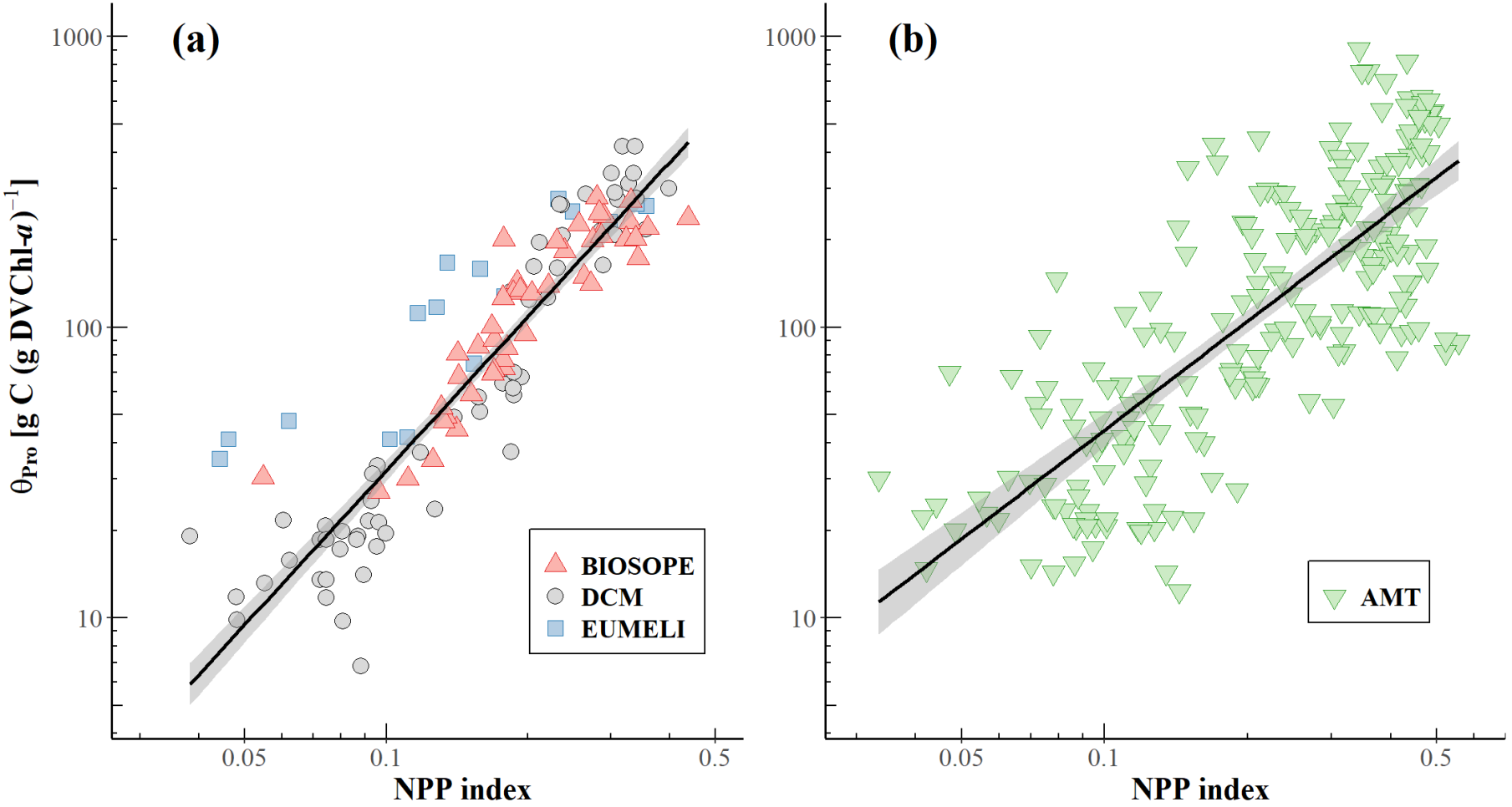


Figure 4.7: The carbon-to-DVChl-*a* ratio for *Prochlorococcus* (θ_{Pro}) plotted against the NPP index measured in the oligotrophic domain for (a) the BIOSOPE, DCM, and EUMELI cruises and (b) the AMT cruises (no. 3, 4, 13-15). The black line represents the line of best fit and the grey shaded area indicates the 95% confidence interval. Symbols are assigned according to different oceanographic cruises.

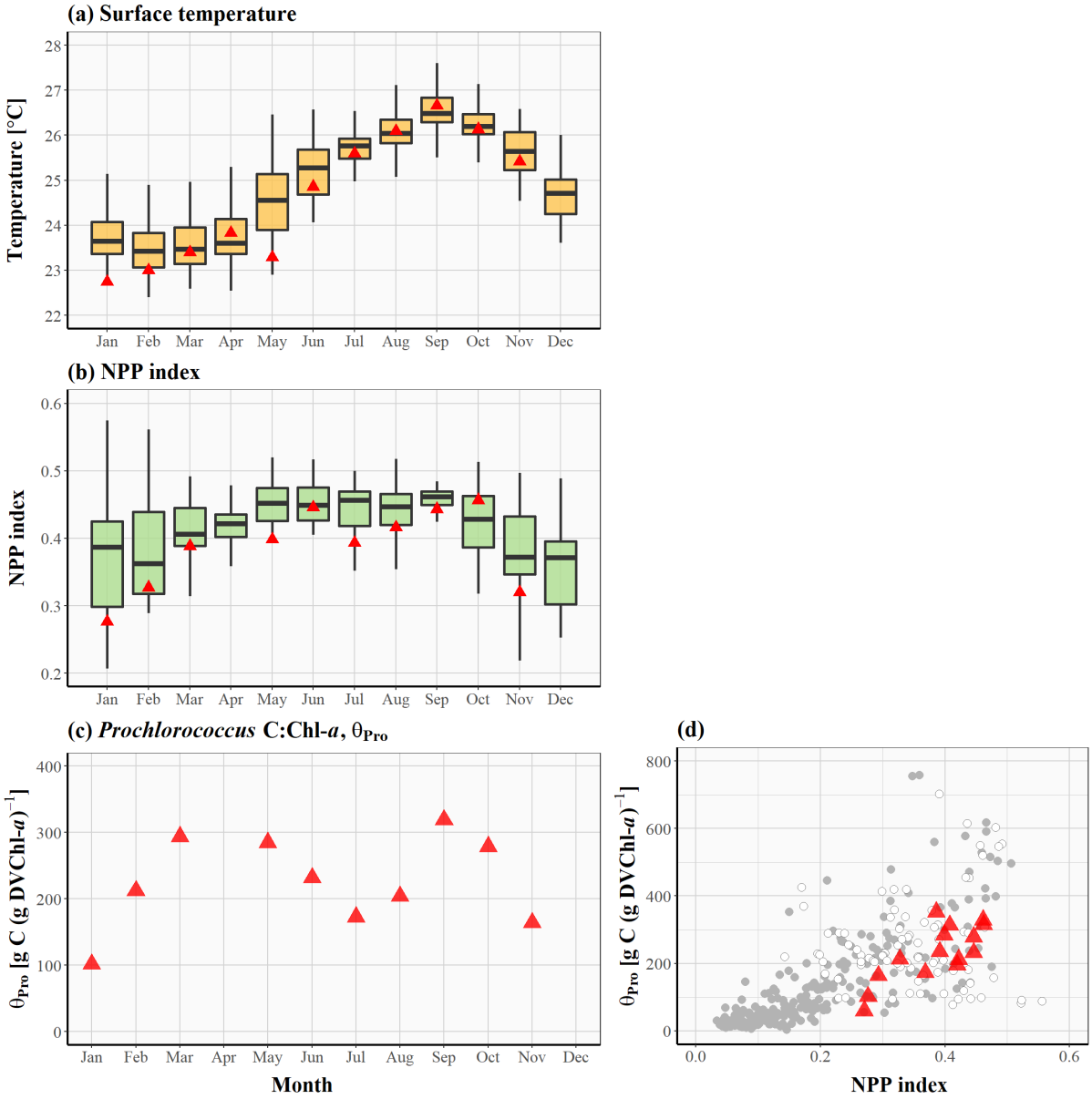


Figure 4.8: Hawaii Ocean Time-series (HOT) observations of (a) sea surface temperature and (b) the NPP index, both of which were collected between 1988 and 2014 (data for the period 1994-1995 are indicated by red triangles), and (c) the carbon-to-DVChl-*a* for *Prochlorococcus* (θ_{Pro}) collected between 1994 and 1995. Data were restricted to within the top 20 m of the water column. For the top and middle panels, the median value is marked by the horizontal line inside the box plot and the lower and upper boundaries correspond to the first and third quartiles (the 25th and 75th percentiles). The Tukey-style whiskers extend 1.5 times the inter-quartile range from the box edges and outliers beyond the end of the whiskers are not shown. The bottom-right panel (d) shows θ_{Pro} plotted against the NPP index for surface (0-20 m) HOT samples collected between 1994 and 1995 (red triangles) along with surface (white circles) and deep (> 20 m, grey circles) samples from the AMT, BIOSOPE, DCM, and EUMELI datasets.

4.3.4 Relationship between the carbon-to-DVChl-*a* ratio for *Prochlorococcus* and the spectral slope of total phytoplankton absorption

Previous studies of the subtropical oligotrophic waters (Allali *et al.*, 1997; Stuart *et al.*, 1998; Letelier *et al.*, 2017) have shown that the shape of $a_{ph}(\lambda)$ is significantly affected by absorption due to NPPs as determined using the spectral reconstruction method of Bidigare *et al.* (1990), and that a numerical index of the spectral shape (spectral slope between 443 and 510 nm) (Hirata *et al.*, 2008) is highly correlated with the NPP index (Figure 2.9 in Chapter 2). Given that θ_{Pro} has been shown to be strongly correlated with the NPP index over various regions and seasons (Figures 4.7-4.8), it is worth exploring whether a spectral slope may also serve as a useful predictor of θ_{Pro} given that it can be routinely measured at sea using sensors mounted on profiling and flow through systems and is also retrievable by ocean-colour remote sensing.

Due to the lack of simultaneous measurements of $a_{ph}(\lambda)$, HPLC phytoplankton pigments, and picophytoplankton cell abundance for both the EUMELI and AMT datasets, only results from the BIOSOPE and DCM cruises are shown. When θ_{Pro} was plotted against values of the spectral slope $S_{443\text{-}550}$ for samples collected during the BIOSOPE and DCM cruises, a clear positive correlation was evident ($\theta_{Pro} = 17035.2\ S_{443\text{-}550} - 349.5$, $R^2 = 0.71$, $p < 0.01$, $N = 80$, Figure 4.9) with a higher degree of scatter observed at higher $S_{443\text{-}550}$.

I also examined the relationship between θ_{Pro} and the spectral slopes between 443 and 510 nm ($S_{443\text{-}510}$) as used in the study of Hirata *et al.* (2008) and between 488 and 532 nm ($S_{488\text{-}532}$) as in Eisner *et al.* (2003) and Chakraborty *et al.*, (2017). The correlation between θ_{Pro} and $S_{443\text{-}510}$ ($R^2 = 0.64$) was slightly weaker than what was found using $S_{443\text{-}550}$, whereas a much weaker relationship was observed between θ_{Pro} and $S_{448\text{-}532}$ ($R^2 = 0.40$).

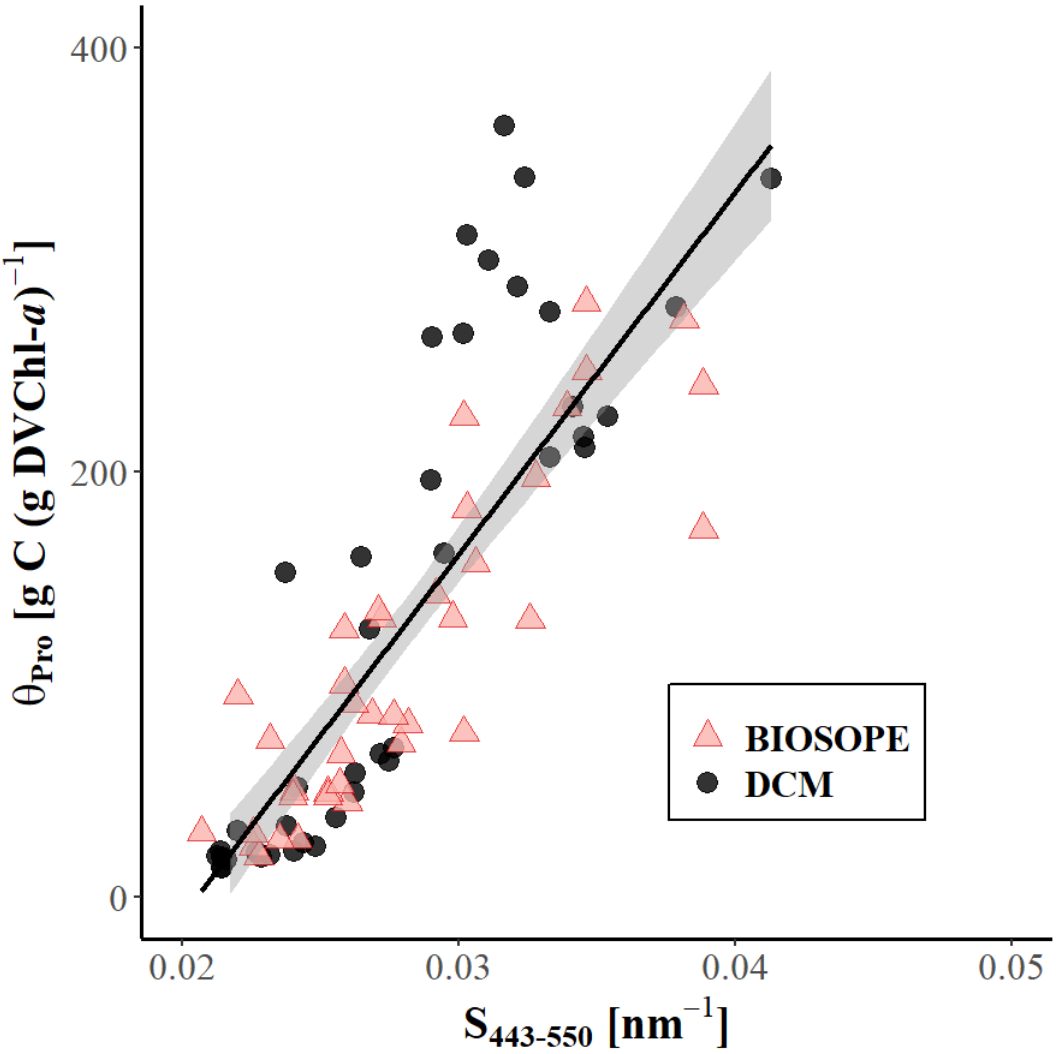


Figure 4.9: The ratio of carbon to DVChl-*a* for *Prochlorococcus* (θ_{Pro}) plotted as a function of the 676 nm-normalised spectral slope of phytoplankton absorption coefficient between 443 nm and 550 nm ($S_{443\text{-}550}$) for samples collected during the BIOSOPE and DCM cruises. Linear regression analysis was performed (black line) and the 95% confidence interval for the linear regression line is shaded in grey. Symbols are assigned according to cruises.

4.3.5 Estimation of the maximum growth rates of *Prochlorococcus*

Understanding the natural variability in *Prochlorococcus* growth rates is critical in assessing their roles in global marine ecosystems and nutrient cycles as well as providing insight of the physiological basis of its ecological success in the oligotrophic ocean (Partensky and Garczarek, 2010). To calculate the maximum growth rates of *Prochlorococcus* ($\mu_{m,\,Pro}$), knowledge of its chlorophyll *a*-specific maximum photosynthetic rate ($P^B_{m,\,Pro}$) along with estimates of θ_{Pro} are required (Geider, 1987; Marañón, 2005). Although direct and simultaneous measurements of these two physiological parameters are rarely obtained from oceanographic cruises, here I provide an approach that derives estimates of θ_{Pro} and $P^B_{m,\,Pro}$ and ultimately $\mu_{m,\,Pro}$ using a suite of ship-board observations.

First, θ_{Pro} is estimated based on its relationship with the NPP index (Figure 4.7) described by Equations 4.4-4.5 for the entire HPLC pigment database (N = 503). Figure 4.10 shows the frequency distribution of the estimates of θ_{Pro} when data is partitioned vertically into layers of different levels of light availability as indexed by the ratio of the sampling depth to the maximum depth of the euphotic zone (z/z_e; Uitz *et al.*, 2008).

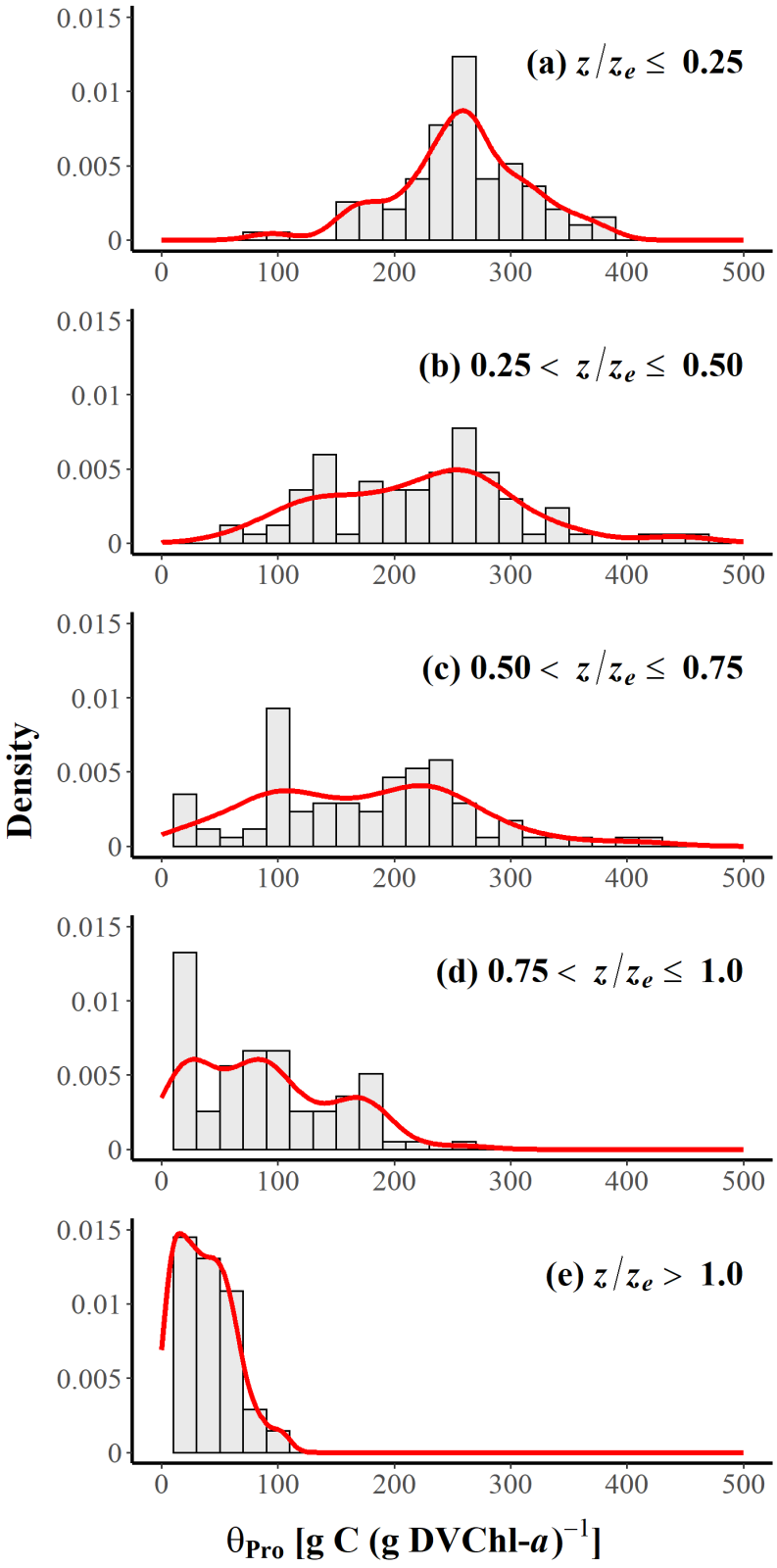


Figure 4.10: Frequency distributions of estimates of the ratio of carbon to DVChl-*a* for *Prochlorococcus* (θ_{Pro}) from the NPP index (Equations 4.4-4.5) for all pigment samples taken on the AMT, BIOSOPE, DCM, and EUMELI cruises. The panels (a) to (e) represent different layers of the water column, from the surface to depth, divided according to the relative availability of light at a given depth indexed by the ratio of that depth to the euphotic depth (z/z_e).

Estimated θ_{Pro} ranged from 2.44 g C (DVChl-*a*)$^{-1}$ (below z_e) to 452.4 g C (DVChl-*a*)$^{-1}$ at 50 m (*ca* 0.5z_e). Within the surface layer ($z/z_e \leq 0.25$, Figure 4.10a), data appeared to be normally distributed with the majority of θ_{Pro} estimates falling in the range of about 220-300 g C (DVChl-*a*)$^{-1}$ and a mean value of 257.32 g C (DVChl-*a*)$^{-1}$ (N = 97). There was a continuing decrease in mean values for each subsequent layer (Figures 4.10b-e) from 223.1 (z/z_e = 0.25-0.5, N = 84) to 174.1 (z/z_e = 0.5-0.75, N = 86), 88.3 (z/z_e = 0.75-1.0, N = 98), and 37.3 ($z/z_e > 1.0$, N = 138), respectively, reflecting photoacclimatory response of *Prochlorococcus* populations to a vertical light gradient. This vertical distribution of θ_{Pro} estimates was consistent with the observed depth-dependent increase in single-cell chlorophyll fluorescence of *Prochlorococcus* in the subtropical oceans (Dusenberry *et al.*, 1999; van den Engh *et al.*, 2017).

Next, estimates of the maximum growth rates ($\mu_{m, Pro}$) [per day, d^{-1}] for surface ($z/z_e \leq 0.25$) *Prochlorococcus* populations were computed as follows (Marañón, 2005):

$$\mu_{m,\,Pro} = \left(\frac{P^B_{m,\,Pro}}{\theta_{Pro}} \right) D \tag{4.6}$$

$P^B_{m,Pro}$ was estimated by averaging values of P^B_m samples identified as *Prochlorococcus*-dominated according to the pigment criteria modified from Sathyendranath *et al.* (2009) observed in the surface waters ($z/z_e \leq 0.25$, i.e. *ca* 30 m). The constant value of 4.01 (±1.58) mg C (mg Chl-*a*)$^{-1}$ h^{-1} was applied to Equation 4.6. θ_{Pro} was estimated based on its relationship with the NPP index (Equation 4.4). *D* is the duration of the photoperiod (i.e. daylength) [hour, h] which was estimated using the R statistical package '*insol*' (Corripio, 2019) based on the sampling dates and the geographic location of each station. It should be noted that there are potential uncertainties associated with the use of the constant $P^B_{m,Pro}$ value for the entire dataset and the prediction of θ_{Pro} by means of linear regression with the NPP index, which are *ca* 39.4% and 34.5%, respectively, and these combined uncertainties could result in *ca* 52.4% error in the

estimation of $\mu_{m,\,Pro}$ using Equation 4.6 (uncertainty propagation analysis; Topping, 1962; Ku, 1966; Platt *et al.*, 1988). The estimated values of $\mu_{m,\,Pro}$ ranged from *ca* 0.11 and 0.85 d^{-1} with a mean of 0.22 d^{-1} and median of 0.18 d^{-1} (N=252).

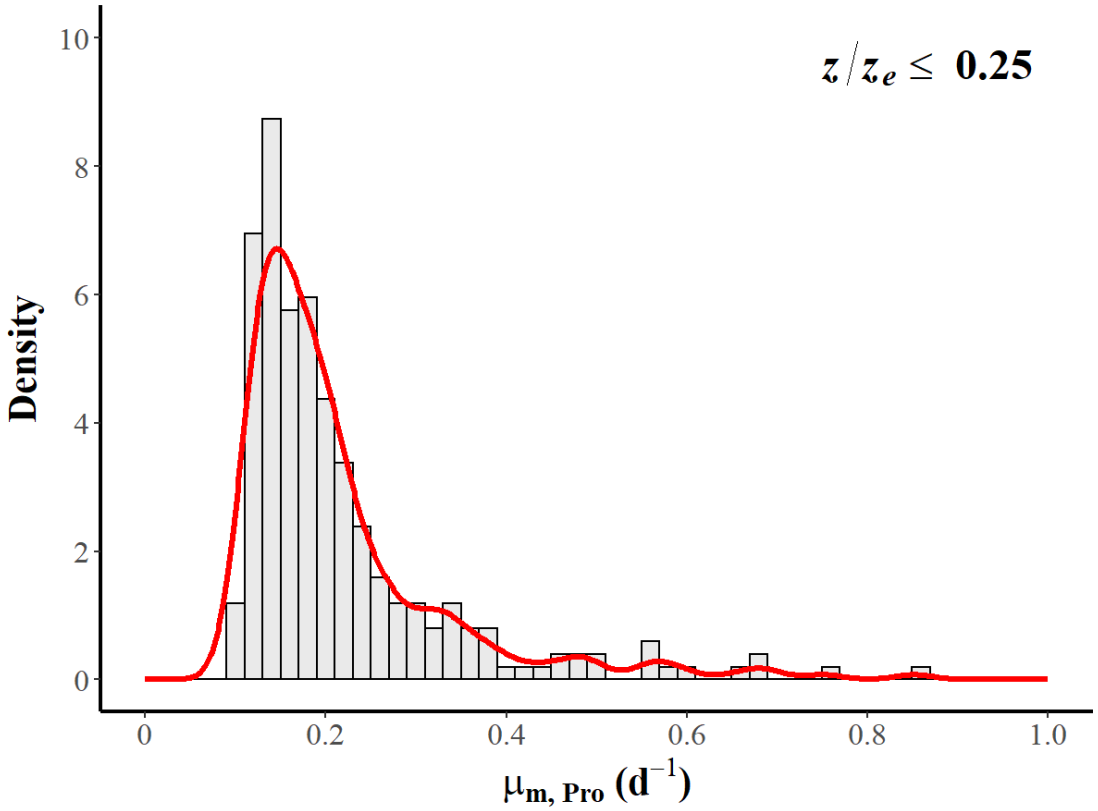


Figure 4.11: Frequency distributions (N = 252) of estimates of the maximum growth rates of *Prochlorococcus* populations ($\mu_{m,\,Pro}$) in the ocean surface (i.e. $z/z_e \leq 0.25$). Calculation was carried out on pooled data combining samples obtained during the AMT, BIOSOPE, DCM, and EUMELI cruises.

4.4 Discussion

4.4.1 Vertical structure of the photosynthetic parameters

Using a global dataset, clear differences in the vertical structure of the photosynthetic parameters between trophic domains were observed: stations in the eutrophic domain (high TChl-*a*, > 2 mg Chl-*a* m^{-3}) typically characterised by well-mixed water columns (Margalef, 1978; Alderkamp *et al.*, 2011) with the mixed layer extending well below the euphotic depth showed

no consistent pattern of depth dependence in the *PE* parameters (Figures 4.2a-4.5a). This suggests that phytoplankton cells, which pigment markers revealed were predominantly large eukaryotes (Claustre and Marty, 1995), tended to be physiologically acclimated to an average mixed-layer irradiance (Falkowski, 1981), and that their rate of photoacclimation was likely slower than the rate of vertical mixing (Lewis *et al.*, 1984). In contrast, for stations within the oligotrophic domain (low TChl-*a*, < 0.2 mg Chl-*a* m^{-3}), the magnitudes of all photosynthetic parameters varied significantly in response to vertical changes in available light with depth. These were predominantly subtropical waters characterised by a relatively shallow and stable mixed layer as a result of both weak wind-induced vertical mixing and strong thermal stratification. Cells confined within the surface mixed layer are continuously exposed to high incident solar irradiances and thus are high light-acclimated as indicated by high values of P_m^B (Figure 4.2c), E_k (Figure 4.4c), and the NPP index (Figure 3.2 in Chapter 3). Cells residing deeper in the water-column below the surface mixed layer were characterised by lower values of P_m^B, E_k, and the NPP index. Deeper samples also displayed higher values of α^B (Figure 4.3c) and ϕ_m (Figure 4.5c). The observed vertical patterns in the photophysiological parameters suggest that the rate of vertical mixing was slower than the rate of photoacclimation (Lewis *et al.*, 1984), allowing phytoplankton cells sufficient time to fully adjust to the ambient light level at a given depth. Pigment and flow cytometric data (Chapter 3, also in Claustre and Marty, 1995; Babin *et al.*, 1996; Bouman, Platt, Kraay, *et al.*, 2000; Veldhuis and Kraay, 2004; Grob, Ulloa, Li, *et al.*, 2007; Hickman *et al.*, 2010) also indicated vertical changes in the dominant picophytoplankton taxa (or ecotypes of a single genus), which are known to exhibit distinct bio-optical properties and photoadaptive strategies. Indeed, both optical characteristics and photosynthetic performance are influenced by the molecular mechanisms underlying responses to light stress, structures of the photosynthetic units, and intracellular pigment complement (Chapters 1-2, also in Morel *et al.*, 1993; Moore *et al.*, 1995; Coleman and Chisholm, 2007; Six *et al.*, 2007,

2008; Hickman *et al.*, 2010; Mella-Flores *et al.*, 2012). Thus, when examining the relationship between taxonomic structure of picophytoplankton-dominated communities and their bio-optical properties, the photoacclimatory state of phytoplankton should be taken into account.

The mesotrophic domain showed vertical gradients of P_m^B (Figure 4.2b) and E_k (Figure 4.4b) while depth dependencies of α^B (Figure 4.3b) and ϕ_m (Figure 4.5b) were not as pronounced. However, when considered separately, the BIOSOPE cruise showed noticeable variations in all three *PE* parameters with depth, and the observed patterns were particularly strong in the HNLC stations where vertical profiles of the photosynthetic parameters were highly comparable, in terms of both the shape of the profiles and the magnitudes of the parameters, to those found at the oligotrophic stations (gyres) of the same transect. This could be explained in part by similarities in the photoacclimatory status (NPP index) and species composition of (picocyanobacteria-dominated) phytoplankton communities residing in both low-latitude HNLC and subtropical gyre conditions. Compared to other mesotrophic sites (i.e. near the Marquises Islands) visited during the BIOSOPE cruise, the HNLC stations also tended to be more hydrodynamically stable (Figure 3 in Claustre *et al.* (2008)) and this is likely due to the influence of the South Pacific Tropical Water (Ras *et al.*, 2008). Consequently, the physico-chemical and biological characteristics of these low latitude HNLC waters more closely resembled those observed in the stratified oligotrophic waters associated with the South Pacific Gyre (Raimbault *et al.*, 2008; Ras *et al.*, 2008).

Within the euphotic zone, samples obtained from the HNLC stations tended to show higher and lower values of E_k and ϕ_m, respectively, relative to those from other mesotrophic sites, potentially as a result of higher relative concentrations of NPPs (Figure 3.2 in Chapter 3) corresponding to both the increased significance of picocyanobacteria and the high light conditions caused by the high optical transparency of these HNLC stations as revealed by deeper

euphotic depths and lower values of the vertical attenuation coefficient for the photosynthetically available radiation (PAR) (Ras *et al.*, 2008). It is also well known that iron limitation of phytoplankton growth and primary production is common in HNLC waters particularly of the tropical Pacific Ocean and the Southern Ocean (Behrenfeld *et al.*, 2006; Moore *et al.*, 2013) and there was clear evidence of iron depletion in the top 400 m of the water column at the HNLC stations of the BIOSOPE transect (Blain *et al.*, 2008). In both culture studies and field experiments, iron stress has been widely shown to cause a marked reduction in the photosynthetic efficiency of marine phytoplankton (Greene *et al.*, 1991, 1992; Vassiliev *et al.*, 1995; Hiscock *et al.*, 2008) and this has been explained to be a result of iron playing a key role in the formation and repair of proteins involved in photosynthesis, including those in the photosystem II reaction centre and the electron transport chain (Greene *et al.*, 1991; Hiscock *et al.*, 2008). Thus iron limitation may be a plausible explanation for the reduced values of ϕ_m at the HNLC stations.

Since information on the time of sample collection was not available for a considerable number of samples in our dataset, I was unable to examine the vertical distribution of the photosynthetic parameters over a diel cycle. Although diel changes could contribute to the variability in *PE* parameters (Prézelin *et al.*, 1986; Bruyant *et al.*, 2005; Xie *et al.*, 2018), they are not likely to be as significant a factor governing large-scale patterns in phytoplankton photophysiology as that caused by basin-scale shifts in abiotic (stability of the water column, light history, and nutrient availability) and biotic (phytoplankton biomass and species composition) factors between trophic domains and across oceanographic regimes encountered during each research cruise (Babin *et al.*, 1996; Bouman *et al.*, 2018).

4.4.2 Relationships between the NPP index and the photosynthetic parameters in the oligotrophic domain

It is important to note that changes in the NPP index in natural populations are not only an indicator of phytoplankton photoacclimation (Babin *et al.*, 1996; Bouman, Platt, Kraay, *et al.*, 2000) but are also related to a shift in gross phytoplankton community structure (Uitz *et al.*, 2008) since most of the variability in this index is driven by changes in zeaxanthin concentration, a marker of picocyanobacteria (*Synechococcus* and *Prochlorococcus*) which I have shown can make up a significant fraction (up to 80%) of the total NPP pool (Chapter 3). Therefore, when accounting for the observed relationships between NPPs and each of the photosynthetic parameters, the effect of both factors must be considered.

(1) The maximum photosynthetic rate (P_m^B)

P_m^B was positively correlated with the NPP index (Figure 4.6a). Theoretically, at steady state, P_m^B can be expressed in terms of a fraction of the number of photosynthetic units to the minimum turnover time for a photosynthetic unit (Dubinsky *et al.*, 1986; Sakshaug *et al.*, 1997). The turnover time represents the time required for electrons to be transported through the electron transport chain, leading to a molecule of oxygen produced per photosynthetic unit (Falkowski, 1981). In phytoplankton, it has been demonstrated that the turnover time is directly proportional to the cellular Chl-*a* content, although the underlying mechanism is not yet fully understood (Mayer and Graham, 1971; Falkowski, 1981). Given that the NPP index in marine picocyanobacteria has been shown to be primarily governed by changes in the intracellular concentration of photosynthetic rather than photoprotective pigments and thus positively correlated to the intracellular (DV)Chl-*a* concentration, one can explain the strong correlations between P_m^B values and the NPP index based strictly on photophysiological terms.

Photosynthetic rates are well known to depend on cell size (Falkowski, 1981; Marañón, 2015) and may provide an alternative explanation for the observed decrease in P_m^B with depth. In the stratified subtropical ocean, deep phytoplankton communities within and below the deep chlorophyll maximum are dominated by larger pico- and nanoeukaryotes, as indicated by both flow cytometry counts and a high relative abundance of the accessory pigments 19′-HEX and 19′-BUT (Ras *et al.*, 2008; Dimier *et al.*, 2009), whereas surface phytoplankton assemblages are dominated by smaller picocyanobacteria (*Prochlorococcus* and *Synechococcus*). The inverse relationship between cell size and P_m^B is consistent with the trends reported in various studies (Malone, 1977; Bouman *et al.*, 2005; Morán, 2007; Strom *et al.*, 2010; Morán and Scharek, 2015; Richardson *et al.*, 2016; Robinson *et al.*, 2018), however, it is also possible that the decrease in P_m^B with depth may also be partially attributed to vertical changes in temperature (*ca* 12°C to over 20°C) which could accelerate the enzymatic activities in the Calvin cycle and thus increase the photosynthetic rate (Robinson *et al.*, 2018). Strong vertical variability in temperature, the size structure of phytoplankton communities, and light history makes the vertical patterns in P_m^B extremely consistent across subtropical datasets.

A larger degree of variability in P_m^B was seen at the higher range of NPP indices (i.e. ≥ 0.4). Although the picocyanobacteria genera *Synechococcus* and *Prochlorococcus* co-existed in these surface samples, when *Prochlorococcus* dominated the pigment biomass as suggested by the elevated ratios of DVChl-*a* to TChl-*a* (i.e. 43-89%), values of P_m^B dropped markedly. This is in accordance with previous studies such as those of Marañón *et al.* (2003) and Xie *et al.* (2015) reporting lower P_m^B values when *Prochlorococcus* became prevalent. These results are also consistent with those obtained in a global study of Richardson *et al.* (2016) who observed

the highest P_m^B associated with *Synechococcus*-dominated communities and relatively low values of P_m^B in the regions where *Prochlorococcus* thrived. Bouman and colleagues (2005) similarly reported a considerable scatter in the relationship between a pigment index of phytoplankton size (comparable to the NPP index in this study) and P_m^B in the picophytoplankton-dominated areas of the Arabian Sea. The authors suggested that, when picophytoplankton dominate, changes in the species composition might be more important than cell size in explaining variation in P_m^B as different picophytoplankton taxa respond differently to short-time environmental variability.

(2) The initial slope (α^B) and the maximum quantum yield of photosynthesis (ϕ_m)

α^B describes the efficiency of light utilisation by marine phytoplankton and is quantitatively related to ϕ_m through light absorption (Dubinsky *et al.*, 1986; Sakshaug *et al.*, 1997). In this study, both α^B and ϕ_m showed a strong negative correlation with the NPP index (Figures 4.6b, d). α^B is proportional to the functional absorption cross-section of photosystem II (σ_{PSII}), which describes the target area where photons are absorbed and the excitation energy is channelled to the reaction centres for photochemistry, and the number of functional PSII reaction centres (i.e. reaction centres that trap the excitation energy; Falkowski *et al.*, 2004) per unit Chl-*a* concentration (Babin *et al.*, 1996; Falkowski and Raven, 2007). NPPs do not transfer their absorbed light energy to the reaction centres, but rather dissipate it so that the reaction centres are protected against over-excitation at harmfully high irradiances. Thus an increase in the NPP index would be accompanied by a reduction in σ_{PSII}, and ultimately α^B and ϕ_m (Cleveland *et al.*, 1989; Kolber *et al.*, 1990; Olaizola *et al.*, 1994; MacIntyre *et al.*, 2002). The xanthophyll-cycle NPPs, such as diadinoxanthin and diatoxanthin as well as zeaxanthin found in higher plants, fulfil the photoprotective function via thermal dissipation of the excitation energy (i.e. non-photochemical quenching) (MacIntyre *et al.*, 2002; Dimier *et al.*, 2009; Kulk *et al.*, 2011).

Zeaxanthin found in picocyanobacteria, on the other hand, is not known to directly be involved in the photoprotective xanthophyll cycles (Latifi *et al.*, 2009), although its insignificant contribution to photosynthesis has been thought to be associated with it being physically disconnected to the photosynthetic machinery (Kana *et al.*, 1988; Masamoto *et al.*, 1999; MacIntyre *et al.*, 2002). Conversely, in low light-acclimated cells, the impact of NPPs was minimal and most of the excitation energy was directed towards photochemistry, leading to increases in σ_{PSII}, α^B and ϕ_m (Moore and Chisholm, 1999; Marra *et al.*, 2000; Uitz *et al.*, 2008; Dubinsky and Stambler, 2009).

The observed decrease in α^B and ϕ_m encountered in the surface phytoplankton communities in the stratified, oligotrophic waters could also be explained in the light of nutrient effects (Cleveland *et al.*, 1989; Kolber *et al.*, 1990). Surface nutrient depletion can suppress the photosynthetic efficiencies in various ways: (1) it may lead to a reduction in the synthesis of proteins constituting the core and the reaction centres of PSII, leading to a decrease in the number of functional PSII reaction centres (Kolber *et al.*, 1988), (2) it may cause a decline in the synthesis of the RuBisCO enzyme used in the Calvin cycle (Geider *et al.*, 1993), and (3) it may trigger an increase in the relative proportion of NPPs and non-photochemical quenching (Geider *et al.*, 1993; Liefer *et al.*, 2018).

(3) Photoadaptation parameter (E_k)

The NPP index has been shown to display a robust positive relationship with the mean daily PAR in the mixed layer in the subtropical ocean (Babin *et al.*, 1996). Thus the observed strong correlation between E_k and the photoacclimatory status as indicated by the NPP index (Figure 4.6c) reflects the photophysiological response of the phytoplankton to light history. Since E_k is defined as P_m^B/α^B, E_k can also be thought of as a reciprocal of both the functional absorption

cross-section of PSII, σ_{PSII}, and the minimum turnover time of a photosynthetic unit (i.e. the maximum rate of photosynthetic electron transport) which, as described earlier, varies with the amount of Chl-*a* per cell (Falkowski, 1981; Falkowski and Raven, 2007). Therefore, high values of E_k observed in surface assemblages dominated by high light-acclimated picocyanobacteria may be a result of a reduced σ_{PSII} caused by the dissipation of excitation energy by NPPs, combined with the slow turnover time related to a decrease in cellular Chl-*a* content. In contrast, increases in both the intracellular concentration of Chl-*a* and the proportion of the excitation energy directed to photochemistry (i.e. low NPP index) were accompanied, respectively, by increases in the turnover time and σ_{PSII} during a downward adjustment of E_k in low light-acclimated eukaryotic phytoplankton residing within and beneath the deep chlorophyll maximum towards the bottom of the euphotic zone.

4.4.3 Relationships between θ_{Pro} and the NPP index

θ_{Pro} was found to be positively correlated with the NPP index across different oceanographic cruises examined (Figure 4.7), although the AMT dataset exhibited a higher degree of variability (Figure 4.7b) owing to its broad latitudinal and temporal coverages. Molecular studies of marine picocyanobacteria conducted on AMT cruises included in our database, such as those of Johnson *et al.* (2006) on AMT-13 and Zwirglmaier *et al.* (2007) on AMT-15, have pointed to strong latitudinal variation in the *Prochlorococcus* community structure in the upper mixed layer with the high light-adapted MED4 (HLI) ecotype dominating at lower latitudes from *ca* 30°N to 30°S, while at higher latitudes (i.e. *ca* 30-40°N and 30-45°S) the MIT9312 (HLII) ecotype was abundant. Zinser and colleagues (2007) investigated the relative effect of light and temperature on differential distributions of *Prochlorococcus* ecotypes in the North Atlantic and found that while light intensity was a good predictor of MED4 abundance, the dependence of the concentration of MIT9312 on light showed greater variability. Temperature, on the other

hand, was found to be more important in explaining the geographical distribution of MIT9312 (Johnson *et al.*, 2006; Zinser *et al.*, 2007), and temperature also appeared to be able to modify the relationship between light and MIT9312 abundance, with a negative correlation, rather than a positive one, observed at low temperature (Zinser *et al.*, 2007). Given that several studies conducted on stations included in our dataset have explicitly shown a significant correlation between the NPP index and light intensities (Babin *et al.*, 1996; Bouman, Platt, Kraay, *et al.*, 2000), these latitudinal differences in the response of *Prochlorococcus* ecotypes to variation in light and temperature conditions might be able to account for the large variability of θ_{Pro} values for the AMT data. Yet, to test this hypothesis, information on *Prochlorococcus* ecotype abundance is required.

Using a large collection of AMT cruise data, a recent study by Smyth *et al.* (2019) showed a bimodal distribution of *Prochlorococcus* cell diameter, one peak at *ca* 0.75 μm and another at ≥ 1.75 μm, which could be observed throughout the water column and across biogeochemical provinces encountered during a series of AMT transects. Such variation in *Prochlorococcus* cell size is likely reflected in a large variation in the intracellular carbon contents (Falkowski, 1981). This could introduce uncertainties in calculations of θ_{Pro} when all cells of this genus are assumed to contain a similar amount of carbon (often derived from an assumed *Prochlorococcus* cell diameter (0.6-0.8 μm) and a fixed value of carbon per cell volume; e.g. Veldhuis and Kraay, 1990; Li *et al.*, 1992; Campbell *et al.*, 1994). These uncertainties could also persist when applying different estimates of carbon per cell to the surface and deep populations of *Prochlorococcus* (e.g. Veldhuis and Kraay, 2004) since, according to Smyth *et al.* (2009), vertical variation in cell size can occur.

The spectral slope ($S_{443\text{-}550}$) was also shown to be a robust predictor of θ_{Pro} (Figure 4.9), highlighting the potential use of this widely observed bio-optical property as an indicator of θ_{Pro}. This relationship will be of use to biogeochemical modellers as θ is known to vary widely in the marine environment and is required to convert fields of phytoplankton carbon biomass that are generated from numerical models into maps of chlorophyll concentration that can be compared with satellite observations. Furthermore, given that information on light absorptive characteristics of phytoplankton can be retrieved through ocean-colour satellite data, the spectral slope may serve as a useful indicator of large-scale change in phytoplankton physiology.

The strong correlation between $S_{443\text{-}550}$ and the NPP index is largely a result of primary and secondary absorption peaks of all major NPPs lying within the blue part of the spectrum with zeaxanthin (found primarily in picocyanobacteria) having *in vivo* peaks at *ca* 445 and 480 nm (Moore *et al.*, 1995) and diadinoxanthin and diatoxanthin (found primarily in eukaryotic algae) centred at *ca* 460 and 490 nm (Johnsen *et al.*, 1994). At wavelengths greater than 550 nm, absorption due to NPPs becomes virtually undetectable.

The correlation between θ_{Pro} and $S_{443\text{-}550}$ (Figure 4.9) was statistically weaker than that between θ_{Pro} and the NPP index (Figure 4.7a) with R^2 values of 0.71 and 0.83, respectively (Fisher's *z*-test, $z = 2.28$, 95% confidence interval, $p < 0.05$). $S_{443\text{-}550}$ was linked to θ_{Pro} through the tight relationship between $a_{ph}(\lambda)$ in the blue-green spectral region and the NPP index. Yet, NPPs (i.e. pigment composition) are not the only source of variation in $a_{ph}(\lambda)$. Pigment packaging also affects the magnitude and shape of $a_{ph}(\lambda)$ (Duyens, 1956; Kirk, 2011), and the variability caused by this factor could propagate to variability in the relationship between θ_{Pro} and $S_{443\text{-}550}$.

Methodological limitations and differences in measurements of $a_{ph}(\lambda)$ by the filter-pad technique between laboratories must also be considered when accounting for the variability in the relationship between $S_{443\text{-}550}$ and θ_{Pro}. Pigment extraction processes for both the BIOSOPE and DCM cruises generally followed the widely-accepted protocol proposed by Kishino *et al.* (1985) in which hot methanol was used as an extracting solvent for the BIOSOPE samples (Bricaud and Stramski, 1990; Bricaud *et al.*, 2010) and the acetone/DMSO solution for the DCM samples (Stuart *et al.*, 1998; Bouman, Platt, Kraay, *et al.*, 2000). Although both methanol and acetone have been shown to generally exhibit no significant differences in extraction efficiencies on samples collected from the oligotrophic ocean (Bricaud and Stramski, 1990), chlorophyll degradation products (e.g. phaeopigments) tend to be extracted better in methanol (thus are included in the extracted phytoplankton fraction) and the water-soluble cyanobacterial phycobiliproteins cannot be extracted in organic solvents (Sosik and Mitchell, 1995). These problems could limit the accuracy of $a_{ph}(\lambda)$ measurements and could translate into uncertainties in the calculation of $S_{443\text{-}550}$.

It is also widely recognised that the filter-pad technique is subjected to errors caused by the extended pathlength of light due to multiple scattering within the filter and between the filter and particles (Allali *et al.*, 1997), and to correct for this filter effect, the pathlength amplification algorithm or β-factor must be applied. A culture study by Moore and colleagues (1995) reported that β-factors for *Prochlorococcus* and *Synechococcus* are different, and they differ significantly from a β-factor derived from cultures of larger eukaryotic cells (diatoms). Taking these considerations into account, the correction algorithm (second-order polynomial) used for DCM samples (Bouman, Platt, Kraay, *et al.*, 2000) combined the β-factor for *Prochlorococcus* taken from Moore *et al*. (1995) with the β-factor for the rest of the phytoplankton community derived by Hoepffner and Sathyendranath (1992) from coastal phytoplankton samples. The two

β-factors were scaled to the relative concentration of DVChl-*a* to TChl-*a* and the remaining fraction of TChl-*a*, respectively (Stuart *et al.*, 1998; Bouman, Platt, Kraay, *et al.*, 2000). On the other hand, group-specific β-factors were not invoked for the BIOSOPE dataset, yet, instead, it was done in a domain-specific manner (Bricaud *et al.*, 2010) in which samples collected in the oligotrophic and mesotrophic waters were assigned a β-factor according to a study by Allali *et al*. (1997) in the equatorial Pacific Ocean, while the algorithm proposed by Bricaud and Stramski (1990) based on observations from the Peruvian upwelling region was assigned to samples obtained from eutrophic stations. Allali *et al*. (1997) noted that the second-order polynomial coefficients for their derived correction algorithm fell between the values reported for *Prochlorococcus* and *Synechococcus* in Moore *et al.* (1995), reflecting the co-dominance of the two picocyanobacteria.

The variation in the pathlength amplification factors applied to $a_{ph}(\lambda)$ measurements could influence the estimates of $S_{443\text{-}550}$ and the differences may be evident when the datasets were pooled. As shown in Figure 4.9, for example, at $\theta_{Pro} > 200$ g C (g DVChl-*a*)$^{-1}$, there appeared to be a cluster of DCM samples with higher θ_{Pro} at lower $S_{443\text{-}550}$ which tended to deviate from the line of best fit. The high θ_{Pro} values estimated for these surface samples resulted from extremely low DVChl-*a* per cell due to high-light photoacclimation. Consequently, the β-factor for *Prochlorococcus* (scaled to DVChl-*a* / TChl-*a*) was not as strongly weighted and the estimated optical densities were governed primarily by the correction factor corresponding to other (eukaryotic) taxa (Hoepffner and Sathyendranath, 1992), which could be slightly biased as this β-factor did not take into account the presence of *Synechococcus* (Stuart *et al.*, 1998) that was particularly abundant in these samples. This uncertainty combined with differences in the correction factor used between datasets might in part explain the deviation of the mentioned cluster of DCM samples from the regression line: when compared to other samples having similarly

high values of θ_{Pro} and the NPP index, these DCM samples tended to show consistently biased $a^*_{ph}(\lambda)$ at 443, 550, and 676 nm towards the lower values, leading to an overall slight underestimation of $S_{443\text{-}550}$ (normalised to $a^*_{ph}(676)$). Note that since the pathlength amplification factor is a function of optical density (Bouman, Platt, Kraay, *et al.*, 2000), errors associated with choices of β-factors are typically more pronounced in the blue spectral region.

4.4.4 *Prochlorococcus* growth rates

The maximum growth rates of *Prochlorococcus* ($\mu_{m,\,Pro}$) in the surface waters ($z/z_e \leq 0.25$) were calculated from θ_{Pro} and the maximum chlorophyll *a*-normalised photosynthetic rates ($P^B_{m,\,Pro}$) (Geider, 1987; Marañón, 2005) (Equation 4.6). θ_{Pro} was estimated based on its relationship with the NPP index (section 4.3.3) and the estimated values showed a clear progressive decrease with depth (Figure 4.10), reflecting the flexibility of *Prochlorococcus* in allocating cellular resources to light-harvesting apparatus under varying light conditions (Talmy *et al.*, 2013; Halsey and Jones, 2015). The extent of θ_{Pro} variability in the field and laboratory cultures has been discussed in the previous chapter. Highly restrictive pigment-marker criteria outlined in Sathyendranath *et al.* (2009) were used to identify *Prochlorococcus*-dominated stations. This pigment approach has also been successfully used elsewhere such as in a recent study by Robinson and colleagues (2018) to derive group- and size class-specific photosynthetic parameters. A major limitation to this approach, however, is that natural phytoplankton assemblages that are dominated only by a single taxonomic group are rare, so a very large number of samples classified as mixed populations would be discarded and there is always a possibility of having a mixed population in a sample even after such stringent criteria are applied. Other potential sources of uncertainties of this approach could be errors associated with pigment measurements, pigments with ambiguous taxonomic affiliations, and the genetic and environmental-related variability in pigment composition within a sub-group level (Llewellyn *et al.*, 2005).

Despite the mentioned potential uncertainties, the estimated $P^B_{m,\mathrm{Pro}}$ value of 4.01 mg C (mg Chl-*a*)$^{-1}$ h^{-1} (or $P^{\mathrm{cell}}_{m,\mathrm{Pro}}$ *ca* 5.52 fg C cell^{-1} h^{-1}) for surface *Prochlorococcus* populations fell within the range reported in various culture studies on high light-adapted (HL) strains such as those of Partensky *et al.* (1993) ($P^B_{m,\mathrm{Pro}}$ = 1.53-4.31 mg C (mg Chl-*a*)$^{-1}$ h^{-1} or $P^{\mathrm{cell}}_{m,\mathrm{Pro}}$ = 4.91-5.85 fg C cell^{-1} h^{-1} for the MED4 strain grown at 3.8-133.0 μmol photons m^{-2} s^{-1}), Shimada *et al*. (1996) (3.89 mg C (mg Chl-*a*)$^{-1}$ h^{-1} or 6.96 fg C cell^{-1} h^{-1} for the GP2 strain grown at 37 μmol photons m^{-2} s^{-1}), Moore and Chisholm (1999) (*ca* 2-5.5 mg C (mg Chl-*a*)$^{-1}$ h^{-1} for six HL strains grown at 70 μmol photons m^{-2} s^{-1}), and Kulk *et al.* (2011) (3.90 mg C (mg Chl-*a*)$^{-1}$ h^{-1} for the MED4 strain at 125 μmol photons m^{-2} s^{-1}). It should be noted that when compared with their low light-adapted (LL) counterparts (typically deeper in the water column), HL strains tend to show a stronger dependence of $P^B_{m,\mathrm{Pro}}$ on growth irradiances (Moore and Chisholm, 1999). Also, when grown under high irradiances, HL strains normally exhibit a higher P^B_m and lower α^B, and therefore their photosynthetic rate saturates at a higher irradiance ($E_k = P^B_m / \alpha^B$), indicating high-light photoacclimation (Moore *et al.*, 1998; Moore and Chisholm, 1999).

A few authors have measured $P^B_{m,\mathrm{Pro}}$ or $P^{\mathrm{cell}}_{m,\mathrm{Pro}}$ for natural *Prochlorococcus* populations, and our results are consistent with these studies. For instance, Li (1994) used a ^{14}C labelling technique combined with flow cytometric cell sorting to estimate photosynthetic rates of *Prochlorococcus* in the Moroccan upwelling region and obtained a $P^{\mathrm{cell}}_{m,\mathrm{Pro}}$ of 4.0 fg C cell^{-1} h^{-1}. In the northern South China Sea, Xie and colleagues (2015) reported a value of P^B_m close to 5.0 mg C (mg Chl-*a*)$^{-1}$ h^{-1} at a station where *Prochlorococcus* was found to predominate, accounting for *ca* 80% of the TChl-*a* biomass (Figure 7 in Xie *et al.*, 2015). The slightly higher P^B_m could be due, in part, to the influence of *Synechococcus* or other picoeukaryotes both of which have been shown

to exhibit significantly higher photosynthetic rates at light saturation than *Prochlorococcus* (Li, 1994; Shimada *et al.*, 1996; Kulk *et al.*, 2011).

A mean $\mu_{m,\,Pro}$ of 0.22 d^{-1} (0.11-0.85 d^{-1}) estimated for surface *Prochlorococcus* populations in this study (Figure 4.11) was consistent with the results reported in several studies. In the oligotrophic Sargasso Sea, Goericke and Welschmeyer (1993) estimated growth rates of *Prochlorococcus*, μ_{Pro}, using ^{14}C pigment labelling and reported mean values of *ca* 0.2 and 0.27 d^{-1} for summer and winter populations, respectively, in the surface layer at 96% incident irradiance (Figure 4B in Goericke and Welschmeyer, 1993). Using a similar pigment labelling technique, Roberts (2001) reported a μ_{Pro} of 0.21 d^{-1} in the surface (0 m) open ocean off the California coast. Liu *et al*. (1995) documented that *Prochlorococcus* populations at the sea surface outside the Kaneohe Bay and at Station ALOHA (October 1993) grew at the rates of 0.33 and 0.38 d^{-1}, respectively as estimated using a selective metabolic inhibitor method. However, the authors also noted that under oligotrophic conditions as observed earlier in May of the same year, the estimated surface μ_{Pro} at Station ALOHA dropped to *ca* 0.20 d^{-1}. Estimates of $\mu_{m,\,Pro}$ obtained in this analysis were also supported by a more recent study by Marañón (2005) who independently used subsets of the AMT data included in the present study along with other observations from the Bermuda Atlantic Time-series (BATS) program to calculate light-saturated growth rates of phytoplankton in the surface (20 m) subtropical gyres and similarly observed that the phytoplankton grew relatively slowly with estimated μ_m values ranging between *ca* 0.18 and 0.52 d^{-1} (Figure 6 in Marañón, 2005). Note that the co-existing *Synechococcus* and picoeukaryotes generally have higher growth rates relative to *Prochlorococcus* (Liu *et al.*, 1995; Moore *et al.*, 1995; Kulk *et al.*, 2011).

The average surface $\mu_{m,\,Pro}$ (0.22 d^{-1}) derived in this study could be considered low when compared to surface observations of $\mu_{m,\,Pro}$ reported in the studies of e.g. Landry *et al*. (1995) (*ca* 0.5 d^{-1} in the central equatorial Pacific, using the dilution technique), Binder *et al*. (1996) (0.49-0.69 d^{-1}, central equatorial Pacific, DNA analysis), and Liu *et al*. (1997) (0.45-0.8 d^{-1}, eastern and western equatorial Pacific, cell cycle analysis). These high surface values are in agreement with some values of $\mu_{m,\,Pro}$ observed in HL ecotypes obtained in culture (Partensky *et al.*, 1993; Moore *et al.*, 1995, 1998; Stawiarski *et al.*, 2018). Yet, it should be emphasised that differences among techniques are a critical source of variation in estimates of *Prochlorococcus* growth rates (Partensky, Hess, *et al.*, 1999), and thus comparisons between datasets have to be done with caution.

High surface values of θ_{Pro} (i.e. 160-400 with a mean of *ca* 260 g C (g DVChl-*a*)$^{-1}$)) might in part explain the relatively low $\mu_{m,\,Pro}$ obtained in this study ($\mu_{m,\,Pro} \sim P^{B}_{m,\,Pro} / \theta_{Pro}$), and support the conclusions of an earlier study by Goldman (1980) that slow phytoplankton growth rates at < 0.2-0.3 d^{-1} were linked to their high carbon-to-Chl-*a* ratios of greater than 120 g C (g Chl-*a*)$^{-1}$. In most cases the surface growth irradiances in subtropical waters far exceed those used in culture studies and this likely results in considerably lower values of DVChl-*a* per *Prochlorococcus* cell and hence higher values of θ_{Pro} reported in field studies. On the other hand, applying the cell-specific carbon conversion factor that was too high could also yield high θ_{Pro}. Several studies stemming from the AMT campaigns (e.g. Zubkov *et al.*, 1998, 2000; Hickman *et al.*, 2010) have used the conversion factor of 29-32 fg C *Prochlorococcus* cell^{-1} derived based on the mean cell size of *ca* 0.6-0.7 μm for their analyses, which is much lower than the conversion factor used here (49 fg C cell^{-1}). However, given recent estimates of *Prochlorococcus* cell diameter (Smyth *et al.*, 2019) showing double peaks at 0.75 and 1.75 μm with a larger average

cell size (*ca* 0.95 μm) than previously recognised in the subtropical gyres, there may be a need for the conversion factor typically used for the AMT datasets to be revisited.

Another possible factor that might limit the accuracy of the estimates of $\mu_{m,\,Pro}$ is the use of a single value of $P^{B}_{m,\,Pro}$ for all surface samples. As discussed earlier, culture studies have shown that $P^{B}_{m,\,Pro}$ varies among HL strains and differs significantly between HL and LL ecotypes, and for HL strains, it increases strongly with increasing light intensities (Partensky *et al.*, 1993; Moore *et al.*, 1995; Moore and Chisholm, 1999; Kulk *et al.*, 2011). The light effects on $P^{B}_{m,\,Pro}$ should be minimal here as all surface samples were exposed to a similar, limited range of light availability indexed by the ratio z/z_e. On the other hand, the intrinsic ecotypic variation in $P^{B}_{m,\,Pro}$ could be more important (Hartmann *et al.*, 2014) given that *Prochlorococcus* ecotype composition can be highly dynamic in the upper water column where HL and LL strains may be distributed differently along environmental (e.g. light, temperature, and nutrient) gradients (Bouman *et al.*, 2006; Johnson *et al.*, 2006; Zinser *et al.*, 2007; Partensky and Garczarek, 2010) in response to seasonal change in physical forcing.

4.5 Concluding Remarks

The first part of this study makes use of an extensive database of *PE* parameters and HPLC-determined pigment concentrations to examine the vertical structure of the photosynthetic properties of marine phytoplankton in the eutrophic, mesotrophic, and oligotrophic domains and then proceeds to examine the role photoacclimation, indicated by the NPP index, plays in governing these vertical patterns. Within the oligotrophic domain which was predominantly highly stratified subtropical waters, the magnitudes of all photophysiological parameters varied significantly in response to strong vertical shifts in the physicochemical characteristics of the

water column (light history, temperature, and nutrient) and phytoplankton community structure. In contrast, the vertical gradients of the photosynthetic parameters were not as strong for stations within the eutrophic and mesotrophic domains. The results clearly demonstrate that the NPP index accounted for a significant fraction of the variability in the photosynthetic parameters observed in the oligotrophic domain.

Next, estimates of θ_{Pro} were calculated based on HPLC pigment data, flow cytometric measurements of cell abundance, and carbon conversion factors from the literature. The strong positive correlation between estimates of θ_{Pro} and the NPP index suggests that the NPP index may serve as a viable indicator of θ_{Pro} in oligotrophic subtropical waters. A major advantage of using the NPP index to estimate θ_{Pro} is that NPPs are unique to phytoplankton, avoiding errors caused by the presence of other organisms and seawater constituents, which could be the case for other techniques including estimates based on bulk ATP and POC concentrations as well as optically-based approaches.

θ_{Pro} was also shown to be positively correlated with the spectral slope $S_{443\text{-}550}$, although the correlation was weaker than that between θ_{Pro} and the NPP index. These results suggest a possibility of using $S_{443\text{-}550}$ to predict θ_{Pro} and hence infer information on variation in phytoplankton physiology. This approach is particularly appealing given that it is an optical property that can be measured autonomously by optical sensors and also from space. Additional datasets comprising simultaneously collected data of phytoplankton absorption, pigment concentrations, and flow cytometry counts are required to more confidently assess the relationship between $S_{443\text{-}550}$ and θ_{Pro} so that the utility of this approach becomes clearer.

Prochlorococcus has long been recognised as a major component of phytoplankton communities in tropical and subtropical regions of the open ocean, although studies reporting its growth rates are surprisingly scarce. Using *in situ* observations of $P^{B}_{m,\,\mathrm{Pro}}$ and estimates of θ_{Pro} derived from the NPP index, the maximum growth rates for surface (20 m) *Prochlorococcus* populations, $\mu_{m,\,\mathrm{Pro}}$, were determined. The estimated values of $\mu_{m,\,\mathrm{Pro}}$ (0.11-0.85 d^{-1}) fall within a reasonable range and suggest that *Prochlorococcus* in the subtropical open-ocean waters grew relatively slowly (mean $\mu_{m,\,\mathrm{Pro}}$ of 0.22 d^{-1}). Future work involves acquiring more direct measurements of $P^{B}_{m,\,\mathrm{Pro}}$ to improve estimates of $\mu_{m,\,\mathrm{Pro}}$ and understanding the physiological mechanisms behind such slow growth rates.

Chapter 5

Summary and Future Work

5.1 Summary

Marine phytoplankton are subjected to extreme variation in both the intensity and spectral quality of light that occurs over seasons, across trophic gradients, and with depth (Kirk, 2011). Photoacclimation is a collection of physiological processes (Falkowski and LaRoche, 1991) to ensure survival of the algal cells under such changes in the ambient light conditions by optimising light absorption and photosynthesis at low light intensities, while protecting photosynthetic units from potential photodamage at excessively high light (Falkowski and Owens, 1980; Olaizola *et al.*, 1994; MacIntyre *et al.*, 2002). When exposed to a new light environment for prolonged duration, photoacclimation typically takes form in the adjustment of the relative abundance of individual pigments present in the cell (MacIntyre *et al.*, 2002). The work presented in this thesis addresses how photoacclimation impacts the pigmentation, bio-optical properties, and photosynthetic performance of marine phytoplankton in natural environments.

Using *in situ* measurements of light absorption spectra of phytoplankton ($a_{ph}(\lambda)$) and HPLC pigment data collected across a broad latitudinal gradient of the Atlantic Basin that covered various oceanic biomes with fundamental differences in physical forcing (Longhurst, 1998), Chapter 2 examined how variation in both the spectral shape and magnitude of the Chl-*a*-specific absorption coefficient $a^*_{ph}(\lambda)$ is related to changes in the pigment composition of phytoplankton communities, with the following principal findings:

- $a^*_{ph}(440)$ was shown to decrease significantly with increasing total Chl-*a* concentration (TChl-*a*) which could be described by a power-law function consistent with previous

studies in different marine regions (Yentsch and Phinney, 1989; Chisholm, 1992; Bricaud *et al*., 1995, 2004, 2010; Sathyendranath *et al*., 1996; Allali *et al*., 1997; Cota *et al*., 2003; Ferreira *et al*., 2013);

- The inverse relationship between $a^*_{ph}(440)$ and TChl-*a* was accompanied by a decrease in the proportion of non-photosynthetic pigments (NPPs) relative to total pigments (NPP index; Babin *et al.*, 1996) from oligotrophic (low TChl-*a*), high-light environments dominated by picocyanobacteria (tropical and subtropical gyres in the Trades Biome) to more productive (higher TChl-*a*), low-light regions abundant with larger eukaryotic phytoplankton (typically in the Westerlies and Polar Biomes);
- The changes in the NPP index along the gradient of the bulk TChl-*a* likely resulted from both photoacclimation and the adaptive variation in pigment composition of dominant prokaryotic and eukaryotic groups (Babin *et al.*, 1996; Moore *et al.*, 2006);
- NPPs accounted for up to 60% of total reconstructed phytoplankton absorption at 440 nm (Bidigare, 1991) in the Trades Biome where variation in the NPP index governed a considerable fraction of the variability in $a^*_{ph}(440)$ and the shape of $a_{ph}(\lambda)$ in the blue-green spectral region as indicated by a spectral slope index; and
- Zeaxanthin (ZEA, a pigment marker for picocyanobacteria) was found to be the most abundant NPP in the Trades Biome and variation in the fractional contribution of ZEA to total pigments was driven largely by changes in the relative contribution of the picocyanobacterium *Prochlorococcus* to total phytoplankton pigment biomass.

Whereas Chapter 2 focused on a broad swath of the Atlantic Basin, Chapter 3 concentrated primarily on the tropical and subtropical regions of both the Atlantic and Pacific Oceans where picophytoplankton are known to be particularly abundant. Using marine picocyanobacterium *Prochlorococcus* as a model organism, Chapter 3 addressed the specific question of how the

relative concentrations of photosynthetic and photoprotective pigments present in phytoplankton cells are modified in response to shifts in irradiance. The principal findings of Chapter 3 are as follows:

- The NPP index showed a strong depth-dependent decrease with a decrease in the relative availability of light in the water column;
- The vertical decline in the NPP index could be attributed in large part to changes in the cellular content of photosynthetic pigments (PSPs). This was supported by information on the intracellular pigment concentrations of the picocyanobacterial community with DVChl-*a* cell^{-1} showing a dramatic increase from the sea surface to the bottom of the euphotic zone whereas ZEA cell^{-1} being relatively uniform with depth;
- Using a simple pigment ratio approach to identify *Prochlorococcus* ecotypes (Partensky *et al*., 1993), this study also shows that the depth-dependent increase in DVChl-*a* cell^{-1} was likely through both changes in the photoacclimatory status of the *Prochlorococcus* population as a whole and an increase in the relative abundance of low light-adapted *Prochlorococcus* ecotypes which intrinsically display higher DVChl-*a* cell^{-1};
- Surface values of the NPP index increased as one moves from coastal upwelling regions to HNLC and oligotrophic open-ocean conditions resulting from a shift in phytoplankton community structure from eukaryotes to small picocyanobacteria subsequent to a progressive deepening of the nitracline;
- Seasonally, NPP indices increased during the summer-autumn months reflecting a photoacclimatory response of the phytoplankton community to the elevated incident solar radiation alongside an increased prevalence of picocyanobacteria during this period of strong water-column stratification, while the depth-dependent variation in the NPP index tended to diminish in the winter and early spring when the density structure of the water column tended to be vertically homogeneous; and

- The carbon-to-(DV)Chl-*a* ratio estimated for *Prochlorococcus* populations (θ_{Pro}) showed a strong photoacclimatory response to changes in irradiance, and θ_{Pro} was relatively high and much more variable in magnitude when compared to those of *Synechococcus* and other eukaryotic picophytoplankton, implying a greater physiological plasticity in this genus (Partensky and Garczarek, 2010; Talmy *et al.*, 2013).

The ability of phytoplankton cells to modify the intracellular composition and concentration of their light harvesting pigments directly impacts biomass-specific photosynthetic rates. Variation in the cellular complement of NPPs relative to PSPs is directly associated with the varying fraction of absorbed energy lost as heat compared to that is transferred to the associated photosystem for photochemistry. Chapter 4 examined the vertical variation in the photophysiological properties of phytoplankton populations in different trophic regimes and how they were related to changes in the NPP index. The following conclusions were drawn from these results:

- The photosynthesis-irradiance (*PE*) parameters exhibited strong depth-dependence for the oligotrophic domain and the HNLC waters of the South Pacific, indicating that the rate of vertical mixing was slower than the rate of photoacclimation, while the vertical patterns observed in eutrophic and mesotrophic waters were not as clear;
- For the oligotrophic domain, the magnitudes of the maximum Chl-*a*-normalised photosynthetic rate (P_m^B) and the photoadaptation parameter (E_k) were positively correlated with the NPP index, while the Chl-*a*-normalised initial slope (α^B) of the *PE* curve and the maximum quantum yield of photosynthesis (ϕ_m) showed a negative correlation with the NPP index;
- θ_{Pro} was positively correlated with both the NPP index and the normalised (to 676 nm) spectral slope of phytoplankton absorption between 443 and 550 nm ($S_{443\text{-}550}$), although the θ_{Pro}-$S_{443\text{-}550}$ relationship showed a slightly higher degree of variability;

- The relationship between the NPP index and θ_{Pro} showed significant seasonal variability with values of both variables increasing toward the summer due to the prevalence of high light-acclimated picocyanobacteria in thermally stratified water columns;
- When the NPP index was used to predict θ_{Pro}, the derived estimates of θ_{Pro} were comparable to the range of values reported in the literature and showed clear depth-dependence as anticipated; and
- Estimation of the maximum growth rates for surface *Prochlorococcus* populations from $P^{B}_{m,\,Pro}$ and estimates of θ_{Pro} derived from its relationship with the NPP index suggested that *Prochlorococcus* growth in the oligotrophic ocean was relatively slow.

5.2 Future work

This thesis has shown that the overall relationship between pigment indices of size and the *in vivo* absorptive properties of phytoplankton was highly variable between oceanic biomes in the Atlantic Basin. Therefore, one area for future study would be to develop a deeper mechanistic understanding of the ecophysiological factors governing the two principal factors known to influence the absorptive properties of cells: pigment diversity and cell size. This will require quantifying the contribution of pigment composition, pigment packaging, and cell size in natural samples and relating these cellular traits to the overall variability in spectral shape and magnitude of light absorption using a combination of theoretical, empirical, and experimental approaches. One way of examining the relative contribution of accessory pigment to phytoplankton absorption is through decomposing *in vivo* absorption spectra of phytoplankton corrected for the package effect into Gaussian absorption bands (Hoepffner and Sathyendranath, 1991; Stuart *et al.*, 1998). This could be an alternative to the spectral reconstruction method (Bidigare *et al.*, 1990) which does not address the potential impact of pigment-binding proteins on the peak heights and peak widths of the absorption spectrum of each pigment. To fully

disentangle the effect of cell size and pigment content on pigment packaging, detailed measurements on the size spectra of natural assemblages would be required, which are, however, still lacking in many bio-optical datasets because no single instrument is able to accurately and unambiguously capture the entire range of cell sizes present in the natural environment. Thus, laboratory experiments using monocultures or mixed populations of known size distributions selected to cover the range of taxonomic groups with contrasting cellular architecture (e.g. number and arrangement of thylakoids) may be necessary to determine how variable the absorptive properties of phytoplankton are within and between the size classes.

Results obtained from this thesis have also advanced our understanding of photoacclimatory characteristics of natural *Prochlorococcus* populations through evaluating the vertical variability in DVChl-*a* cell^{-1} and θ_{Pro}. By supplementing bio-optical data with molecular analyses on *Prochlorococcus* ecotype diversity, we should be able to address the relative importance of ecotypic versus photoacclimatory effects (Thompson *et al.*, 2018) in governing the vertical variability in the intracellular concentration of DVChl-*a*. Another outstanding question of *Prochlorococcus* photoacclimation would be to understand how *Prochlorococcus* communities residing in oligotrophic, transparent waters differ from those in more productive, turbid environments in terms of their acclimation or adaptation to changes in the spectral quality of the underwater light field.

Variation in θ_{Pro} is not only a function of light, but also registers changes in division rates driven by other environmental factors (Geider, 1987; Graff *et al.*, 2016). Future work involving multifactorial bioassays on cultures and natural populations could allow a greater insight into the nutrient and temperature effects on photoacclimatory and subsequent bio-optical characteristics of *Prochlorococcus*. In addition to the role that abiotic, bottom-up factors (Bouman *et*

al., 2006, 2011; Johnson *et al.*, 2006; Zinser *et al.*, 2007) play in governing the absorptive properties of *Prochlorococcus*, the effect of biotic stressors (e.g. viral infection and selective grazing) are less well understood. How these top-down factors impact the spatio-temporal variability in the bio-optical properties of *Prochlorococcus* warrants further investigation.

Knowledge of how large-scale trends in the concentrations of PSPs and NPPs (and their specific binding proteins) vary relative to one another in the course of photoacclimation and photoadaptation is also of fundamental importance to understand and predict ocean biogeochemical cycles as it is critical not only for quantifying phytoplankton photosynthetic performance and productivity, but also for determining the flow of the fixed energy through various functional components (i.e. light harvesting, photoprotection, carbon fixation, and biosynthesis (especially of ribosomes)) within phytoplankton cells (Geider *et al.*, 1996; Talmy *et al.*, 2013) which, in turn, regulates the particulate organic matter composition and stoichiometry of phytoplankton communities and higher trophic levels (Finkel *et al.*, 2010; Martiny *et al.*, 2013, 2016).

With increasing interest in predicting future effects of climate change, there would be a pressing need to better understand the physiological and molecular mechanisms involved in photoacclimation of marine phytoplankton in response to high light, including the cellular localisation and photoprotective role of NPPs in picocyanobacteria, as photoprotection would critically determine their ecological success in the future ocean (Katayama *et al.*, 2017) where global warming is postulated to enhance upper ocean stratification and, thereby, increase the average light availability within the mixed layer (Boyd *et al.*, 2010).

References

Acevedo-Trejos, E., Brandt, G., Bruggeman, J. and Merico, A. (2015) 'Mechanisms shaping size structure and functional diversity of phytoplankton communities in the ocean', *Scientific Reports*, 5(8918).

Agustí, S., González-Gordillo, J. I., Vaqué, D., Estrada, M., Cerezo, M. I., Salazar, G., Gasol, J. M. and Duarte, C. M. (2015) 'Ubiquitous healthy diatoms in the deep sea confirm deep carbon injection by the biological pump', *Nature Communications*, 6(7608).

Aiken, J., Pradhan, Y., Barlow, R. G., Lavender, S. J., Poulton, A. and Hardman-Mountford, N. J. (2009) 'Phytoplankton pigments and functional types in the Atlantic Ocean: a decadal assessment, 1995-2005', *Deep-Sea Research Part II: Topical Studies in Oceanography*, 56(15), pp. 899–917.

Aksnes, D. L., Ohman, M. D. and Rivière, P. (2007) 'Optical effect on the nitracline in a coastal upwelling area', *Limnology and Oceanography*, 52(3), pp. 1179–1187.

Alberts, B., Johnson, A., Lewis, J., Raff, M., Roberts, K. and Walter, P. (2015) *Molecular Biology of the Cell*. Garland Science.

Alderkamp, A.-C., de Baar, H. J. W., Visser, R. J. W. and Arrigo, K. R. (2010) 'Can photoinhibition control phytoplankton abundance in deeply mixed water columns of the Southern Ocean?', *Limnology and Oceanography*, 55(3), pp. 1248–1264.

Alderkamp, A.-C., Garcon, V., de Baar, H. J. W. and Arrigo, K. R. (2011) 'Short-term photoacclimation effects on photoinhibition of phytoplankton in the Drake Passage (Southern Ocean)', *Deep-Sea Research Part I: Oceanographic Research Papers*, 58(9), pp. 943–955.

Allali, K., Bricaud, A. and Claustre, H. (1997) 'Spatial variations in the chlorophyll-specific absorption coefficients of phytoplankton and photosynthetically active pigments in the equatorial Pacific', *Journal of Geophysical Research: Oceans*, 102(C6), pp. 12413–12423.

Aquino-Cruz, A., Hernández-Becerril, D. U., Signoret-Poillon, M., Salas-de-León, D. A. and Monreal-Gómez, M. A. (2013) 'Studies on picophytoplankton in the southern Gulf of Mexico: recognition of picoprokaryotes and abundances of picophytoplankton during "dry season"', *Brazilian Journal of Oceanography*, 61(4), pp. 265–276.

Aro, E. M., Virgin, I. and Andersson, B. (1993) 'Photoinhibition of Photosystem II. Inactivation, protein damage and turnover', *Biochimica et Biophysica Acta*, 1143(2), pp. 113–134.

Babin, M., Morel, A., Claustre, H., Bricaud, A., Kolber, Z. and Falkowski, P. G. (1996) 'Nitrogen- and irradiance-dependent variations of the maximum quantum yield of carbon fixation in eutrophic, mesotrophic and oligotrophic marine systems', *Deep-Sea Research Part I: Oceanographic Research Papers*, 43(8), pp. 1241–1272.

Babin, M., Morel, A. and Gagnon, R. (1994) 'An incubator designed for extensive and sensitive measurements of phytoplankton photosynthetic parameters', *Limnology and Oceanography*, 39(3), pp. 694–702.

Balch, W., Drapeau, D., Bowler, B. and Booth, E. (2007) 'Prediction of pelagic calcification rates using satellite measurements', *Deep-Sea Research Part II: Topical Studies in Oceanography*, 54(5–7), pp. 478–495.

Barlow, R. G., Aiken, J., Holligan, P. M., Cummings, D. G., Maritorena, S. and Hooker, S. B. (2002) 'Phytoplankton pigment and absorption characteristics along meridional transects in the Atlantic Ocean', *Deep-Sea Research Part I: Oceanographic Research Papers*, 49(4), pp. 637–660.

Barlow, R. G., Aiken, J., Moore, G. F., Holligan, P. M. and Lavender, S. J. (2004) 'Pigment adaptations in surface phytoplankton along the eastern boundary of the Atlantic Ocean', *Marine Ecology Progress Series*, 281, pp. 13–26.

Barlow, R. G., Cummings, D. G. and Gibb, S. W. (1997) 'Improved resolution of mono- and divinyl chlorophylls *a* and *b* and zeaxanthin and lutein in phytoplankton extracts using reverse phase C-8 HPLC', *Marine Ecology Progress Series*, 161, pp. 303–307.

Barton, A. D., Finkel, Z. V., Ward, B. A., Johns, D. G. and Follows, M. J. (2013) 'On the roles of cell size and trophic strategy in North Atlantic diatom and dinoflagellate communities', *Limnology and Oceanography*, 58(1), pp. 254–266.

Behrenfeld, M. J. and Boss, E. S. (2006) 'Beam attenuation and chlorophyll concentration as alternative optical indices of phytoplankton biomass', *Journal of Marine Research*, 64, pp. 431–451.

Behrenfeld, M. J., Boss, E. S., Siegel, D. A. and Shea, D. M. (2005) 'Carbon-based ocean productivity and phytoplankton physiology from space', *Global Biogeochemical Cycles*, 19(1), pp. 1–14.

Behrenfeld, M. J. and Falkowski, P. G. (1997) 'A consumer's guide to phytoplankton primary productivity models', *Limnology and Oceanography*, 42(7), pp. 1479–1491.

Behrenfeld, M. J., Worthington, K., Sherrell, R. M., Chavez, F. P., Strutton, P., McPhaden, M. and Shea, D. M. (2006) 'Controls on tropical Pacific Ocean productivity revealed through nutrient stress diagnostics', *Nature*, 442(7106), pp. 1025–1028.

Berner, T., Dubinsky, Z., Wyman, K. and Falkowski, P. G. (1989) 'Photoadaptation and the package effect in *Dunaliella tertiolecta* (Chlorophyceae)', *Journal of Phycology*, 25(1), pp. 70–78.

Bertilsson, S., Berglund, O., Karl, D. M. and Chisholm, S. W. (2003) 'Elemental composition of marine *Prochlorococcus* and *Synechococcus*: implications for the ecological stoichiometry of the sea', *Limnology and Oceanography*, 48(5), pp. 1721–1731.

Berube, P. M., Biller, S. J., Kent, A. G., Berta-Thompson, J. W., Roggensack, S. E., Roache-Johnson, K. H., Ackerman, M., Moore, L. R., Meisel, J. D., Sher, D., Thompson, L. R., Campbell, L., Martiny, A. C. and Chisholm, S. W. (2015) 'Physiology and evolution of nitrate acquisition in *Prochlorococcus*', *The ISME Journal*, 9(5), pp. 1195–1207.

Bidigare, R. R. (1991) 'Analysis of algal chlorophylls and carotenoids', in Hurd, D. C. and Spencer, D. W. (eds) *Marine Particles: Analysis and Characterization*. American Geophysical Union, pp. 119–123.

Bidigare, R. R., Van Heukelem, L. and Trees, C. C. (2003) 'HPLC phytoplankton pigments: sampling, laboratory methods, and quality assurance procedures', in Mueller, J. L., Fargion, G. S., and McClain, C. R. (eds) *Ocean Optics Protocols for Satellite Ocean Color Sensor Validation, Revision 4, Volume VNASA/TM-2003-211621*. Greenbelt, Maryland: NASA Goddard Space Flight Center, pp. 5–14.

Bidigare, R. R., Van Heukelem, L. and Trees, C. C. (2005) 'Analysis of algal pigments by high-performance liquid chromatography', in Andersen, R. A. (ed.) *Algal Culturing Techniques*. New York, USA: Academic Press, pp. 432–435.

Bidigare, R. R., Ondrusek, M. E., Morrow, J. . and Kiefer, D. A. (1990) '*In vivo* absorption properties of algal pigments', *SPIE Proceedings 1302, Ocean Optics X*, 290, pp. 290–302.

Bidigare, R. R., Schofield, O. and Prézelin, B. B. (1989) 'Influence of zeaxanthin on quantum yield of photosynthesis of *Synechococcus* clone WH7803 (DC2)', *Marine Ecology Progress Series*, 56, pp. 177–188.

Biller, S. J., Berube, P. M., Lindell, D. and Chisholm, S. W. (2015) '*Prochlorococcus*: the structure and function of collective diversity', *Nature Reviews Microbiology*, 13(1), pp. 13–27.

Binder, B. J., Chisholm, S. W., Olson, R. J., Frankel, S. L. and Worden, A. Z. (1996) 'Dynamics of picophytoplankton, ultraphytoplankton and bacteria in the central equatorial Pacific', *Deep-Sea Research Part II: Topical Studies in Oceanography*, 43(4–6), pp. 907–931.

Bird, C. and Wyman, M. (2003) 'Nitrate/nitrite assimilation system of the marine picoplanktonic cyanobacterium *Synechococcus* sp. Strain WH 8103: effect of nitrogen source and availability on gene expression', *Applied and Environmental Microbiology*, 69(12), pp. 7009–7018.

Blain, S., Bonnet, S. and Guieu, C. (2008) 'Dissolved iron distribution in the tropical and sub tropical South Eastern Pacific', *Biogeosciences*, 5, pp. 269–280.

Blanchot, J., André, J. M., Navarette, C., Neveux, J. and Radenac, M. H. (2001) 'Picophytoplankton in the equatorial pacific: vertical distributions in the warm pool and in the high nutrient low chlorophyll conditions', *Deep-Sea Research Part I: Oceanographic Research Papers*, 48(1), pp. 297–314.

Blanchot, J. and Rodier, M. (1996) 'Picophytoplankton abundance and biomass in the western tropical Pacific Ocean during the 1992 El Nino year: results from flow cytometry', *Deep-Sea Research Part I: Oceanographic Research Papers*, 43(6), pp. 877–895.

Bouman, H. A. (1998) *Photosynthetic and Optical Properties of Subtropical North Atlantic Phytoplankton*. Dalhousie University.

Bouman, H. A., Platt, T., Doblin, M., Figueiras, F. G., Gudmundsson, K., Gudfinnsson, H. G., Huang, B., Hickman, A. E., Hiscock, M. R., Jackson, T., Lutz, V. A., Mélin, F., Rey, F., Pepin, P., Segura, V., Tilstone, G. H., Van Dongen-Vogels, V. and Sathyendranath, S. (2018) 'Photosynthesis-irradiance parameters of marine phytoplankton: synthesis of a global data set', *Earth System Science Data*, 10(1), pp. 251–266.

Bouman, H. A., Platt, T., Kraay, G. W., Sathyendranath, S. and Irwin, B. D. (2000) 'Bio-optical properties of the subtropical North Atlantic. I. Vertical variability', *Marine Ecology Progress Series*, 200, pp. 3–18.

Bouman, H. A., Platt, T., Sathyendranath, S., Irwin, B. D., Wernand, M. R. and Kraay, G. W. (2000) 'Bio-optical properties of the subtropical North Atlantic. II. Relevance to models of primary production', *Marine Ecology Progress Series*, 200, pp. 19–34.

Bouman, H. A., Platt, T., Sathyendranath, S., Li, W. K. W., Stuart, V., Fuentes-Yaco, C., Maass, H., Horne, E. P. W., Ulloa, O., Lutz, V. A. and Kyewalyanga, M. (2003) 'Temperature as indicator of optical properties and community structure of marine phytoplankton: implications for remote sensing', *Marine Ecology Progress Series*, 258, pp. 19–30.

Bouman, H. A., Platt, T., Sathyendranath, S. and Stuart, V. (2005) 'Dependence of light-saturated photosynthesis on temperature and community structure', *Deep-Sea Research Part I: Oceanographic Research Papers*, 52(7), pp. 1284–1299.

Bouman, H. A., Ulloa, O., Barlow, R. G., Li, W. K. W., Platt, T., Zwirglmaier, K., Scanlan, D. J. and Sathyendranath, S. (2011) 'Water-column stratification governs the community structure of subtropical marine picophytoplankton', *Environmental Microbiology Reports*, 3(4), pp. 473–482.

Bouman, H. A., Ulloa, O., Scanlan, D. J., Zwirglmaier, K., Li, W. K. W., Platt, T., Stuart, V., Barlow, R. G., Leth, O., Clementson, L. A., Lutz, V. A., Fukasawa, M., Watanabe, S. and Sathyendranath, S. (2006) 'Oceanographic basis of the global surface distribution of *Prochlorococcus* ecotypes', *Science*, 312(5775), pp. 918–21.

Boyd, P. W., Rynearson, T. A., Armstrong, E. A., Fu, F., Hayashi, K., Hu, Z., Hutchins, D. A., Kudela, R. M., Litchman, E., Mulholland, M. R., Passow, U., Strzepek, R. F., Whittaker, K. A., Yu, E. and Thomas, M. K. (2013) 'Marine phytoplankton temperature versus growth responses from polar to tropical waters – outcome of a scientific community-wide study', *PLoS ONE*, 8(5).

Boyd, P. W., Strzepek, R., Fu, F. and Hutchins, D. A. (2010) 'Environmental control of open-ocean phytoplankton groups: Now and in the future', *Limnology and Oceanography*, 55(3), pp. 1353–1376.

Brewin, R. J. W., Devred, E., Sathyendranath, S., Lavender, S. J. and Hardman-Mountford, N. J. (2011) 'Model of phytoplankton absorption based on three size classes', *Applied Optics*, 50(22), pp. 4535–4549.

Brewin, R. J. W., Sathyendranath, S., Jackson, T., Barlow, R. G., Brotas, V., Airs, R. L. and Lamont, T. (2015) 'Influence of light in the mixed-layer on the parameters of a three-component model of phytoplankton size class', *Remote Sensing of Environment*, 168, pp. 437–450.

Bricaud, A., Babin, M., Claustre, H., Ras, J. and Tièche, F. (2010) 'Light absorption properties and absorption budget of Southeast Pacific waters', *Journal of Geophysical Research*, 115(C8).

Bricaud, A., Babin, M., Morel, A. and Claustre, H. (1995) 'Variability in the chlorophyll-specific absorption coefficients of natural phytoplankton: analysis and parameterization', *Journal of Geophysical Research*, 100, pp. 13321–13332.

Bricaud, A., Claustre, H., Ras, J. and Oubelkheir, K. (2004) 'Natural variability of phytoplanktonic absorption in oceanic waters: influence of the size structure of algal populations', *Journal of Geophysical Research: Oceans*, 109(11), pp. 1–12.

Bricaud, A. and Stramski, D. (1990) 'Spectral absorption coefficients of living phytoplankton and nonalgal biogenous matter: a comparison between the Peru upwelling area and the Sargasso Sea', *Limnology and Oceanography*, 35(3), pp. 562–582.

Brown, M. and Wittwer, C. (2000) 'Flow cytometry: principles and clinical applications in hematology', *Clinical Chemistry*, 46(8), pp. 1221–1229.

Browning, T. J., Bouman, H. A. and Moore, C. M. (2014) 'Satellite-detected fluorescence: decoupling nonphotochemical quenching from iron stress signals in the South Atlantic and Southern Ocean', *Global Biogeochemical Cycles*, 28, pp. 510–524.

Brunet, C., Johnsen, G., Lavaud, J. and Roy, S. (2011) 'Pigments and photoacclimation processes', in Roy, S., Llewellyn, C. A., Egeland, E. S., and Johnsen, G. (eds) *Phytoplankton*

Pigments: Characterization, Chemotaxonomy and Application in Oceanography. Cambridge University Press, pp. 465–471.

Bruyant, F., Babin, M., Genty, B., Prasil, O., Behrenfeld, M. J., Claustre, H., Bricaud, A., Garczarek, L., Holtzendorff, J., Koblizek, M., Dousova, H. and Partensky, F. (2005) 'Diel variations in the photosynthetic parameters of *Prochlorococcus* strain PCC 9511: combined effects of light and cell cycle', *Limnology and Oceanography*, 50(3), pp. 850–863.

Buck, K. R., Chavez, F. P. and Campbell, L. (1996) 'Basin-wide distributions of living carbon components and the inverted trophic pyramid of the central gyre of the North Atlantic Ocean, summer 1993', *Aquatic Microbial Ecology*, 10(3), pp. 283–298.

Buitenhuis, E. T., Li, W. K. W., Vaulot, D., Lomas, M. W., Landry, M. R., Partensky, F., Karl, D. M., Ulloa, O., Campbell, L., Jacquet, S., Lantoine, F., Chavez, F. P., MacIas, D., Gosselin, M. and McManus, G. B. (2012) 'Picophytoplankton biomass distribution in the global ocean', *Earth System Science Data*, 4(1), pp. 37–46.

Butcher, R. W. (1952) 'Contributions to our knowledge of the smaller marine algae', *Journal of the Marine Biological Association of the United Kingdom*, 31(1), pp. 175–191.

Cailliau, C., Claustre, H., Vidussi, F., Marie, D. and Vaulot, D. (1996) 'Carbon biomass, and gross growth rates as estimated from 14C pigment labelling, during photoacclimation in Prochlorococcus CCMP 1378', *Marine Ecology Progress Series*, 145, pp. 209–221.

Campbell, L., Nolla, H. A. and Vaulot, D. (1994) 'The importance of *Prochlorococcus* to community structure in the central North Pacific Ocean', *Limnology and Oceanography*, 39(4), pp. 954–961.

Campbell, L. and Vaulot, D. (1993) 'Photosynthetic picoplankton community structure in the subtropical North Pacific Ocean near Hawaii (station ALOHA)', *Deep-Sea Research Part I: Oceanographic Research Papers*, 40(10), pp. 2043–2060.

Casey, J. R., Lomas, M. W., Mandecki, J. and Walker, D. E. (2007) '*Prochlorococcus* contributes to new production in the Sargasso Sea deep chlorophyll maximum', *Geophysical Research Letters*, 37(10).

Cermeño, P., Dutkiewicz, S., Harris, R. P., Follows, M. J., Schofield, O. M. and Falkowski, P. G. (2008) 'The role of nutricline depth in regulating the ocean carbon cycle', *Proceedings of the National Academy of Sciences of the United States of America*, 105(51), pp. 20344–20349.

Chakraborty, S., Lohrenz, S. E. and Gundersen, K. (2017) 'Photophysiological and light absorption properties of phytoplankton communities in the river-dominated margin of the northern Gulf of Mexico', *Journal of Geophysical Research: Oceans*, 122(6), pp. 4922–4938.

Charlson, R. J., Lovelock, J. E., Andreae, M. O. and Warren, S. G. (1987) 'Oceanic phytoplankton, atmospheric sulphur, cloud albedo and climate', *Nature*, 326, pp. 655–661.

Cheah, W., McMinn, A., Griffiths, F. B., Westwood, K. J., Wright, S. W. and Clementson, L. A. (2013) 'Response of phytoplankton photophysiology to varying environmental conditions in the Sub-Antarctic and Polar Frontal Zone', *PLoS ONE*, 8(8).

Chisholm, S. W. (1992) 'Phytoplankton size', in Falkowski, P. G., Woodhead, A. D., and Vivirito, K. (eds) *Primary Productivity and Biogeochemical Cycles in the Sea*. Boston, USA: Springer, pp. 213–237.

Chisholm, S. W., Olson, R. J., Zettler, E. R., Goericke, R., Waterbury, J. B. and Welschmeyer, N. A. (1988) 'A novel free-living prochlorophyte abundant in the oceanic euphotic zone', *Nature*, 334(6180), pp. 340–343.

Ciotti, Á. M., Lewis, M. R. and Cullen, J. J. (2002) 'Assessment of the relationships between dominant cell size in natural phytoplankton communities and the spectral shape of the absorption coefficient', *Limnology and Oceanography*, 47(2), pp. 404–417.

Claustre, H. (1994) 'The trophic status of various oceanic provinces as revealed by phytoplankton pigment signatures', *Limnology and Oceanography*, 39(5), pp. 1206–1210.

Claustre, H., Bricaud, A., Babin, M., Bruyant, F., Guillou, L., Le Gall, F., Marie, D. and Partensky, F. (2002) 'Diel variations in *Prochlorococcus* optical properties', *Limnology and Oceanography*, 47(6), pp. 1637–1647.

Claustre, H., Kerhervé, P., Marty, J.-C. and Prieur, L. (1994) 'Phytoplankton photoadaptation related to some frontal physical processes', *Journal of Marine Systems*, 5(3–5), pp. 251–265.

Claustre, H. and Marty, J.-C. (1995) 'Specific phytoplankton biomasses and their relation to primary production in the tropical North Atlantic', *Deep-Sea Research Part I: Oceanographic Research Papers*, 42(8), pp. 1475–1493.

Claustre, H., Sciandra, A. and Vaulot, D. (2008) 'Introduction to the special section bio-optical and biogeochemical conditions in the South East Pacific in late 2004: the BIOSOPE program', *Biogeosciences*, 5, pp. 679–691.

Cleveland, J. S., Perry, M. J., Kiefer, D. A. and Talbot, M. C. (1989) 'Maximal quantum yield of photosynthesis in the northwestern Sargasso Sea', *Journal of Marine Research*, 47, pp. 869–886.

Cleveland, J. S. and Weidemann, A. D. (1993) 'Quantifying absorption by aquatic particles: a multiple scattering correction for glass-fiber filters', *Limnology and Oceanography*, 38, pp. 1321–1327.

Coleman, M. L. and Chisholm, S. W. (2007) 'Code and context: *Prochlorococcus* as a model for cross-scale biology', *Trends in Microbiology*, 15(9), pp. 398–407.

Collier, J. L., Brahamsha, B. and Palenik, B. (1999) 'The marine cyanobacterium *Synechococcus* sp. WH7805 requires urease (urea amidohydrolase, EC 3.5.1.5) to utilize urea as a nitrogen source: molecular-genetic and biochemical analysis of the enzyme', *Microbiology*, 145(2), pp. 447–459.

Corhlan, W. P. and Harrison, P. J. (1991) 'Uptake of nitrate, ammonium, and urea by nitrogen-straved cultures of *Micromonas pusilla* (Prasinophyceae): transient responses', *Journal of Phycology*, 27(6), pp. 673–679.

Corripio, J. G. (2019) 'Solar Radiation'. Available at: https://meteoexploration.com/R/insol/index.html.

Coutinho, F., Tschoeke, D. A., Thompson, F. and Thompson, C. (2016) 'Comparative genomics of *Synechococcus* and proposal of the new genus *Parasynechococcus*', *PeerJ*, 2016(1).

Cullen, J. J., Franks, P. J. S., Karl, D. M. and Longhurst, A. R. (2002) 'Physical influences on marine ecosystem dynamics', in Robinson, A. R., McCarthy, J. J., and Rothschild, B. J. (eds) *The Sea*. New York, USA: John Willey & Sons, pp. 297–336.

Cullen, J. J., Stewart, E., Renger, E., Eppley, R. W. and Winant, C. D. (1983) 'Vertical motion of the thermocline, nitracline and chlorophyll maximum layers in relation to currents on the Southern California Shelf', *Journal of Marine Research*, 41, pp. 239–262.

Cuvelier, M. L., Allen, A. E., Monier, A., Mccrow, J. P., Messié, M., Tringe, S. G., Woyke, T., Welsh, R. M., Ishoey, T., Lee, J.-H., Binder, B. J., Dupont, C. L., Latasa, M., Guigand, C., Buck, K. R., Hilton, J., Thiagarajan, M., Caler, E., Read, B., Lasken, R. S., Chavez, F. P., Worden, A. Z. and Karl, D. M. (2010) 'Targeted metagenomics and ecology of globally important uncultured eukaryotic phytoplankton', *Proceedings of the National Academy of Sciences of the United States of America*, 107, pp. 14679–14684.

Demmig-Adams, B. (1990) 'Carotenoids and photoprotection in plants: a role for the xanthophyll zeaxanthin', *Biochimica et Biophysica Acta*, pp. 1–24.

Devred, E., Sathyendranath, S., Stuart, V. and Platt, T. (2011) 'A three component classification of phytoplankton absorption spectra: application to ocean-color data', *Remote Sensing of Environment*, 115(9), pp. 2255–2266.

Dimier, C., Giovanni, S., Ferdinando, T. and Brunet, C. (2009) 'Comparative ecophysiology of the xanthophyll cycle in six marine phytoplanktonic species', *Protist*, 160(3), pp. 397–411.

Dubinsky, Z., Falkowski, P. G. and Wyman, K. (1986) 'Light harvesting and utilization by phytoplankton', *Plant Cell Physiology*, 27(7), pp. 1335–1349.

Dubinsky, Z. and Stambler, N. (2009) 'Photoacclimation processes in phytoplankton: mechanisms, consequences, and applications', *Aquatic Microbial Ecology*, 56, pp. 163–176.

DuRand, M. D., Olson, R. J. and Chisholm, S. W. (2001) 'Phytoplankton population dynamics at the Bermuda Atlantic Time-series station in the Sargasso Sea', *Deep-Sea Research Part II: Topical Studies in Oceanography*, 48(8–9), pp. 1983–2003.

Dusenberry, J. A., Olson, R. J. and Chisholm, S. W. (1999) 'Frequency distributions of phytoplankton single-cell fluorescence and vertical mixing in the surface ocean', *Limnology and Oceanography*, 44(2), pp. 431–435.

Duyens, L. N. M. (1956) 'The flattering of the absorption spectrum of suspensions, as compared to that of solutions', *Biochimica et Biophysica Acta*, 19, pp. 1–12.

Eisner, L. B., Twardowski, M. S., Cowles, T. J. and Perry, M. J. (2003) 'Resolving phytoplankton photoprotective : photosynthetic carotenoid ratios on fine scales using in situ spectral absorption measurements', *Limnology and Oceanography*, 48(2), pp. 632–646.

van den Engh, G. J., Doggett, J. K., Thompson, A. W., Doblin, M. A., Gimpel, C. N. G. and Karl, D. M. (2017) 'Dynamics of *Prochlorococcus* and *Synechococcus* at station ALOHA revealed through flow cytometry and high-resolution vertical sampling', *Frontiers in Marine Science*, 4(359).

Eppley, R. W., Renger, E. H. and Harrison, W. G. (1979) 'Nitrate and phytoplankton production in southern California', *Limnology and Oceanography*, 24(3), pp. 483–494.

Falkowski, P. G. (1981) 'Light-shade adaptation and assimilation numbers', *Journal of Plankton Research*, 3(2), pp. 203–216.

Falkowski, P. G. (1983) 'Light-shade adaptation and vertical mixing of marine phytoplankton: a comparative field study', *Journal of Marine Research*, 41, pp. 215–237.

Falkowski, P. G. (1994) ‘The role of phytoplankton photosynthesis in global biogeochemical cycles’, *Photosynthesis Research*, 39(3), pp. 235–258.

Falkowski, P. G., Barber, R. T. and Smetacek, V. (1998) ‘Biogeochemical controls and feedbacks on ocean primary production’, *Science*, 281(5374), pp. 200–206.

Falkowski, P. G. and LaRoche, J. (1991) ‘Acclimation to spectral irradiance in algae’, *Journal of Phycology*, 27(1), pp. 8–14.

Falkowski, P. G. and Owens, T. G. (1980) ‘Light-shade adaptation: two strategies in marine phytoplankton’, *Plant Physiology*, 66(4), pp. 592–595.

Falkowski, P. G. and Raven, J. A. (2007) *Aquatic Photosynthesis*. 2nd edn. Princeton University Press.

Falkowski, P. G., Scholes, R. J., Boyle, E., Canadell, J., Canfield, D., Elser, J., Gruber, N., Hibbard, K., Hogberg, P., Linder, S., Mackenzie, F. T., Moore, B., Pedersen, T., Rosental, Y., Seitzinger, S., Smetacek, V. and Steffen, W. (2000) ‘The global carbon cycle: a test of our knowledge of earth as a system’, *Science*, 290(5490), pp. 291–296.

Falkowski, P. G., Žek, M. K., Gorbunov, M. Y. and Kolber, Z. (2004) ‘Development and application of variable chlorophyll fluorescence techniques in marine ecosystems’, in Papageorgiou, G. C. and Govindjee (eds) *Chlorophyll a Fluorescence : A Signature of Photosynthesis*. The Netherlands: Springer, p. 819.

Fanesi, A., Wagner, H. and Wilhelm, C. (2017) ‘Phytoplankton growth rate modelling: can spectroscopic cell chemotyping be superior to physiological predictors?’, *Proceedings of the Royal Society B: Biological Sciences*, 284(1848).

Fawcett, S. E., Lomas, M. W., Casey, J. R., Ward, B. B. and Sigman, D. M. (2011) ‘Assimilation of upwelled nitrate by small eukaryotes in the Sargasso Sea’, *Nature Geoscience*, 4(10), pp. 717–722.

Fernández, A., Mour No-Carballido, B., Bode, A., Varela, M. and Marañón, E. (2010) ‘Latitudinal distribution of *Trichodesmium* spp. and N_2 fixation in the Atlantic Ocean’, *Biogeosciences*, 7, pp. 3167–3176.

Ferreira, A., Ciotti, Á. M., Mendes, C. R. B., Uitz, J. and Bricaud, A. (2017) ‘Phytoplankton light absorption and the package effect in relation to photosynthetic and photoprotective pigments in the northern tip of Antarctic Peninsula’, *Journal of Geophysical Research: Oceans*, 122, pp. 7344–7363.

Ferreira, A., Stramski, D., Garcia, C. A. E., Garcia, V. M. T., Ciotti, Á. M. and Mendes, C. R. B. (2013) ‘Variability in light absorption and scattering of phytoplankton in Patagonian waters: role of community size structure and pigment composition’, *Journal of Geophysical Research: Oceans*, 118.

Field, C. B., Behrenfeld, M. J., Randerson, J. T. and Falkowski, P. G. (1998) ‘Primary production of the biosphere: integrating terrestrial and oceanic components’, *Science*, 281(5374), pp. 237–240.

Finkel, Z. V., Beardall, J., Flynn, K. J., Quigg, A., Rees, T. A. V and Raven, J. A. (2010) ‘Phytoplankton in a changing world: cell size and elemental stoichiometry’, *Journal of Plankton Research*, 32(1), pp. 119–137.

Flombaum, P., Gallegos, J. L., Gordillo, R. a, Rincón, J., Zabala, L. L., Jiao, N., Karl, D. M., Li, W. K. W., Lomas, M. W., Veneziano, D., Vera, C. S., Vrugt, J. A. and Martiny, A. C. (2013) 'Present and future global distributions of the marine cyanobacteria *Prochlrococcus* and *Synechococcus*', *Proceedings of the National Academy of Sciences*, 110(24), pp. 9824–9829.

Fogg, G. E. (1986) 'Picoplankton', *Proceedings of the Royal Society of London B: Biological Science*, 228(1250), pp. 1–30.

Frouin, R. J. and Iacobellis, S. F. (2002) 'Influence of phytoplankton on the global radiation budget', *Journal of Geophysical Research*, 107(D19).

Fujieki, L. A., Santiago-Mandujano, F., Deppe, W., McCoy, R. and Church, M. J. (2016) *Hawaii Ocean Time-series Data Report 26: 2014*. Honolulu, Hawaii.

Fujiki, T., Toda, T., Kikuchi, T. and Taguchi, S. (2003) 'Photoprotective response of xanthophyll pigments during phytoplankton blooms in Sagami Bay, Japan', *Journal of Plankton Research*, 25(3), pp. 317–322.

Fujita, Y., Ohki, K. and Murakami, A. (1985) 'Chromatic regulation of photosystem composition in the photosynthetic system of red and blue-green algae', *Plant and Cell Physiology*, 26(8), pp. 1541–1548.

Fuller, N. J., Marie, D., Partensky, F., Vaulot, D., Post, A. F. and Scanlan, D. J. (2003) 'Clade-specific 16S ribosomal DNA oligonucleotides reveal the predominance of a single marine *Synechococcus* clade throughout a stratified water column in the Red Sea', *Applied and Environmental Microbiology*, 69(5), pp. 2430–2443.

Garczarek, L., Hess, W. R., Holtzendorff, J., van der Staay, G. W. M. and Partensky, F. (2000) 'Multiplication of antenna genes as a major adaptation to low light in a marine prokaryote', *Proceedings of the National Academy of Sciences of the United States of America*, 97(8), pp. 4098–4101.

Garrido, J. L., Airs, R. L., Rodríguez, F., Van Heukelem, L. and Zapata, M. (2011) 'New HPLC separation techniques', in Roy, S., Llewellyn, C. A., Egeland, E. S., and Johnsen, G. (eds) *Phytoplankton Pigments: Characterization, Chemotaxonomy and Application in Oceanography*. Cambridge, UK: Cambridge University Press, pp. 165–194.

Geider, R. J. (1987) 'Light and temperature dependence of the carbon to chlorophyll a ratio in microalgae and cyanobacteria: implications for physiology and growth of phytoplankton', *New Phytologist*, 106(1), pp. 1–34.

Geider, R. J. (1993) 'Quantitative phytoplankton physiology: implications for primary production and phytoplankton growth', *ICES Marine Science Symposia*, 197, pp. 52–62.

Geider, R. J., MacIntyre, H. L. and Kana, T. M. (1996) 'A dynamic-model of photoadaptation in phytoplankton', *Limnology and Oceanography*, 41(1), pp. 1–15.

Geider, R. J., MacIntyre, H. L. and Kana, T. M. (1997) 'Dynamic model of phytoplankton growth and acclimation: responses of the balanced growth rate and the chlorophyll a:carbon ratio to light, nutrient-limitation and temperature', *Marine Ecology Progress Series*, 148, pp. 187–200.

Geider, R. J., La Roche, J., Greene, R. M. and Olaizola, M. (1993) 'Response of the photosynthetic apparatus of *Phaeodactylum tricornatum* (Bacillariophycea) to nitrate, phosphate, or iron starvation', *Journal of Phycology*, 29(6), pp. 755–766.

Gibb, S. W., Barlow, R. G., Cummings, D. G., Rees, N. ., Trees, C. C., Holligan, P. M. and Suggett, D. (2000) 'Surface phytoplankton pigment distributions in the Atlantic Ocean: an assessment of basin scale variability between 50°N and 50°S', *Progress in Oceanography*, 45(3–4), pp. 339–368.

Gibb, S. W., Cummings, D. G., Irigoien, X., Barlow, R. G., Fauzi, R. and Mantoura, C. (2001) 'Phytoplankton pigment chemotaxonomy of the northeastern Atlantic', *Deep-Sea Research Part II: Topical Studies in Oceanography*, 48(4–5), pp. 795–823.

Gieskes, W. W. C., Kraay, G. W., Nontji, A., Setiapermana, D. and Sutomo (1988) 'Monsoonal alternation of a mixed and a layered structure in the phytoplankton of the euphotic zone of the banda sea (Indonesia): a mathematical analysis of algal pigment fingerprints', *Netherlands Journal of Sea Research*, 22(2), pp. 123–137.

Goericke, R. and Repeta, D. J. (1992) 'The pigments of *Prochlorococcus marinus*: the presence of divinyl chlorophyll a and b in a marine procaryote', *Limnology and Oceanography*, 37(2), pp. 425–433.

Goericke, R. and Welschmeyer, N. A. (1993) 'The marine prochlorophyte *Prochlorococcus* contributes significantly to phytoplankton biomass and primary production in the Sargasso Sea', *Deep-Sea Research Part I: Oceanographic Research Papers*, 40(11–12), pp. 2283–2294.

Goldman, J. C. (1980) 'Physiological processes, nutrient availability, and the concept of relative growth rate in marine phytoplankton ecology', in Falkowski, P. G. (ed.) *Primary Productivity in the Sea*. Springer, pp. 179–194.

Graff, J. R., Westberry, T. K., Milligan, A. J., Brown, M. B., Dall'Olmo, G., van Dongen-Vogels, V., Reifel, K. M. and Behrenfeld, M. J. (2015) 'Analytical phytoplankton carbon measurements spanning diverse ecosystems', *Deep-Sea Research Part I: Oceanographic Research Papers*, 102, pp. 16–25.

Graff, J. R., Westberry, T. K., Milligan, A. J., Brown, M. B., Dall'Olmo, G., Reifel, K. M. and Behrenfeld, M. J. (2016) 'Photoacclimation of natural phytoplankton communities', *Marine Ecology Progress Series*, 542, pp. 51–62.

de Grazia, A. (2015) *A Raman Flow Cytometer*. King Abdullah University of Science and Technology.

Grébert, T., Doré, H., Partensky, F., Farrant, G. K., Boss, E. S., Picheral, M., Guidi, L., Pesant, S., Scanlan, D. J., Wincker, P., Acinas, S. G., Kehoe, D. M. and Garczarek, L. (2018) 'Light color acclimation is a key process in the global ocean distribution of *Synechococcus* cyanobacteria', *Proceedings of the National Academy of Sciences*, 115(9), pp. E2010–E2019.

Greene, R. M., Geider, R. J. and Falkowski, P. G. (1991) 'Effect of iron limitation on photosynthesis in a marine diatom', *Limnology and Oceanography*, 36(8), pp. 1772–1782.

Greene, R. M., Geider, R. J., Kolber, Z. and Falkowski, P. G. (1992) 'Iron-induced changes in light harvesting and photochemical energy-conversion processes in eukaryotic marine algae', *Plant Physiology*, 100, pp. 565–575.

Grob, C., Ulloa, O., Claustre, H., Huot, Y., Alarcón, G. and Marie, D. (2007) 'Contribution of picoplankton to the total particulate organic carbon (POC) concentration in the eastern South Pacific', *Biogeosciences*, 4, pp. 837–852.

Grob, C., Ulloa, O., Li, W. K. W., Alarcón, G., Fukasawa, M. and Watanabe, S. (2007) 'Picoplankton abundance and biomass across the eastern South Pacific Ocean along latitude 32.5°S', *Marine Ecology Progress Series*, 332, pp. 53–62.

Grossman, A. R., Schaefer, M. R., Chiang, G. G. and Collier, J. L. (1993) 'The phycobilisome, a light-harvesting complex responsive to environmental conditions', *Microbiological Reviews*, pp. 725–749.

Halsey, K. H. and Jones, B. M. (2015) 'Phytoplankton strategies for photosynthetic energy allocation', *Annual Review of Marine Science*, 7(1), pp. 265–297.

Halsey, K. H., Milligan, A. and Behrenfeld, M. J. (2014) 'Contrasting strategies of photosynthetic energy utilization drive lifestyle strategies in ecologically important picoeukaryotes', *Metabolites*, 4(2), pp. 260–280.

Hammer, A. C. and Pitchford, J. W. (2005) 'The role of mixotrophy in plankton bloom dynamics, and the consequences for productivity', *ICES Journal of Marine Science*, 62(5), pp. 833–840.

Harrison, W. G. and Platt, T. (1986) 'Photosynthesis-irradiance relationships in polar and temperate phytoplankton populations', *Polar Biology*, 5, pp. 153–164.

Hartmann, M., Gomez-Pereira, P., Grob, C., Ostrowski, M., Scanlan, D. J. and Zubkov, M. V. (2014) 'Efficient CO_2 fixation by surface *Prochlorococcus* in the Atlantic Ocean', *The ISME Journal*, 8(11), pp. 2280–2289.

He, Q., Dolganov, N., Björkman, O. and Grossman, A. R. (2001) 'The high light-inducible polypeptides in *Synechocystis* PCC6803. Expression and function in high light', *Journal of Biological Chemistry*, 276, pp. 306–314.

Head, E. J. H. and Horne, E. P. W. (1993) 'Pigment transformation and vertical flux in an area of convergence in the North Atlantic', *Deep-Sea Research Part II: Topical Studies in Oceanography*, 40(1–2), pp. 329–346.

Hess, W. R., Rocap, G., Ting, C. S., Larimer, F., Stilwagen, S., Lamerdin, J. and Chisholm, S. W. (2001) 'The photosynthetic apparatus of *Prochlorococcus*: insights through comparative genomics', *Photosynthesis Research*, 70, pp. 53–71.

van Heukelem, L. and Thomas, C. S. (2001) 'Computer-assisted high performance liquid chromatography method development with applications to the isolation and analysis of phytoplankton pigments', *Journal of Chromatography A*, 910(1), pp. 31–49.

Heywood, J. L., Zubkov, M. V., Tarran, G. A., Fuchs, B. M. and Holligan, P. M. (2006) 'Prokaryoplankton standing stock in oligotrophic gyre and equatorial provinces of the Atlantic Ocean: evaluation of inter-annual variability', *Deep-Sea Research Part I: Oceanographic Research Papers*, 53, pp. 1530–1547.

Hickman, A. E. (2007) *The Photophysiology and Primary Productivity of Phytoplankton within the Deep Chlorophyll Maximum*. University of Southampton.

Hickman, A. E., Dutkiewicz, S., Williams, R. G. and Follows, M. J. (2010) 'Modelling the effects of chromatic adaptation on phytoplankton community structure in the oligotrophic ocean', *Marine Ecology Progress Series*, 406, pp. 1–17.

Hirata, T., Aiken, J., Hardman-Mountford, N. J., Smyth, T. J. and Barlow, R. G. (2008) 'An absorption model to determine phytoplankton size classes from satellite ocean colour', *Remote Sensing of Environment*, 112(6), pp. 3153–3159.

Hiscock, M. R., Lance, V. P., Apprill, A. M., Bidigare, R. R., Johnson, Z. I., Mitchell, B. G., Smith, W. O. and Barber, R. T. (2008) 'Photosynthetic maximum quantum yield increases are an essential component of the Southern Ocean phytoplankton response to iron', *Proceedings of the National Academy of Sciences of the United States of America*, 105(12), pp. 4775–4780.

Hoepffner, N. and Sathyendranath, S. (1991) 'Effect of pigment composition on absorption properties of phytoplankton', *Marine Ecology Progress Series*, 73, pp. 11–23.

Hoepffner, N. and Sathyendranath, S. (1992) 'Bio-optical characteristics of coastal waters: absorption spectra of phytoplankton and pigment distribution in the western North Atlantic', *Limnology and Oceanography*, 37(8), pp. 1660–1679.

Holm-Hansen, O., Lorenzen, C. J., Holmes, R. W. and Strickland, J. D. H. (1965) 'Fluorometric determination of chlorophyll', *ICES Journal of Marine Science*, 30(1), pp. 3–15.

Hunter, B. L. and Laws, E. A. (1981) 'ATP and chlorophyll a as estimators of phytoplankton carbon biomass', *Limnology and Oceanography*, 26(5), pp. 944–956.

Huot, Y., Babin, M., Bruyant, F., Grob, C., Twardowski, M. S. and Claustre, H. (2007) 'Relationship between photosynthetic parameters and different proxies of phytoplankton biomass in the subtropical ocean', *Biogeosciences*, 4(5), pp. 853–868.

Ichinomiya, M., Dos Santos, A. L., Gourvil, P., Yoshikawa, S., Kamiya, M., Ohki, K., Audic, S., de Vargas, C., Noël, M. H., Vaulot, D. and Kuwata, A. (2016) 'Diversity and oceanic distribution of the Parmales (Bolidophyceae), a picoplanktonic group closely related to diatoms', *The ISME Journal*, 10(10), pp. 2419–2434.

IOCCG (2008) *Why ocean colour? The societal benefits of ocean colour technology*. Edited by V. Stuart. Dartmouth, Canada.

IOCCG (2014) *Phytoplankton functional types from space*. Edited by S. Sathyendranath. Dartmouth, Canada.

Jackson, T. (2013) *Phytoplankton Community Structure, Photophysiology and Primary Production in the Atlantic Arctic*. University of Oxford.

Jakobsen, H. H. and Markager, S. (2016) 'Carbon-to-chlorophyll ratio for phytoplankton in temperate coastal waters: seasonal patterns and relationship to nutrients', *Limnology and Oceanography*, 61(5), pp. 1853–1868.

Jassby, A. D. and Platt, T. (1976) 'Mathematical formulation of the relationship between photosynthesis and light for phytoplankton', *Limnology and Oceanography*, 21(4), pp. 540–547.

Jeffrey, S. W. and Mantoura, R. F. C. (1997) 'Development of pigment methods for oceanography: SCOR-supported Working Groups and objectives', in Jeffrey, S. W., Mantoura, R. F. C., and Wright, S. W. (eds) *Phytoplankton Pigments in Oceanography: Guidelines to Modern Methods*. Paris, France: UNESCO Publishing, pp. 19–36.

Jeffrey, S. W. and Vesk, M. (1997) 'Introduction to marine phytoplankton and their pigment signatures', in Jeffrey, S. W., Mantoura, R. F. C., and Wright, S. W. (eds) *Phytoplankton Pigments in Oceanography: Guidelines to Modern Methods*. Paris, France: UNESCO Publishing, pp. 37–84.

Jeffrey, S. W., Wright, S. W. and Zapata, M. (2011) 'Microalgal classes and their signature pigments', in Roy, S., Llewellyn, C. A., Egeland, E. S., and Johnsen, G. (eds) *Phytoplankton Pigments: Characterization, Chemotaxonomy and Application in Oceanography*. Cambridge, UK: Cambridge University Press, pp. 3–45.

Johnsen, G., Norli, M., Moline, M. A., Robbins, I., von Quillfeldt, C., Sørensen, K., Cottier, F. and Berge, J. (2018) 'The advective origin of an under-ice spring bloom in the Arctic Ocean using multiple observational platforms', *Polar Biology*, 41(6), pp. 1197–1216.

Johnsen, G. and Sakshaug, E. (1996) 'Light harvesting in bloom-forming marine phytoplankton: species-specificity and photoacclimation', *Scientia Marina*, 60, pp. 47–56.

Johnsen, G., Samset, O., Granskog, L. and Sakshaug, E. (1994) '*In vivo* absorption characteristics in 10 classes of bloom-forming phytoplankton: taxonomic characteristics and responses to photoadaptation by means of discriminant and HPLC analysis', *Marine Ecology Progress Series*, 105, pp. 149–157.

Johnson, Z. I. and Lin, Y. (2009) '*Prochlorococcus*: approved for export', *Proceedings of the National Academy of Sciences of the United States of America*, 106(26), pp. 10400–10401.

Johnson, Z. I., Zinser, E. R., Coe, A., McNulty, N. P., Woodward, E. M. S. and Chisholm, S. W. (2006) 'Niche partitioning among *Prochlorococcus* ecotypes along ocean-scale environmental gradients', *Science*, 311, pp. 1737–1740.

Jones, H. L. J., Leadbeater, B. S. C. and Green, J. C. (1993) 'Mixotrophy in marine species of *Chrysochromulina* (Prymnesiophyceae): ingestion and digestion of a small green flagellate', *Journal of the Marine Biological Association of the United Kingdom*, 73, pp. 283–296.

Jonkers, L., Hillebrand, H. and Kucera, M. (2019) 'Global change drives modern plankton communities away from the pre-industrial state', *Nature*, 570(7761), pp. 372–375.

Kana, T. M. and Glibert, P. M. (1987) 'Effect of irradiances up to 2000 μE m^{-2} s^{-1} on marine *Synechococcus* WH7803—I. Growth, pigmentation, and cell composition', *Deep Sea Research Part A. Oceanographic Research Papers*, 34(4), pp. 479–495.

Kana, T. M., Glibert, P. M., Goericke, R. and Welschmeyer, N. A. (1988) 'Zeaxanthin and beta-carotene in *Synechococcus* WH7803 respond differently to irradiance', *Limnology and Oceanography*, 33(6), pp. 1623–1627.

Karl, D. M. (1999) 'A sea of change: biogeochemical variability in the North Pacific Subtropical Gyre', *Ecosystems*, 2(3), pp. 181–214.

Karl, D. M., Bidigare, R. R. and Letelier, R. M. (2001) 'Long-term changes in plankton community structure and productivity in the North Pacific Subtropical Gyre: the domain shift hypothesis', *Deep-Sea Research Part II: Topical Studies in Oceanography*, 48, pp. 1449–1470.

Karl, D. M. and Church, M. J. (2014) 'Microbial oceanography and the Hawaii Ocean Time-series programme', *Nature Reviews Microbiology*, 12, pp. 699–713.

Katayama, T., Makabe, R., Sampei, M., Hattori, H., Sasaki, H. and Taguchi, S. (2017) 'Photoprotection and recovery of photosystem II in the Southern Ocean phytoplankton', *Polar Science*, 12, pp. 5–11.

Kelly, D. E. (2018) *Oceanographic Analysis with R*. New York, USA: Spinger-Verlag.

Key, T., McCarthy, A., Campbell, D. A., Six, C., Roy, S. and Finkel, Z. V. (2010) 'Cell size trade-offs govern light exploitation strategies in marine phytoplankton', *Environmental Microbiology*, 12(1), pp. 95–104.

Kirk, J. T. O. (1975) 'A theoretical analysis of the contribution of algal cells to the attenuation of light within natural waters I. General treatment of suspensions of pigmented cells', *New Phytologist*, 75(1), pp. 11–20.

Kirk, J. T. O. (2011) *Light and Photosynthesis in Aquatic Ecosystems*. 3rd edn. Cambridge, UK: Cambridge University Press.

Kirkham, A. R., Jardillier, L. E., Tiganescu, A., Pearman, J., Zubkov, M. V. and Scanlan, D. J. (2011) 'Basin-scale distribution patterns of photosynthetic picoeukaryotes along an Atlantic Meridional Transect', *Environmental Microbiology*, 13(4), pp. 975–990.

Kirkham, A. R., Lepère, C., Jardillier, L. E., Not, F., Bouman, H. A., Mead, A. and Scanlan, D. J. (2013) 'A global perspective on marine photosynthetic picoeukaryote community structure', *The ISME journal*, 7(5), pp. 922–36.

Kishino, M., Takahashi, M., Okami, N. and Ichimura, S. (1985) 'Estimation of the spectral absorption coefficients of phytoplankton in the sea', *Bulletin of Marine Science*, 37(2), pp. 634–642.

Koenker, R. and Bassett, G. (1978) 'Regression quantiles', *Econometrica*, 46, pp. 33–50.

Kolber, Z., Wyman, K. V. and Falkowski, P. G. (1990) 'Natural variability in photosynthetic energy conversion efficiency: a field study in the Gulf of Maine', *Limnology and Oceanography*, 35(1), pp. 72–79.

Kolber, Z., Zehr, J. and Falkowski, P. G. (1988) 'Effects of growth irradiance and nitrogen limitation on photosynthetic energy conversion in photosystem II', *Plant Physiology*, 88(3), pp. 923–929.

Kraay, G. W., Zapata, M. and Veldhuis, M. J. W. (1992) 'Separation of chlorophylls c_1, c_2, and c_3 of marine phytoplankton by reversed-phase-C18-high-performance liquid chromatography', *Journal of Phycology*, 28(5), pp. 708–712.

Kremp, A., Tamminen, T. and Spilling, K. (2008) 'Dinoflagellate bloom formation in natural assemblages with diatoms: nutrient competition and growth strategies in Baltic spring phytoplankton', *Aquatic Microbial Ecology*, 50(2), pp. 181–196.

Ku, H. H. (1966) 'Notes on the use of propagation of error formulas', *Journal of Research of the National Bureau of Standards - C. Engineering and Instrumentation*, 70(4), pp. 263–273.

Kulk, G., de Poll, W. H. van, Visser, R. J. W. and Buma, A. G. J. (2011) 'Distinct differences in photoacclimation potential between prokaryotic and eukaryotic oceanic phytoplankton', *Journal of Experimental Marine Biology and Ecology*, 398(1–2), pp. 63–72.

Landry, M. R., Kirshtein, J. and Constantinou, J. (1995) 'A refined dilution technique for measuring the community grazing impact of microzooplankton, with experimental tests in the central equatorial Pacific', *Marine Ecology Progress Series*, 120, pp. 53–63.

Lange, P. K., Brewin, R. J. W., Dall'Olmo, G., Tarran, G. A., Sathyendranath, S., Zubkov, M. V. and Bouman, H. A. (2018) 'Scratching beneath the surface: a model to predict the vertical distribution of *Prochlorococcus* using remote sensing', *Remote Sensing*, 10(6), p. 847.

Latifi, A., Ruiz, M. and Zhang, C.-C. (2009) ‘Oxidative stress in cyanobacteria’, *FEMS Microbiology Reviews*, 33, pp. 258–278.

Lavaud, J. (2007) ‘Fast regulation of photosynthesis in diatoms: mechanisms, evolution and ecophysiology’, *Functional Plant Science and Biotechnology*, 1, pp. 267–287.

Lawrenz, E., Silsbe, G., Capuzzo, E., Ylöstalo, P., Forster, R. M., Simis, S. G. H., Prášil, O., Kromkamp, J. C., Hickman, A. E., Moore, C. M., Forget, M. H., Geider, R. J. and Suggett, D. J. (2013) ‘Predicting the electron requirement for carbon fixation in seas and cceans’, *PLoS ONE*, 8(3).

Laws, E. A. (2013) ‘Evaluation of *in situ* phytoplankton growth rates: a synthesis of data from varied approaches’, *Annual Review of Marine Science*, 5, pp. 247–268.

Lazzara, L., Bricaud, A. and Claustre, H. (1996) ‘Spectral absorption and fluorescence excitation properties of phytoplanktonic populations at a mesotrophic and an oligotrophic site in the tropical North Atlantic (EUMELI program)’, *Deep-Sea Research Part I: Oceanographic Research Papers*, 43(8), pp. 1215–1240.

Lehmuskero, A., Skogen Chauton, M. and Boström, T. (2018) ‘Light and photosynthetic microalgae: a review of cellular- and molecular-scale optical processes’, *Progress in Oceanography*, 168, pp. 43–56.

Letelier, R. M., White, A. E., Bidigare, R. R., Barone, B., Church, M. J. and Karl, D. M. (2017) ‘Light absorption by phytoplankton in the North Pacific Subtropical Gyre’, *Limnology and Oceanography*, 62, pp. 1526–1540.

Lewis, M. R., Cullen, J. J. and Platt, T. (1984) ‘Relationships between vertical mixing and photoadaptation of phytoplankton: similarity criteria’, *Marine Ecology Progress Series*, 15, pp. 141–149.

Li, W. K. W. (1989) ‘Shipboard analytical flow cytometry of oceanic ultraphytoplankton’, *Cytometry*, 10(5), pp. 564–579.

Li, W. K. W. (1994) ‘Primary production of prochlorophytes, cyanobacteria, and eukaryotic ultraphytoplankton: measurements from flow cytometric sorting’, *Limnology and Oceanography*, 39(1), pp. 169–175.

Li, W. K. W. (1995) ‘Composition of ultraphytoplankton in the central North Atlantic’, *Marine Ecology Progress Series*, 122, pp. 1–8.

Li, W. K. W., Dickie, P. M., Irwin, B. D. and Wood, A. M. (1992) ‘Biomass of bacteria, cyanobacteria, prochlorophytes and photosynthetic eukaryotes in the Sargasso Sea’, *Deep-Sea Research Part A. Oceanographic Research Papers*, 39(3–4), pp. 501–519.

Li, W. K. W., Jellett, J. F. and Dickie, P. M. (1995) ‘DNA distributions in planktonic bacteria stained with TOTO or TO-PRO’, *Limnology and Oceanography*, 40(8), pp. 1485–1495.

Li, W. K. W., Mclaughlin, F. A., Lovejoy, C. and Carmack, E. C. (2009) ‘Smallest algae thrive as the Arctic Ocean freshens’, *Science*, 326, p. 539.

Liberton, M., Austin, J. R., Berg, R. H. and Pakraski, H. B. (2011) ‘Unique thylakoid membrane architecture of a unicellular N_2-fixing cyanobacterium revealed by electron tomography’, *Plant Physiology*, 155(4), pp. 1656–1666.

Lichtlé, C., Thomas, J. C., Spilar, A. and Partensky, F. (1995) 'Immunological and ultrastructural characterization of the photosynthetic complexes of the prochlorophyte *Prochlorococcus* (Oxychlorobacteria)', *Journal of Phycology*, 31(6), pp. 934–941.

Liefer, J. D., Garg, A., Campbell, D. A., Irwin, A. J. and Finkel, Z. V. (2018) 'Nitrogen starvation induces distinct photosynthetic responses and recovery dynamics in diatoms and prasinophytes', *PLoS ONE*, 13(4).

Lindell, D., Erdner, D., Marie, D., Prášil, O., Žek, M. K., Le Gall, F., Rippka, R., Partensky, F., Scanlan, D. J. and Post, A. F. (2002) 'Nitrogen stress response of *Prochlorococcus* strain PCC 9511 (Oxyphotobacteria) involves contrasting regulation of *ntcA* and *amt1*', *Journal of Phycology*, 38(6), pp. 1113–1124.

Lindley, S. T., Bidigare, R. R. and Barber, R. T. (1995) 'Phytoplankton photosynthesis parameters along 140°W in the equatorial Pacific', *Deep-Sea Research Part II: Topical Studies in Oceanography*, 42(2–3), pp. 441–463.

Liu, H., Campbell, L. and Landry, M. R. (1995) 'Growth and mortality rates of *Prochlorococcus* and *Synechococcus* measured with a selective inhibitor technique', *Marine Ecology Progress Series*, 116, pp. 277–287.

Liu, H., Nolla, H. A. and Campbell, L. (1997) '*Prochlorococcus* growth rate and contribution to primary production in the equatorial and subtropical North Pacific Ocean', *Aquatic Microbial Ecology*, 12, pp. 39–47.

Liu, H., Probert, I., Uitz, J., Claustre, H., Aris-Brosou, S., Frada, M., Not, F. and de Vargas, C. (2009) 'Extreme diversity in noncalcifying haptophytes explains a major pigment paradox in open oceans', *Proceedings of the National Academy of Sciences*, 106(31), pp. 12803–12808.

Llewellyn, C. A., Fishwick, J. R. and Blackford, J. C. (2005) 'Phytoplankton community assemblage in the English Channel: a comparison using chlorophyll a derived from HPLC-CHEMTAX and carbon derived from microscopy cell counts', *Journal of Plankton Research*, 27(1), pp. 103–119.

Lohrenz, S. E., Weidemann, A. D. and Tuel, M. (2003) 'Phytoplankton spectral absorption as influenced by community size structure and pigment composition', *Journal of Plankton Research*, 25(1), pp. 35–61.

Longhurst, A. R. (1998) *Ecological Geography of the Sea*. Academic Press.

Lovejoy, C., Vincent, W. F., Bonilla, S., Roy, S., Martineau, M.-J., Terrado, R., Potvin, M., Massana, R. and Pedrós-Alió, C. (2007) 'Distribution, phylogeny, and growth of cold-adapted picoprasinophytes in Arctic seas', *Journal of Phycology*, 43, pp. 78–89.

Lutz, V. A., Sathyendranath, S. and Head, E. J. H. (1996) 'Absorption coefficient of phytoplankton: regional variations in the North Atlantic', *Marine Ecology Progress Series*, 135, pp. 197–213.

Lutz, V. A., Sathyendranath, S., Head, E. J. H. and Li, W. K. W. (2003) 'Variability in pigment composition and optical characteristics of phytoplankton in the Labrador Sea and the Central North Atlantic', *Marine Ecology Progress Series*, 260, pp. 1–18.

MacIntyre, H. L., Kana, T. M., Anning, T. and Geider, R. J. (2002) 'Photoacclimation of photosynthesis irradiance response curves and photosynthetic pigments in microalgae and cyanobacteria', *Journal of Phycology*, 38(1), pp. 17–38.

Maeda, S., Murakami, A., Ito, H., Tanaka, A. and Omata, T. (2015) 'Functional characterization of the FNT Family Nitrite Transporter of marine picocyanobacteria', *Life*, 5(1), pp. 432–446.

Mahmoud, R. M., Sanfilippo, J. E., Nguyen, A. A., Strnat, J. A., Partensky, F., Garczarek, L., Abo El Kassem, N., Kehoe, D. M. and Schluchter, W. M. (2017) 'Adaptation to blue light in marine *Synechococcus* requires MpeU, an enzyme with similarity to phycoerythrobilin lyase isomerases', *Frontiers in Microbiology*, 8(243).

Malmstrom, R. R., Coe, A., Kettler, G. C., Martiny, A. C., Frias-Lopez, J., Zinser, E. R. and Chisholm, S. W. (2010) 'Temporal dynamics of *Prochlorococcus* ecotypes in the Atlantic and Pacific Oceans', *The ISME Journal*, 4, pp. 1252–1264.

Malmstrom, R. R., Rodrigue, S., Huang, K. H., Kelly, L., Kern, S. E., Thompson, A., Roggensack, S., Berube, P. M., Henn, M. R. and Chisholm, S. W. (2013) 'Ecology of uncultured *Prochlorococcus* clades revealed through single-cell genomics and biogeographic analysis', *The ISME Journal*, 7(1), pp. 184–198.

Malone, T. C. (1977) 'Light-saturated photosynthesis by phytoplankton size fractions in the New York bight, USA', *Marine Biology*, 42(4), pp. 281–292.

Marañón, E. (2005) 'Phytoplankton growth rates in the Atlantic subtropical gyres', *Limnology and Oceanography*, 50(1), pp. 299–310.

Marañón, E. (2015) 'Cell size as a key determinant of phytoplankton metabolism and community structure', *Annual Review of Marine Science*, 7, pp. 241–264.

Marañón, E., Behrenfeld, M. J., González, N., Mouriño, B. and Zubkov, M. V. (2003) 'High variability of primary production in oligotrophic waters of the Atlantic Ocean: uncoupling from phytoplankton biomass and size structure', *Marine Ecology Progress Series*, 257, pp. 1–11.

Marañón, E., Cermeño, P., Rodríguez, J., Zubkov, M. V. and Harris, R. P. (2007) 'Scaling of phytoplankton photosynthesis and cell size in the ocean', *Limnology and Oceanography*, 52(5), pp. 2190–2198.

Marañón, E., Holligan, P. M., Barciela, R. M., González, N., Mouriño, B., Pazó, M. J. and Varela, M. (2001) 'Patterns of phytoplankton size structure and productivity in contrasting open-ocean environments', *Marine Ecology Progress Series*, 216, pp. 43–56.

Mareš, J., Strunecký, O., Bučinská, L. and Wiedermannová, J. (2019) 'Evolutionary patterns of thylakoid architecture in cyanobacteria', *Frontiers in Microbiology*, 10(277).

Margalef, R. (1978) 'Life-forms of phytoplankton as survival alternatives in an unstable environment', *Oceanologica Acta*, 1, pp. 493–509.

Marie, D., Partensky, F., Jacquet, S. and Vaulot, D. (1997) 'Enumeration and cell cycle analysis of natural populations of marine picoplankton by flow cytometry using the nucleic acid stain SYBR Green I', *Applied and Environmental Microbiology*, 63, pp. 186–193.

Marie, D., Simon, N. and Vaulot, D. (2005) 'Phytoplankton cell counting by flow cytometry', in Anderson, R. A. (ed.) *Algal Culturing Techniques*. Amsterdam: Elsevier, pp. 253–267.

Marra, J., Trees, C. C., Bidigare, R. R. and Barber, R. T. (2000) 'Pigment absorption and quantum yields in the Arabian Sea', *Deep-Sea Research Part II: Topical Studies in Oceanography*, 47(7–8), pp. 1279–1299.

Martiny, A. C., Pham, C. T. A., Primeau, F. W., Vrugt, J. A., Moore, J. K., Levin, S. A. and Lomas, M. W. (2013) 'Strong latitudinal patterns in the elemental ratios of marine plankton and organic matter', *Nature Geoscience*, 6(4), pp. 279–283.

Martiny, A. C., Talarmin, A., Mouginot, C., Lee, J. A., Huang, J. S., Gellene, A. G. and Caron, D. A. (2016) 'Biogeochemical interactions control a temporal succession in the elemental composition of marine communities', *Limnology and Oceanography*. Wiley Blackwell, 61(2), pp. 531–542.

Masamoto, K., Zsiros, O. and Gombos, Z. (1999) 'Accumulation of zeaxanthin in cytoplasmic membranes of the cyanobacterium *Synechococcus* sp. strain PCC7942 grown under high light condition', *Journal of Plant Physiology*, 155, pp. 136–138.

Massana, R. (2011) 'Eukaryotic picoplankton in surface oceans', *Annual Review of Microbiology*, 65, pp. 91–110.

Matsumoto, K. and Ando, K. (2009) 'Use of cyanobacterial pigments to characterize the ocean surface mixed layer in the western Pacific warm pool', *Journal of Marine Systems*, 75, pp. 245–252.

Matsuoka, A., Larouche, P., Poulin, M., Vincent, W. and Hattori, H. (2009) 'Phytoplankton community adaptation to changing light levels in the southern Beaufort Sea, Canadian Arctic', *Estuarine, Coastal and Shelf Science*, 82(3), pp. 537–546.

Mauzerall, D. and Greenbaum, N. L. (1989) 'The absolute size of a photosynthetic unit', *Biochimica et Biophysica Acta*, 974(2), pp. 119–140.

Mayer, J. and Graham, J. (1971) 'The photosynthetic unit in *Chlorella* measured by repetitive short flashes', *Plant Physiology*, 48, pp. 282–286.

McGillicuddy, D. J., Robinson, A. R., Siegel, D. A., Jannasch, H. W., Robinson, R., Dickey, T. D., McNeil, J., Michaels, A. F. and Knap, A. H. (1998) 'Influence of mesoscale eddies on new production in the Sargasso Sea', *Nature*, 394, pp. 263–266.

McKie-Krisberg, Z. M. and Sanders, R. W. (2014) 'Phagotrophy by the picoeukaryotic green alga *Micromonas*: implications for Arctic Oceans', *The ISME Journal*, 8(10), pp. 1953–1961.

Mella-Flores, D., Six, C., Ratin, M., Partensky, F., Boutte, C., Le Corguille, G., Marie, D., Blot, N., Gourvil, P., Kolowrat, C. and Garczarek, L. (2012) '*Prochlorococcus* and *Synechococcus* have evolved different adaptive mechanisms to cope with light and UV stress', *Frontiers in Microbiology*, 3(285).

Mitchell, B. G. (1990) 'Algorithms for determining the absorption coefficient of aquatic particulates using the Quantitative Filter Technique (QFT)', *SPIE Proceedings 1302, Ocean Optics X*, 290, pp. 137–148.

Mitchell, B. G. (2002) 'Bio-optical measurement and modeling of the California Current and Southern Oceans', in Fargion, G. S. and McClain, C. R. (eds) *SIMBIOS Project 2001 Annual Report, NASA/TM-2002-210005*. Greenbelt, Maryland: NASA Goddard Space Flight Center, pp. 84–87.

Mitchell, B. G., Bricaud, A., Carder, K. L., Cleveland, J. S., Ferrari, G. M., Gould, R. W., Kahru, M., Kishino, M., Maske, H., Tiffany, M., Moore, L. R., Nelson, N. B., Phinney, D. a., Reynolds, R. A., Sosik, H. M., Stramski, D., Tassan, S., Trees, C. C., Weidemann, A. D., Wieland, J. and Vodecek, A. (2000) 'Determination of spectral absorption coefficients of particles, dissolved material and phytoplankton for discrete water samples', in Fargion, G. S. and

Mueller, J. L. (eds) *Ocean Optics Protocols for Satellite Ocean Color Sensor Validation, Revision 2, NASA/TM-2000-20996*. Greenbelt, Maryland: NASA Goddard Space Flight Center, pp. 125–153.

Mitchell, B. G., Kahru, M., Wieland, J. and Stramska, M. (2002) 'Determination of spectral absorption coefficients of particles, dissolved material and phytoplankton for discrete water samples', in Fargion, G. S. and Mueller, J. L. (eds) *Ocean Optics Protocols for Satellite Ocean Color Sensor Validation, Revision 3, NASA/TM-2002-21004*. Greenbelt, Maryland: NASA Goddard Space Flight Center, pp. 231–257.

Mobley, C. D. (1994) *Light and Water: Radiative Transfer in Natural Waters*. Academic Press.

Moon-van der Staay, S. Y., van der Staay, G. W. M., Guillou, L., Vaulot, D., Claustre, H. and Medlin, L. K. (2000) 'Abundance and diversity of prymnesiophytes in the picoplankton community from the equatorial Pacific Ocean inferred from 18S rDNA sequences', *Limnology and Oceanography*, 45(1), pp. 98–109.

Moore, C. M., Mills, M. M., Arrigo, K. R., Berman-Frank, I., Bopp, L., Boyd, P. W., Galbraith, E. D., Geider, R. J., Guieu, C., Jaccard, S. L., Jickells, T. D., La Roche, J., Lenton, T. M., Mahowald, N. M., Marañón, E., Marinov, I., Moore, J. K., Nakatsuka, T., Oschlies, A., Saito, M. A., Thingstad, T. F., Tsuda, A. and Ulloa, O. (2013) 'Processes and patterns of oceanic nutrient limitation', *Nature Geoscience*, 6(9), pp. 701–710.

Moore, C. M., Suggett, D. J., Hickman, A. E., Kim, Y.-N. K., Tweddle, J. F., Sharples, J., Geider, R. J. and Holligan, P. M. (2006) 'Phytoplankton photoacclimation and photoadaptation in response to environmental gradients in a shelf sea', *Limnology and Oceanography*, 51(2), pp. 936–949.

Moore, L. R. and Chisholm, S. W. (1999) 'Photophysiology of the marine cyanobacterium *Prochlorococcus*: ecotypic differences among cultured isolates', *Limnology and Oceanography*, 44, pp. 628–638.

Moore, L. R., Goericke, R. and Chisholm, S. W. (1995) 'Comparative physiology of *Synechococcus* and *Prochlorococcus*: influence of light and temperature on growth, pigment, fluorescence and absorptive properties', *Marine Ecology Progress Series*, 116, pp. 259–275.

Moore, L. R., Post, A. F., Rocap, G. and Chisholm, S. W. (2002) 'Utilization of different nitrogen sources by the marine cyanobacteria *Prochlorococcus* and *Synechococcus*', *Limnology and Oceanography*, 47(4), pp. 989–996.

Moore, L. R., Rocap, G. and Chisholm, S. W. (1998) 'Physiology and molecular phylogeny of coexisting *Prochlorococcus* ecotypes', *Nature*, 393, pp. 464–467.

van Mooy, B. A. S., Rocap, G., Fredricks, H. F., Evans, C. T. and Devol, A. H. (2006) 'Sulfolipids dramatically decrease phosphorus demand by picocyanobacteria in oligotrophic marine environments', *Proceedings of the National Academy of Sciences of the United States of America*, 103(23), pp. 8607–8612.

Morán, X. A. G. (2007) 'Annual cycle of picophytoplankton photosynthesis and growth rates in a temperate coastal ecosystem: a major contribution to carbon fluxes', *Aquatic Microbial Ecology*, 49, pp. 267–279.

Morán, X. A. G., Lopez-Urrutia, A., Calvo-Dıaz, A. and Li, W. K. W. (2010) 'Increasing importance of small phytoplankton in a warmer ocean', *Global Change Biology*, 16(3), pp. 1137–1144.

Morán, X. A. G. and Scharek, R. (2015) ‘Photosynthetic parameters and primary production, with focus on large phytoplankton, in a temperate mid-shelf ecosystem’, *Estuarine, Coastal and Shelf Science*, 154, pp. 255–263.

Morel, A. (1988) ‘Optical modeling of the upper ocean in relation to its biogenous matter content (case I waters)’, *Journal of Geophysical Research*, 93(C9), pp. 749–759.

Morel, A., Ahn, Y.-W., Partensky, F., Vaulot, D. and Claustre, H. (1993) ‘*Prochlorococcus* and *Synechococcus*: a comparative study of their size, pigmentation and related optical properties’, *Journal of Marine Research*, 51, pp. 617–649.

Morel, A., Antoine, D., Babin, M. and Dandonneau, Y. (1996) ‘Measured and modeled primary production in the northeast Atlantic (EUMELI JGOFS program): the impact of natural variations in photosynthetic parameters on model predictive skill’, *Deep-Sea Research Part I: Oceanographic Research Papers*, 43(8), pp. 1273–1304.

Morel, A. and Bricaud, A. (1981) ‘Theoretical results concerning light-absorption in a discrete medium, and application to specific absorption of phytoplankton’, *Deep-Sea Research*, 28(11), pp. 1375–1393.

Morel, A. and Bricaud, A. (1986) ‘Inherent optical properties of algal cells including picoplankton: theoretical and experimental results’, *Canadian Bulletin of Fisheries and Aquatic Science*, 214, pp. 521–559.

Morel, A., Huot, Y., Gentili, B., Werdell, P. J., Hooker, S. B. and Franz, B. A. (2007) ‘Examining the consistency of products derived from various ocean color sensors in open ocean (Case I) waters in the perspective of a multi-sensor approach’, *Remote Sensing of Environment*, 111, pp. 69–88.

Morel, A. and Maritorena, S. (2001) ‘Bio-optical properties of oceanic waters: a reappraisal’, *Journal of Geophysical Research: Oceans*, 106(C4), pp. 7163–7180.

Müller, P., Li, X.-P. and Niyogi, K. K. (2001) ‘Non-photochemical quenching. A response to excess light energy’, *Plant Physiology*, 125(4), pp. 1558–1566.

Nair, A., Sathyendranath, S., Platt, T., Morales, J., Stuart, V., Forget, M. H., Devred, E. and Bouman, H. A. (2008) ‘Remote sensing of phytoplankton functional types’, *Remote Sensing of Environment*, 112(8), pp. 3366–3375.

Nanba, O. and Satoh, K. (1987) ‘Isolation of a photosystem II reaction center consisting of D-1 and D-2 polypeptides and cytochrome b-559’, *Proceedings of the National Academy of Sciences*, 84(1), pp. 109–112.

Nevo, R., Chuartzman, S. G., Tsabari, O., Reich, Z., Charuvi, D. and Shimoni, E. (2009) ‘Architecture of thylakoid membrane networks’, in Wada, H. and Murata, N. (eds) *Lipids in Photosynthesis. Advances in Photosynthesis and Respiration, vol 30.* Springer Dordrecht, pp. 295–328.

Not, F., Gausling, R., Azam, F., Heidelberg, J. F. and Worden, A. Z. (2007) ‘Vertical distribution of picoeukaryotic diversity in the Sargasso Sea’, *Environmental Microbiology*, 9(5), pp. 1233–1252.

Olaizola, M., La Roche, J., Kolber, Z. and Falkowski, P. G. (1994) ‘Non-photochemical fluorescence quenching and the diadinoxanthin cycle in a marine diatom’, *Photosynthesis Research*, 41, pp. 357–370.

Olson, R. J., Chisholm, S. W., Zettler, E. R., Altabet, M. A. and Dusenberry, J. A. (1990) 'Spatial and temporal distributions of prochlorophytes picoplankton in the North Atlantic Ocean', *Deep-Sea Research Part I: Oceanographic Research Papers*, 37(6), pp. 1033–1051.

Olson, R. J., Frankel, S. L., Chisholm, S. W. and Shapiro, H. M. (1983) 'An inexpensive flow cytometer for the analysis of fluorescence signals in phytoplankton: chlorophyll and DNA distributions', *Journal of Experimental Marine Biology and Ecology*, 68(2), pp. 129–144.

Olson, R. J., Vaulot, D. and Chisholm, S. W. (1985) 'Marine phytoplankton distributions measured using shipboard flow cytometry', *Deep-Sea Research Part A. Oceanographic Research Papers*, 32(10), pp. 1273–1280.

Olson, R. J., Zettler, E. R. and DuRand, M. D. (1993) 'Phytoplankton analysis using flow cytometry', in Kemp, P. F., Sherr, E. B., and Cole, J. J. (eds) *Handbook of Methods in Aquatic Microbial Ecology*. Lewis Publishers, pp. 175–186.

Omand, M. M., Feddersen, F., Guza, R. T. and Franks, P. J. S. (2012) 'Episodic vertical nutrient fluxes and nearshore phytoplankton blooms in Southern California', *Limnology and Oceanography*, 57(6), pp. 1673–1688.

Palinska, K. A., Jahns, T., Rippka, R. and de Marsac, N. T. (2000) '*Prochlorococcus marinus* strain PCC 9511, a picoplanktonic cyanobacterium, synthesizes the smallest urease', *Microbiology*, 146(12), pp. 3099–3107.

Pan, X., Wong, G. T. F., Ho, T.-Y., Shiah, F.-K. and Liu, H. (2013) 'Remote sensing of picophytoplankton distribution in the northern South China Sea', *Remote Sensing of Environment*, 128, pp. 162–175.

Park, J. Y., Kug, J. S., Bader, J., Rolph, R. and Kwon, M. (2015) 'Amplified Arctic warming by phytoplankton under greenhouse warming', *Proceedings of the National Academy of Sciences of the United States of America*, 112(19), pp. 5921–5926.

Partensky, F., Blanchot, J., Lantoine, F., Neveux, J. and Marie, D. (1996) 'Vertical structure of picophytoplankton at different trophic sites of the tropical northeastern Atlantic Ocean', *Deep-Sea Research Part I: Oceanographic Research Papers*, 43, pp. 1191–1213.

Partensky, F., Blanchot, J. and Vaulot, D. (1999) 'Differential distribution and ecology of *Prochlorococcus* and *Synechococcus* in oceanic waters : a review', *Bulletin de l'Institut océanographique de Monaco*, 19, pp. 457–475.

Partensky, F. and Garczarek, L. (2010) '*Prochlorococcus*: advantages and limits of minimalism', *Annual Review of Marine Science*, 2, pp. 305–331.

Partensky, F., Hess, W. R. and Vaulot, D. (1999) '*Prochlorococcus*, a marine photosynthetic prokaryote of global significance', *Microbiology and Molecular Biology Reviews*, 63(1), pp. 106–127.

Partensky, F., Hoepffner, N., Li, W. K. W., Ulloa, O. and Vaulot, D. (1993) 'Photoacclimation of *Prochlorococcus* sp. (Prochlorophyta) strains isolated from the North Atlantic and the Mediterranean Sea', *Plant Physiology*, 101, pp. 285–296.

Paulsen, M. L., Doré, H., Garczarek, L., Seuthe, L., Müller, O., Sandaa, R.-A., Bratbak, G. and Larsen, A. (2016) '*Synechococcus* in the Atlantic gateway to the Arctic Ocean', *Frontiers in Marine Science*, 3(191).

Perry, M. J., Talbot, M. C. and Alberte, R. S. (1981) 'Photoadaption in marine phytoplankton: response of the photosynthetic unit', *Marine Biology*, 62, pp. 91–101.

Petrou, K., Trimborn, S., Rost, B., Ralph, P. J. and Hassler, C. S. (2014) 'The impact of iron limitation on the physiology of the Antarctic diatom *Chaetoceros simplex*', *Marine Bology*, 161(4), pp. 925–937.

Platt, T., Bouman, H. A., Devred, E., Fuentes-Yaco, C. and Sathyendranath, S. (2005) 'Physical forcing and phytoplankton distributions', *Scientia Marina*, 69, pp. 55–73.

Platt, T., Gallegos, C. L. and Harrison, W. G. (1980) 'Photoinhibition of photosynthesis in natural assemblages of marine phytoplankton', *Journal of Marine Research*, 38(687–701).

Platt, T. and Sathyendranath, S. (1988) 'Oceanic primary production: estimation by remote sensing at local and regional scales', *Science*, 241(4873), pp. 1613–1620.

Platt, T., Sathyendranath, S., Caverhill, C. M. and Lewis, M. R. (1988) 'Ocean primary production and available light: further algorithms for remote sensing', *Deep-Sea Research Part I: Oceanographic Research Papers*, 35(6), pp. 855–879.

Polimene, L., Brunet, C., Butenschön, M., Martinez-Vicente, V., Widdicombe, C., Torres, R. and Allen, J. I. (2014) 'Modelling a light-driven phytoplankton succession', *Journal of Plankton Research*, 36(1), pp. 214–229.

van de Poll, W. H., Visser, R. J. W. and Buma, A. G. . J. (2007) 'Acclimation to a dynamic irradiance regime changes excessive irradiance sensitivity of *Emiliania huxleyi* and *Thalassiosira weissflogii*', *Limnology and Oceanography*, 52(4), pp. 1430–1438.

Polovina, J. J., Howell, E. A. and Abecassis, M. (2008) 'Ocean's least productive waters are expanding', *Geophysical Research Letters*, 35(3).

Post, A. F., Ohad, I., Warner, K. M. and Bullerjahn, G. S. (1993) 'Energy distribution between Photosystems I and II in the photosynthetic prokaryote *Prochlorothrix hollandica* involves a chlorophyll ab antenna which associates with Photosystem I', *Biochimica et Biophysica Acta*, 1144(3), pp. 374–384.

Poulton, A. J., Holligan, P. M., Hickman, A. E., Kim, Y.-N. K., Adey, T. R., Stinchcombe, M. C., Holeton, C., Root, S. and Woodward, E. M. S. (2006) 'Phytoplankton carbon fixation, chlorophyll-biomass and diagnostic pigments in the Atlantic Ocean', *Deep-Sea Research Part II: Topical Studies in Oceanography*, 53, pp. 1593–1610.

Preisendorfer, R. W. (1961) 'Application of radiative transfer theory to light measurements in the sea', *Union of Geodetic Geophysical Institute Monograph*, 10, pp. 11–30.

Prézelin, B. B. (1981) 'Light reaction in photosynthesis', in Platt, T. (ed.) *Physiological Bases of Phytoplankton Ecology*. Ottawa, Canada: Department of Fisheries and Oceans, pp. 1–43.

Prézelin, B. B., Putt, M. and Glover, H. E. (1986) 'Diurnal patterns in photosynthetic capacity and depth-dependent photosynthesis-irradiance relationships in *Synechococcus* spp. and larger phytoplankton in three water masses in the Northwest Atlantic Ocean', *Marine Biology*, 91, pp. 205–217.

Prieur, L. and Sathyendranath, S. (1981) 'An optical classification of coastal and oceanic waters based on the specific spectral absorption curves of phytoplankton pigments, dissolved organic matters, and other particulate materials', *Limnology And Oceanography*, 26(4), pp. 671–689.

Le Quéré, C., Harrison, S. P., Colin Prentice, I., Buitenhuis, E. T., Aumont, O., Bopp, L., Claustre, H., Cotrim Da Cunha, L., Geider, R. J., Giraud, X., Klaas, C., Kohfeld, K. E., Legendre, L., Manizza, M., Platt, T., Rivkin, R. B., Sathyendranath, S., Uitz, J., Watson, A. J. and Wolf-Gladrow, D. (2005) 'Ecosystem dynamics based on plankton functional types for global ocean biogeochemistry models', *Global Change Biology*, 11, pp. 2016–2040.

Raimbault, P., Garcia, N. and Cerutti, F. (2008) 'Distribution of inorganic and organic nutrients in the South Pacific Ocean - evidence for long-term accumulation of organic matter in nitrogen-depleted waters', *Biogeosciences*, 5, pp. 281–298.

Ras, J., Claustre, H. and Uitz, J. (2008) 'Spatial variability of phytoplankton pigment distributions in the Subtropical South Pacific Ocean: comparison between in situ and predicted data', *Biogeosciences*, 5, pp. 353–369.

Raven, J. A. (1984) 'A cost-benefit-analysis of photon-absorption by photosynthetic unicells', *New Phytologist*, 98(4), pp. 593–625.

Raven, J. A. (1991) 'Responses of aquatic photosynthetic organisms to increased solar UVB', *Journal of Photochemistry and Photobiology B: Biology*, 9(2), pp. 239–244.

Raven, J. A. (1998) 'The twelfth Tansley Lecture. Small is beautiful: the picophytoplankton', *Functional Ecology*, 12(4), pp. 503–513.

Reckermann, M. and Veldhuis, M. J. W. (1997) 'Trophic interactions between picophytoplankton and micro- and nanozooplankton in the western Arabian Sea during the NE monsoon 1993', *Aquatic Microbial Ecology*, 12, pp. 263–273.

Richardson, K., Beardall, J. and Raven, J. A. (1983) 'Adaptation of unicellular algae to irradiance: an analysis of strategies', *New Phytologist*, 93, pp. 157–191.

Richardson, K., Bendtsen, J., Kragh, T. and Mousing, E. A. (2016) 'Constraining the distribution of photosynthetic parameters in the global ocean', *Frontiers in Marine Science*, 3.

Roberts, A. E. (2001) *Growth Rate Dynamics of* Prochlorococcus *spp. in the Eastern North Pacific: Carbon 14 Pigment Labeling Estimates*. California State University, Fresno.

Robinson, A., Bouman, H. A., Tilstone, G. H. and Sathyendranath, S. (2018) 'Size class dependent relationships between temperature and phytoplankton photosynthesis-irradiance parameters in the Atlantic Ocean', *Frontiers in Marine Science*, 4(435).

Rocap, G., Distel, D. L., Waterbury, J. B. and Chisholm, S. W. (2002) 'Resolution of *Prochlorococcus* and *Synechococcus* ecotypes by using 16S-23S Ribosomal DNA Internal Transcribed Spacer Sequences', *Applied and Environmental Microbiology*, 68(3), pp. 1180–1191.

Rocap, G., Larimer, F. W., Lamerdin, J., Malfatti, S., Chain, P., Ahlgren, N. A., Arellano, A., Coleman, M. L., Hauser, L., Hess, W. R., Johnson, Z. I., Land, M., Lindell, D., Post, A. F., Regala, W., Shah, M., Shaw, S. L., Steglich, C., Sullivan, M. B., Ting, C. S., Tolonen, A., Webb, E. A., Zinser, E. R. and Chisholm, S. W. (2003) 'Genome divergence in two *Prochlorococcus* ecotypes reflects oceanic niche differentiation', *Nature*, 424, pp. 1042–1047.

Rochaix, J.-D. (2016) 'The dynamics of the photosynthetic apparatus in algae', in Najafpour, M. M. (ed.) *Applied Photosynthesis - New Progress*. IntechOpen, pp. 23–52.

Rogers, W. (1992) 'Quantile regression standard errors', *Stata Technical Bulletin*, 2, pp. 133–137.

Ross, O. N., Moore, C. M., Suggett, D. J., MacIntyre, H. L. and Geider, R. J. (2008) 'A model of photosynthesis and photo-protection based on reaction center damage and repair', *Limnology and Oceanography*, 53(5), pp. 1835–1852.

Rudorff, F., Gonzalez-Silvera, A. G., Dogliotti, A. I., Garcia-Llano, C. F., Santamaría-del-Angel, E., de Oliveira, E. N., de Souza, E. M., Chalhoub, E. S., de Souza, M. S., Noernberg, M. A., Pompeu, M., Carvalho, M., Ayala, R., Cerdeira, S., Frouin, R. J., Kampel, M., Kopelevich, O. and Lutz, V. A. (2007) 'Analysis of SeaWiFS imagery over the Southwestern Atlantic Ocean during the March 2002 R/V IOFFE Cruise', in *SPIE Proceedings 6680, Coastal Ocean Remote Sensing*.

Rusch, D. B., Martiny, A. C., Dupont, C. L., Halpern, A. L. and Venter, J. C. (2010) 'Characterization of *Prochlorococcus* clades from iron-depleted oceanic regions', *Proceedings of the National Academy of Sciences of the United States of America*, 107(37), pp. 16184–16189.

Sakshaug, E., Bricaud, A., Dandonneau, Y., Falkowski, P. G., Kiefer, D. A., Legendre, L., Morel, A., Parslow, J. and Takahashi, M. (1997) 'Parameters of photosynthesis: definitions, theory and interpretation of results', *Journal of Plankton Research*, 19(11), pp. 1637–1670.

Sathyendranath, S., Gouveia, A. D., Shetye, S. R., Ravindran, P. and Platt, T. (1991) 'Biological control of surface temperature in the Arabian Sea', *Nature*, 349, pp. 54–56.

Sathyendranath, S. and Platt, T. (1988) 'The spectral irradiance field at the surface and in the interior of the ocean : a model for application in oceanography and remote sensing', *Journal of Geophysical Research*, 93(C8), pp. 9270–9280.

Sathyendranath, S. and Platt, T. (1993) 'Remote sensing of water-column primary production', *ICES Marine Science Symposia*, 197, pp. 236–243.

Sathyendranath, S., Platt, T., Kovač, Ž., Dingle, J., Jackson, T., Brewin, R. J. W., Franks, P., Marañón, E., Kulk, G. and Bouman, H. A. (2020) 'Reconciling models of primary production and photoacclimation', *Applied Optics*, 59(10).

Sathyendranath, S., Platt, T., Stuart, V., Veldhuis, M. J. W., Kraay, G. W. and Glen Harrison, W. (1996) 'Some bio-optical characteristics of phytoplankton in the NW Indian Ocean', *Marine Ecology Progress Series*, 132, pp. 299–311.

Sathyendranath, S., Stuart, V., Nair, A., Oka, K., Nakane, T., Bouman, H. A., Forget, M. H., Maass, H. and Platt, T. (2009) 'Carbon-to-chlorophyll ratio and growth rate of phytoplankton in the sea', *Marine Ecology Progress Series*, 383, pp. 73–84.

Sathyendranath, S., Watts, L., Devred, E., Platt, T., Caverhill, C. and Maass, H. (2004) 'Discrimination of diatoms from other phytoplankton using ocean-colour data', *Marine Ecology Progress Series*, 272, pp. 59–68.

Scanlan, D. J. and West, N. J. (2002) 'Molecular ecology of the marine cyanobacterial genera *Prochlorococcus* and *Synechococcus*', *FEMS Microbiology Ecology*, 40, pp. 1–12.

Scharien, R. K., Segal, R., Nasonova, S., Nandan, V., Howell, S. E. L. and Haas, C. (2017) 'Winter sentinel-1 backscatter as a predictor of spring Arctic sea ice melt pond fraction', *Geophysical Research Letters*, 44(24), pp. 262–270.

Searle, G. F. W. and Wessels, J. S. C. (1978) 'Role of β-carotene in the reaction centres of Photosystems I and II of spinach chloroplasts prepared in non-polar solvents', *Biochimica et Biophysica Acta*, 504(1), pp. 84–99.

Shen, P., Qi, Y., Wang, Y. and Huang, L. (2011) '*Phaeocystis globosa* Scherffel, a harmful microalga, and its production of dimethylsulfoniopropionate', *Chinese Journal of Oceanology and Limnology*, 29(4), pp. 869–873.

Shimada, A., Maruyama, T. and Miyashi, S. (1996) 'Vertical distributions and photosynthetic action spectra of two oceanic picophytoplankters, *Prochlorococcus marinus* and *Synechococcus* sp.', *Marine Biology*, 127, pp. 15–23.

Sieburth, J. M., Smetacek, V. and Lenz, J. (1978) 'Pelagic ecosystem structure: heterotrophic compartments of the plankton and their relationship to plankton size fractions', *Limnology and Oceanography*, 23(6), pp. 1256–1263.

Siefermann-Harms, D. (1985) 'Carotenoids in photosynthesis. I. Location in photosynthetic membranes and light-harvesting function', *Biochimica et Biophysica Acta*, 811, pp. 325–355.

Simon, N., Foulon, E., Grulois, D., Six, C., Desdevises, Y., Latimier, M., Le Gall, F., Tragin, M., Houdan, A., Derelle, E., Jouenne, F., Marie, D., Le Panse, S., Vaulot, D. and Marin, B. (2017) 'Revision of the genus *Micromonas* Manton et Parke (Chlorophyta, Mamiellophyceae), of the type species *M. pusilla* (Butcher) Manton et Parke and of the species *M. commoda* van Baren, Bachy and Worden and description of two new species', *Protist*, 168(5), pp. 612–635.

Sinclair, M., Keighan, E. and Jones, J. (1979) 'ATP as a measure of living phytoplankton carbon in estuaries', *Journal of the Fisheries Research Board of Canada*, 36(2), pp. 180–186.

Six, C., Finkel, Z. V., Irwin, A. J. and Campbell, D. A. (2007) 'Light variability illuminates niche-partitioning among marine picocyanobacteria', *PLoS ONE*, 2(12).

Six, C., Finkel, Z. V., Rodriguez, F., Marie, D., Partensky, F. and Campbell, D. A. (2008) 'Contrasting photoacclimation costs in ecotypes of the marine eukaryotic picoplankter *Ostreococcus*', *Limnology and Oceanography*, 53(1), pp. 255–265.

Six, C., Sherrard, R., Lionard, M., Roy, S. and Campbell, D. A. (2009) 'Photosystem II and pigment dynamics among ecotypes of the green alga *Ostreococcus*', *Plant Physiology*, 151, pp. 379–390.

Six, C., Thomas, J. C., Brahamsha, B., Lemoine, Y. and Partensky, F. (2004) 'Photophysiology of the marine cyanobacterium *Synechococcus* sp. WH8102, a new model organism', *Aquatic Microbial Ecology*, 35, pp. 17–29.

Smith, E. L. (1936) 'Photosynthesis in relation to light and carbon dioxide', *Proceedings of the National Academy of Sciences*, 22(8), pp. 504–511.

Smyth, T. J., Tarran, G. A. and Sathyendranath, S. (2019) 'Marine picoplankton size distribution and optical property contrasts throughout the Atlantic Ocean revealed using flow cytometry', *Applied Optics*, 58(32), pp. 8802–8815.

SooHoo, J. B., Kiefer, D. A., Collins, D. J. and Mcdermid, I. S. (1986) 'In vivo fluorescence excitation and absorption spectra of marine phytoplankton: I. Taxonomic characteristics and responses to photoadaptation', *Journal of Plankton Research*, 8(1), pp. 197–214.

Sosik, H. M. and Mitchell, B. G. (1995) 'Light absorption by phytoplankton, photosynthetic pigments and detritus in the California Current System', *Deep-Sea Research Part I: Oceanographic Research Papers*, 42(10), pp. 1717–1748.

Sosik, H. M., Olson, R. J. and Armbrust, E. V. (2010) 'Flow cytometry in phytoplankton research', in *Chlorophyll a Fluorescence in Aquatic Sciences: Methods and Applications*. Springer Netherlands, pp. 171–185.

Stawiarski, B., Buitenhuis, E. T. and Fallens, M. (2018) 'The physiological response of seven strains of picophytoplankton to light, and its representation in a dynamic photosynthesis model', *Limnology and Oceanography*, 63, pp. S367–S380.

Steinberg, D. K., Carlson, C. A., Bates, N. R., Johnson, R. J., Michaels, A. F. and Knap, A. H. (2001) 'Overview of the US JGOFS Bermuda Atlantic Time-series Study (BATS): a decade-scale look at ocean biology and biogeochemistry', *Deep-Sea Research Part II: Topical Studies in Oceanography*, 48, pp. 1405–1447.

Strom, S. L., Marcri, E. L. and Fredrickson, K. A. (2010) 'Light limitation of summer primary production in the coastal Gulf of Alaska: physiological and environmental causes', *Marine Ecology Progress Series*, 402, pp. 45–57.

Stuart, V., Sathyendranath, S., Head, E. J. H., Platt, T., Irwin, B. and Maass, H. (2000) 'Bio-optical characteristics of diatom and prymnesiophyte populations in the Labrador Sea', *Marine Ecology Progress Series*, 201(1991), pp. 91–106.

Stuart, V., Sathyendranath, S., Platt, T., Maass, H. and Irwin, B. D. (1998) 'Pigments and species composition of natural phytoplankton populations: effect on the absorption spectra', *Journal of Plankton Research*, 20(2), pp. 187–217.

Stuart, V., Ulloa, O., Alarcón, G., Sathyendranath, S., Major, H., Head, E. J. H. and Platt, T. (2004) 'Bio-optical characteristics of phytoplankton populations in the upwelling system off the coast of Chile', *Revista Chilena de Historia Natural*, 77, pp. 87–105.

Suggett, D. J., Moore, C. M., Hickman, A. E. and Geider, R. J. (2009) 'Interpretation of fast repetition rate (FRR) fluorescence: signatures of phytoplankton community structure versus physiological state', *Marine Ecology Progress Series*, 376, pp. 1–19.

Talmy, D., Blackford, J., Hardman-Mountford, N. J., Dumbrell, A. J. and Geider, R. J. (2013) 'An optimality model of photoadaptation in contrasting aquatic light regimes', *Limnology and Oceanography*, 58(5), pp. 1802–1818.

Tarran, G. A., Heywood, J. L. and Zubkov, M. V. (2006) 'Latitudinal changes in the standing stocks of nano- and picoeukaryotic phytoplankton in the Atlantic Ocean', *Deep-Sea Research Part II: Topical Studies in Oceanography*, 53, pp. 1516–1529.

Taylor, A. R., Brownlee, C. and Wheeler, G. (2016) 'Coccolithophore cell biology: chalking up progress', *Annual Review of Marine Science*, 9, pp. 283–310.

Taylor, F. J. R., Hoppenrath, M. and Saldarriaga, J. F. (2008) 'Dinoflagellate diversity and distribution', *Biodiversity and Conservation*. Springer Netherlands, 17(2), pp. 407–418.

Telfer, A. (2002) 'What is b-carotene doing in the photosystem II reaction centre?', *Philosophical Transactions of the Royal Society B: Biological Sciences*, 357, pp. 1431–1440.

Thompson, A. W., van den Engh, G. J., Ahlgren, N. A., Kouba, K., Ward, S., Wilson, S. T. and Karl, D. M. (2018) 'Dynamics of *Prochlorococcus* diversity and photoacclimation during short-term shifts in water column stratification at station ALOHA', *Frontiers in Marine Science*, 5, p. 488.

Thornber, J. P. (1975) ‘Chlorophyll-proteins: light-harvesting and reaction center components of plants’, *Annual Review of Plant Physiology*, 26, pp. 127–158.

Tilstone, G. H., Lange, P. K., Misra, A., Brewin, R. J. W. and Cain, T. (2017) ‘Micro-phytoplankton photosynthesis, primary production and potential export production in the Atlantic Ocean’, *Progress in Oceanography*, 158, pp. 109–129.

Ting, C. S., Rocap, G., King, J. and Chisholm, S. W. (2002) ‘Cyanobacterial photosynthesis in the oceans: the origins and significance of divergent light-harvesting strategies’, *Trends in Microbiology*, 10(3), pp. 134–142.

Topping, J. (1962) *Errors of Observation and Their Treatment*. 3rd edn. London: Chapman and Hall.

Tragin, M. and Vaulot, D. (2019) ‘Novel diversity within marine Mamiellophyceae (Chlorophyta) unveiled by metabarcoding’, *Scientific Reports*, 9.

Trees, C. C., Clark, D. K., Bidigare, R. R., Ondrusek, M. E. and Mueller, J. L. (2000) ‘Accessory pigments versus chlorophyll a concentrations within the euphotic zone: a ubiquitous relationship’, *Limnology and Oceanography*, 45(5), pp. 1130–1143.

Turner, S. M., Malin, G., Liss, P. S., Harbour, D. S. and Holligan, P. M. (1988) ‘The seasonal variation of dimethyl sulfide and dimethylsulfoniopropionate concentrations in nearshore waters’, *Limnology and Oceanography*, 33(3), pp. 364–375.

Ueyoshi, K., Frouin, R. J., Nakamoto, S. and Subrahmanyam, B. (2005) ‘Sensitivity of equatorial Pacific Ocean circulation to solar radiation absorbed by phytoplankton’, in *SPIE Proceedings 5585, Remote Sensing of the Coastal Oceanic Environment, 58850R*.

Uitz, J., Claustre, H., Gentili, B. and Stramski, D. (2010) ‘Phytoplankton class-specific primary production in the world’s oceans: seasonal and interannual variability from satellite observations’, *Global Biogeochemical Cycles*, 24(3).

Uitz, J., Claustre, H., Griffiths, F. B., Ras, J., Garcia, N. and Sandroni, V. (2009) ‘A phytoplankton class-specific primary production model applied to the Kerguelen Islands region (Southern Ocean)’, *Deep-Sea Research Part I: Oceanographic Research Papers*, 56(4), pp. 541–560.

Uitz, J., Claustre, H., Morel, A. and Hooker, S. B. (2006) ‘Vertical distribution of phytoplankton communities in open ocean: an assessment based on surface chlorophyll’, *Journal of Geophysical Research: Oceans*, 111(8).

Uitz, J., Huot, Y., Bruyant, F., Babin, M. and Claustre, H. (2008) ‘Relating phytoplankton photophysiological properties to community structure on large scales’, *Limnology and Oceanography*, 53(2), pp. 614–630.

Urbach, E., Scanlan, D. J., Distel, D. L., Waterbury, J. B. and Chisholm, S. W. (1998) ‘Rapid diversification of marine picophytoplankton within dissimilar light harvesting structures inferred from sequences of *Prochlorococcus* and *Synechococcus* (cyanobacteria)’, *Journal of Molecular Evolution*, 46, pp. 188–201.

Urry, L. A., Cain, M. L., Wasserman, S. A., Minorsky, P. V. and Jackson, R. B. (2013) *Campbell Biology*. Benjamin Cummings.

Vassiliev, I. R., Kolber, Z., Wyman, K. D., Mauzerall, D., Shukla, V. K. and Falkowski, P. G. (1995) 'Effects of iron limitation on Photosystem II composition and light utilization in *Dunaliella tertiolecta*', *Plant Physiology*, 109(3), pp. 963–972.

Vaulot, D., Eikrem, W., Viprey, M. and Moreau, H. (2008) 'The diversity of small eukaryotic phytoplankton in marine ecosystems', *FEMS Microbiology Reviews*, 32(5), pp. 795–820.

Vaulot, D., Marie, D., Olson, R. J. and Chisholm, S. W. (1995) 'Growth of *Prochlorococcus*, a photosynthetic prokaryote, in the equatorial Pacific Ocean', *Science*, 268(5216), pp. 1480–1482.

del Vecchio, R. and Subramaniam, A. (2004) 'Influence of the Amazon River on the surface optical properties of the western tropical North Atlantic Ocean', *Journal of Geophysical Research*, 109.

Veldhuis, M. J. W., Cucci, T. L. and Sieracki, M. E. (1997) 'Cellular DNA content of marine phytoplankton using two new fluorochromes: taxonomic and ecological implications', *Journal of Phycology*, 33, pp. 527–541.

Veldhuis, M. J. W. and Kraay, G. W. (1990) 'Vertical distribution and pigment composition of a picoplanktonic prochlorophyte in the subtropical North Atlantic: a combined study of HPLC-analysis of pigments and flow cytometry', *Marine Ecology Progress Series*, 68, pp. 121–127.

Veldhuis, M. J. W. and Kraay, G. W. (2000) 'Application of flow cytometry in marine phytoplankton research: current applications and future perspectives', *Scientia Marina*, 64(2), pp. 121–134.

Veldhuis, M. J. W. and Kraay, G. W. (2004) 'Phytoplankton in the subtropical Atlantic Ocean: towards a better assessment of biomass and composition', *Deep-Sea Research Part I: Oceanographic Research Papers*, 51(4), pp. 507–530.

Verity, P. G., Robertson, C. Y., Tronzo, C. R., Andrews, M. G., Nelson, J. R. and Sieracki, M. E. (1992) 'Relationships between cell volume and the carbon and nitrogen content of marine photosynthetic nanoplankton', *Limnology and Oceanography*, 37(7), pp. 1434–1446.

Vidussi, F., Claustre, H., Manca, B. B., Luchetta, A. and Jean-Claude, M. (2001) 'Phytoplankton pigment distribution in relation to upper thermocline circulation in the eastern Mediterranean Sea during winter', *Journal of Geophysical Research*, 106, pp. 939–956.

Volk, T. and Hoffert, M. I. (1985) 'Ocean carbon pumps: analysis of relative strengths and efficiencies in ocean-driven atmospheric CO_2 changes', in Sundquist, E. T. and Broecker, W. S. (eds) *The Carbon Cycle and Atmospheric CO_2: Natural Variations Archean to Present*. Washington, D. C.: American Geophysical Union, pp. 99–110.

Ward, B. A. (2015) 'Temperature-correlated changes in phytoplankton community structure are restricted to polar waters', *PLoS ONE*, 10(8).

Wei, Y., Sun, J., Zhang, X., Wang, J. and Huang, K. (2019) 'Picophytoplankton size and biomass around equatorial eastern Indian Ocean', *Microbiology Open*, 8(2).

Weier, T. E. and Benson, A. A. (1967) 'The molecular organization of chloroplast membranes', *American Journal of Botany*, 54(4), pp. 389–402.

Werdell, P. J. and Bailey, S. W. (2005) 'An improved in-situ bio-optical data set for ocean color algorithm development and satellite data product validation', *Remote Sensing of Environment*, 98(1), pp. 122–140.

West, N. J., Lebaron, P., Strutton, P. G. and Suzuki, M. (2011) 'A novel clade of *Prochlorococcus* found in high nutrient low chlorophyll waters in the South and Equatorial Pacific Ocean', *The ISME Journal*, 5, pp. 933–944.

West, N. J. and Scanlan, D. J. (1999) 'Niche-partitioning of *Prochlorococcus* populations in a stratified water column in the Eastern North Atlantic Ocean', *Applied and Environmental Microbiology*, 65, pp. 2585–2591.

Williams, R. G. and Follows, M. J. (2011) *Ocean Dynamics and the Carbon Cycle*. Cambridge, UK: Cambridge University Press.

Wright, S. W., Jeffrey, S. W., Mantoura, R. F. C., Llewellyn, F. C., Bjornland, C. A. and Repeta, D. J. (1991) 'Improved HPLC method for the analysis of chlorophylls and caratenoids from marine phytoplankton', *Marine Ecology Progress Series*, 77, pp. 183–196.

Wu, H., Cockshutt, A. M., McCarthy, A. and Campbell, D. A. (2011) 'Distinctive photosystem II photoinactivation and protein dynamics in marine diatoms', *Plant Physiology*, 156(4), pp. 2184–95.

Wu, H., Roy, S., Alami, M., Green, B. R. and Campbell, D. A. (2012) 'Photosystem II photoinactivation, repair, and protection in marine centric diatoms', *Plant physiology*, 160(1), pp. 464–76.

Xie, Y., Huang, B., Lin, L., Laws, E. A., Wang, L., Shang, S., Zhang, T. and Dai, M. (2015) 'Photosynthetic parameters in the northern South China Sea in relation to phytoplankton community structure', *Journal of Geophysical Research: Oceans*, 120(6), pp. 4187–4204.

Xie, Y., Laws, E. A., Yang, L. and Huang, B. (2018) 'Diel patterns of variable fluorescence and carbon fixation of picocyanobacteria *Prochlorococcus*-dominated phytoplankton in the South China Sea Basin', *Frontiers in Microbiology*, 9(1589).

Yentsch, C. S. and Phinney, D. a. (1989) 'A bridge between ocean optics and microbial ecology', *Limnology and Oceanography*, 34(8), pp. 1694–1705.

Yoch, D. C. (2002) 'Dimethylsulfoniopropionate: its sources, role in the marine food web, and biological degradation to dimethylsulfide', *Applied and Environmental Microbiology*, 68(12), pp. 5804–5815.

Zinser, E. R., Johnson, Z. I., Coe, A., Karaca, E., Veneziano, D. and Chisholm, S. W. (2007) 'Influence of light and temperature on *Prochlorococcus* distributions in the Atlantic Ocean', *Limnology and Oceanography*, 52(5), pp. 2205–2220.

Zouni, A., Witt, H. T., Kern, J., Fromme, P., Krauss, N., Saenger, W. and Orth, P. (2001) 'Crystal structure of photosystem II from *Synechococcus elongatus* at 3.8 Å resolution', *Nature*, 409(6821), pp. 739–743.

Zubkov, M. V., Burkill, P. H. and Topping, J. N. (2007) 'Flow cytometric enumeration of DNA-stained oceanic planktonic protists', *Journal of Plankton Research*, 29, pp. 79–86.

Zubkov, M. V., Sleigh, M. A., Burkill, P. H. and Leakey, R. J. G. (2000) 'Picoplankton community structure on the Atlantic Meridional Transect: a comparison between seasons', *Progress in Oceanography*, 45, pp. 369–386.

Zubkov, M. V., Sleigh, M. A., Tarran, G. A., Burkill, P. H. and Leakey, R. J. G. (1998) 'Picophytoplanktonic community structure on an Atlantic transect from 50N to 50S', *Deep-Sea Research Part I: Oceanographic Research Papers*, 45, pp. 1339–1355.

Zwirglmaier, K., Heywood, J. L., Chamberlain, K., Woodward, E. M. S., Zubkov, M. V. and Scanlan, D. J. (2007) ‘Basin-scale distribution patterns of picocyanobacterial lineages in the Atlantic Ocean’, *Environmental Microbiology*, 9(5), pp. 1278–1290.

Appendix

List of the original sources of oceanographic data included in this thesis

1. Phytoplankton pigments and absorption coefficients

Dataset	Dates	Data contributors / online repositories	Relevant publications
AMT (no. 3, 4, 6, 12-15)	1996-2004	https://www.bodc.ac.uk/data/bodc_database/samples/ (BODC Database)	Gibb *et al*. (2000); Barlow *et al*. (2002, 2004); Hickman *et al*. (2010)
BATS	2002-2007	http://batsftp.bios.edu/BATS/bottle/ (Pigments)	Steinberg *et al*. (2001)
BEAGLE (JAMSTEC)	2003	Heather Bouman	Bouman *et al*. (2006)
BIOSOPE (IFREMER)	2004	Annick Bricaud (Absorption) & Josephine Ras (Pigments) https://doi.org/10.17600/4010100	Claustre *et al*. (2008); Raimbault *et al*. (2008); Ras *et al*. (2008); Bricaud *et al*. (2010)
BIO	1997-2003	Shuba Sathyendranath	Stuart *et al*. (2000); Sathyendranath *et al*. (2009)
D357 (UK-GEOTRACE)	2010	Heather Bouman & Thomas Browning (BODC Database)	Browning *et al*. (2014)
DCM (NIOZ)	1996	Marcel Veldhuis, George Fransz & Taco de Bruin https://doi.org/10.1594/PANGAEA.761694 (Absorption) https://doi.org/10.1594/PANGAEA.93815 (Pigments)	Bouman, Platt, Kraay, *et al*. (2000) Bouman, Platt, Sathyendranath, *et al*. (2000) Veldhuis and Kraay (2004)
EUMELI-3 (IFREMER)	1991	Annick Bricaud https://doi.org/10.1594/PANGAEA.804915 (Absorption) Hervé Claustre https://doi.org/10.1594/PANGAEA.804914 (Pigments)	Bricaud *et al*. (1995, 2004); Claustre and Marty (1995); Uitz *et al*. (2008)

Phytoplankton pigments and absorption spectra (continued)

Dataset	Dates	Data contributors / online repositories	Relevant publications
EUMELI-4 (IFREMER)	1992	Annick Bricaud https://doi.org/10.1594/PANGAEA.804946 (Absorption) Hervé Claustre https://doi.org/10.1594/PANGAEA.804944 (Pigments)	Bricaud *et al*. (1995, 2004); Claustre and Marty (1995); Babin *et al*. (1996); Uitz *et al*. (2008)
HOT	2002-2008	https://hahana.soest.hawaii.edu/hot/hot-dogs/bextraction.html or ftp://ftp.soest.hawaii.edu/hot/water (Pigments)	Karl *et al*. (2001); Letelier *et al*. (2014)
ICE-CHASER-2 (SAMS)	2010	Heather Bouman & Thomas Jackson	Jackson (2013)
JC068 (UK-GEOTRACE)	2011-2012	Heather Bouman & Thomas Browning (BODC Database)	Browning *et al*. (2014)
JC069 (UK-GEOTRACE)	2013	Heather Bouman & Thomas Browning (BODC Database)	Browning *et al*. (2014)
AMLR (NOAA)	2000-2002	Greg Mitchell (NOMAD Database) https://seabass.gsfc.nasa.gov/cruise/amlr2000 (AMLR 2000) https://seabass.gsfc.nasa.gov/cruise/amlr2001 (AMLR 2001) https://seabass.gsfc.nasa.gov/cruise/amlr2002 (AMLR 2002)	Werdell and Bailey (2008)
EN355 (WHOI)	2001	Ru Morrison (NOMAD Database) https://seabass.gsfc.nasa.gov/cruise/en355	Werdell and Bailey (2008)
IOFFE	2001	Oleg Kopelevich (NOMAD Database) https://seabass.gsfc.nasa.gov/cruise/ioffe01	Werdell and Bailey (2008)

2. Picocyanobacterial abundance (analytical flow cytometry)

Dataset	Dates	Data contributors / online repositories	Relevant publications
AMT (no. 3, 4, 6, 12-15)	1996-2004	https://www.bodc.ac.uk/data/bodc_database/samples/ (BODC Database)	Zubkov *et al*. (1998, 2000); Heywood *et al*. (2006); Tarran *et al*. (2006); Hickman *et al*. (2010); Lange *et al*. (2018);
BATS	2002-2007	http://batsftp.bios.edu/BATS/bottle/	Steinberg *et al*. (2001); Maranón *et al*. (2003); Maranón (2005); Malmstrom *et al*. (2010);
BIOSOPE	2004	Osvaldo Ulloa https://doi.org/10.17600/4010100	Grob, Ulloa, Claustre, *et al*. (2007); Claustre *et al*. (2008); West *et al*. (2011)
DCM	1996	Marcel Veldhuis, George Fransz & Taco de Bruin https://doi.org/10.1594/PANGAEA.761718	Veldhuis and Kraay (2004)
HOT	2002-2008	https://hahana.soest.hawaii.edu/hot/hot-dogs/bextraction.html or ftp://ftp.soest.hawaii.edu/hot/water	Malmstrom *et al*. (2010); Karl and Church (2014); Thompson *et al*. (2018)

3. Photosynthesis-irradiance (*PE*) parameters

Dataset	Dates	Data contributors / online repositories	Relevant publications
AMT-3, 4	1996-1997	Emilio Maranón	Maranón *et al.* (2003, 2007); Maranón (2005)
AMT-6	1998	Gavin Tilstone / https://doi.org/10.1594/PANGAEA.874087 (supplement to Bouman *et al*., 2018)	Lawrenz *et al*. (2013); Tilstone *et al*. (2017); Bouman *et al*. (2018)
AMT-15	2004	Anna Hickman / https://doi.org/10.1594/PANGAEA.874087 (supplement to Bouman *et al*., 2018)	Hickman (2007); Lawrenz *et al*. (2013); Bouman *et al*. (2018)
BIOSOPE	2004	Marcel Babin / https://doi.org/10.17600/4010100	Huot *et al*. (2007)
DCM	1996	Marcel Veldhuis, George Fransz & Taco de Bruin https://doi.org/10.1594/PANGAEA.761718 (the original dataset can be found on pages 17-18 of the cruise report available at https://epic.awi.de/id/eprint/29909/1/Vel1996a.pdf)	Bouman, Platt, Sathyendranath, *et al*. (2000)
EUMELI-4	1992	Marcel Babin http://www.obs-vlfr.fr/cd_rom_dmtt/EUMELI/EU4/pb-vs-e/eu4_pbvse_babin.htm	Babin *et al*. (1994, 1996)

4. Physical properties of the water column (CTD profiles) (for calculation of the depth of the mixed layer in Chapter 3)

Dataset	Dates	Data contributors / online repositories	Relevant publications
AMT (no. 3, 4, 6, 12-15)	1996-2004	https://www.bodc.ac.uk/data/bodc_database/ctd/search/ (BODC Database)	
BATS	2002-2007	http://batsftp.bios.edu/BATS/prelim/ctd/	
BIOSOPE	2004	Data on the mixed-layer depth can be downloaded from http://www.obs-vlfr.fr/proof/php/bio_log_basicfiles.php	Claustre *et al*. (2008); Raimbault *et al*. (2008); Ras *et al*. (2008); Uitz et *al*. (2008)
DCM	1996	Marcel Veldhuis, George Fransz & Taco de Bruin https://doi.org/10.1594/PANGAEA.761693 Estimates of the mixed-layer depth along with other hydro-graphic data can also be found on Table 2 in Bouman (1998) or Table 1 in Veldhuis and Kraay (2004).	Bouman (1998); Veldhuis and Kraay (2004)
HOT	2002-2008	https://hahana.soest.hawaii.edu/hot/hot-dogs/bextraction.html or ftp://ftp.soest.hawaii.edu/hot/ctd/	